

MECHANISTIC INVESTIGATION OF (DHQD)₂PHAL CATALYSIS IN
CHLORINATION AND DIHYDROXYLATION REACTIONS USING A
NAPHTHALENE-BASED ANALOGUE

By

Calvin Grant

A DISSERTATION

Submitted to
Michigan State University
in partial fulfillment of the requirements
for the degree of

Chemistry—Doctor of Philosophy

2018

ABSTRACT

MECHANISTIC INVESTIGATION OF (DHQD)₂PHAL CATALYSIS IN CHLORINATION AND DIHYDROXYLATION REACTIONS USING A NAPHTHALENE-BASED ANALOGUE

By

Calvin Grant

This dissertation is composed of three different projects, each discussed in a chapter. Following are short descriptions of the contained chapters.

Because of the low financial potential gains in antimicrobial drug development, companies have not invested much capital into the area, relying on naturally occurring compounds found within the last twenty to thirty years to keep the microbes at bay. In the mean time, microbes have been developing resistance to the most consistently used antimicrobials. Strains such as *pseudomonas aeruginosa* and *methicillin-resistant staphylococcus* are becoming more prevalent with the ubiquitous use of antimicrobials in animal feeds, cosmetics, and medications. In order to contribute to the search for new antibiotics, we pursued antimicrobial lead compounds by tapping an easily accessible resource - repurposed laboratory compounds. The first chapter of this dissertation addresses the process of organizing, testing, and analyzing a library for antibacterial assays. A few of the positive antibacterial hits have been analyzed to investigate the mode-of-action of their class.

In another study, discussed in chapter two, addresses a total synthesis of Alexine, a polyhydroxylated pyrrolizidine found to exhibit antiretroviral activity. While most syntheses of this family of pyrrolizidines utilized amino acids or sugars as templates, this synthesis relied on an aza-payne rearrangement and a one-carbon homologative relay ring expansion after incorporation of all necessary carbons required in the structure of alexine. This synthesis attempt ends with the formation of the initial pyrrolidine via our methodology and a proposal for the completion of the total synthesis.

In the final chapter, for which the dissertation has been titled, new advancements in halofunctionalization that have been uncovered in the Borhan laboratory are further investigated. In particular, the hypothesis regarding the enantioselectivities seen when utilizing (DHQD)₂PHAL under optimized conditions suggests that the high enantioselectivities seen in the halofunctionalization of unfunctionalized alkenes done by Borhan and coworkers are due to the rigidity of DHQD ligand-linker bonds C-O-C=N facilitated by the sp² character of pendant oxygen as it donates into the electron deficient aromatic linker. In order to probe this, a naphthalene linker analogue (DHQD)₂NAPH was synthesized and used as a catalyst in the optimized reactions. Computational studies were used to confirm the results and confirm the validity of the hypothesis.

Copyright by
CALVIN GRANT
2018

For my wife, my family, and the God who made all things possible.

ACKNOWLEDGEMENTS

To Babak, you made worlds of knowledge accessible to me and trusted me to use it well.

To Chrysoula, when I didn't know where to step, you made all the paths visible and even walked me down some of them.

To Crystal, you stood by me when I just stood there and even when I just sat, but your expectations of me and your support never waivered.

To my family, through blood and through circumstance, your constant support and laughter was a wellspring of life.

To my church, you made my successes your successes and made me a part of the whole.

To my God, you provided everything, inside and outside of me, to pull success from a place within me where there was none.

TABLE OF CONTENTS

LIST OF TABLES	ix
LIST OF FIGURES	xi
LIST OF SCHEMES	xiii
KEY TO SYMBOLS AND ABBREVIATIONS	xvi
Chapter I	1
Antibacterial Assay and Evaluation of Laboratory Compounds	1
I.1. Introduction	1
I.2. Results and Discussion	4
I.2.1. High Throughput Assay Screening of Laboratory Compounds	4
I.2.2. Synthesis and Assay of 3-alkyl-3-hydroxytetrahydrofurans	86
I.2.3. Mode-of-Action Studies of 3-alkyl-3-hydroxytetrahydrofurans Using Hemolysis Assays	95
I.2.4. General Hemolytic Assays	101
I.3. Conclusion	103
I.4. Experimental	106
REFERENCES	121
Chapter II	127
Steps Towards the Total Synthesis of (+)-Alexine via One-Carbon Homologative Relay Ring Expansion	127
II.1. Introduction	127
II.1.1. Discovery of Alexine	127
II.1.2. Biological Activity of Alexine	127
II.1.3. Previous Synthetic Approaches to Alexine and Other Members of the Family	131
II.1.4. Retrosynthesis of Alexine	139
II.2. Results and Discussion	141
II.2.1. Synthesis of Alexine	141
II.3. Conclusion	149
II.4. Experimental	153
REFERENCES	174

Chapter III	177
Mechanistic Investigation of (DHQD)₂PHAL Catalysis in Chlorination and Dihydroxylation Reactions Using a Naphthalene-Based Analogue	177
III.1. Introduction	177
III.1.1. Overview	177
III.1.2. Phase-transfer Catalysis in Asymmetric Halofunctionalization	183
III.1.3. Mechanistic Insights into Asymmetric Chlorocyclization	186
III.2. Results and Discussion	201
III.2.1. Synthesis of (DHQD) ₂ NAPH	201
III.2.2. Intramolecular Chlorofunctionalization	205
III.2.3. Intermolecular Chlorofunctionalization	210
III.2.3.1. Chloroetherification	211
III.2.3.2. Dichlorination	217
III.2.4. Computational Derivations	221
III.2.5. Sharpless Dihydroxylation	227
III.3. Conclusion	232
III.4. Experimental	234
III.4.1. Synthesis	234
III.4.2. Quantum Mechanics Modeling Experiments	249
REFERENCES	268

LIST OF TABLES

Table I-1: Antimicrobial activity of Squalamine and comparable molecules.	73
Table I-2: Substituted tetrahydrofuran activity against Gram-positive bacteria.	86
Table I-3: EC ₅₀ Values of 3,3-alkylhydroxytetrahydrofuran analogues of differing chain lengths.	91
Table I-4: EC ₅₀ Values of branched and aromatic 3,3-alkylhydroxytetrahydrofuran analogues on Gram-positive bacteria.	93
Table I-5: Evaluation of hydroxyl group importance in antibacterial activity of 3,3-alkylhydroxytetrahydrofuran analogues and EC ₅₀ values on Gram-positive bacteria.	94
Table II-1: Action of naturally occurring alexines on mouse gut digestive glucosidase activity compared with those of DMP and castanospermine. Concentration (M) of alkaloid giving 50% inhibition. $>3.3 \times 10^{-4}$ required for 50% inhibition. ^{3 4}	130
Table III-1: Erosion of enantiospecificity in acetolysis from olefin-to-olefin transfer. HFIP = hexafluoroisopropanol, Tf = trifluoromethanesulfonyl, Ts = 4-toluenesulfonyl. $es = (ee_{\text{product}}/ee_{\text{starting material}}) \times 100\%$.	180
Table III-2: (DHQD) ₂ PHAL mediated halolactonization. ^a NR = no reaction after 3 h.	181
Table III-3: Selections from the chlorolactonization substrate scope.	188
Table III-4: Effect of benzoyl substitution on 1,1-disubstituted amide chlorocyclization.	189
Table III-5: Olefinic aryl effects on chlorocyclization of 1,1-disubstituted amides.	190

Table III-6: Chlorocyclization of 1,2-disubstituted and trisubstituted allyl amides. ^a Reaction was run in 1-nitropropane in the presence of 300 wt% molecular sieves (4Å).	191
Table III-7: Comparison of Chloramine-T•3H ₂ O/(DHQD) ₂ PHAL to DCDPH/(DHQD) ₂ PHAL in the cyclization of allyl amines.	194
Table III-8: Limited substrate scope of intermolecular chloroetherification by Soltanzadeh, et al.	212
Table III-9: A comparison of intermolecular chloroetherification of aliphatic and aromatic allylic amides using (DHQD) ₂ PHAL and (DHQD) ₂ NAPH catalysts.	214
Table III-10: Limited substrate scope of intermolecular dichlorination by Soltanzadeh, et al.	219
Table III-11: A comparison of intermolecular dichlorination of aliphatic and aromatic allylic amides using (DHQD) ₂ PHAL and (DHQD) ₂ NAPH catalysts.	221
Table III-12: DFT B3LYP 6-31G* energies (kcal) of single (DHQD) ₂ Ar bond rotation.	226
Table III-13: Dihydroxylation of <i>trans</i> -5-decene and <i>trans</i> -stilbene using a variety of 9-O-aromatic DHQD catalysts.	230
Table III-14: Oxidation of <i>trans</i> -stilbene via Sharpless Dihydroxylation with (DHQD) ₂ PHAL and (DHQD) ₂ NAPH ligands.	248
Table III-15: Oxidation of <i>trans</i> -decene via Sharpless Dihydroxylation with (DHQD) ₂ PHAL and (DHQD) ₂ NAPH ligands.	249

LIST OF FIGURES

Figure I-1: Teixobactin is a gram-positive antibacterial isolated from β -proteobacteria <i>Eleftheria terrae</i> .	3
Figure I-2: Gram-positive and Gram-negative activity of general repurposed laboratory compounds.	6
Figure I-3: Squalamine, an aminosterol isolated from the stomach of the dogshark <i>Squalus acanthias</i> .	72
Figure I-4: Squalamine and select squalamine mimics.	74
Figure I-5: A. Select polymyxins, cyclic members of the cationic peptide antibiotic class. B. Select polymyxin mimics and their minimum inhibitory concentrations ($\mu\text{g/mL}$) against Gram-positive and Gram-negative bacteria compared to polymyxin B. Minimum hemolytic concentration (MHC) was also recorded in $\mu\text{g/mL}$.	75
Figure I-6: Synthesis and antibacterial testing of benzothiazine steroids and their ketone precursors against Gram-positive and Gram-negative strains of bacteria.	76
Figure I-7: Minimum inhibitory concentration of Gram-positive and Gram-negative bacteria by steroidal compounds from an assay of general lab compounds.	78
Figure I-8: Minimum inhibitory concentration of Gram-positive and Gram-negative bacteria by select compounds from an assay of general lab compounds.	80
Figure I-9: Minimum inhibitory concentration of select compounds from an assay of general lab compounds against Gram-positive and Gram-negative bacteria.	81
Figure I-10: Minimum inhibitory concentration of charged compounds in an assay of general lab compounds against Gram-positive and Gram-negative bacteria.	82

Figure I-11: Allicin, a compound found in garlic that has shown promising antibacterial activity in Gram-positive and Gram-negative bacteria.	83
Figure I-12: Minimum inhibitory concentration of Gram-positive and Gram-negative bacteria by select compounds from an assay of general lab compounds.	85
Figure I-13: UV/Vis absorption of hemolysis assay supernatant of 3,3-alkylhydroxytetrahydrofurans at 550 nm.	96
Figure I-14: Red blood cell viability after incubation with 3,3-alkylhydroxytetrahydrofurans.	98
Figure I-15: Minimum inhibitory concentration of general laboratory compounds that exhibited no hemolytic activity.	102
Figure II-1: Alexine structural comparison to DMDP.	128
Figure II-2: Retrosynthetic analysis of (+)-Alexine (II-1) via one-carbon homologative relay ring expansion.	139
Figure II-3: One-carbon homologative relay ring expansion of aziridinols.	140
Figure III-1: Iodolactonization via phase-transfer catalysis..	185
Figure III-2: Relative energy of rotation of anisole and dimethoxybenzenes. ^a Relative energy (E_{rel}) is in kcal/mol.	222
Figure III-3: Relative rotational energy of 1,4-dimethoxypyridazine, a simple model system for (DHQD) ₂ PHAL bond rotation.	224
Figure III-4: DFT calculation (B3LYP 6-31G*) of relative energy of (DHQD) ₂ PHAL (<i>a</i>) and (DHQD) ₂ NAPH (<i>b</i>). =C-O-C dihedral angle and relative energy for each structure is written below.	227
Figure III-5: A comparison of DHQD ether catalysts divided into quadrants.	231
Figure III-6: Possible electron deficient naphthyl linkers to test for the recovery of selectivity in chlorofunctionalization.	233

LIST OF SCHEMES

Scheme I-1: Resazurin is reduced by viable cells to resorufin.	5
Scheme I-2: Synthesis of 3,3-alkylhydroxytetrahydrofuran analogues via one-carbon homologative relay ring expansion. ^a Yields were calculated in relation to the alkyl halide.	89
Scheme I-3: Synthesis of 3,3-alkylhydroxytetrahydrofuran analogues via nucleophilic addition. ^a Used <i>n</i> BuLi as nucleophile. ^b Unless otherwise mentioned, nucleophiles were generated through magnesium insertion to form the corresponding Grignard reagent.	90
Scheme II-1: Synthesis of pyrrolizidine natural products isoretronecanol (II-8) and trachelanthamidine (II-9).	131
Scheme II-2: Synthesis of (-)-Trachelanthamidine (II-9).	132
Scheme II-3: First synthesis of (+)-Alexine (II-1). This initial synthesis was based on the inherent chirality of D-glucose.	133
Scheme II-4: Synthesis of (+)-Casuarine.	135
Scheme II-5: Attempted synthesis of 3-epialexine analogues.	137
Scheme II-6: Asymmetric synthesis of 1,2-diepi-alexine and 1,2,7-triepi-australine via Sharpless aminohydroxylation.	138
Scheme II-7: Synthesis of aziridinal fragment II-57.	142
Scheme II-8: Synthesis of vinyl halide fragment II-58.	143
Scheme II-9: Initial nucleophilic combination of fragments.	144
Scheme II-10: Dehydrohalogenation of <i>cis</i> -vinyl halide II-58b and lithiation of <i>in situ</i> formed alkyne.	145

Scheme II-11: Nucleophilic addition using Grignard bases.	145
Scheme II-12: Alkyne reduction. a. Phillips NBSH reduction provided 93% of desired product. b. NBSH reduction of propargyl aziridinol proved more reactive and difficult to partially reduce. c. Palladium on barium sulfate proved sufficient for a quantitative partial reduction to give the desired <i>cis</i> -alkene.	147
Scheme II-13: Silyl exchange and one-carbon homologative relay ring - expansion.	148
Scheme II-14: Remaining steps in the synthesis of alexine.	152
Scheme III-1: Spectroscopically observable haliranium ions.	178
Scheme III-2: Mechanisms of olefin-to-olefin transfer of bromenium ions.	179
Scheme III-3: Comparison of halenium source reactivity exhibited through bromolactonization with NBS and chlorolactonization with NCS.	183
Scheme III-4: Iodolactonization using phase-transfer catalysis.	184
Scheme III-5: Fluorocyclization of benzamides using an anionic phase-transfer catalyst.	186
Scheme III-6: Importance of hydantoin structure in chlorolactonization.	192
Scheme III-7: Evaluation of the importance of phthalazine linker in relation to enantioselectivity.	195
Scheme III-8: Enantioselective cost evaluation of monomer modification in dimeric chlorolactonization catalysts. ^a The enantioselectivities of lactone III-19e are documented below the structure of the catalyst used. ^b Each arrow indicates the enantioselective cost of a specified modification.	197
Scheme III-9: Probing the importance of the phthalazine nitrogens.	199
Scheme III-10: Synthesis of (DHQD) ₂ PHAL.	201

Scheme III-11: Sharpless synthesis of dihydroquinidine 9- <i>O</i> -(9'-phenanthryl)ether (DHQD-PHN) using Ullmann coupling. ²	202
Scheme III-12: Synthesis of naphthyl dimer (DHQD) ₂ NAPH. (a) Attempted Ullmann coupling with 1,4-dibromonaphthalene. (b) Synthesis of 1,4-diiodonaphthalene. (c) Ullmann coupling and reduction to form (DHQD) ₂ NAPH dimer.	204
Scheme III-13: Synthesis of hydroquinidine-1,4-naphthalenediyl diether (DHQD) ₂ NAPH.	205
Scheme III-14: Comparison of (QD) ₂ PHAL and (QD) ₂ NAPH in chlorolactonization and allyl amide chlorocyclization.	206
Scheme III-15: Substrate scope for the intramolecular chlorocyclization of allene amides.	209
Scheme III-16: Allene chlorocyclization enantioselectivities.	210
Scheme III-17: Bromoesterification of allyl sulfonamides using (DHQD) ₂ PHAL.	211
Scheme III-18: Regioselectivity challenge associated with asymmetric dichlorination of unactivated olefins.	218
Scheme III-19: Nicolaou asymmetric dichlorination of allyl alcohols.	218
Scheme III-20: Recommended ligand for each olefin class and their enantioselectivity range. ¹	228
Scheme III-21: Dihydroxylation of <i>trans</i> -stilbene and <i>trans</i> -5-decene with (DHQD) ₂ NAPH and (DHQD) ₂ PHAL.	229

KEY TO SYMBOLS AND ABBREVIATIONS

Å	Angstrom
Ar	Aryl
B3LYP	Beck, three-parameter, Lee-Yang-Parr Hybrid Functional
BenzoPHAL	1,4-Benzophthalazine
BINOL	1,1'-Bi(2-naphthol)
CN	Cinchonidine
CPA	Cationic Peptide Antibiotic
CSA	Cationic Steroid Antibiotic
DCDMH	1,3-Dichloro-5,5-dimethylhydantoin
DCDPH	1,3-Dichloro-5,5-diphenylhydantoin
δ	Delta (chemical shift)
DFT	Density Functional Theory
DHQD	Dihydroquinidine
(DHQD) ₂ NAPH	Hydroquinidine 1,4-naphthalenediyl diether
(DHQD) ₂ PHAL	Hydroquinidine 1,4-phthalazinediyl diether
DMSO	Dimethylsulfoxide
DMDP	(2 <i>R</i> ,3 <i>R</i> ,4 <i>R</i> ,5 <i>R</i>)-2,5-dihydroxymethyl-3,4-Dihydroxypyrrolidine
DME	Dimethoxyethane
DNA	Deoxyribonucleic Acid

EC ₅₀	Effective Concentration, 50%
<i>ee</i>	Enantiomeric Excess
EtOAc	Ethyl Acetate
HFIP	Hexafluoroisopropanol
LB	Lysogeny broth, Luria Broth, Luria-Bertani
λ	Lamda (wavelength)
λ_{max}	Maximum Wavelength
LD ₅₀	Lethal Dose, 50% (Median Lethal Dose)
M	Molar
<i>m</i> CPBA	<i>meta</i> -Chloroperoxybenzoic acid
MeCN	Acetonitrile
MeOH	Methanol
μg	Microgram
μL	Microliter
MHC	Minimum Hemolytic Concentration
MIC	Minimum Inhibitory Concentration
mg	Milligram
MHz	Megahertz
mL	Milliliter
mM	Millimolar
MOM	Methoxymethyl
MOMCl	Methoxymethyl chloride

MP2	2 nd Order Møller-Plesset <i>ab initio</i> method
NAM	<i>N</i> -acetylmuramic acid
NAPY	2,7-Disubstituted-1,8-naphthyridine
NBSH	2-Nitrobenzene sulfonyl hydrazide
nBuLi	<i>n</i> -Butyl lithium
nm	Nanometer
NMR	Nuclear Magnetic Resonance
PCC	Pyridinium Chlorochromate
PhSCI	Benzenesulfonyl Chloride
PMB	<i>para</i> -Methoxybenzyl
PPTS	Pyridinium <i>para</i> -Toluenesulfonic Acid
PYDZ	3,6-Disubstituted Pyridazine
QD	Quinidine
REDOX	Reduction-oxidation reaction
RNA	Ribonucleic Acid
rt	Room temperature
SER	Structure-Enantioselectivity Relationship
STO	Slater-Type Orbital Basis Set
TBAI	Tetrabutylammonium iodide
TBSCI	<i>t</i> -Butylsilyl Chloride
TFE	Trifluoroethanol
THF	Tetrahydrofuran

TLC	Thin Layer Chromatography
TMEDA	Tetramethylethylenediamine
TMS	Trimethylsilyl
UV	Ultraviolet light
wt%	Weight Percent

Chapter I

Antibacterial Assay and Evaluation of Laboratory Compounds

I.1. Introduction

Many of well-known antimicrobials have been discovered in nature. Penicillin, streptomycin, tetracyclin, chloramphenicol, erythromycin, and vancomycin were all isolated from natural sources or were derived from natural product leads. This may lead to the assumption that the antimicrobial drugs were initially a serendipitous isolation from a natural source. In reality, the inception of antimicrobial drugs outside of the realm of naturopathic medicine began in the laboratory with such compounds as salvarsan, an organic arsenic compound used in the treatment of syphilis, and prontosil, an oral precursor to sulfanilamide and a specific activity against gram-positive cocci.⁵

In order to combat the high mortality of the day, Paul Ehrlich envisioned the use of small molecules to combat bacterial diseases, or as he referred to it, “chemotherapy”. Relying on the advancement of knowledge of bacteria and developments in organic chemistry, particularly in dye synthesis, Ehrlich worked to synthesize a compound that would have a specific affinity for the microorganisms and a toxic element that would eliminate them. With this in mind, he was able to develop compound 606, also referred to as Salvarsan. This compound was effective against syphilis and therefore represented the first real chemotherapeutic success.

Today, we are in the midst of another crisis, ironically, stemming from the ubiquitous use of antimicrobials in addition to the amazing adaptability of microbes. The number of antibiotic-resistant infections is increasing worldwide. That, along with the low return on investments for companies (antibiotics being short-course treatments typically taken for 2 weeks as opposed to chronic illnesses and their noncurative treatments), creates a perfect storm.⁶ This problem has increased in urgency so much that the Infectious Disease Society of America are making regular calls for new antimicrobials and enacting policies to encourage the search for new antimicrobials.^{7 8}

In light of such dire circumstances, there have been a few advancements. For example, Lewis and coworkers have recently developed new methods to grow previously uncultured organisms and have, consequently, isolated a new antibiotic dubbed teixobactin that kills Gram-positive bacteria without detectable resistance.⁹ Teixobactin, shown in Figure I-1, prevents cell wall synthesis by binding to highly conserved lipid II and lipid III domains. As yet, all *Staphylococcus aureus* and *Mycobacterium tuberculosis* mutants have not shown any resistance to teixobactin.

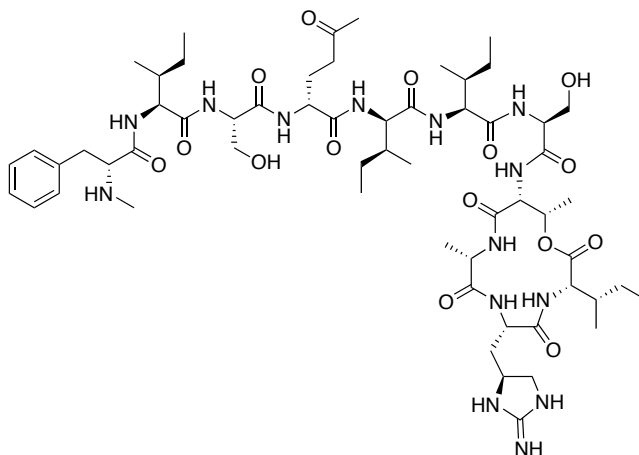


Figure I-1: Teixobactin is a gram-positive antibacterial isolated from β -proteobacteria *Eleftheria terrae*.

While the pursuit of microbe-produced antibacterials is a wise and promising course, to neglect other avenues in the pursuit of new antimicrobials would not be wise. With this in mind, we decided to submit laboratory-synthesized compounds to an antibacterial assay as another means to search for leads. Synthesis provides an ever-increasing amount of compounds to test, whether they are intermediates in a total synthesis or repurposed compounds from methodologies and mechanistic studies. The structural complexity of each individual compound is limited only by its original purpose and the imagination of the scientists involved.

Of course, to attempt an endeavor like this, a library must be created to catalog the compounds and their activity. After submission of these compounds to antimicrobial assays, the hits would be evaluated. Analogues would be synthesized and studied in order to fully understand the contribution their

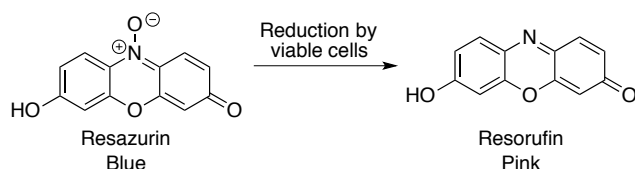
structure makes to their activity. Finally, elucidating the mode of action would determine if this compound could be considered a viable lead.

I.2. Results and Discussion

I.2.1. High Throughput Assay Screening of Laboratory Compounds

In order to test the lab compounds for antibacterial activity, it was important to organize them systemically in a library format that would be conducive to tracking their testing results. To this end, approximately 1,400 compounds were labeled and assigned a number. A portion of each compound was diluted to a concentration of 10 mg/mL in DMSO and stored separately at -20 °C. Gram-positive (specifically, *bacillus cereus*, *bacillus subtilis*, *micrococcus luteus*, and *staphylococcus aureus*) and Gram-negative bacterias (*escherichia coli*, *klebsiella pneumoniae*, *pseudomonas aeruginosa*, and *serratia marcescens*), were inoculated into 5 mL portions of autoclaved lysogeny broth (LB) and allowed to incubate in a shaker for 6 to 8 hours. 1 mL of the cell culture was diluted by adding 10 mL of LB. To prepare the well-plates, 170 µL of LB were added to each well, followed by 30 µL of the bacterial cell solution. 10 µl of the 10 mg/ml solutions of laboratory compounds was added to each well in triplicate. A streptomycin control of the same concentration was added to a well to provide a positive control with respect to Gram-positive bacteria. Tetracyclin was used as the positive control with respect to Gram-negative bacteria. The 96 well-plates were incubated at 37 °C for another 6 to 8 hours.

In order to test the viability of bacterial cells after incubation with the laboratory compounds, resazurin dye was used. Resazurin is a blue dye that is irreversibly reduced to resorufin, a pink compound by mitochondrial enzymes after intake by living cells, making it a useful REDOX indicator of cell viability.^{10 11 12} The metabolism of resazurin to resorufin is an indication of the existence of viable cells and, in our case, an indication that the tested laboratory compound proved ineffective as an antibacterial. 1 μ L of a 3.3 mg/mL solution of resazurin in water was added to each well and monitored visually and via the Benchmark Biorad microplate reader (at λ =595 nm, 655 nm) every 5 minutes until 30 minutes had passed. Compounds that maintained high concentrations of resazurin after this incubation were considered active, requiring less than 476 μ g/mL to inhibit bacterial proliferation. Upon treatment with resazurin dye, 29 compounds were found to be active.



Scheme I-1: Resazurin is reduced by viable cells to resorufin.

entry	compound	Gram (+)	Gram (-)	entry	compound	Gram (+)	Gram (-)
1		✗	✗	9		✗	✗
2		✗	✗	10		✗	✗
3		✗	✗	11		✗	✗
4		✗	✗	12		✗	✗
5		✗	✗	13		✗	✗
6		✗	✗	14		✗	✗
7		✗	✗	15		✗	✗
8		✗	✗	16		✗	✗

Figure I-2: Gram-positive and Gram-negative activity of general repurposed laboratory compounds.

Figure I-2 (cont'd)

entry	compound	Gram (+)	Gram (-)	entry	compound	Gram (+)	Gram (-)
17		✗	✗	25		✗	✗
18		✗	✗	26		✗	✗
19		✗	✗	27		✗	✗
20		✗	✗	28		✗	✗
21		✗	✗	29		✗	✗
22		✗	✗	30		✗	✗
23		✗	✗	31		✗	✗
24		✗	✗	32		✗	✗

Figure I-2 (cont'd)

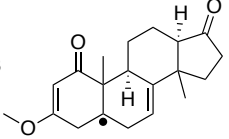
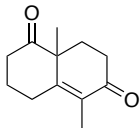
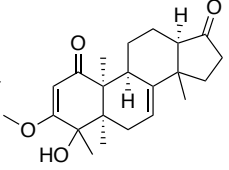
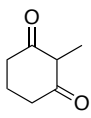
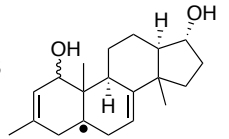
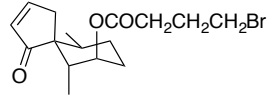
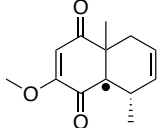
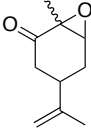
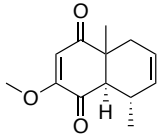
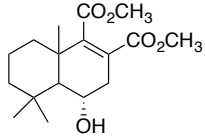
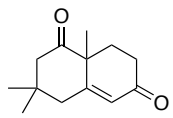
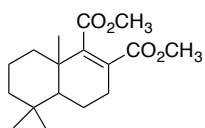
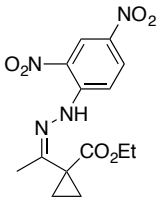
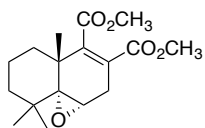
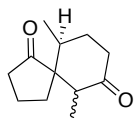
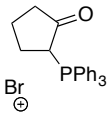
entry	compound	Gram (+)	Gram (-)	entry	compound	Gram (+)	Gram (-)
33		✗	✗	41		✗	✗
34		✗	✗	42		✗	✗
35		✗	✗	43		✗	✗
36		✗	✗	44		✗	✗
37		✗	✗	45		✗	✗
38		✗	✗	46		✗	✗
39		✗	✗	47		✗	✗
40		✗	✗	48		✗	✗

Figure I-2 (cont'd)

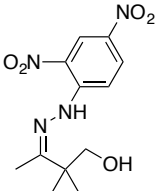
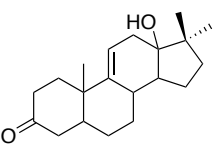
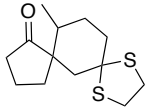
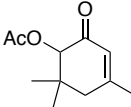
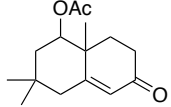
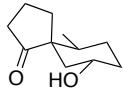
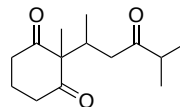
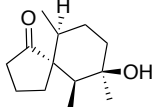
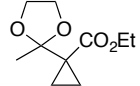
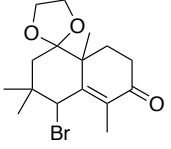
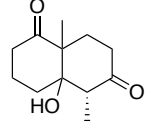
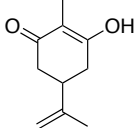
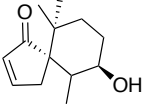
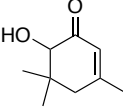
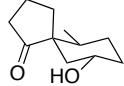
entry	compound	Gram (+)	Gram (-)	entry	compound	Gram (+)	Gram (-)
49		✗	✗	57		✗	✗
50		✗	✗	58		✗	✗
51		✗	✗	59	$\text{Ph}_3\text{PCH}_2\text{PPh}_3 \cdot 2\text{Br}$	✓	✓
52		✗	✗	60		✗	✗
53		✗	✗	61		✗	✗
54		✗	✗	62		✗	✗
55		✗	✗	63		✗	✗
56		✗	✗	64		✗	✗

Figure I-2 (cont'd)

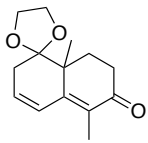
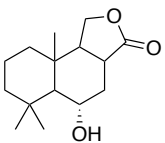
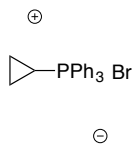
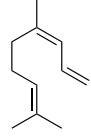
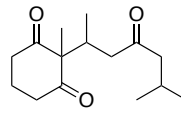
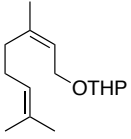
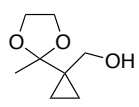
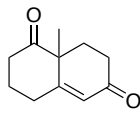
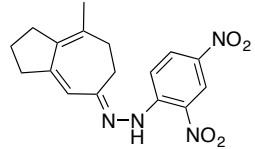
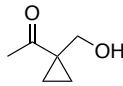
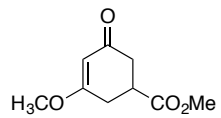
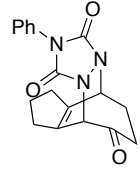
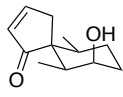
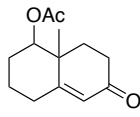
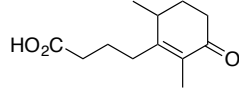
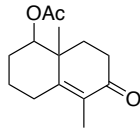
entry	compound	Gram (+)	Gram (-)	entry	compound	Gram (+)	Gram (-)
65		✗	✗	73		✗	✗
66		✗	✗	74		✗	✗
67		✗	✗	75		✗	✗
68		✗	✗	76		✗	✗
69		✗	✗	77		✗	✗
70		✗	✗	78		✗	✗
71		✗	✗	79		✗	✗
72		✗	✗	80		✗	✗

Figure I-2 (cont'd)

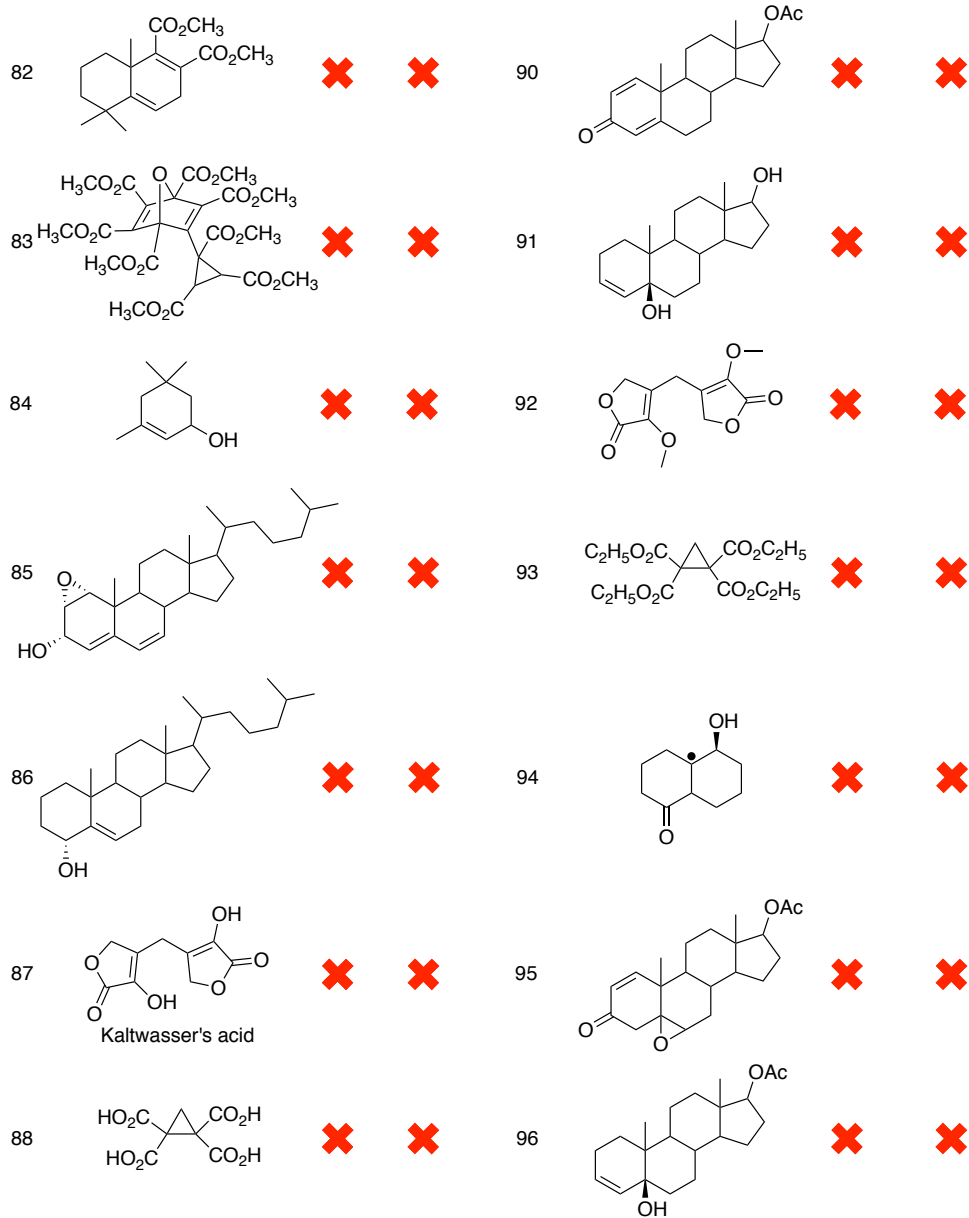


Figure I-2 (cont'd)

entry	compound	Gram (+)	Gram (-)	entry	compound	Gram (+)	Gram (-)
97		✗	✗	105		✗	✗
98		✗	✗	106		✗	✗
99	$\text{C}_2\text{H}_5\text{O}_2\text{C}-\text{CH}_2-\text{CH}_2-\text{CO}_2\text{C}_2\text{H}_5$	✗	✗	107		✗	✗
100		✗	✗	108		✗	✗
101		✗	✗	109		✗	✗
102		✗	✗	110	$\text{H}_3\text{CO}_2\text{C}-\text{CH}_2-\text{CH}_2-\text{CO}_2\text{CH}_3$	✗	✗
103		✗	✗	111		✗	✗
104		✗	✗	112	$\left[\begin{array}{c} \text{O}_2\text{C} \\ \text{O}_2\text{C} \end{array} \right]^{-4} 2\text{BA}^{+2}$	✗	✗

Figure I-2 (cont'd)

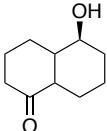
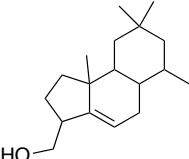
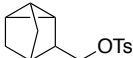
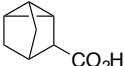
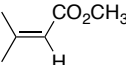
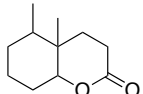
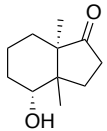
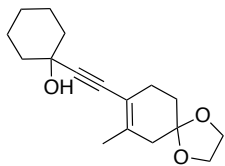
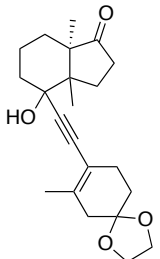
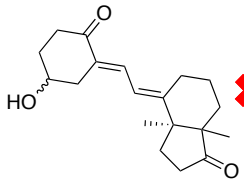
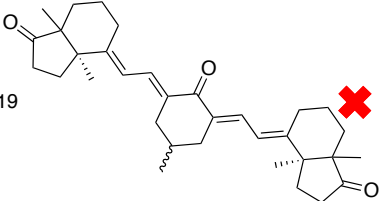
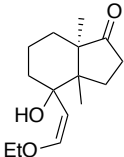
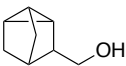
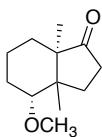
entry	compound	Gram (+)	Gram (-)	entry	compound	Gram (+)	Gram (-)
113		✗	✗	121	alpha-bromocamphor	✗	✗
114		✗	✗	122		✗	✗
115	para-bromocamphor	✗	✗	123		✗	✗
116		✗	✗	124		✗	✗
117		✗	✗	125		✗	✗
118		✗	✗	126		✗	✗
119		✗	✗	127		✗	✗
120		✗	✗	128		✗	✗

Figure I-2 (cont'd)

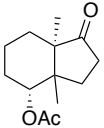
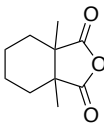
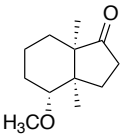
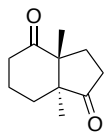
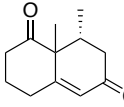
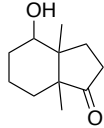
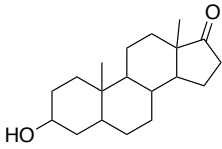
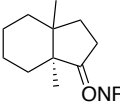
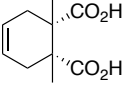
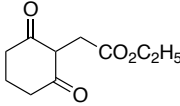
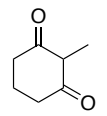
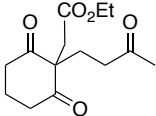
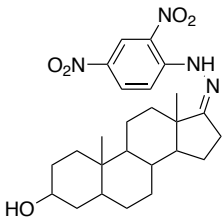
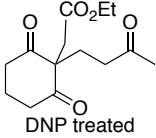
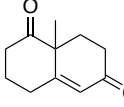
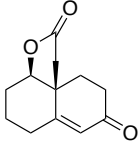
entry	compound	Gram (+)	Gram (-)	entry	compound	Gram (+)	Gram (-)
129		✗	✗	137		✗	✗
130		✗	✗	138		✗	✗
131		✗	✗	139		✗	✗
132		✗	✗	140		✗	✗
133		✗	✗	141		✗	✗
134		✗	✗	142		✗	✗
135		✗	✗	143		✗	✗
136		✗	✗	144		✗	✗

Figure I-2 (cont'd)

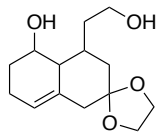
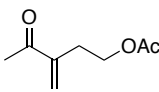
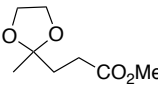
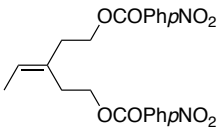
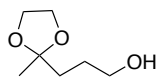
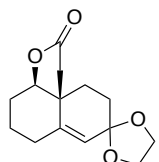
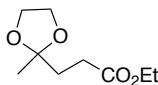
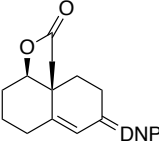
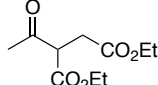
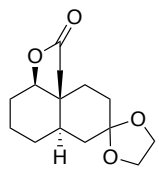
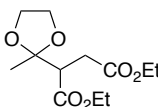
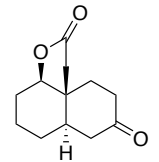
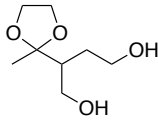
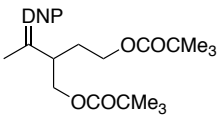
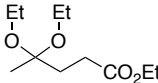
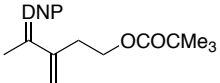
entry	compound	Gram (+)	Gram (–)	entry	compound	Gram (+)	Gram (–)
145		✗	✗	153		✗	✗
146		✗	✗	154		✗	✗
147		✗	✗	155		✗	✗
148		✗	✗	156		✗	✗
149		✗	✗	157		✗	✗
150		✗	✗	158		✗	✗
151		✗	✗	159		✗	✗
152		✗	✗	160		✗	✗

Figure I-2 (cont'd)

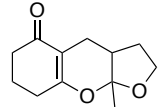
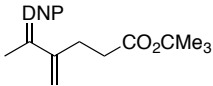
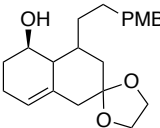
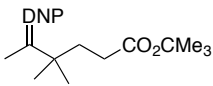
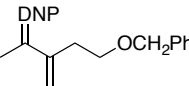
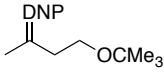
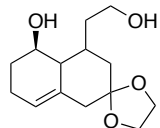
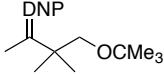
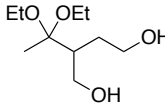
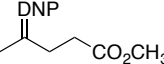
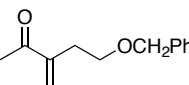
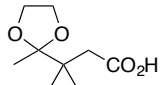
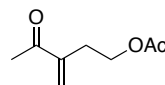
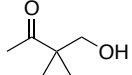
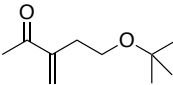
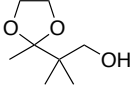
entry	compound	Gram (+)	Gram (-)	entry	compound	Gram (+)	Gram (-)
161		✗	✗	169		✗	✗
162		✗	✗	170		✗	✗
163		✗	✗	171		✗	✗
164		✗	✗	172		✗	✗
165		✗	✗	173		✗	✗
166		✗	✗	174		✗	✗
167		✗	✗	175		✗	✗
168		✗	✗	176		✗	✗

Figure I-2 (cont'd)

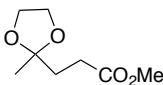
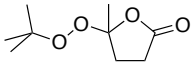
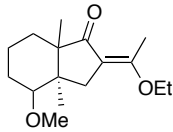
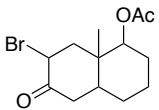
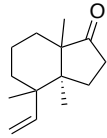
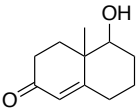
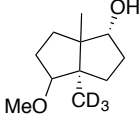
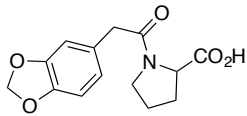
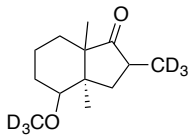
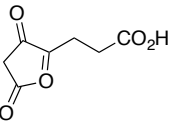
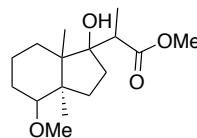
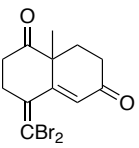
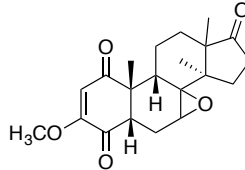
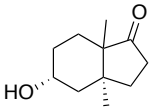
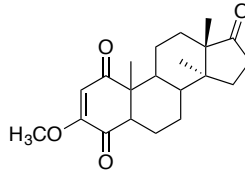
entry	compound	Gram (+)	Gram (-)	entry	compound	Gram (+)	Gram (-)
177		✗	✗	185	Geranyl phenyl ether	✗	✗
178		✗	✗	186		✗	✗
179		✗	✗	187		✗	✗
180		✗	✗	188		✗	✗
181		✗	✗	189		✗	✗
182		✓	✓	190		✗	✗
183		✗	✗	191		✗	✗
184		✗	✗	192		✗	✗

Figure I-2 (cont'd)

entry	compound	Gram (+)	Gram (-)	entry	compound	Gram (+)	Gram (-)
193		✗	✗	201		✗	✗
194		✗	✗	202		✗	✗
195		✗	✗	203		✗	✗
196		✗	✗	204		✗	✗
197		✗	✗	205		✗	✗
198		✗	✗	206		✗	✗
199		✗	✗	207		✗	✗
200		✗	✗	208		✗	✗

Figure I-2 (cont'd)

entry	compound	Gram (+)	Gram (-)	entry	compound	Gram (+)	Gram (-)
209		✗	✗	217		✗	✗
210		✗	✗	218		✗	✗
211		✗	✗	219		✗	✗
212		✗	✗	220		✗	✗
213		✗	✗	221		✗	✗
214		✗	✗	222		✗	✗
215		✗	✗	223		✗	✗
216		✗	✗	224		✗	✗

Figure I-2 (cont'd)

entry	compound	Gram (+)	Gram (–)	entry	compound	Gram (+)	Gram (–)
209		✗	✗	217		✗	✗
210		✗	✗	218		✗	✗
211		✗	✗	219		✗	✗
212		✗	✗	220		✗	✗
213		✗	✗	221		✗	✗
214		✗	✗	222		✗	✗
215		✗	✗	223		✗	✗
216		✗	✗	224		✗	✗

Figure I-2 (cont'd)

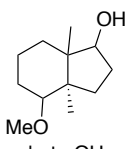
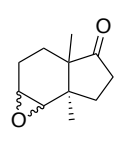
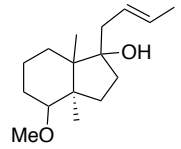
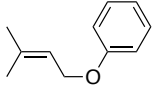
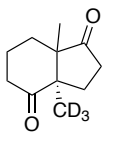
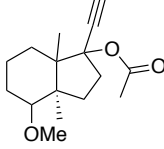
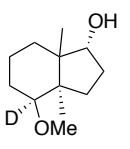
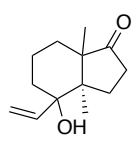
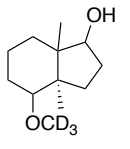
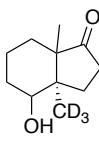
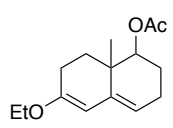
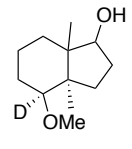
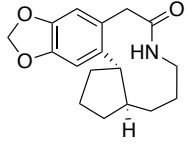
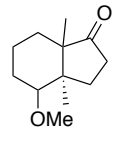
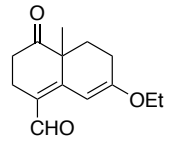
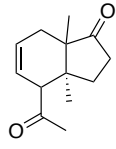
entry	compound	Gram (+)	Gram (–)	entry	compound	Gram (+)	Gram (–)
225	 beta-OH	✗	✗	233		✗	✗
226		✗	✗	234		✗	✗
227		✗	✗	235		✗	✗
228		✗	✗	236		✗	✗
229		✗	✗	237		✗	✗
230		✗	✗	238		✗	✗
231		✗	✗	239		✗	✗
232		✗	✗	240		✗	✗

Figure I-2 (cont'd)

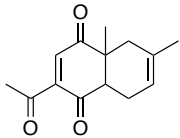
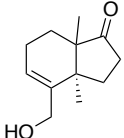
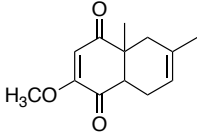
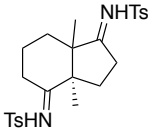
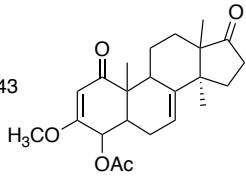
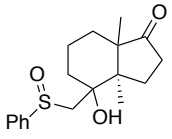
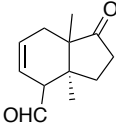
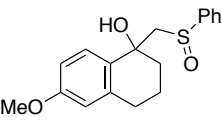
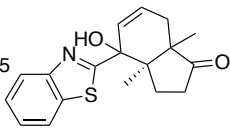
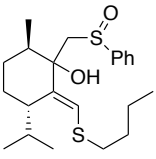
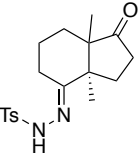
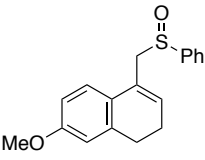
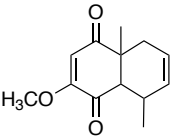
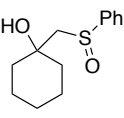
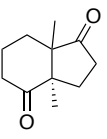
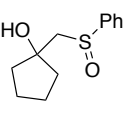
entry	compound	Gram (+)	Gram (-)	entry	compound	Gram (+)	Gram (-)
241		✗	✗	249		✗	✗
242		✗	✗	250		✗	✗
243		✗	✗	251		✗	✗
244		✗	✗	252		✗	✗
245		✗	✗	253		✗	✗
246		✗	✗	254		✗	✗
247		✗	✗	255		✗	✗
248		✗	✗	256		✗	✗

Figure I-2 (cont'd)

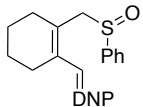
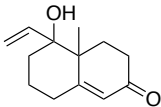
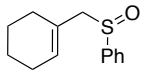
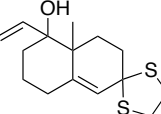
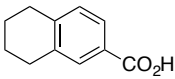
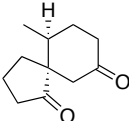
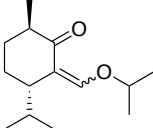
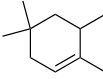
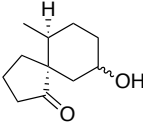
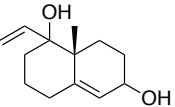
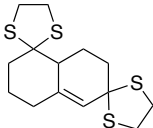
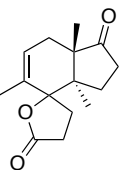
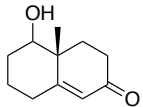
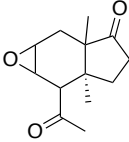
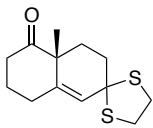
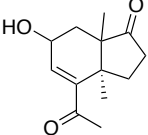
entry	compound	Gram (+)	Gram (–)	entry	compound	Gram (+)	Gram (–)
257		✗	✗	265		✗	✗
258		✗	✗	266		✗	✗
259		✗	✗	267		✗	✗
260		✗	✗	268		✗	✗
261		✗	✗	269		✗	✗
262		✗	✗	270		✗	✗
263		✗	✗	271		✗	✗
264		✗	✗	272		✗	✗

Figure I-2 (cont'd)

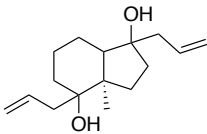
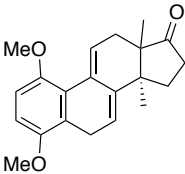
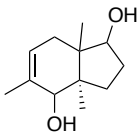
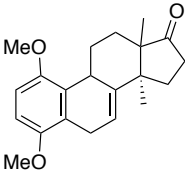
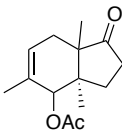
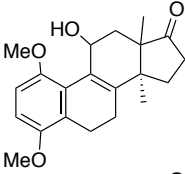
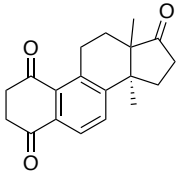
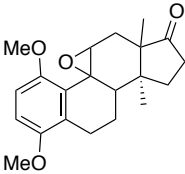
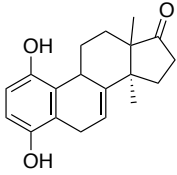
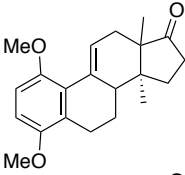
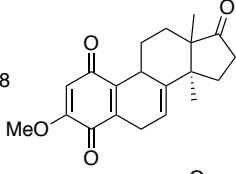
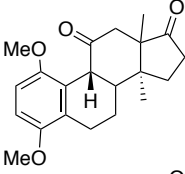
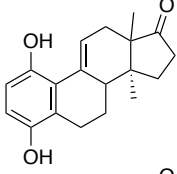
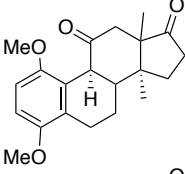
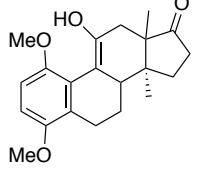
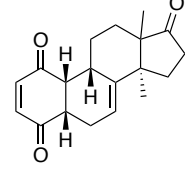
entry	compound	Gram (+)	Gram (–)	entry	compound	Gram (+)	Gram (–)
273		✗	✗	281		✗	✗
274		✗	✗	282		✗	✗
275		✗	✗	283		✗	✗
276		✗	✗	284		✗	✗
277		✗	✗	285		✗	✗
278		✗	✗	286		✗	✗
279		✗	✗	287		✗	✗
280		✗	✗	288		✓	✗

Figure I-2 (cont'd)

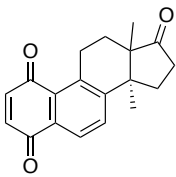


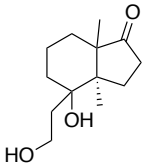


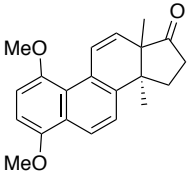


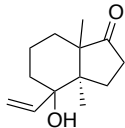


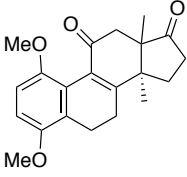


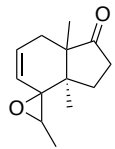


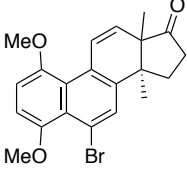


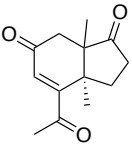


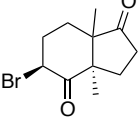


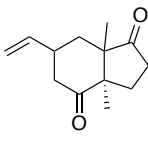


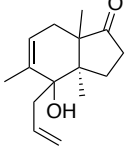


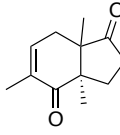


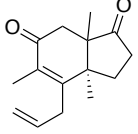


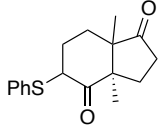


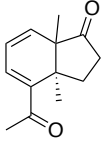


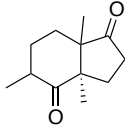


entry	compound	Gram (+)	Gram (-)	entry	compound	Gram (+)	Gram (-)
289				297			
290				298			
291				299			
292				300			
293				301			
294				302			
295				303			
296				304			

Figure I-2 (cont'd)

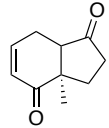
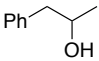
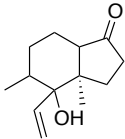
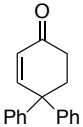
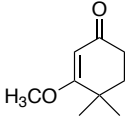
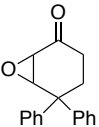
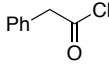
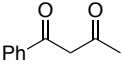
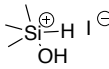
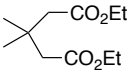
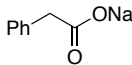
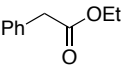
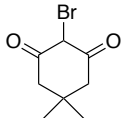
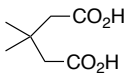
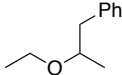
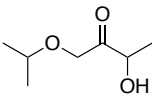
entry	compound	Gram (+)	Gram (–)	entry	compound	Gram (+)	Gram (–)
305		✗	✗	313		✗	✗
306		✗	✗	314		✗	✗
307		✗	✗	315		✗	✗
308		✗	✗	316		✗	✗
309		✗	✗	317		✗	✗
310		✗	✗	318		✗	✗
311		✗	✗	319		✗	✗
312		✗	✗	320		✗	✗

Figure I-2 (cont'd)

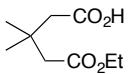
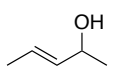
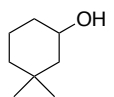
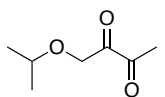
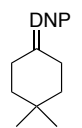
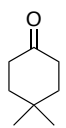
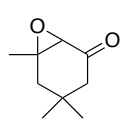
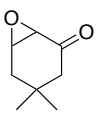
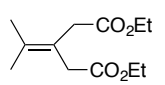
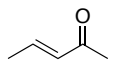
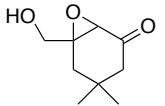
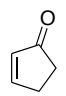
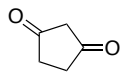
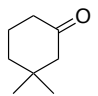
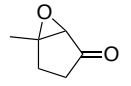
entry	compound	Gram (+)	Gram (-)	entry	compound	Gram (+)	Gram (-)
321		✗	✗	329		✗	✗
322		✗	✗	330		✗	✗
323		✗	✗	331	Formalin dimedone	✗	✗
324		✗	✗	332		✗	✗
325		✗	✗	333		✗	✗
326		✗	✗	334		✗	✗
327		✗	✗	335		✗	✗
328		✗	✗	336		✗	✗

Figure I-2 (cont'd)

entry	compound	Gram (+)	Gram (-)	entry	compound	Gram (+)	Gram (-)
337		✗	✗	345		✗	✗
338		✗	✗	346		✓	✗
339		✗	✗	347		✓	✗
340		✗	✗	348		✗	✗
341		✗	✗	349		✗	✗
342		✗	✗	350		✗	✗
343		✗	✗	351		✗	✗
344		✗	✗	352		✗	✗

Figure I-2 (cont'd)

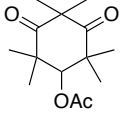
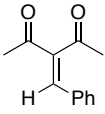
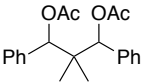
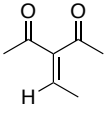
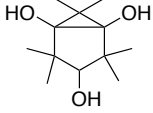
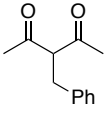
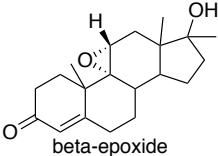
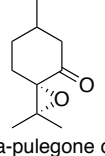
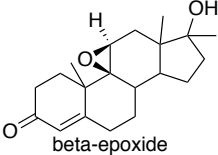
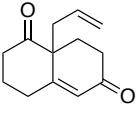
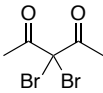
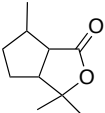
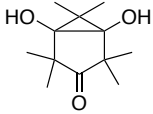
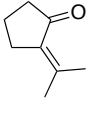
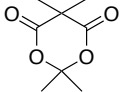
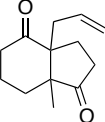
entry	compound	Gram (+)	Gram (–)	entry	compound	Gram (+)	Gram (–)
353		✗	✗	361		✗	✗
354		✗	✗	362		✗	✗
355		✗	✗	363		✗	✗
356	 beta-epoxide	✗	✗	364	 alpha-pulegone oxide	✗	✗
357	 beta-epoxide	✗	✗	365		✗	✗
358		✗	✗	366		✗	✗
359		✗	✗	367		✗	✗
360		✗	✗	368		✗	✗

Figure I-2 (cont'd)

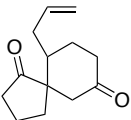
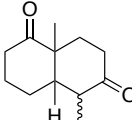
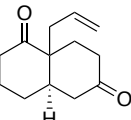
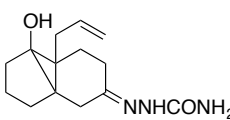
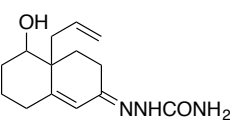
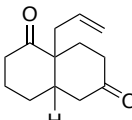
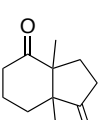
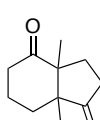
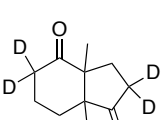
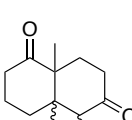
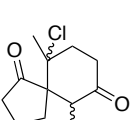
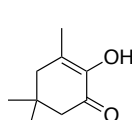
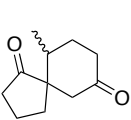
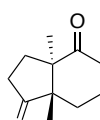
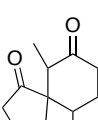
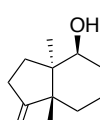
entry	compound	Gram (+)	Gram (-)	entry	compound	Gram (+)	Gram (-)
369		✗	✗	377		✗	✗
370		✗	✗	378		✗	✗
371		✗	✗	379		✗	✗
372		✗	✗	380		✗	✗
373		✗	✗	381		✗	✗
374		✗	✗	382		✗	✗
375		✗	✗	383		✗	✗
376		✗	✗	384		✗	✗

Figure I-2 (cont'd)

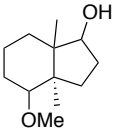
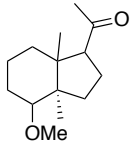
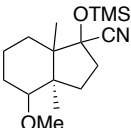
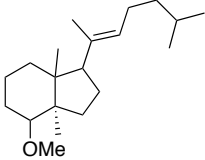
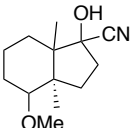
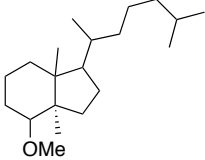
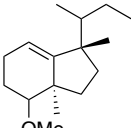
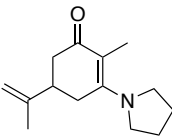
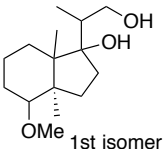
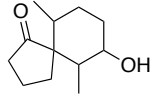
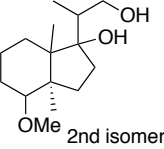
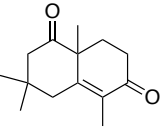
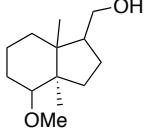
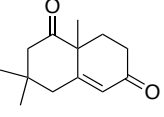
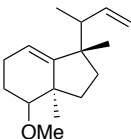
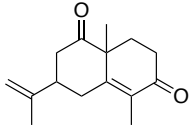
entry	compound	Gram (+)	Gram (–)	entry	compound	Gram (+)	Gram (–)
385		✗	✗	393		✗	✗
386		✗	✗	394		✗	✗
387		✗	✗	395		✗	✗
388		✗	✗	396		✗	✗
389	 1st isomer	✗	✗	397		✗	✗
390	 2nd isomer	✗	✗	398		✗	✗
391		✗	✗	399		✗	✗
392		✗	✗	400		✗	✗

Figure I-2 (cont'd)

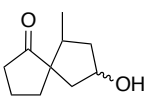
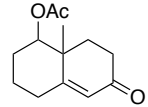
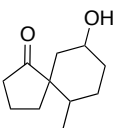
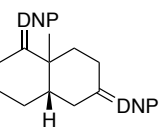
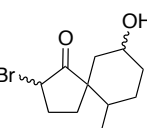
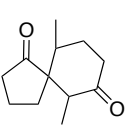
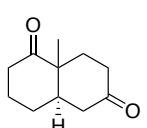
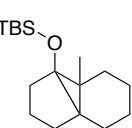
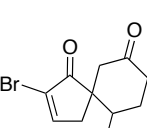
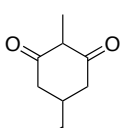
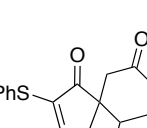
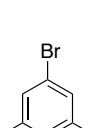
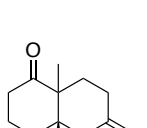
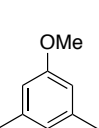
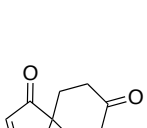
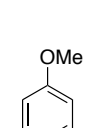
entry	compound	Gram (+)	Gram (-)	entry	compound	Gram (+)	Gram (-)
401		✗	✗	409		✗	✗
402		✗	✗	410		✗	✗
403		✗	✗	411		✗	✗
404		✗	✗	412		✗	✗
405		✗	✗	413		✗	✗
406		✗	✗	414		✗	✗
407		✗	✗	415		✗	✗
408		✗	✗	416		✗	✗

Figure I-2 (cont'd)

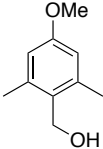
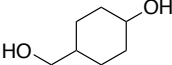
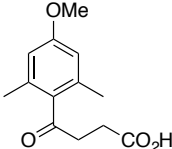
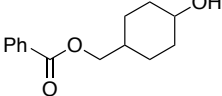
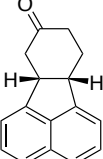
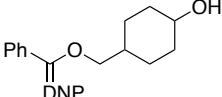
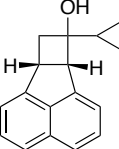
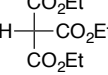
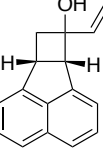
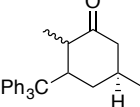
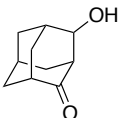
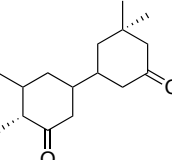
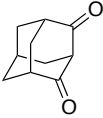
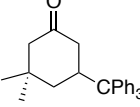
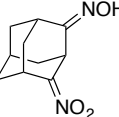
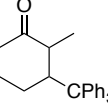
entry	compound	Gram (+)	Gram (-)	entry	compound	Gram (+)	Gram (-)
417		✗	✗	425		✗	✗
418		✗	✗	426		✗	✗
419		✗	✗	427		✗	✗
420		✓	✗	428		✗	✗
421		✓	✗	429		✗	✗
422		✗	✗	430		✗	✗
423		✗	✗	431		✗	✗
424		✗	✗	432		✗	✗

Figure I-2 (cont'd)

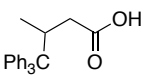


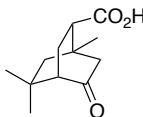


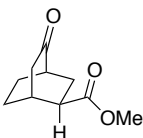


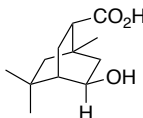


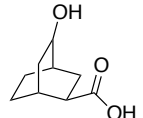


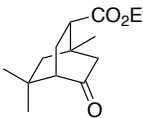


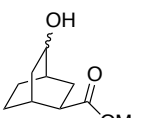


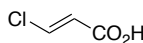


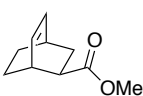


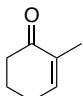


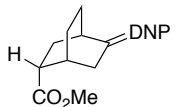


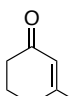


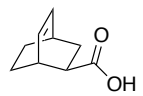


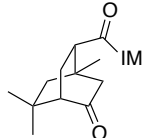


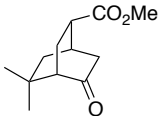


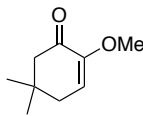


entry	compound	Gram (+)	Gram (–)	entry	compound	Gram (+)	Gram (–)
433				441			
434				442			
435				443			
436				444			
437				445			
438				446			
439				447			
440				448			

Figure I-2 (cont'd)

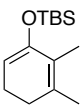
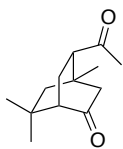
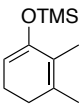
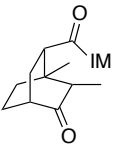
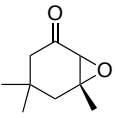
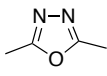
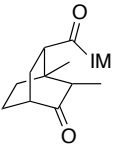
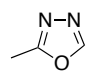
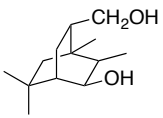
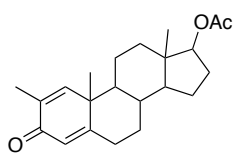
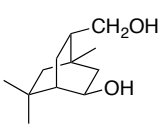
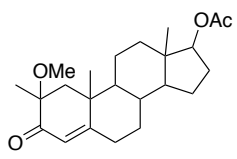
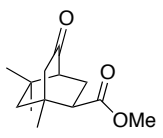
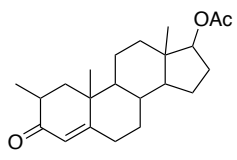
entry	compound	Gram (+)	Gram (-)	entry	compound	Gram (+)	Gram (-)
449		✗	✗	457		✗	✗
450		✗	✗	458	<chem>CH3CONHNH2</chem>	✗	✗
451		✗	✗	459	<chem>CH3CONHN=CHOEt</chem>	✗	✗
452		✗	✗	460		✗	✗
453		✗	✗	461		✗	✗
454		✗	✗	462		✗	✗
455		✗	✗	463		✗	✗
456		✗	✗	464		✗	✗

Figure I-2 (cont'd)

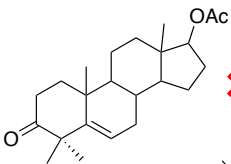
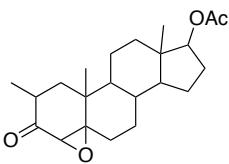
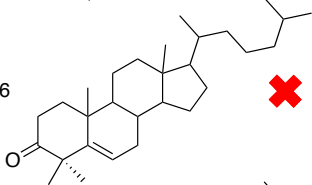
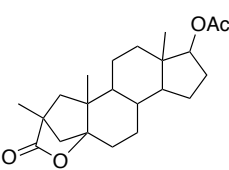
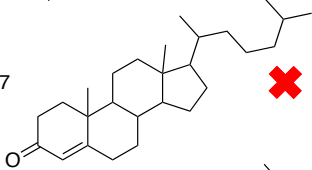
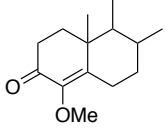
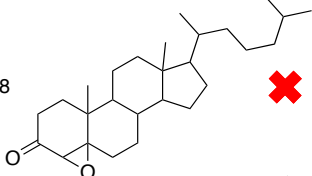
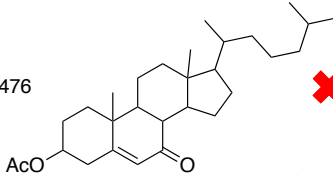
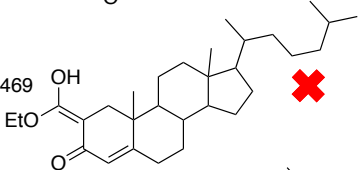
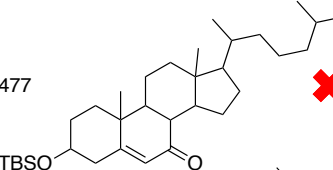
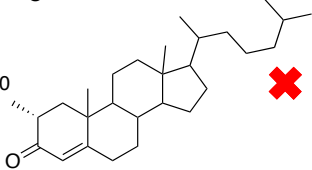
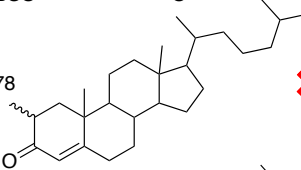
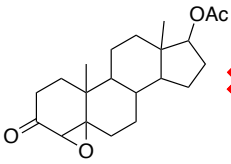
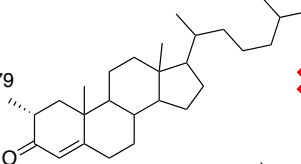
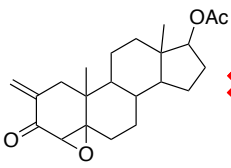
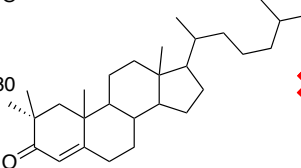
entry	compound	Gram (+)	Gram (-)	entry	compound	Gram (+)	Gram (-)
465		✗	✗	473		✗	✗
466		✗	✗	474		✗	✗
467		✗	✗	475		✗	✗
468		✗	✗	476		✗	✗
469		✗	✗	477		✗	✗
470		✗	✗	478		✗	✗
471		✗	✗	479		✗	✗
472		✗	✗	480		✗	✗

Figure I-2 (cont'd)

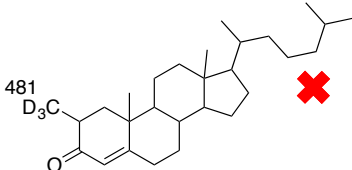
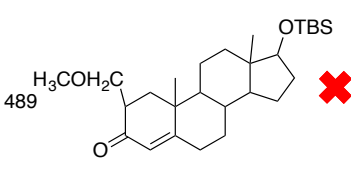
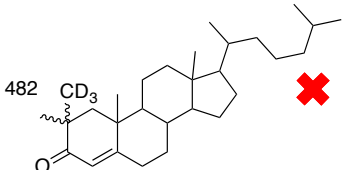
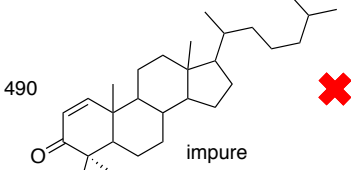
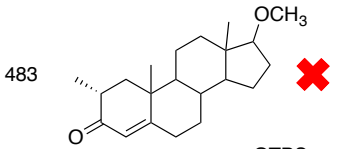
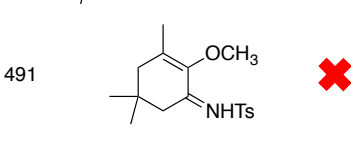
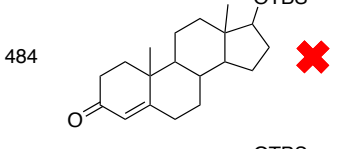
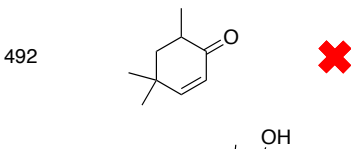
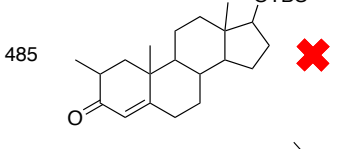
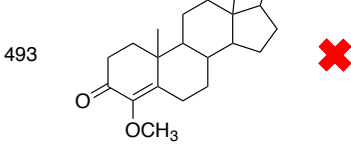
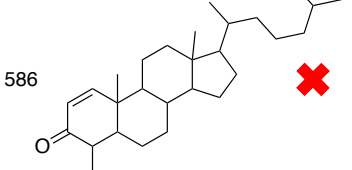
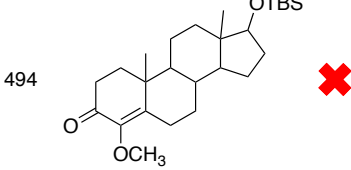
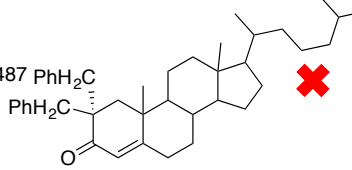
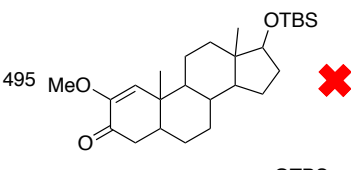
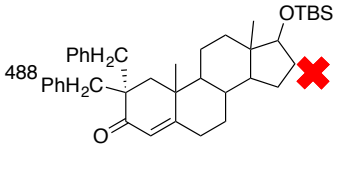
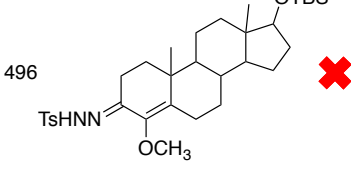
entry	compound	Gram (+)	Gram (-)	entry	compound	Gram (+)	Gram (-)
481		✗	✗	489		✗	✗
482		✗	✗	490		✗	✗
483		✗	✗	491		✗	✗
484		✗	✗	492		✗	✗
485		✗	✗	493		✗	✗
586		✗	✗	494		✗	✗
487		✗	✗	495		✗	✗
488		✗	✗	496		✗	✗

Figure I-2 (cont'd)

entry	compound	Gram (+)	Gram (-)	entry	compound	Gram (+)	Gram (-)
497		✗	✗	505		✗	✗
498		✗	✗	506		✗	✗
499		✗	✗	507		✗	✗
500		✗	✗	508		✗	✗
501		✗	✗	509		✗	✗
502		✗	✗	510		✗	✗
503		✗	✗	511		✗	✗
504		✗	✗	512		✗	✗

Figure I-2 (cont'd)

entry	compound	Gram (+)	Gram (-)	entry	compound	Gram (+)	Gram (-)
513		✗	✗	521		✗	✗
514		✗	✗	522		✗	✗
515		✗	✗	523		✗	✗
516		✗	✗	524		✗	✗
517		✗	✗	525		✗	✗
518		✗	✗	526		✗	✗
519		✗	✗	527		✗	✗
520		✗	✗	528		✗	✗

Figure I-2 (cont'd)

entry	compound	Gram (+)	Gram (-)	entry	compound	Gram (+)	Gram (-)
529		✗	✗	537		✗	✗
530		✗	✗	538		✗	✗
531		✗	✗	539		✗	✗
532		✗	✗	540		✗	✗
533		✗	✗	541		✗	✗
534		✗	✗	542		✗	✗
535		✗	✗	543		✗	✗
536		✗	✗	544		✗	✗

Figure I-2 (cont'd)

entry	compound	Gram (+)	Gram (-)	entry	compound	Gram (+)	Gram (-)
545		✗	✗	553		✗	✗
546		✗	✗	554		✗	✗
547		✗	✗	555		✗	✗
548		✗	✗	556		✗	✗
549		✗	✗	557		✗	✗
550		✗	✗	558		✗	✗
551		✗	✗	559		✗	✗
552		✗	✗	560		✗	✗

Figure I-2 (cont'd)

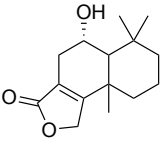
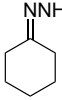
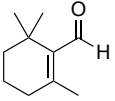
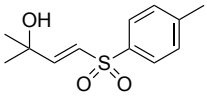
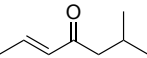
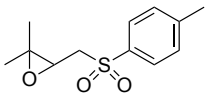
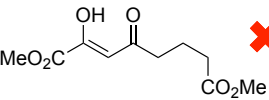
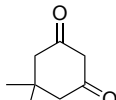
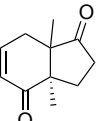
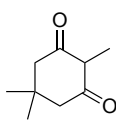
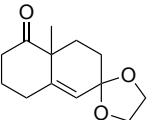
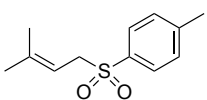
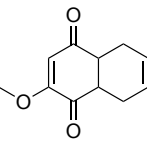
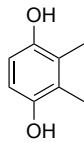
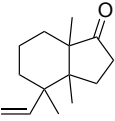
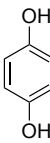
entry	compound	Gram (+)	Gram (-)	entry	compound	Gram (+)	Gram (-)
561		✗	✗	569		✗	✗
562		✗	✗	570		✗	✗
563		✗	✗	571		✗	✗
564		✗	✗	572		✗	✗
565		✗	✗	573		✗	✗
566		✗	✗	574		✗	✗
567		✗	✗	575		✗	✗
568		✗	✗	576		✗	✗

Figure I-2 (cont'd)

entry	compound	Gram (+)	Gram (–)	entry	compound	Gram (+)	Gram (–)
577		✗	✗	585		✗	✗
578		✗	✗	586		✗	✗
579		✗	✗	587		✗	✗
580		✗	✗	588		✗	✗
581		✗	✗	589		✗	✗
582		✗	✗	590		✗	✗
583		✗	✗	591		✗	✗
584		✗	✗	592		✗	✗

Figure I-2 (cont'd)

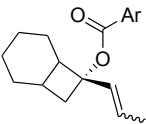
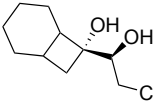
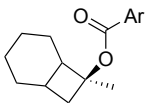
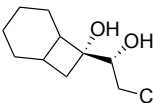
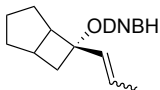
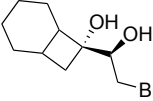
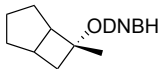
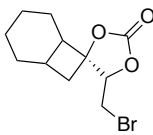
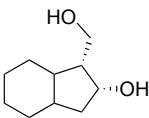
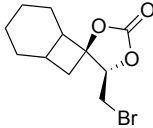
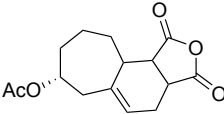
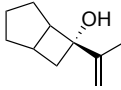
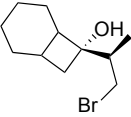
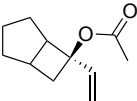
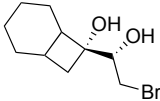
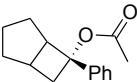
entry	compound	Gram (+)	Gram (-)	entry	compound	Gram (+)	Gram (-)
593		✗	✗	601		✗	✗
594		✗	✗	602		✗	✗
595		✗	✗	603		✗	✗
596		✗	✗	604		✗	✗
597		✗	✗	605		✗	✗
598		✗	✗	606		✗	✗
599		✗	✗	607		✗	✗
600		✗	✗	608		✗	✗

Figure I-2 (cont'd)

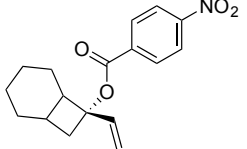
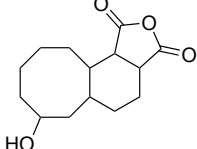
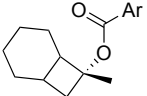
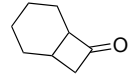
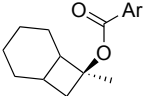
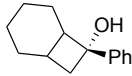
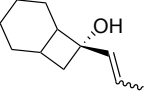
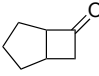
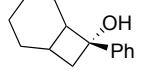
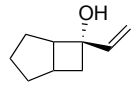
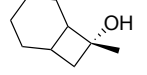
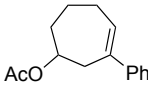
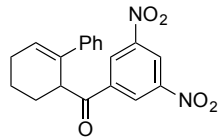
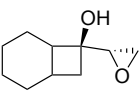
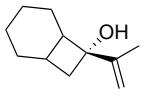
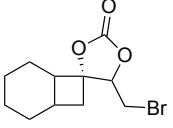
entry	compound	Gram (+)	Gram (-)	entry	compound	Gram (+)	Gram (-)
609		✗	✗	617		✗	✗
610		✗	✗	618		✗	✗
611		✗	✗	619		✗	✗
612		✗	✗	620		✗	✗
613		✗	✗	621		✗	✗
614		✗	✗	622		✗	✗
615		✗	✗	623		✗	✗
616		✗	✗	624		✗	✗

Figure I-2 (cont'd)

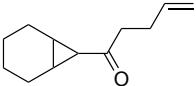
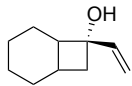
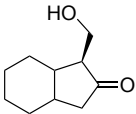
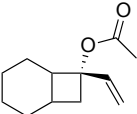
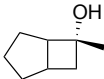
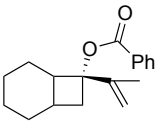
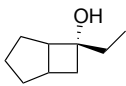
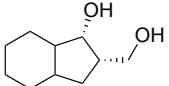
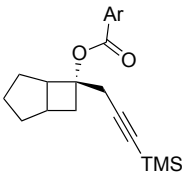
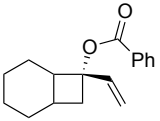
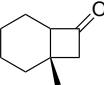
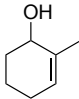
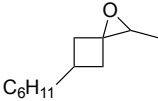
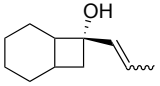
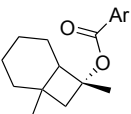
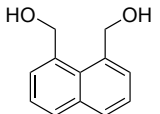
entry	compound	Gram (+)	Gram (-)	entry	compound	Gram (+)	Gram (-)
625		✗	✗	633		✗	✗
626		✗	✗	634		✗	✗
627		✗	✗	635		✗	✗
628		✗	✗	636		✗	✗
629		✗	✗	637		✗	✗
630		✗	✗	638		✗	✗
631		✗	✗	639		✗	✗
632		✗	✗	640		✗	✗

Figure I-2 (cont'd)

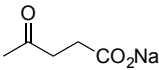
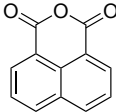
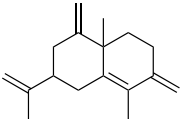
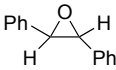
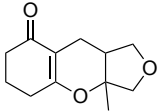
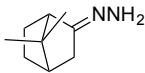
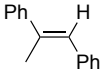
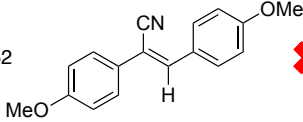
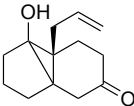
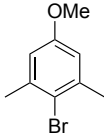
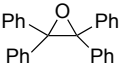
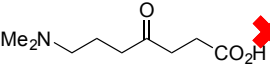
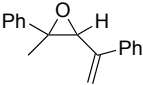

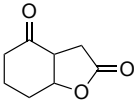
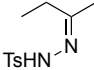
entry	compound	Gram (+)	Gram (-)	entry	compound	Gram (+)	Gram (-)
641		✗	✗	649		✗	✗
642		✗	✗	650		✗	✗
643		✗	✗	651		✗	✗
644		✗	✗	652		✗	✗
645		✗	✗	653		✗	✗
646		✗	✗	654		✗	✗
647		✗	✗	655		✗	✗
648		✗	✗	656		✗	✗

Figure I-2 (cont'd)

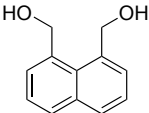
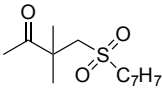
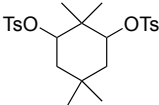
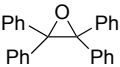
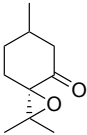
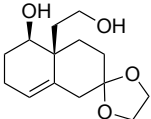
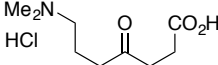
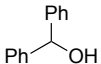
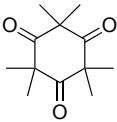
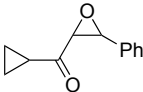
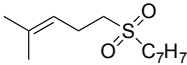
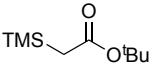
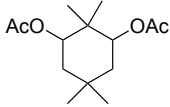
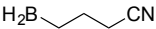
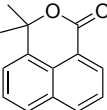
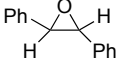
entry	compound	Gram (+)	Gram (-)	entry	compound	Gram (+)	Gram (-)
657		✗	✗	665		✗	✗
658		✗	✗	666		✗	✗
659		✗	✗	667		✗	✗
660		✗	✗	668		✗	✗
661		✗	✗	669		✗	✗
662		✗	✗	670		✗	✗
663		✗	✗	671		✗	✗
664		✗	✗	672		✗	✗

Figure I-2 (cont'd)

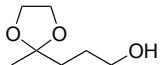
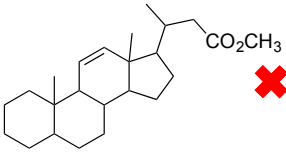
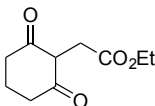
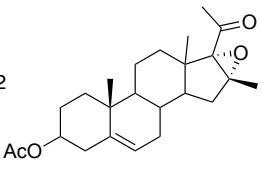
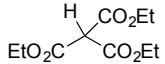
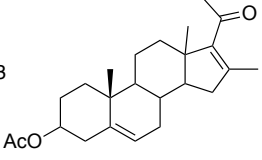
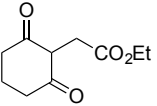
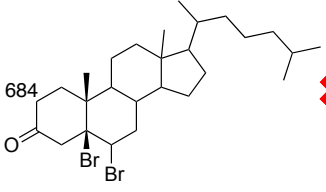
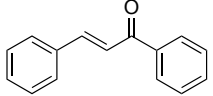
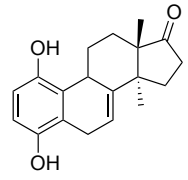
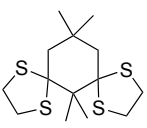
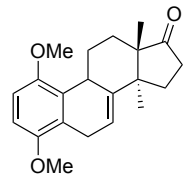
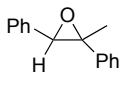
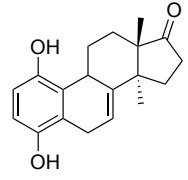
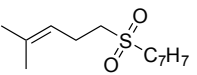
entry	compound	Gram (+)	Gram (-)	entry	compound	Gram (+)	Gram (-)
673		✗	✗	681		✗	✗
674		✗	✗	682		✗	✗
675		✗	✗	683		✗	✗
676		✗	✗	684		✗	✗
677		✗	✗	685		✓	✗
678		✗	✗	686		✗	✗
679		✗	✗	687		✓	✗
780		✗	✗				

Figure I-2 (cont'd)

entry	compound	Gram (+)	Gram (-)	entry	compound	Gram (+)	Gram (-)
688		✓	✗	696		✗	✗
689		✓	✗	697		✗	✗
691		✗	✗	698		✗	✗
692		✗	✗	699		✗	✗
693		✓	✗	700		✗	✗
694		✗	✗	701		✗	✗
695		✗	✗	702		✗	✗
				703		✗	✗

Figure I-2 (cont'd)

entry	compound	Gram (+)	Gram (-)	entry	compound	Gram (+)	Gram (-)
704		✗	✗	712		✗	✗
705		✗	✗	713		✗	✗
706		✗	✗	714		✗	✗
707		✗	✗	715		✗	✗
708		✗	✗	716		✗	✗
709		✗	✗	717		✗	✗
710		✗	✗	718		✗	✗
711		✗	✗	719		✗	✗

Figure I-2 (cont'd)

entry	compound	Gram (+)	Gram (-)	entry	compound	Gram (+)	Gram (-)
720		✗	✗	728		✗	✗
721		✗	✗	729		✗	✗
722		✗	✗	730		✗	✗
723		✗	✗	731		✗	✗
724		✗	✗	732		✗	✗
725		✗	✗	733		✗	✗
726		✗	✗	734		✗	✗
727		✗	✗	735		✗	✗

Figure I-2 (cont'd)

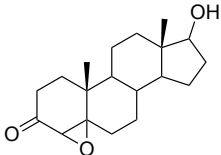
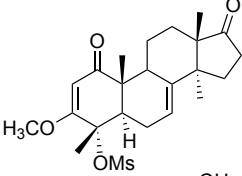
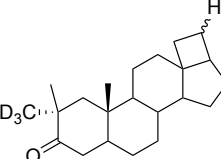
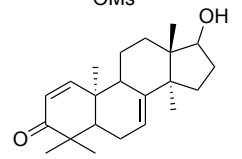
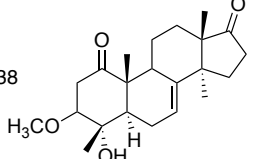
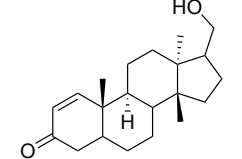
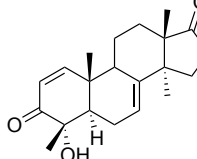
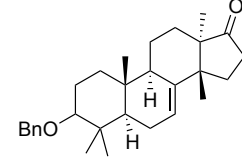
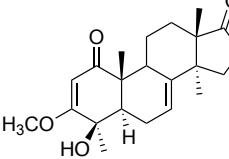
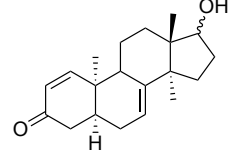
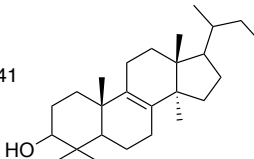
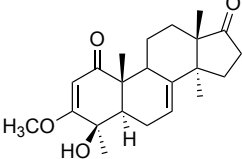
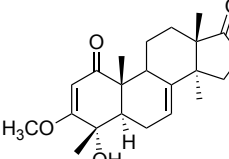
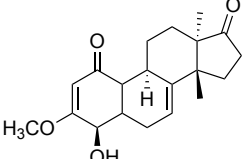
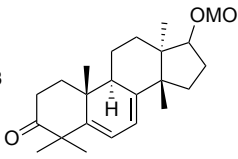
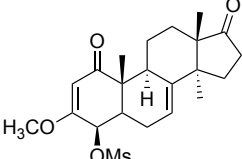
entry	compound	Gram (+)	Gram (-)	entry	compound	Gram (+)	Gram (-)
736		✗	✗	744		✗	✗
737		✗	✗	745		✗	✗
738		✗	✗	746		✗	✗
739		✗	✗	747		✗	✗
740		✗	✗	748		✗	✗
741		✗	✗	749		✗	✗
742		✗	✗	750		✗	✗
743		✗	✗	751		✗	✗

Figure I-2 (cont'd)

entry	compound	Gram (+)	Gram (-)	entry	compound	Gram (+)	Gram (-)
752		✗	✗	760		✗	✗
735		✗	✗	761		✗	✗
754		✗	✗	762		✗	✗
755		✗	✗	763		✗	✗
756		✗	✗	764		✗	✗
757		✗	✗	765		✗	✗
758		✗	✗	766		✗	✗
759		✗	✗	767		✗	✗

Figure I-2 (cont'd)

entry	compound	Gram (+)	Gram (-)	entry	compound	Gram (+)	Gram (-)
768		✗	✗	776		✗	✗
769		✗	✗	777		✗	✗
770		✗	✗	778		✗	✗
771		✗	✗	779		✗	✗
772		✗	✗	780		✗	✗
773		✗	✗	781		✗	✗
774		✗	✗	782		✗	✗
775		✗	✗	783		✗	✗

Figure I-2 (cont'd)

entry	compound	Gram (+)	Gram (-)	entry	compound	Gram (+)	Gram (-)
784		✗	✗	792		✗	✗
785		✗	✗	793		✗	✗
786		✗	✗	794		✗	✗
787		✗	✗	795		✗	✗
788		✗	✗	796		✗	✗
789		✗	✗	797		✗	✗
790		✗	✗	798		✗	✗
791		✗	✗	799		✗	✗

Figure I-2 (cont'd)

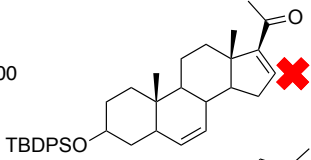
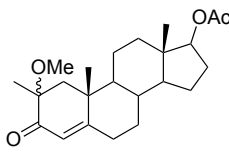
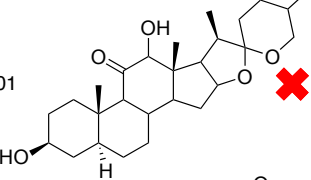
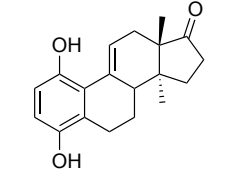
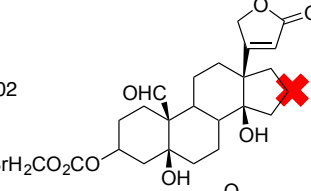
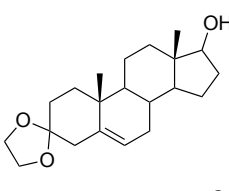
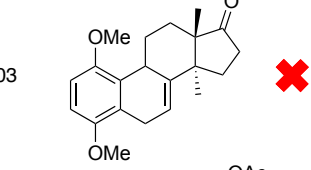
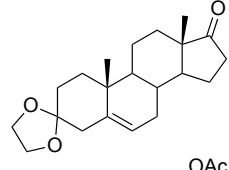
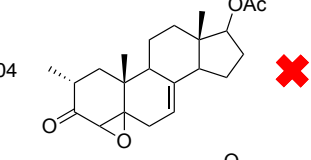
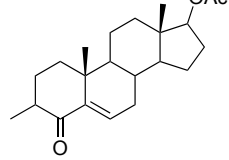
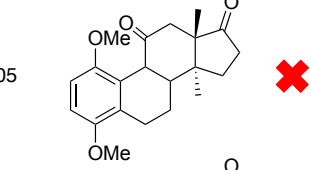
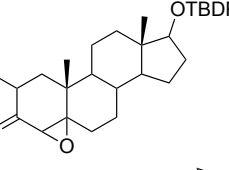
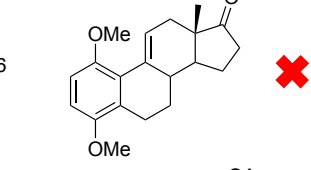
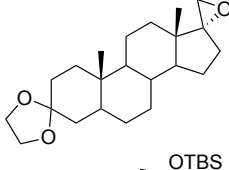
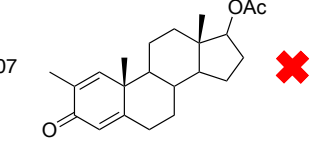
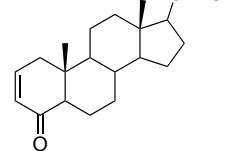
entry	compound	Gram (+)	Gram (-)	entry	compound	Gram (+)	Gram (-)
800		✗	✗	808		✗	✗
801		✗	✗	809		✓	✗
802		✗	✗	810		✗	✗
803		✗	✗	811		✗	✗
804		✗	✗	812		✗	✗
805		✗	✗	813		✗	✗
806		✗	✗	814		✗	✗
807		✗	✗	815		✗	✗

Figure I-2 (cont'd)

entry	compound	Gram (+)	Gram (-)	entry	compound	Gram (+)	Gram (-)
816		✗	✗	824		✗	✗
817		✗	✗	825		✗	✗
818		✗	✗	826		✗	✗
819		✗	✗	827		✗	✗
820		✗	✗	828		✗	✗
821		✗	✗	829		✗	✗
822		✓	✗	830		✗	✗
823		✗	✗	831		✗	✗

Figure I-2 (cont'd)

entry	compound	Gram (+)	Gram (-)	entry	compound	Gram (+)	Gram (-)
832		✗	✗	840	<chem>CC(=O)c1ccccc1</chem>	✗	✗
833		✗	✗	841	<chem>CC(O)(c1ccccc1)C(=O)c2ccccc2</chem>	✗	✗
834		✗	✗	842	<chem>CC(O)(c1ccccc1)C(=O)c2ccccc2</chem>	✗	✗
835		✗	✗	843	<chem>CC(=O)c1ccccc1</chem>	✗	✗
836		✗	✗	844	<chem>c1ccccc1C2(Cc3ccccc3)OC2c4ccccc4</chem>	✗	✗
837		✗	✗	845		✗	✗
838	<chem>CC(=O)c1ccccc1</chem>	✗	✗	846		✗	✗
839	<chem>CC(O)(c1ccccc1)C(=O)c2ccccc2</chem>	✓	✗	847		✗	✗

Figure I-2 (cont'd)

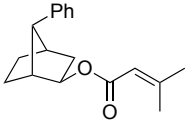
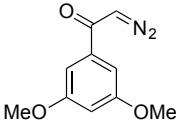
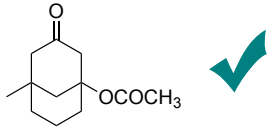
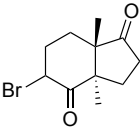
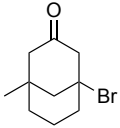
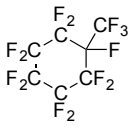
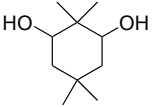
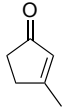
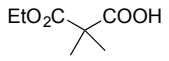
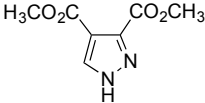
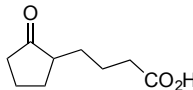
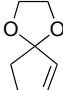
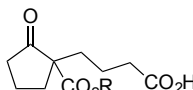
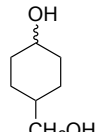
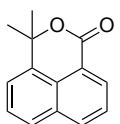
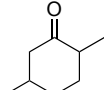
entry	compound	Gram (+)	Gram (–)	entry	compound	Gram (+)	Gram (–)
848		✗	✗	856		✗	✗
849		✓	✗	857		✗	✗
850		✗	✗	508		✗	✗
851		✗	✗	859		✗	✗
852		✗	✗	860		✗	✗
853		✗	✗	861		✗	✗
854		✗	✗	862		✗	✗
855		✗	✗	863		✗	✗

Figure I-2 (cont'd)

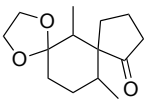
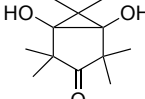
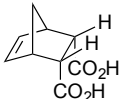
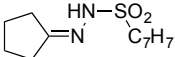
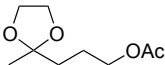
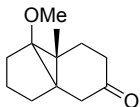
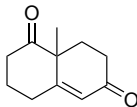
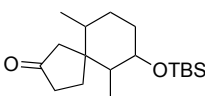
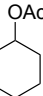
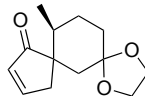
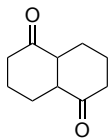
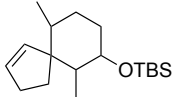
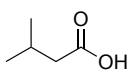
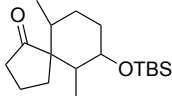
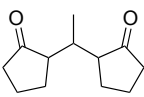
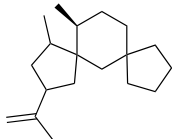
entry	compound	Gram (+)	Gram (-)	entry	compound	Gram (+)	Gram (-)
864		✗	✗	872		✗	✗
865		✗	✗	873		✗	✗
866		✗	✗	874		✗	✗
867		✗	✗	875		✗	✗
868		✗	✗	876		✗	✗
869		✗	✗	877		✗	✗
870		✗	✗	878		✗	✗
871		✗	✗	879		✗	✗

Figure I-2 (cont'd)

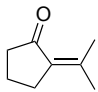
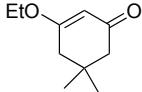
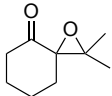
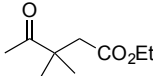

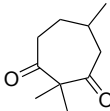
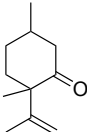
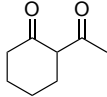
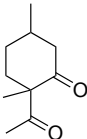
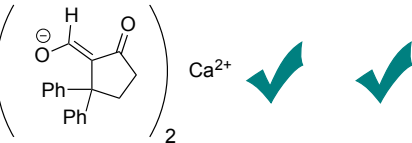
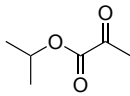
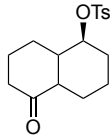
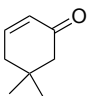
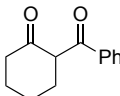
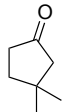
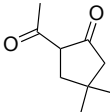
entry	compound	Gram (+)	Gram (-)	entry	compound	Gram (+)	Gram (-)
880		✗	✗	888		✗	✗
881		✗	✗	889		✗	✗
882		✗	✗	890		✗	✗
883		✗	✗	891		✗	✗
884		✗	✗	892		✓	✓
885		✗	✗	893		✗	✗
886		✗	✗	894		✗	✗
887		✗	✗	895		✗	✗

Figure I-2 (cont'd)

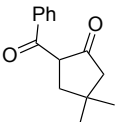


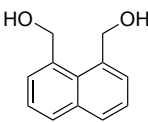


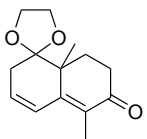


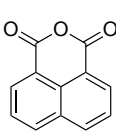


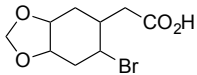


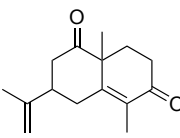


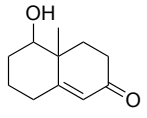


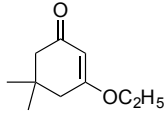


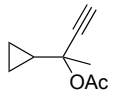


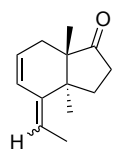


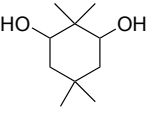


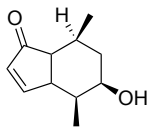


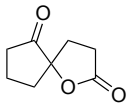


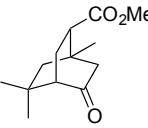


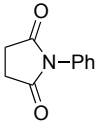


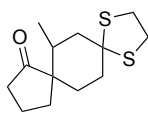


entry	compound	Gram (+)	Gram (-)	entry	compound	Gram (+)	Gram (-)
896				904			
897				905			
898				906			
899				907			
900				908			
901				909			
902				910			
903				911			

Figure I-2 (cont'd)

entry	compound	Gram (+)	Gram (-)	entry	compound	Gram (+)	Gram (-)
912		✓	✗	920		✗	✗
913		✗	✗	921		✗	✗
914		✗	✗	922		✗	✗
915		✗	✗	923		✗	✗
916		✓	✗	924		✓	✓
917		✗	✗	925		✗	✗
918		✗	✗	926		✗	✗
919		✗	✗	927		✓	✓

Figure I-2 (cont'd)

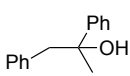


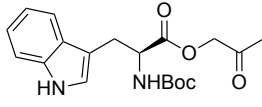


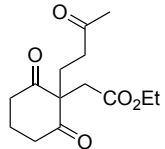


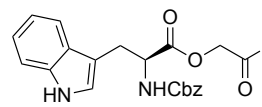


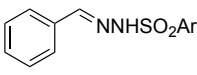


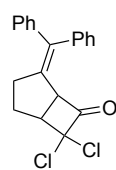


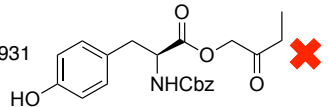


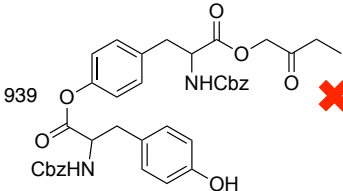


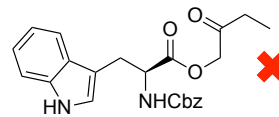


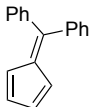


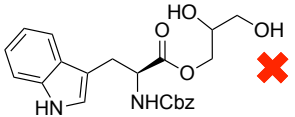


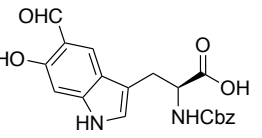


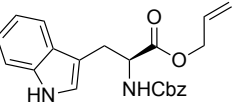


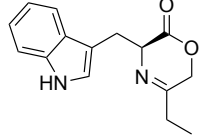


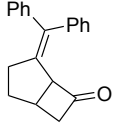


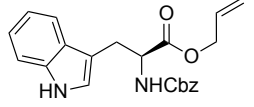


entry	compound	Gram (+)	Gram (-)	entry	compound	Gram (+)	Gram (-)
928				936			
929				937			
930				938			
931				939			
932				940			
933				941			
934				942			
935				943			

Figure I-2 (cont'd)

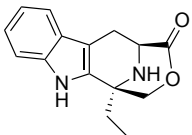
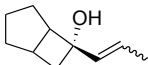
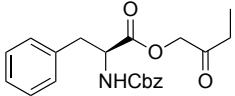
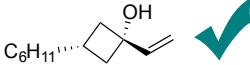
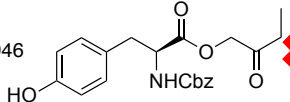

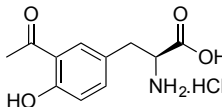
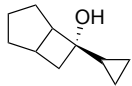
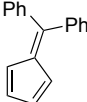
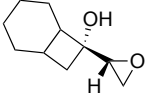
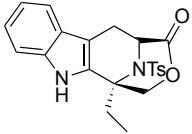
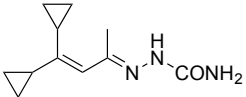
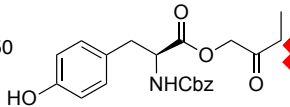
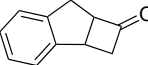
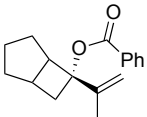
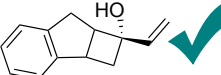
entry	compound	Gram (+)	Gram (-)	entry	compound	Gram (+)	Gram (-)
944		✗	✗	952		✗	✗
945		✗	✗	953		✓	✗
946		✗	✗	954		✗	✗
947		✗	✗	955		✗	✗
948		✗	✗	956		✗	✗
949		✗	✗	957		✗	✗
950		✗	✗	958		✗	✗
951		✗	✗	959		✓	✗

Figure I-2 (cont'd)

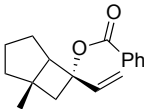
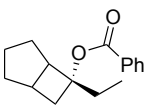
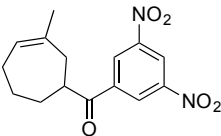
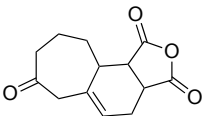
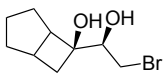
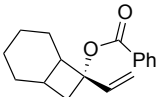
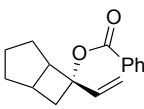
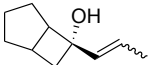
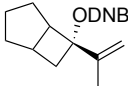
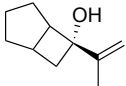
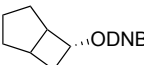
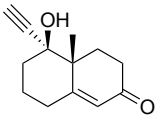
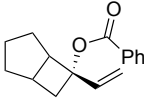
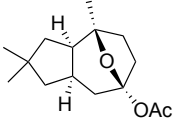
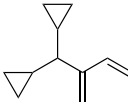
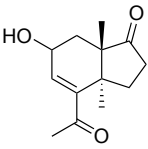
entry	compound	Gram (+)	Gram (-)	entry	compound	Gram (+)	Gram (-)
960		✗	✗	968		✗	✗
961		✗	✗	969		✗	✗
962		✗	✗	970		✗	✗
963		✗	✗	971		✗	✗
964		✗	✗	972		✗	✗
965		✗	✗	973		✓	✗
966		✗	✗	974		✗	✗
967		✗	✗	975		✗	✗

Figure I-2 (cont'd)

entry	compound	Gram (+)	Gram (-)	entry	compound	Gram (+)	Gram (-)
976		✗	✗	984		✗	✗
977		✗	✗	985		✗	✗
978		✗	✗	986		✗	✗
979		✗	✗	987		✗	✗
980		✗	✗	988		✗	✗
981		✗	✗	989		✗	✗
982		✗	✗	990		✗	✗
983		✗	✗	991		✗	✗

Figure I-2 (cont'd)

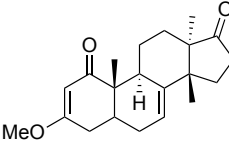
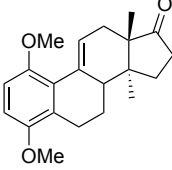
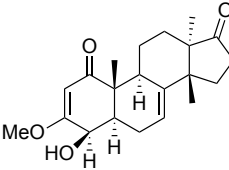
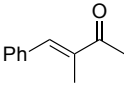
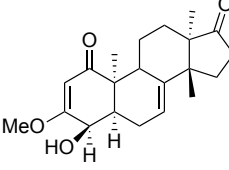
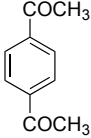
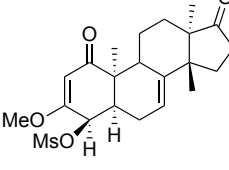
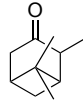
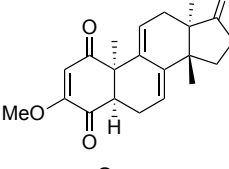
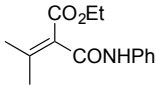
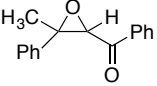
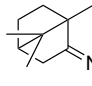
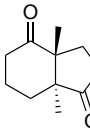
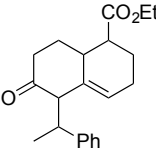
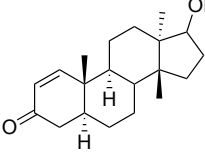
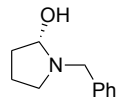
entry	compound	Gram (+)	Gram (-)	entry	compound	Gram (+)	Gram (-)
992		✗	✗	1000		✗	✗
993		✗	✗	1001		✗	✗
994		✗	✗	1002		✗	✗
995		✗	✗	1003		✗	✗
996		✗	✗	1004		✗	✗
997		✗	✗	1005		✗	✗
998		✗	✗	1006		✗	✗
999		✗	✗	1007		✗	✗

Figure I-2 (cont'd)

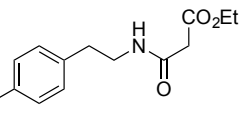
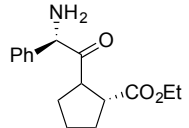
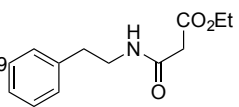
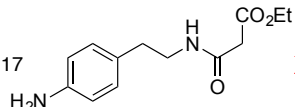
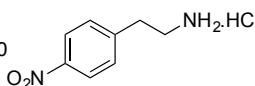
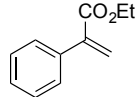
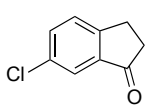
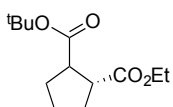
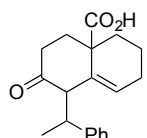
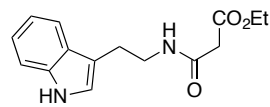
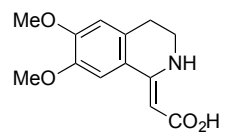
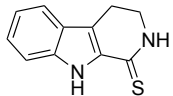
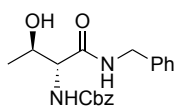
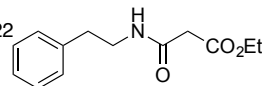
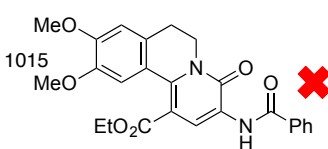
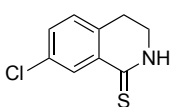
entry	compound	Gram (+)	Gram (-)	entry	compound	Gram (+)	Gram (-)
1008		✗	✗	1016		✗	✗
1009		✗	✗	1017		✗	✗
1010		✗	✗	1018		✗	✗
1011		✗	✗	1019		✗	✗
1012		✗	✗	1020		✗	✗
1013		✗	✗	1021		✗	✗
1014		✗	✗	1022		✗	✗
1015		✗	✗	1023		✗	✗

Figure I-2 (cont'd)

entry	compound	Gram (+)	Gram (-)
1024		✗	✗
1025		✗	✗
1026		✗	✗
1027		✗	✗

Amongst the biologically active molecules, we noticed a group of steroidal compounds that were active against Gram-positive bacteria. While it is not common, steroidal compounds have been isolated that have shown antibiotic activity.¹³ Squalamine, an aminosterol antibiotic shown in Figure I-3, was isolated from the stomach of the dogfish shark *Squalus acanthias*. This steroid exhibits significant antibacterial activity in both Gram-positive bacteria, such as the *Staphylococci* strains (1-2 µg/mL for both *aureus* and *faecalis*), and Gram-negative bacteria, such as *Eschericia coli*, *Pseudomonas aeruginosa*, and *Serratia marcescens* (1-2 µg/mL, 4-8 µg/mL, and >125 µg/mL, respectively) as shown in Table I-1. This is notable when compared to ampicillin, a known and therapeutically utilized broad-spectrum antibacterial that interestingly exhibits comparable activity to the natural steroid with *S. aureus* at <1 µg/mL, *S. faecalis* at <0.25 µg/mL, *E. coli* at 2.4 µg/mL, *P. aeruginosa* at 62-125 µg/mL, and *S. marcescens* at 4-62 µg/mL.

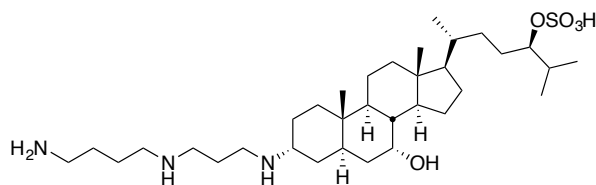
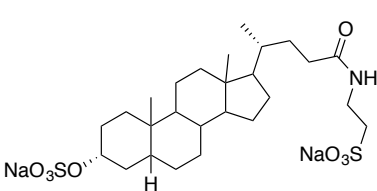


Figure I-3: Squalamine, an aminosterol isolated from the stomach of the dogshark *Squalus acanthias*.

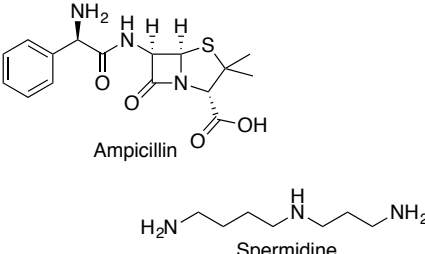
In order to highlight the importance of the specific combination that makes up squalamine, tauroolithocholic acid 3-sulfate, a bile acid salt, and spermidine, a

polyamine found in living tissue that has various metabolic functions, were both tested and demonstrated no activity at concentrations less than 500 µg/mL. Individually, neither compound is an effective antibacterial. It should be noted, however, that bile acids have been found to exhibit some protection against bacteria.^{14 15}

Squalamine was found to be more active against bacterial strains than magainin-II, a cationic peptide antibiotic. For example, where squalamine exhibited a 1-2 µg/mL minimum inhibitory concentration with respect to *E. coli*, magainin-II required 31-62 µg/mL. This trend spanned all evaluated strains of bacteria and the tested fungus and protozoa. Cationic peptide antibiotics (CPAs) are a class of peptide that adopt α -helical conformations or β -sheet conformations and subsequently, exhibit facially amphiphilic secondary structure that has been



Tauroolithocholic acid 3-sulfate



Ampicillin

Spermidine

Antimicrobial activity (MIC), µg/mL					
Sample	<i>E. coli</i>	<i>Pseudomonas aeruginosa</i>	<i>Staphylococcus aureus</i>	<i>Staphylococcus faecalis</i>	<i>Serratia marcescens</i>
Ampicillin	2-4	62-125	<1	<0.25	4-62
Squalamine	1-2	4-8	1-2	1-2	>125
Tauroolithocholic acid 3-sulfate	>500	>500	>500	>500	>500
Spermidine	>500	>500	>500	250-500	>500
Magainin-II amide	31-62	31-62	>250	125-250	>250

MIC = Minimum Inhibitory Concentration

Table I-1: Antimicrobial activity of Squalamine and comparable molecules.

found to have potent antibacterial properties via two models that exist to represent the modes of action: (1) In the “carpet model”, the amphiphilic peptides adhere to the negatively charged bacterial membrane and remove portions of the membrane once they’ve reached a high enough concentration, compromising the membrane. (2) In the “barrel-and-stave model”, the cationic peptides reach into the anionic cell membrane like the staves of a barrel, creating stable pores.¹⁶

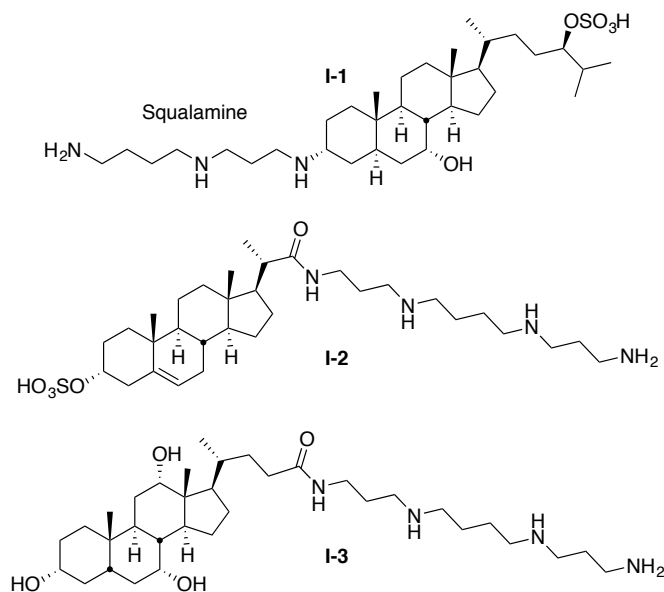


Figure I-4: Squalamine and select squalamine mimics.

Antibacterial steroids have also been the subject of synthesis.^{17 18} Savage and coworkers synthesized cationic steroid antibiotics (CSAs) based on the rigid and predictable structure of steroids and the overall amphiphilic nature of the previously mentioned CPAs. CSAs have been classed into two categories: (1) Squalamine and the squalamine mimics synthesized and tested by Regen and

coworkers^{19 20} featured in Figure I-4 and (2) polymyxin mimics. Polymyxins (shown in Figure I-5A) are cyclic CPAs known for their ability to rupture the outer and inner membranes of Gram-negative bacteria.²¹ Similarly, polymyxin mimics were found to be selective for bacterial cells, exhibiting a bacteriocidal propensity not mirrored in its higher hemolytic activity. For example, compound **I-5c** had a minimum inhibitory concentration of 3.0 µg/mL with *Streptococcus pyogenes* with a minimum hemolytic concentration of greater than 200 µg/mL (Figure I-5B).

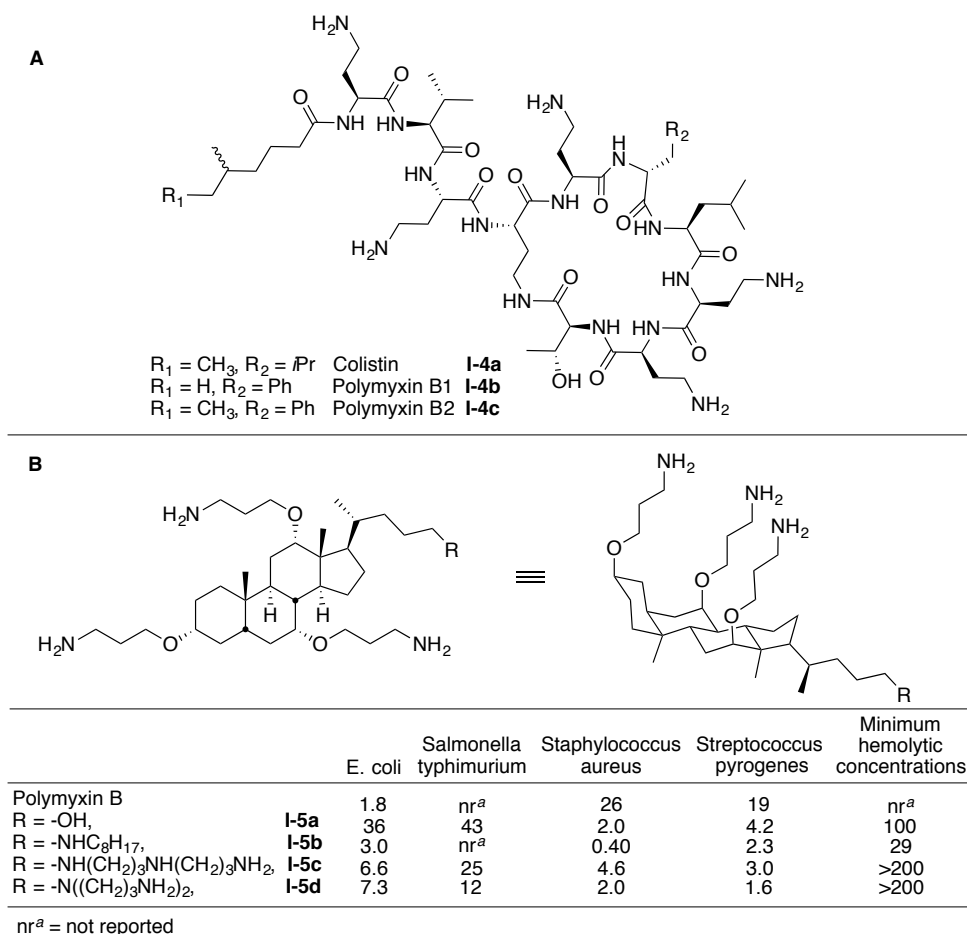


Figure I-5: A. Select polymyxins, cyclic members of the cationic peptide antibiotic class. B. Select polymyxin mimics and their minimum inhibitory concentrations (µg/mL) against Gram-positive and Gram-negative bacteria compared to polymyxin B. Minimum hemolytic concentration (MHC) was also recorded in µg/mL.

These compounds have shown broad-spectrum antibacterial activity comparable to polymyxin B in the case of both Gram-positive and Gram-negative bacteria.²²

Shamsuzzaman and coworkers synthesized another class of steroids, featured in Figure I-6, that target internal bacterial pathways instead of directly compromising cell integrity.²³ They found steroidal compounds advantageous because of their low toxicity, the ease with which they penetrate the cell wall, and their high bioavailability. With this in mind, steroidal ketones were modified into benzothiazines. These compounds are known to exhibit antibacterial effects via inhibition of bacterial topoisomerase II (also known as DNA-gyrase), an enzyme

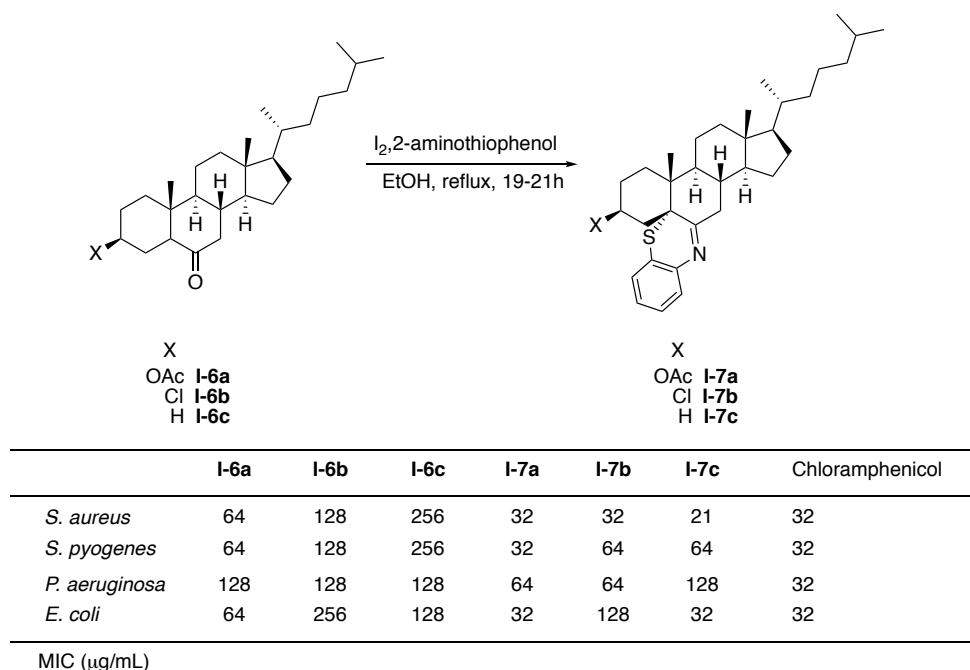


Figure I-6: Synthesis and antibacterial testing of benzothiazine steroids and their ketone precursors against Gram-positive and Gram-negative strains of bacteria.

necessary for DNA replication.²⁴ Submission of three steroidal ketones to a one-pot α -iodination and subsequent cyclization using 2-aminothiophenol led to formation of the three desired benzothiazine products (Figure I-6). Benzothiazines I-7a-c were incubated with *S. pyogenes*, *S. aureus*, *P. aeruginosa*, and *E. coli* along with their ketone predecessors and a chloramphenicol control. When looking at Figure I-6, it is apparent that the steroidal ketones are not as effective as the benzothiazines (all ketones were two to five fold higher in effective concentration than their benzothiazine counterparts). Compound **I-7a** proved especially effective with comparative activity to that of chloramphenicol (32 $\mu\text{g/mL}$ with all bacteria except *P. aeruginosa*, 64 $\mu\text{g/mL}$).

Interestingly, all active steroids tested in our laboratory manifested activity only against Gram-positive strains of bacteria. With regard to the assayed steroids (Figure I-7), diepoxide **I-8a** was compared with other ketone steroids that lacked the epoxidation of the polar α,β -unsaturation and, in the absence of the oxirane, lacked any notable activity against any of the evaluated bacteria. In a search for assayed steroids with α,β -epoxidation, we found no steroid similar enough for a direct comparison. The tested α,β -oxo-keto-steroids exhibited no activity against either of the tested classes of bacteria.

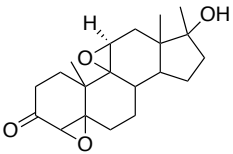
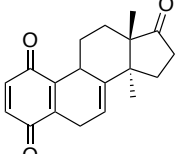
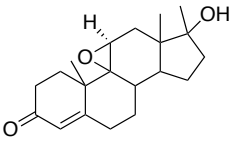
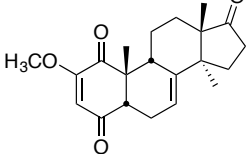
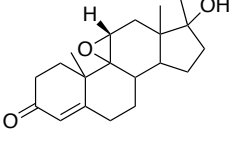
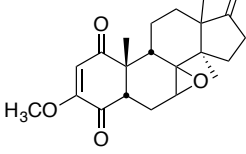
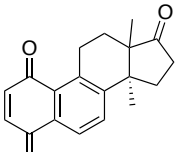
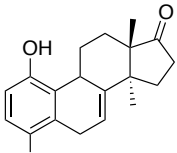
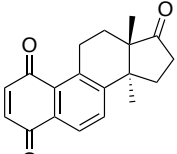
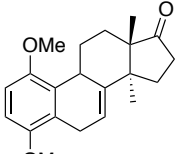
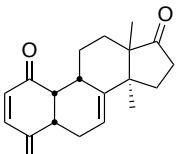
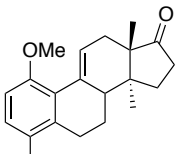
	Gram (+)	Gram (-)		Gram (+)	Gram (-)	
 I-8a	✓	✗	 I-10b	✓	✗	
 I-8b	✗	✗	 I-10c	✗	✗	
 I-8c	✗	✗	 I-10d	✗	✗	✓ MIC ≤ 476 µg/mL
 I-9a	✓	✗	 I-11a	✓	✗	✗ MIC > 476 µg/mL
 I-9b	✓	✗	 I-11b	✗	✗	
 I-10a	✓	✗	 I-11c	✗	✗	

Figure I-7: Minimum inhibitory concentration of Gram-positive and Gram-negative bacteria by steroidal compounds from an assay of general lab compounds.

1,4-benzoquinone based steroids **I-9** and **I-10** were found to exhibit antibacterial activity for as long as there was no substitution on carbons 2 and 3 of the

quinone moiety. This may be due to the reduced electron deficient nature of the olefin as exemplified by the methoxy-substituted steroids **I-10c** and **I-10d**. Naturally isolated²⁵ and synthetic²⁶ benzoquinones have been previously used as bacteriocides and have been found to block essential enzymes via combination with sulfhydryl groups of the enzymes themselves or essential bacterial metabolites²⁷. Hydroquinone derived steroid **I-11a** and like steroids showed Gram-positive inhibition though methyl protection of the diol moiety resulted in complete loss of observable activity. Such activity has been seen in hydroquinone derivatives such as natural products culpin²⁸ and avarol²⁹. We suspect that the mode of action is similar to that of the benzoquinone derivatives, requiring only prior oxidation to become active³⁰.

Cyclobutanols, pictured in Figure I-8, have also been found to provide Gram-positive bioactivity. Activity was consistently observed whether or not the aryl substitution persisted. The pendant hydroxyl group seems to be essential for antibacterial activity. Upon oxidation of this group (as seen in compound **I-12c**) or protection of the hydroxyl group (namely, as an ester as demonstrated by compound **I-12f**), the activity is lost. While cyclobutanes have been moieties present in many natural products and patented for their use as antivirals³¹, we have found none used as antibacterials.

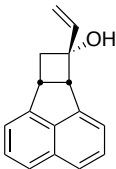
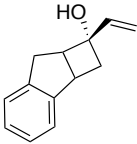
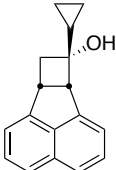
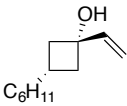

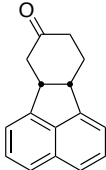
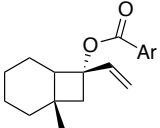

	Gram (+)	Gram (-)		Gram (+)	Gram (-)	
 I-12a	✓	✗	 I-12d	✓	✗	
 I-12b	✓	✗	 I-12e	✓	✗	 MIC ≤ 476 µg/mL
 I-12c	✗	✗	 I-12f	✗	✗	 MIC > 476 µg/mL

Figure I-8: Minimum inhibitory concentration of Gram-positive and Gram-negative bacteria by select compounds from an assay of general lab compounds.

Aryl compounds **I-13a-e**, when tested, provided Gram-positive activity for diketones and alcohols (Figure I-9). Ester **I-13e** provided no detectable activity for Gram-negative cells. Even more interestingly, in a comparison of **I-13b** and **I-13c**, the loss of a carbonyl seems to have contributed to the new activity in Gram-negative bacteria. Among the tested carboxylic acids, **I-14a** also exhibited activity against both Gram-positive and Gram-negative bacteria. While it could be suggested that this is due to the amphiphilic nature of the compound, it appears that **I-14b**, exhibiting singular Gram-positive activity, and **I-14c**, lacking

completely in activity, would be more drastically amphiphilic due to their more extensive hydrophobic regions.

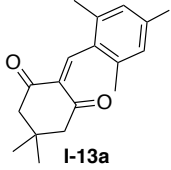
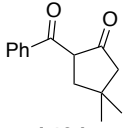
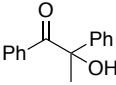
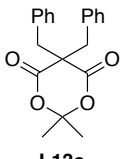
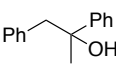
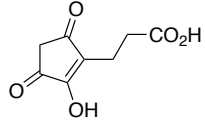
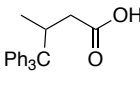
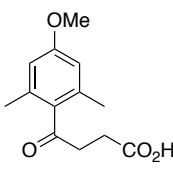
 I-13a	Gram (+) ✓	Gram (-) ✗	 I-13d	Gram (+) ✓	Gram (-) ✗
 I-13b	Gram (+) ✓	Gram (-) ✗	 I-13e	Gram (+) ✓	Gram (-) ✗
 I-13c	Gram (+) ✓	Gram (-) ✓			
 I-14a	Gram (+) ✓	Gram (-) ✓	<div>✓ MIC £ 476 µg/mL</div> <div>✗ MIC > 476 µg/mL</div>		
 I-14b	Gram (+) ✓	Gram (-) ✗			
 I-14c	Gram (+) ✗	Gram (-) ✗			

Figure I-9: Minimum inhibitory concentration of select compounds from an assay of general lab compounds against Gram-positive and Gram-negative bacteria.

Also among the tested compounds, we found two hits **I-15a** and **I-15b**, anionic and cationic, respectively, that inhibited growth in both Gram-positive and Gram-negative bacteria in a subclass of charged molecules (Figure I-10). This type of activity has been seen before^{17 32} and theoretically results in the lysis of the cell membrane and, eventually, cell death. This is not to say, however, that charged compounds will always produce activity in bacterial cell lines. Compound **I-15c** produced no activity in either Gram-positive or Gram-negative bacteria though it is a highly charged molecule. This may be due to the limited hydrophobic portions in the molecule. It would seem likely that this compound is highly soluble in water and would have no considerable effect on the cell membrane.

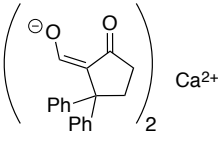
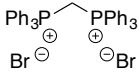
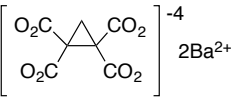
	Gram (+)	Gram (-)	
 I-15a	✓	✓	✓ MIC ≤ 476 µg/mL
 I-15b	✓	✓	✗ MIC > 476 µg/mL
 I-15c	✗	✗	

Figure I-10: Minimum inhibitory concentration of charged compounds in an assay of general lab compounds against Gram-positive and Gram-negative bacteria.

Sulfur based compounds had varying activity (Figure I-12). It appeared that sulfur compounds specifically containing S-S and S-N bonds were found to be bacteriocidal against Gram-positive bacteria. Compounds **I-16a** and **I-16b** provided activity where **I-16c** and **I-16d** did not. Notably, allicin (pictured in Figure I-11), a disulfide compound found in *Allium sativum* (garlic), has displayed Gram-positive (*S. aureus* with a 50% lethal dose concentration or LD₅₀ of 12 µg/mL) and Gram-negative (*E. coli* with an LD₅₀ of 15 µg/mL) bacteriocidal activity^{33, 34}. Allicin was found to inhibit certain important thiol containing enzymes, such as acetate kinase and phosphotransacetyl-CoA synthetase. For example, allicin has shown partially inhibit DNA and protein synthesis in *Salmonella typhimurium* while completely shutting down RNA synthesis at bacteriostatic concentrations of 0.2 to 0.5 mM.

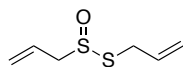


Figure I-11: Allicin, a compound found in garlic that has shown promising antibacterial activity in Gram-positive and Gram-negative bacteria.

Still, disulfides as antibacterials are rare outside of peptide antibiotics³⁵. Hocquellet and coworkers have found that hepcidin 25, a 25 amino acid antibacterial peptide known for its function as an iron regulator in humans³⁶, does not kill bacteria by destroying their membrane. Instead, the disulfide bonds

are necessary in order for peptide to bind to DNA. It is not clear whether these disulfide bonds are solely to maintain the structure of the peptide or if it also participates directly in binding to DNA.

Some less obvious hits produced interesting results. Bicyclic compound **I-17** exhibited activity in Gram-positive strains. Interestingly, alkynyl compounds produced activity in Gram-positive strains (**I-18a** and **I-19a**) and, in some cases, both Gram-positive and –negative strains (**I-19b**). In order to try to better understand the activity of compound **I-18a**, we compared it to **I-18b**. **I-18a** is biologically active because of the terminal alkyne moiety.

Internal alkyne esters **I-19a** and **I-19b** differ only in the substitution of C3. The difference is not very great but the results are substantially different. The activity seen in Gram-negative cells in the case of the protected propargyl alcohol **I-19b** is lost when the CH₂OBn is absent. While there are other in the literature with antimicrobial activity,^{37,38} their complexity complicates the direct association of their activity to the alkynes within.

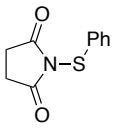
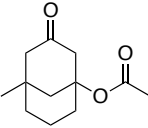
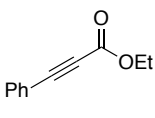
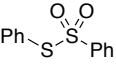
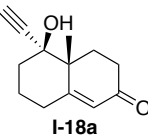
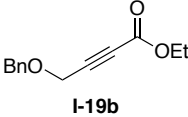
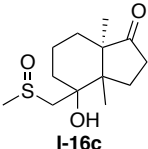
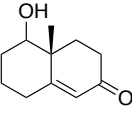

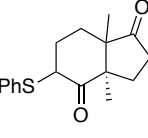

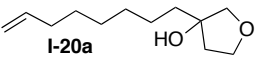
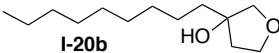
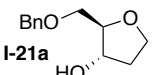
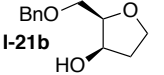
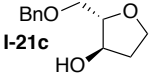
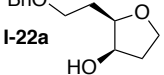
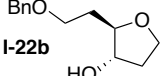
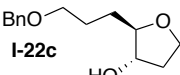
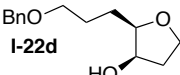
 I-16a	Gram (+) ✓	Gram (-) ✗	 I-17	Gram (+) ✓	Gram (-) ✗	 I-19a	Gram (+) ✓	Gram (-) ✗
 I-16b	Gram (+) ✓	Gram (-) ✗	 I-18a	Gram (+) ✓	Gram (-) ✗	 I-19b	Gram (+) ✓	Gram (-) ✓
 I-16c	✗	✗	 I-18b	✗	✗	 MIC ≤ 476 µg/mL		
 I-16d	✗	✗				 MIC > 476 µg/mL		

Figure I-12: Minimum inhibitory concentration of Gram-positive and Gram-negative bacteria by select compounds from an assay of general lab compounds.

I.2.2. Synthesis and Assay of 3-alkyl-3-hydroxytetrahydrofurans

In 2004, Borhan and coworkers published work on the sulfoxonium ylide induced one-carbon homologative relay ring expansion of 2,3-epoxyalcohols to form substituted tetrahydrofurans while maintaining the initial stereochemical enrichment.³⁹ The methodology relied on Payne rearrangement of enantiomerically pure epoxyalcohols, followed by sulfoxonium ylide attack on the least substituted side of the generated epoxide. The displacement of DMSO

		<i>Bacillus cereus</i>	<i>Bacillus subtilis</i>	<i>Microc. luteus</i>	<i>Staph. aureus</i>
	Streptomycin	167	333	<23	<23
1	 I-20a	250	ND	<23	ND
2	 I-20b	33	74	ND	ND
3	 I-21a	NA	NA	167	NA
4	 I-21b	NA	NA	1000	NA
5	 I-21c	NA	NA	NA	NA
6	 I-22a	NA	NA	NA	NA
7	 I-22b	NA	NA	NA	NA
8	 I-22c	NA	NA	NA	NA
9	 I-22d	NA	NA	NA	NA

*Numbers represent EC₅₀ values (μg/ml). Compounds were added until activity was observed.
 ND = Active but EC₅₀ not determined NA = No Activity

Table I-2: Substituted tetrahydrofuran activity against Gram-positive bacteria.

Table I-2 (cont'd)

		<i>Bacillus cereus</i>	<i>Bacillus subtilis</i>	<i>Microc. luteus</i>	<i>Staph. aureus</i>
	Streptomycin	167	333	<23	<23
10		NA	NA	833	NA
11		NA	NA	NA	NA
12		NA	NA	NA	NA
13		NA	NA	NA	NA
14		NA	NA	NA	NA
15		952	1333	666	NA
16		NA	NA	NA	NA
17		NA	NA	NA	NA
18		NA	NA	NA	NA

*Numbers represent EC₅₀ values (μg/ml). Compounds were added until activity was observed.

ND = Active but EC₅₀ not determined

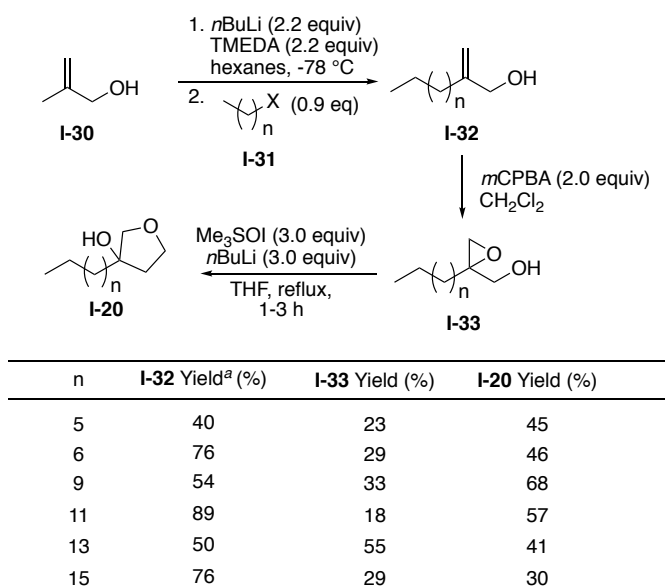
NA = No Activity

intramolecularly (5-endo-tet) by the alkoxide yielded enantiomerically sustained 2,3- disubstituted tetrahydrofurans. This methodology provided a new subclass of molecules to be repurposed and a great opportunity display the utility of this project.

Initial tests on substituted tetrahydrofuran compounds by Vaseliou and the Borhan group provided two hits across Gram-positive cell lines (*Bacillus cereus*,

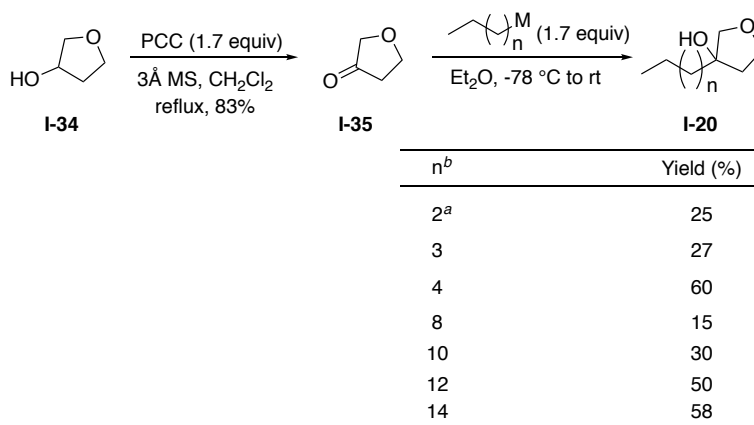
Bacillus subtilis, *Micrococcus luteus*, and *Staphylococcus aureus*) featured in Table I-2. Resazurin antimicrobial assays revealed that compound **I-20a** showed activity comparable to that of streptomycin, prompting the synthesis and evaluation of **I-20b** to probe the importance of the terminal alkene. The larger number of stereochemical groups and halogen incorporated into the structures of the other tetrahydrofurans tested did not seem to contribute to antibacterial activity, though spirocyclic compound **I-27** did manifest activity at very high concentrations (EC₅₀ values of 952 µg/mL for *Bacillus cereus*, 1333 µg/mL for *Bacillus subtilis*, and 666 µg/mL for *Micrococcus luteus*).

The promising activity observed in 3,3-substituted tetrahydrofurans **I-20a** and **I-20b** persuaded us to pursue structure-activity relationship studies in order to determine the optimum antibacterial lead compound. We began by varying alkyl chain length in order to determine its importance and the ideal length. One mode of synthesis required the formation of the 2-methyl-2-propen-1-ol dianion, using *n*-butyl lithium and TMEDA at -78 °C (Scheme I-2). The added alkyl halides reacted selectively with the carbanion forming extended chain 1,1-alkenols. *m*CPBA epoxidation provided epoxy alcohols **I-33** which were subsequently submitted to the sulfoxonium ylide induced relay ring expansion to form the 3,3-alkylhydroxytetrahydrofurans **I-20** in moderate yields.



Scheme I-2: Synthesis of 3,3-alkylhydroxytetrahydrofuran analogues via one-carbon homologative relay ring expansion. ^a Yields were calculated in relation to the alkyl halide.

An alternate method of synthesis, pictured in Scheme I-3, required the initial synthesis of 3-oxatetrahydrofuran from commercially available 3-hydroxytetrahydrofuran via PCC oxidation. The resulting ketone was submitted to multiple metalloalkane attacks in order to form other 3,3-alkylhydroxytetrahydrofurans. These two synthetic methods resulted in the formation of 3,3-disubstituted THF molecules with alkyl chains ranging from 4 to 17 carbons long.



Scheme I-3: Synthesis of 3,3-alkylhydroxytetrahydrofuran analogues via nucleophilic addition. ^aUsed *n*BuLi as nucleophile. ^bUnless otherwise mentioned, nucleophiles were generated through magnesium insertion to form the corresponding Grignard reagent.

Evaluation of the EC₅₀ values of 3,3-alkylhydroxytetrahydrofurans was done in duplicate using a 45 well plate and a Biorad Benchmark microplate reader and based on the metabolism of resazurin dye by viable Gram-positive bacteria after incubation with the tested compound. We found that the activity did vary in accordance with the lengths of the alkyl chains of the tested substrates, with an optimal range of seven to thirteen carbons. The increase in activity seen in the shorter length seemed to increase gradually culminating at a chain length of twelve carbons (**I-20j**) (EC₅₀ values of 4 µg/mL for *Bacillus cereus*, <10 µg/mL for *Bacillus subtilis*, and 12 µg/mL for *Micrococcus luteus*). Tests of the twelve-carbon substrate **I-20j** against *Staphylococcus aureus* activity proved inconclusive. We began to see a rapid decrease in activity as the chain lengths exceeded twelve carbons. This rapid drop in activity can be explained by the increasing insolubility of the substrates in the growth media. Though we began to

see problems with the determination of antibacterial activity of **I-20k**, the activity *Bacillus* strains suggested we had reached the pinnacle of activity for these analogues and were beginning the decline of activity due to both the interaction with the cells and the decreasing solubility of the more hydrophobic lengthy chain substrates in the cell media.

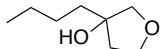
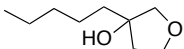
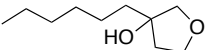
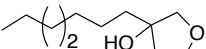
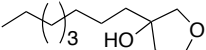
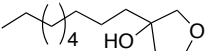
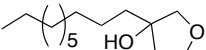
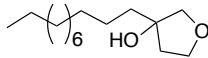
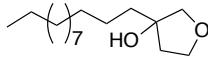
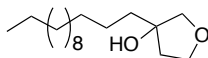
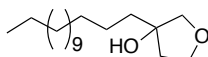
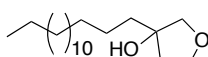
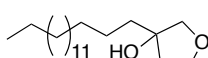
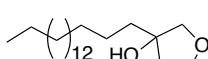
			<i>Bacillus cereus</i>	<i>Bacillus subtilis</i>	<i>Microc. luteus</i>	<i>Staph. aureus</i>
	Streptomycin		111	133	133	133
1	4C		>476	>476	>476	>476
	I-20c					
2	5C		>476	>476	>476	>476
	I-20d					
3	6C		>476	>476	>476	>476
	I-20e					
4	7C		222	200	167	ND
	I-20f					
5	8C		190	222	56	222
	I-20g					
6	9C		111	67	29	95
	I-20b					
7	10C		22	58	32	42
	I-20h					
*Numbers represent EC ₅₀ values (μg/ml).			ND = Not Determined			

Table I-3: EC₅₀ Values of 3,3-alkylhydroxytetrahydrofuran analogues of differing chain lengths.

Table I-3 (cont'd)

			<i>Bacillus cereus</i>	<i>Bacillus subtilis</i>	<i>Microc. luteus</i>	<i>Staph. aureus</i>
		Streptomycin	111	133	133	133
8	11C		13	14	22	12
		I-20i				
9	12C		4	<10	12	ND
		I-20j				
10	13C		7	<19	>476	ND
		I-20k				
11	14C		ND	ND	>476	>476
		I-20l				
12	15C		>476	>476	>476	>476
		I-20m				
13	16C		>476	>476	>476	>476
		I-20n				
14	17C		>476	>476	>476	>476
		I-20o				
*Numbers represent EC ₅₀ values (μg/ml).			ND = Not Determined			

To briefly scan the effects of branching and aromaticity in 3,3-alkylhydroxytetrahydrofuran analogues, compounds **I-20p-I-20r** were made via the one carbon homologative relay ring expansion of the corresponding starting epoxide using the sulfoxonium ylide as previously done. As illustrated in Table I-3, we found no measurable effects on tested Gram-positive bacterial strains.

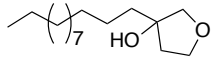
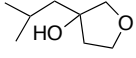
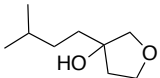
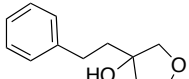
			<i>Bacillus cereus</i>	<i>Bacillus subtilis</i>	<i>Microc. luteus</i>	<i>Staph. aureus</i>
	Streptomycin		111	133	133	133
1	12C		4	<10	12	ND
		I-20j				
2	iBu		>476	>476	>476	>476
		I-20p				
3	iPn		>476	>476	>476	>476
		I-20q				
4	hBn		>476	>476	>476	>476
		I-20r				
*Numbers represent EC ₅₀ values (μg/ml).			ND = Not Determined			

Table I-4: EC₅₀ Values of branched and aromatic 3,3-alkylhydroxytetrahydrofuran analogues on Gram-positive bacteria.

To test the necessity of the hydroxyl moiety (Table I-5), two active analogues, **I-20i** and **I-20k**, were protected with trimethylsilyl chloride and methyl iodide, respectively. The activity initially seen in hydroxytetrahydrofuran **I-20k** was completely muted when converted to the methyl ether. The shorter more universally active **I-20i** seemed to maintain activity even after protection with the silyl group. We suspected that the silyl ether was deprotected upon addition to the cellular medium. Trimethylsilyl ethers have a well-known susceptibility to solvolysis, especially in acidic media.⁴⁰

The importance of the hydroxyl group and the chain length to the antibacterial activity of the 3,3-alkylhydroxytetrahydrofurans suggested a mode of action similar to that exhibited by surfactants and other amphiphiles, namely, the rupture or dissolution of the cell membrane.⁴¹

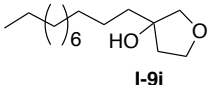
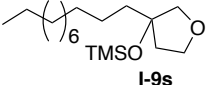
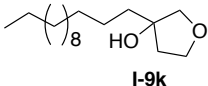
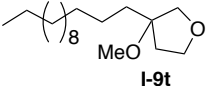
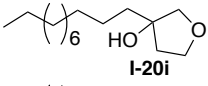
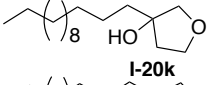
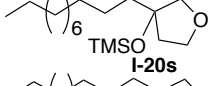
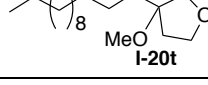
<hr/>				
11C	 I-9i	$\xrightarrow[\text{CH}_2\text{Cl}_2, 68\%]{\text{TMSCl (1.1 equiv) imidazole (1.2 equiv)}}$	 I-9s	
13C	 I-9k	$\xrightarrow[\text{THF, 84\%}]{\text{NaH (1.5 equiv) MeI (1.5 equiv)}}$	 I-9t	
		<i>Bacillus cereus</i>	<i>Bacillus subtilis</i>	<i>Microc. luteus</i>
		<i>Staph. aureus</i>		
Streptomycin		111	133	133
1	11C  I-20i	13	14	22
2	13C  I-20k	7	<19	>476
3	11C  I-20s	4	<10	12
4	13C  I-20t	>476	>476	>476
*Numbers represent EC ₅₀ values (μg/ml).		ND = Not Determined		

Table I-5: Evaluation of hydroxyl group importance in antibacterial activity of 3,3-alkylhydroxytetrahydrofuran analogues and EC₅₀ values on Gram-positive bacteria.

Kubo and coworkers have shown similarly that long chain alcohols are effective antibacterials against *Streptococcus mutans*.^{42 43} Interestingly, amongst the various alcohols tested, the simple thirteen-carbon alcohol, 1-tridecanol, showed the lowest minimum inhibitory concentration (6.25 μg/mL). Linalool and

Geranylacetol gave MICs of >800 and 25 $\mu\text{g/mL}$, respectively. The fact that this activity is manifested solely in Gram-positive cells further suggests the disassembly of the cell membrane generally seen with detergents.

I.2.3. Mode-of-Action Studies of 3-alkyl-3-hydroxytetrahydrofurans

Using Hemolysis Assays

To probe the merits of this hypothesis, we employed a hemolysis assay. 20 μL of each 10 mg/mL alkylhydroxytetrahydrofuran solution was added to 400 μL of a buffered solution of red blood cells (5.0×10^7 cells/mL) creating a 420 μL solution that was mixed and allowed to sit for 30 minutes. Triton X-100, a commercially available surfactant, was used as a positive control (20 μL of 10mg/mL solution) with isotonic buffer (20 μL), pure DMSO (20 μL), and streptomycin (20 μL of 10mg/mL) serving as negative controls. 100 μL of each solution was placed in a 96 well plate were used to observe cell viability under a microscope and the remaining 100 μL was centrifuged. The supernatant of the centrifuged samples was submitted to UV analysis on a 96 well plate at 550 nm using the Benchmark Biorad microplate reader. Hemolysis of red blood cells results in the release of hemoglobin ($\lambda_{\text{max}} = 540 \text{ nm}$) into the solution, giving higher absorptions than samples wherein hemolysis did not occur.

The results of the analysis of the supernatant after hemolysis are shown in Figure I-13. The red blood cell control showed little absorption at 550 nm, indicating minimal cell lysis. Addition of 20 μ L of pure DMSO caused a small amount of cell lysis as indicated by the moderate absorbance. Studies have shown that DMSO does have the ability to lyse erythrocytes in the absence of saline.⁴⁴ Conversely, while the presence of saline does not completely prevent the osmolysis of erythrocytes, it greatly reduces it. 20 μ L of a 10 mg/mL solution of Triton X-100 was added to the cell solution and provided extensive cell lysis. The streptomycin control produced no notable cell lysis as expected.

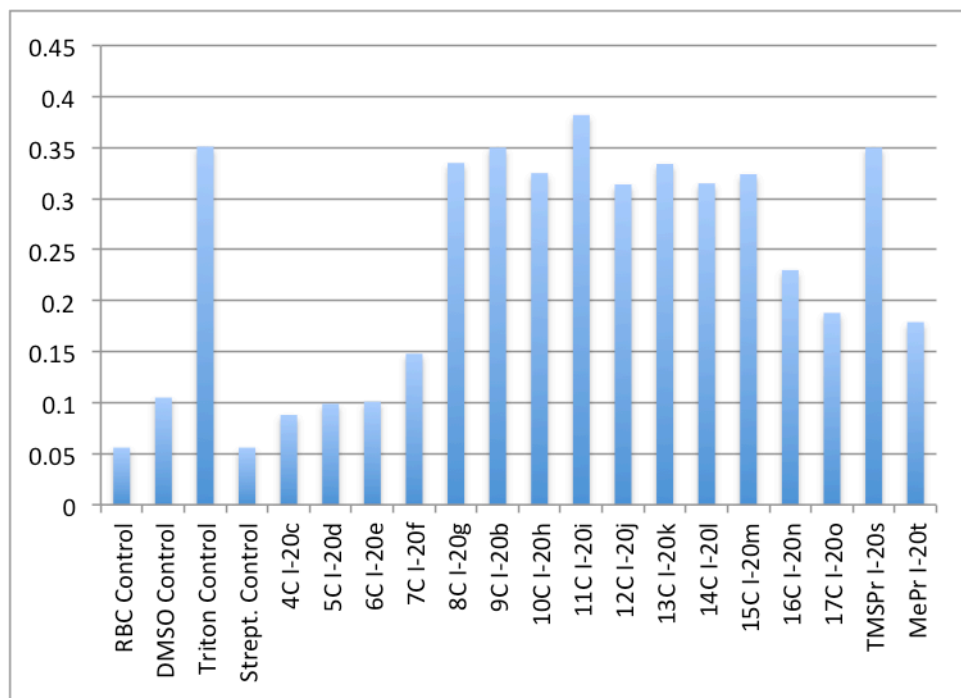


Figure I-13: UV/Vis absorption of hemolysis assay supernatant of 3,3-alkylhydroxytetrahydrofurans at 550 nm.

While our shorter analogues, specifically the 4 to 7 carbon chain analogues (**I-20c-f**), exhibited moderate hemolysis, it seemed comparable to that of DMSO. This is likely due to the solvent itself instead of the short chain 3,3-hydroxytetrahydrofuran compounds. As a matter of fact, the first signs of significant activity are not observed until the 8-carbon chain length of **I-20g** is utilized. Major lysis of the red blood cells occurred with carbon chain lengths between eight and fifteen carbons, a range closely comparable with the antibacterial activity seen in the previous assays (7 carbons to 13 carbons). Figure I-14 illustrates the surviving cell populations resulting from incubation with differing carbon chains.

The protected 3,3-alkylhydroxytetrahydrofurans have shown hemolytic activity very similar to the antibacterial activity observed earlier. The methyl-protected alcohol (**I-20t**) showed little activity while the TMS-protected alcohol (**I-20s**) lysed the red blood cells efficiently. This is in line with the theory that the trimethylsilyl group was solvolyzed, facilitating the lysis of the red blood cells by the free 11-carbon 3,3-alkylhydroxytetrahydrofuran (**I-20i**).

Based on these results, it is apparent that the mode of action of the 3,3-alkylhydroxytetrahydrofurans is the rupture of the cell, a mechanism commonly seen in detergents. This theory is supported by the fact that addition of high

doses of the substrates to Gram-negative cells showed no significant activity while exhibiting substantial activity with Gram-positive cell lines.

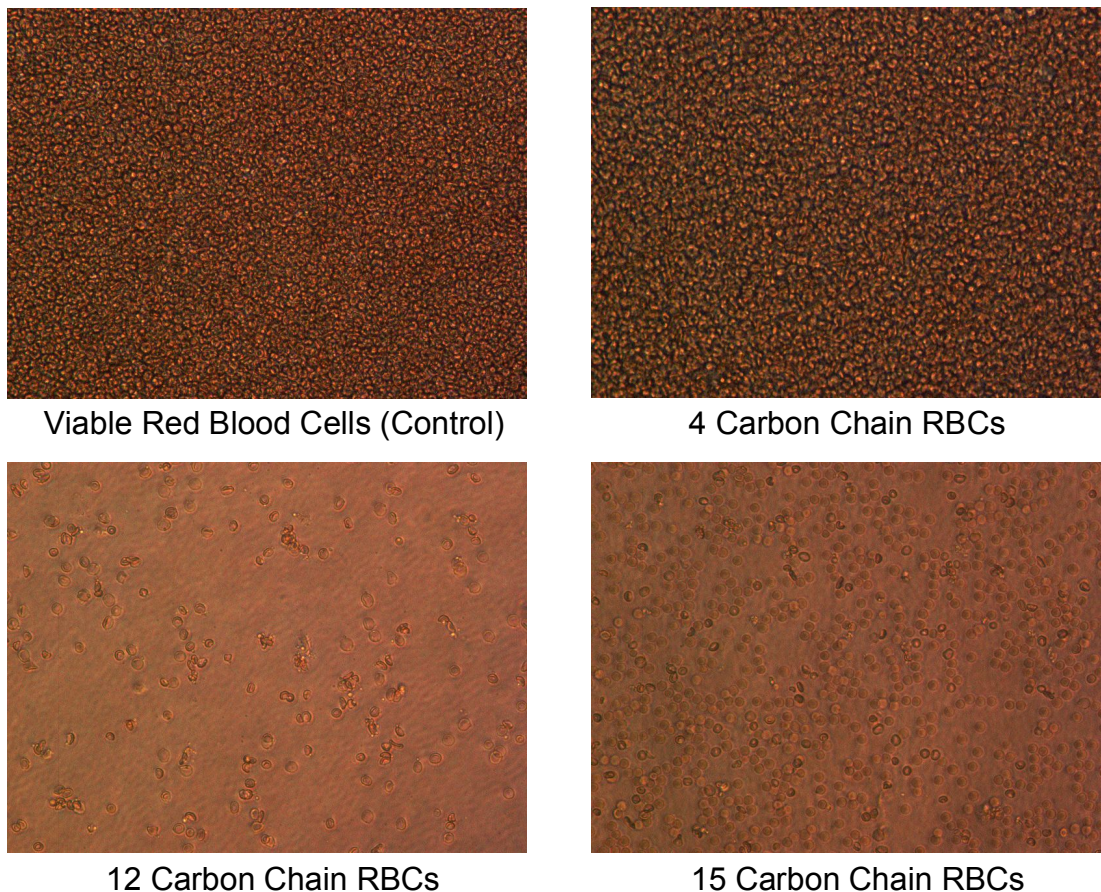


Figure I-14: Red blood cell viability after incubation with 3,3-alkylhydroxytetrahydrofurans.

Gram-positive and Gram-negative bacteria differ in many ways. One of the major differences that directly affect the passage of antimicrobials into the cell is the peptidoglycan cell “wall”. While both bacterial classes have this rigid structure that stabilizes the cytoplasmic membrane, their thicknesses are very different. Gram-positive bacteria possess 40-80 peptidoglycan layers 40-80 nm thick that

account for 90% of the dry weight of the cell. Gram-negative bacteria contain one layer of peptidoglycan 7-8 nm thick that account for roughly 10% of the dry weight of the cell.⁴⁵ This difference justifies the persistence of the Gram stain by Gram-positive bacteria and inability of the Gram stain to persist in Gram-negative bacteria. It also explains the purpose of the peptidoglycan cell wall: scaffolding for the bacteria to maintain the cell's structure.^{46, 47} The cell wall is not a protective barrier against antimicrobial compounds and in some instances, may even attract antibacterial peptides to the bacteria as a first step in the bacteriocidal mechanism. For example, the 34 amino acid peptide antibacterial nisin primarily inhibits peptidoglycan synthesis by initially binding to the peptidoglycan precursor lipid II.^{48, 49} This means the alkylhydroxytetrahydrofurans tested would not be hindered greatly by the cell wall of Gram-positive bacteria.

The incorporation of teichoic acid polymers into the cell surface is another difference seen between Gram-positive and Gram-negative bacteria. Teichoic acid is a soluble glycerolphosphate or ribitolphosphate polymer found in most Gram-positive bacteria linked either to the cytoplasmic membrane via a pendant glycolipid anchor (lipoteichoic acid) or covalently linked to *N*-acetylmuramic acid (NAM) of the peptidoglycan cell wall (wall teichoic acid).⁵⁰ Because of their phosphate heads, these polymers create a relatively negative charge on the cell envelope. It has been found that the absence of these polymers in the bacterial

casing will negatively affect the growth and viability of the cells.⁵¹ Consequently, these polymers provide a foothold for cationic and hydrogen bonding antimicrobials to adhere to bacterial cells, promoting the initial entry into the cell membrane.⁴⁷

A final major contributing difference between Gram-positive and Gram-negative is the outer membrane of Gram-negative bacteria. This is the most significant difference between the two Gram classifications in terms of antimicrobial contact. The outer membrane serves as a layer of protection. The inner leaflet of the outer membrane is made up of Zwitterionic phospholipids while the outer leaflet consists of Zwitterionic phospholipids and lipopolysaccharides.⁵² Because of their neutral heads, it is more difficult to distinguish between eukaryotic cells and Gram-negative cells using electrostatic interactions.

In terms of antibiotics, Savage and coworkers suggest that this layer of protection can be disrupted by the introduction of amphiphilic compounds (specifically cationic antibiotics) that can sensitize the cell to hydrophobic bacteria that, alone, could not traverse the outer membrane.¹⁸ Similarly, Helander and coworkers found that lactic acid served to permeabilize Gram-negative bacteria by similarly compromising the outer membrane.⁵³

With regard to Gram-positive bacteria, Kubo and coworkers shed light on the specific effects of alcohols as antimicrobials. They note that Gram-negative bacteria show no loss in viability when treated with alcohols of different lengths (MIC > 800 $\mu\text{g/mL}$) and Gram-positive bacteria are inhibited with chain lengths between 8 and 13 carbons. They suggest that the rapid decrease in activity with longer chains is due to the dispersion of the alcohol into the phospholipid bilayer, resulting in the breaking of the hydrogen bond.

Since a compound with a mode-of-action of nonselective cell lysis would not serve well as an effective antibacterial administered to eukaryotic organisms, 3,3-alkylhydroxytetrahydrofurans were not investigated further as a viable antibacterial.

I.2.4. General Hemolytic Assays

In order to seek out other compounds that exhibit hemolytic activity, the antibacterial hits were submitted to new hemolytic assays. The compounds that were found active against gram-positive and both gram classes of bacteria were submitted to a similar assay to that of 3,3-alkylhydroxytetrahydrofurans.

While many of the compounds were found to have slight hemolytic activity, there were a select few that had none. Steroids **I-10a** and **I-11a** were found to exhibit little to no cell lysis. This seems reasonable when we consider the mode of action of natural antibiotic benzoquinones and hydroquinones suggested previously.

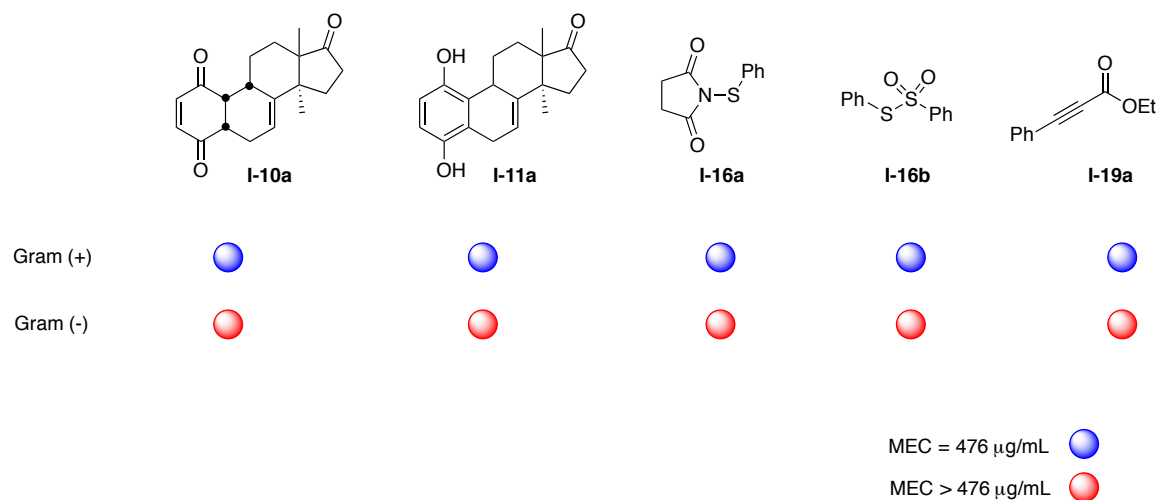


Figure I-15: Minimum inhibitory concentration of general laboratory compounds that exhibited no hemolytic activity.

Sulfide compounds **I-16a** and **I-16b** also did not rupture the red blood cell. This fits with the observations by Mirelman and coworkers that disulfides such as allicin inhibit cellular function by reacting with thiol moieties in important enzymes. Finally, internal alkyne **I-19a** also did not lyse the cells.

We also noted that every compound that was found to be effective against both Gram-positive and Gram-negative bacteria (alcohol **I-13c**, carboxylic acid **I-14a**, anionic salt **I-15a**, cationic salt **I-15b**, and alkyne **I-19b**) provided hemolysis

comparable to that of the Triton X-100 control. To some extent, all of these compounds discouraged cell viability via a compromised membrane.

I.3. Conclusion

In attempts to combat the increasing resistance of bacteria to antimicrobials, we began to search for hits in a rarely accessed library: synthesized laboratory compounds that have outlived their usefulness in other academic pursuits. Out of approximately 1400 compounds tested for antibacterial activity, approximately 29 compounds, not accounting for redundancies, were found to be biologically active at the appropriate concentrations against gram-positive bacteria. 5 of those compounds were found to be active against gram-negative bacteria.

Among these compounds, we found that 3,3-alkylhydroxytetrahydrofurans showed substantial activity. With that, we began to further explore the source of this activity and found that the chain length and the hydroxyl group were responsible for the activity seen. In terms of chain length, the compounds within the range of 7-13 carbons were the ones in which activity was observed. Activity was gradually introduced as the chain length grew from 4 carbons to 7 carbons, suggesting the appropriate chain length was important with respect to the inhibition of cell function. However, activity seemed to quickly subside from 14 to 15 carbons, suggesting the loss of activity was directly connected to the solubility

of the substrate in the cellular media. Protection of the hydroxyl moiety completely shut down activity.

The combination of these two ideas led us to believe that these 3,3-alkylhydroxytetrahydrofurans were acting as surfactants and destroying the cell membranes of the bacteria. In order to test this hypothesis, we submitted the compounds to a hemolytic assay and found that there was a substantial correlation between the activity exhibited in gram-positive bacteria and the hemolysis of red blood cells, substantial hemolysis occurring between 8 and 15 carbons.

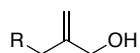
In order to rule out unselective membrane rupture as a mode of action, we submitted all other antibacterial hits found in this probe to the hemolysis assay. While many provided moderate hemolysis, only five gave rise to little to no hemolysis. Four of these were expected to be due to mechanisms suggested by other compounds with similar moieties. The fifth, however, an internal alkyne ester, seemed to have precedence only with largely complex compounds wherein other functionalities could be implicated in the antibacterial activity seen. More study of the simple alkynes utilized in these experiments is necessary to fully understand the contribution of the alkyne to the activity seen in those more complex structures.

Since new compounds are continually synthesized and utilized in the laboratory, this method of searching for new antibacterial hits is continually evolving to incorporate new and different compounds. The perpetual revision of such a library could prove essential in the fight for new antimicrobials and further increases the probability of quickly finding new weapons in the struggle against antibiotic resistant strains.

I.4. Experimental

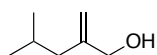
General Antimicrobial Assay. Gram-positive cell lines *Bacillus cereus* ATCC-1778, *Bacillus subtilis* ATCC-6633, *Micrococcus luteus* ATCC-7468D, *Staphylococcus aureus* ATCC-6538 and Gram-negative cell lines *Escherichia coli* ATCC-8739, *Klebsiella pneumonia* ATCC-4352, *Pseudomonas aeruginosa* ATCC-9027, *Serratia marcescens* ATCC-14756, *Enterobacter aerogenes* ATCC-13048 were inoculated into 5 mL autoclaved LB solution and allowed to stir on an incubator shaker for 6 to 8 hours. 1 mL of the bacterial solution was added to 10 mL of autoclaved LB. 30 μ L of the cell solution is added to each well of a 96 well plate after the addition of 170 μ L of autoclaved LB. 10 μ L of a 10mg/mL solution of the tested compound was added to the assigned well (done in duplicate or triplicate). The 96 well plate was incubated at 37 °C overnight.

1 μ L of 3.3 mg/mL Resazurin in water was added to each well after incubation. The plate was analyzed using UV/Visible spectroscopy via Benchmark Biorad microplate reader (595 and 655 nm), scanning incrementally every 5 minutes until the unaffected wells were light pink.

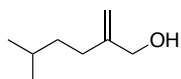


Preparation of 1,1-disubstituted alkenyl alcohols (I-32). A flame-dried flask (3-neck) was charged with a stir bar and equipped with an argon balloon. TMEDA (10.32 ml, 8g, 69 mmol) was added in 15ml hexanes (spectro. grade) followed by

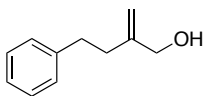
the addition of nBuLi (30 ml, 2.5M in hexanes, 69 mmol) while maintaining a temperature below -10 °C. After stirring for 30 minutes, 2-methyl-2-propen-1-ol (2.8 ml, 2.38g, 32 mmol) was added at -78 °C. The solution was allowed to stir overnight providing a yellowish-orange opaque texture. At this point the alkyl halide (28 mmol) was added after cooling the suspension again to -78 °C. The mixture was again allowed to stir overnight. The reaction was quenched with saturated ammonium chloride solution. The mixture was extracted (EtOAc 30 ml x 3), dried over sodium sulfate, and concentrated in vacuo. The compound was purified by column chromatography (10% EtOAc in hexanes) to give yields varying from 30-75%.



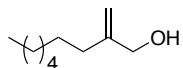
^1H NMR (500 MHz, CDCl_3) δ 5.02 (s, 1 H), 4.83 (s, 1 H), 4.05 (s, 1 H), 1.91 (d, $J = 7.0$ Hz, 2 H), 1.79-1.64 (m, 1 H), 0.851 (d, $J = 11$ Hz, 6 H).



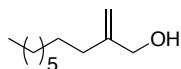
^1H NMR (500 MHz, CDCl_3) δ 4.98 (s, 1 H), 4.84 (s, 1 H), 4.05 (s, 2 H), 2.35 (dd, $J = 2.0$ Hz, 1.5 Hz, 2 H), 1.53 (m, 1 H), 1.31 (m, 2 H), 0.873 (d, $J = 11$ Hz, 6 H).



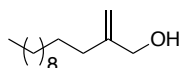
^1H NMR (500 MHz, CDCl_3) δ 7.50-7.24 (m, 5 H), 5.22 (s, 1 H), 5.06 (s, 1 H), 4.22 (s, 2 H), 2.91 (t, $J = 10$, 2 H), 2.52 (t, $J = 10$ Hz, 2 H).



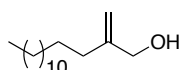
^1H NMR (500 MHz, CDCl_3) δ 4.99 (dt, $J = 0.5, 1.0$ Hz, 1 H), 4.84 (dt, $J = 1.0, 1.5$ Hz, 1 H), 4.05 (s, 2 H), 2.03 (d, $J = 7.5$ Hz, 2 H), 1.09-1.34 (m, 12 H), 0.865 (t, $J = 7.5$ Hz, 3 H).



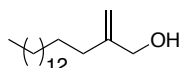
^1H NMR (500 MHz, CDCl_3) δ 4.99 (dt, $J = 0.5, 1.0$ Hz, 1 H), 4.84 (dt, $J = 1.0, 1.5$ Hz, 1 H), 4.05 (s, 2 H), 2.03 (t, $J = 7.5$ Hz, 2 H), 1.34-1.09 (m, 12 H), 0.865 (t, $J = 7.5$ Hz, 3 H). ^{13}C NMR (125 MHz, CDCl_3) δ 149.3, 108.9, 65.9, 33.0, 31.9, 29.4, 29.3, 27.8, 22.7, 14.1.



^1H NMR (500 MHz, CDCl_3) δ 4.99 (dt, $J = 0.5, 1.0$ Hz, 1 H), 4.84 (dt, $J = 1.0, 1.5$ Hz, 1 H), 4.05 (s, 2 H), 2.03 (t, $J = 7.5$ Hz, 2 H), 1.37-1.08 (m, 18 H), 0.865 (t, $J = 7.5$ Hz, 3 H).

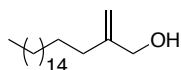


^1H NMR (500 MHz, CDCl_3) δ 4.99 (dt, $J = 0.5, 1.0$ Hz, 1 H), 4.84 (dt, $J = 1.0, 1.5$ Hz, 1 H), 4.05 (s, 2 H), 2.03 (d, $J = 7.5$ Hz, 2 H), 1.09-1.34 (m, 12 H), 0.865 (t, $J = 7.5$ Hz, 3 H). ^{13}C NMR (125 MHz, CDCl_3) δ 149.3, 108.9, 65.9, 33.0, 31.9, 29.4, 29.3, 27.8, 22.7, 14.1.

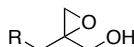


^1H NMR (500 MHz, CDCl_3) δ 4.99 (dt, $J = 0.5, 1.0$ Hz, 1 H), 4.85 (dt, $J = 1.0, 1.5$ Hz, 1 H), 4.05 (s, 2 H), 2.03 (t, $J = 7.5$ Hz, 2 H), 1.16-1.32 (m, 26 H), 0.867 (t, $J =$

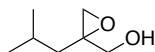
7.5 Hz, 3 H). ^{13}C NMR (125 MHz, CDCl_3) δ 149.3, 108.9, 70.0, 34.1, 33.0, 32.8, 31.9, 29.7, 29.6, 29.5, 29.4, 29.3, 28.8, 28.2, 27.8, 22.7, 14.1.



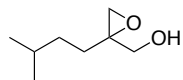
^1H NMR (500 MHz, CDCl_3) δ 4.99 (dt, $J = 0.5, 1.0$ Hz, 1 H), 4.85 (dt, $J = 1.0, 1.5$ Hz, 1 H), 4.05 (s, 2 H), 2.03 (t, $J = 7.5$ Hz, 2 H), 1.16-1.32 (m, 26 H), 0.867 (t, $J = 7.5$ Hz, 3 H).



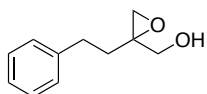
Preparation of 2-alkyl-2-hydroxymethyl epoxide. The alkene substrate was stirred in dry methylene chloride (50 ml) at 0 $^{\circ}\text{C}$. *m*CPBA (2.0 equiv.) was dissolved in the necessary methylene chloride and added via cannula to the stirring solution. The ice bath was left in place and the mixture was allowed to war to room temperature and then left for three hours. The reaction was also monitored via TLC. The reaction was quenched with saturated sodium carbonate. Extraction was done with methylene chloride (30 ml x 3). The organic layer was concentrated in vacuo and dried over sodium sulfate. Purification was achieved via column chromatography (15% EtOAc in hexane). The pure compounds generally resulted in yellowish-brown oils. In the case of the 17-carbon analogue, it resulted in a yellow gel like solid. Yields were approx. 30%.



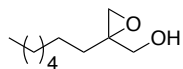
^1H NMR (500 MHz, CDCl_3) δ 3.53 (d, $J = 20$ Hz, 1 H), 3.51 (d, $J = 20$ Hz, 1 H), 2.54 (d, $J = 8.0$ Hz, 1 H), 2.51 (d, $J = 8.0$ Hz, 1 H), 1.53-1.52 (m, 1 H), 1.22 (d, $J = 9.5$ Hz, 2 H), 0.913 (d, $J = 11$ Hz, 6 H).



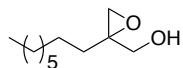
^1H NMR (500 MHz, CDCl_3) δ 3.91 (d, $J = 20.5$ Hz, 1 H), 3.76 (d, $J = 20.5$ Hz, 1 H), 3.02 (d, $J = 7.5$ Hz, 1 H), 2.80 (d, $J = 7.5$ Hz, 1 H), 2.48 (bs, 1 H), 1.90 (dt, $J = 14, 23.5$ Hz, 1 H), 1.72-1.56 (m, 1 H), 1.37 (dt, $J = 12, 15.5$ Hz, 1 H), 1.01 (d, $J = 11$ Hz, 6 H).



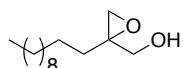
^1H NMR (500 MHz, CDCl_3) δ 7.49-7.22 (m, 5 H), 3.95 (d, $J = 20$ Hz, 1 H), 3.85 (d, $J = 20$ Hz, 1 H), 3.34 (d, $J = 8.0$ Hz, 1 H), 2.81 (d, $J = 8.0$ Hz, 1 H), 2.36-2.20 (m, 2 H), 2.10-1.94 (m, 2 H).



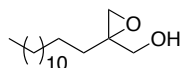
^1H NMR (500 MHz, CDCl_3) δ 3.76 (d, $J = 20$ Hz, 1 H), 3.63 (d, $J = 20$ Hz, 1 H), 2.87 (d, $J = 5.0$ Hz, 1 H), 2.65 (d, $J = 5.0$ Hz, 1 H), 1.82-1.66 (m, 2 H), 1.40-1.14 (m, 2 H), 0.862 (t, $J = 13$ Hz, 3 H).



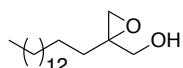
^1H NMR (500 MHz, CDCl_3) δ 3.75 (d, $J = 12$ Hz, 1 H), 3.62 (d, $J = 12$ Hz, 1 H), 2.86 (d, $J = 4.5$ Hz, 1 H), 2.64 (d, $J = 4.5$ Hz, 1 H), 1.74 (dt, $J = 7.0, 15$ Hz, 1 H), 1.62 (bs, 1 H), 1.48 (dt, $J = 8.0, 16$ Hz, 1 H), 1.35-1.16 (m, 12 H), 0.857 (t, $J = 7.0$ Hz, 3 H). ^{13}C NMR (125 MHz, CDCl_3) δ 62.8, 59.7, 49.8, 32.0, 31.8, 29.7, 29.4, 29.2, 24.6, 22.6, 14.1.



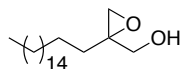
^1H NMR (500 MHz, CDCl_3) δ 3.76 (d, $J = 20$ Hz, 1 H), 3.63 (d, $J = 20$ Hz, 1 H), 2.87 (d, $J = 8.0$ Hz, 1 H), 2.65 (d, $J = 8.0$ Hz, 1 H), 1.82-1.66 (m, 2 H), 1.40-1.14 (m, 2 H), 0.862 (t, $J = 13$ Hz, 3 H).



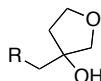
^1H NMR (500 MHz, CDCl_3) δ 3.76 (d, $J = 12$ Hz, 1 H), 3.62 (d, $J = 12$ Hz, 1 H), 2.87 (d, $J = 5.0$ Hz, 1 H), 2.65 (d, $J = 5.0$ Hz, 1 H), 1.74 (dt, $J = 7.0, 15$ Hz, 1 H), 1.48 (dt, $J = 8.0, 16$ Hz, 1 H), 1.35-1.14 (m, 24 H), 0.860 (t, $J = 6.5$ Hz, 3 H). ^{13}C NMR (125 MHz, CDCl_3) δ 62.97, 50.06, 32.25, 32.16, 29.97, 29.91, 29.88, 29.85, 29.76, 29.72, 29.58, 24.86, 22.92, 14.35.



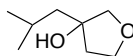
^1H NMR (500 MHz, CDCl_3) δ 3.76 (d, $J = 12$ Hz, 1 H), 3.62 (d, $J = 12$ Hz, 1 H), 2.87 (d, $J = 5.0$ Hz, 1 H), 2.65 (d, $J = 5.0$ Hz, 1 H), 1.74 (dt, $J = 7.0, 15$ Hz, 1 H), 1.48 (dt, $J = 8.0, 16$ Hz, 1 H), 1.35-1.14 (m, 26 H), 0.860 (t, $J = 6.5$ Hz, 3 H).



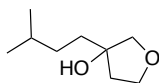
^1H NMR (500 MHz, CDCl_3) δ 3.91 (d, $J = 20.5$ Hz, 1 H), 3.79 (d, $J = 20.5$ Hz, 1 H), 3.02 (d, $J = 8.0$ Hz, 1 H), 2.80 (d, $J = 8.0$ Hz, 1 H), 1.92 (dt, $J = 7.0, 15$ Hz, 1 H), 1.63 (dt, $J = 8.0, 16$ Hz, 1 H), 1.52-1.26 (m, 30 H), 1.01 (t, $J = 10$ Hz, 3 H).



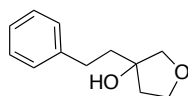
Preparation of 3-alkyl-3-hydroxytetrahydrofuran. Trimethylsulfoxonium iodide was dried under high vacuum at 40 °C overnight. In preparation of 3-hydroxyTHF derivatives, dimethylsulfoxonium methylide was generated from trimethylsulfoxonium iodide and $n\text{BuLi}$ in THF at -78 °C. Addition of the epoxy alcohol precursor followed by heating to reflux for 3 hours resulted in a darker tinted liquid that was quenched with ammonium chloride after cooling. The mixture was extracted several times with EtOAc. The organic layer was washed with brine, dried over sodium sulfate, and concentrated in vacuo. The crude mixture was purified via column chromatography (10% EtOAc in hexanes) resulting in a yellow oil in most cases and a brown gel in the case of the 17 carbon chain analogue. Yields varied (30-74%).



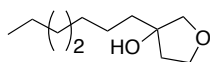
^1H NMR (500 MHz, CDCl_3) δ 3.98 (dt, $J = 10$ Hz, 15 Hz, 1 H), 3.86 (td, $J = 6$ Hz, 13 Hz, 1 H), 3.72 (dd, $J = 1$ Hz, 15 Hz, 1 H), 3.51 (d, $J = 17.5$ Hz, 1 H), 1.97-1.82 (m, 3 H), 1.56 (dd, $J = 9.5$ Hz, 11.5, 2 H), 0.955 (dd, $J = 12$ Hz, 15.5 Hz, 6 H).



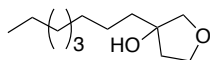
^1H NMR (500 MHz, CDCl_3) δ 4.01 (dt, $J = 6.5$ Hz, 9 Hz, 1 H), 3.90-3.84 (m, 1 H), 3.68 (d, $J = 10$ Hz, 1 H), 3.53 (d, $J = 9.5$ Hz, 1 H), 1.93-1.86 (m, 1 H), 1.62 (dd, $J = 9.5$ Hz, 10.5, 2 H), 1.56-1.46 (m, 1 H), 1.38-1.20 (m, 3 H), 0.891 (d, $J = 11$ Hz, 6 H).



^1H NMR (500 MHz, CDCl_3) δ 7.34-7.25 (m, 2 H), 7.26-7.15 (m, 3 H), 4.03 (dt, $J = 8$ Hz, 10 Hz, 1 H), 3.89 (td, $J = 4.5$ Hz, 9.0 Hz, 1 H), 3.72 (d, $J = 10$ Hz, 1 H), 3.57 (d, $J = 9$ Hz, 1 H), 2.86-2.70 (m, 2 H), 2.02-1.93 (m, 4 H). ^{13}C NMR (125 MHz, CDCl_3) δ 142.1, 128.8, 128.5, 126.3, 110.0, 81.3, 79.2, 67.6, 40.2, 31.32.

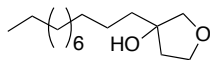


^1H NMR (500 MHz, CDCl_3) δ 4.01 (dt, $J = 7.5$ Hz, 8.5 Hz, 1 H), 3.87 (td, $J = 5.5$ Hz, 8 Hz, 1 H), 3.68 (d, $J = 9$ Hz, 1 H), 3.53 (d, $J = 9$ Hz, 1 H), 1.90 (dd, $J = 5$ Hz, 7 Hz, 2 H), 1.62 (t, $J = 8.5$ Hz, 2 H), 1.34-1.18 (m, 10 H), 0.864 (t, $J = 7$ Hz, 3 H). ^{13}C NMR (125 MHz, CDCl_3) δ 84.5, 79.1, 67.7, 40.0, 38.2, 32.0, 30.3, 29.4, 24.9, 22.9, 14.3.

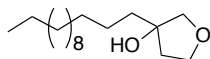


^1H NMR (500 MHz, CDCl_3) δ 4.01 (td, $J = 7.5$ Hz, 8.5 Hz, 16 Hz, 1 H), 3.87 (dt, $J = 5$ Hz, 7.5 Hz, 1 H), 3.68 (d, $J = 9$ Hz, 1 H), 3.53 (d, $J = 9$ Hz, 1 H), 1.90 (dd, $J = 6$ Hz, 7.5 Hz, 2 H), 1.63 (t, $J = 8.5$ Hz, 2 H), 1.32-1.18 (m, 18), 0.863 (d, $J = 7$ Hz,

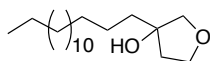
3 H). ^{13}C NMR (125 MHz, CDCl_3) δ 81.2, 78.9, 67.4, 39.8, 37.9, 31.9, 30.1, 29.5, 29.2, 24.6, 22.6, 14.1.



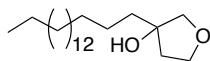
^1H NMR (500 MHz, CDCl_3) δ 4.00 (dd, $J = 8.5$ Hz, 16.5 Hz, 1 H), 3.90-3.84 (m, 1 H), 3.67 (d, $J = 9.5$ Hz, 1 H), 3.53 (d, $J = 9.5$ Hz, 1 H), 1.90 (d, $J = 5$ Hz, 7.5 Hz, 2 H), 1.62 (t, $J = 8.5$ Hz, 2 H), 1.34-1.18 (m, 24 H), 0.859 (t, $J = 7$ Hz, 3 H). ^{13}C NMR (125 MHz, CDCl_3) δ 81.5, 79.1, 67.7, 40.0, 38.2, 32.1, 30.3, 29.9, 29.85, 29.81, 29.79, 29.6, 24.9, 22.9, 14.3.



^1H NMR (500 MHz, CDCl_3) δ 4.00 (dd, $J = 7$ Hz, 14 Hz, 1 H), 3.87 (dd, $J = 9$ Hz, 16.5 Hz, 1 H), 3.67 (d, $J = 9$ Hz, 1 H), 3.53 (d, $J = 9$ Hz, 1 H), 1.90 (dd, $J = 6$ Hz, 7.5 Hz, 2 H), 1.62 (t, $J = 8.5$ Hz, 2 H), 1.32-1.18 (m, 22), 0.860 (d, $J = 7$ Hz, 3 H). ^{13}C NMR (125 MHz, CDCl_3) δ 81.2, 78.9, 67.4, 60.4, 39.8, 37.9, 31.9, 30.1, 29.7, 29.6, 29.5, 29.3, 24.6, 22.7, 21.0, 14.2, 14.1.



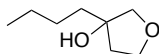
^1H NMR (500 MHz, CDCl_3) δ 4.04 (dd, $J = 7$ Hz, 14 Hz, 1 H), 3.91 (dd, $J = 9$ Hz, 16.5 Hz, 1 H), 3.72 (d, $J = 9$ Hz, 1 H), 3.57 (d, $J = 9$ Hz, 1 H), 1.93 (dd, $J = 6$ Hz, 7.5 Hz, 2 H), 1.66 (t, $J = 8.5$ Hz, 2 H), 1.38-1.22 (m, 24), 0.897 (t, $J = 7$ Hz, 3 H). ^{13}C NMR (125 MHz, CDCl_3) δ 81.4, 79.1, 67.7, 40.0, 38.2, 32.2, 30.3, 29.92, 29.89, 29.88, 29.82, 29.80, 29.51, 24.9, 22.9, 14.3.



^1H NMR (500 MHz, CDCl_3) δ 4.14 (dd, $J = 7$ Hz, 14 Hz, 1 H), 4.05 (dd, $J = 8.5$ Hz, 16.5 Hz, 1 H), 3.92 (dt, $J = 5$ Hz, 8 Hz, 1 H), 3.73 (d, $J = 9$ Hz, 1H) 3.58 (d, $J = 9.5$ Hz, 1 H), 1.36-1.26 (m, 18 H), 0.902 (t, $J = 7$ Hz, 3 H).

Lithium Reagent

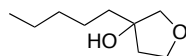
n-Butyllithium was added to dry diethyl ether and stirred while purging with N_2 gas. After lowering the temperature to -78°C , 3-oxa-THF was added. The reaction was monitored via TLC and diluted with H_2O upon completion. NH_4Cl was added to the solution before extraction several times with CH_2Cl_2 . The organic layer was dried over sodium sulfate, and concentrated in vacuo. The crude mixture was purified via column chromatography (20% EtOAc in hexanes) to reveal a clear liquid. The yield was low (25%).



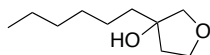
^1H NMR (300 MHz, CDCl_3) δ 4.01 (dd, $J = 7$ Hz, 14 Hz, 1 H), 3.87 (td, $J = 5$ Hz, 8 Hz, 12.5 Hz, 1 H), 3.68 (d, $J = 9$ Hz, 1 H), 3.54 (d, $J = 9$ Hz, 1 H), 1.90(d, $J = 5$ Hz, 8 Hz, 2 H), 1.64 (t, $J = 8.5$ Hz, 2 H), 1.38-1.30 (m, 4 H), 0.908 (t, $J = 7$ Hz, 3 H).

Grignard Reagents

Magnesium metal and a very small amount of iodine was charged into a small dry flask with a stir bar and sealed. After purging, dry diethyl ether was added via syringe and the solution was stirred for 30 minutes. The alkyl halide was added and allowed to stir for 30 more minutes. The disappearance of the brownish tint produced by the iodine was a coloremtric gauge to mark initiation of magnesium insertion. The temperature was lowered to $-78\text{ }^{\circ}\text{C}$ and 3-oxaTHF was added. The reaction was monitored via TLC and diluted with H_2O upon completion. After the solution stilled, NH_4Cl was added to the solution before extraction several times with CH_2Cl_2 . The organic layer was dried over sodium sulfate, and concentrated in vacuo. The crude mixture was purified via column chromatography (20% EtOAc in hexanes) to reveal a clear liquid. The yield was low (25%).

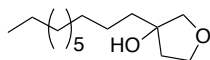


^1H NMR (500 MHz, CDCl_3) δ 4.01 (dd, $J = 7\text{ Hz}, 14\text{ Hz}$, 1 H), 3.87 (dd, $J = 9\text{ Hz}, 16.5\text{ Hz}$, 1 H), 3.68 (d, $J = 9.5\text{ Hz}$, 1 H), 3.53 (d, $J = 9.5\text{ Hz}$, 1 H), 1.90 (dd, $J = 6\text{ Hz}, 8.5\text{ Hz}$, 2 H), 1.62 (t, $J = 9\text{ Hz}$, 2 H), 1.34-1.16 (m, 6), 0.881 (t, $J = 6.5\text{ Hz}$, 3 H). ^{13}C NMR (125 MHz, CDCl_3) δ 81.2, 78.9, 67.4, 39.8, 37.9, 32.3, 24.3, 22.6, 14.0.

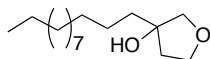


^1H NMR (500 MHz, CDCl_3) δ 4.01 (dd, $J = 8.5\text{ Hz}, 16.5\text{ Hz}$, 1 H), 3.87 (dd, $J = 9\text{ Hz}, 16.5\text{ Hz}$, 1 H), 3.68 (d, $J = 9.5\text{ Hz}$, 1 H), 3.53 (d, $J = 9\text{ Hz}$, 1 H), 1.90 (dd, $J = 6\text{ Hz}, 8.5\text{ Hz}$, 2 H), 1.63 (t, $J = 9\text{ Hz}$, 2 H), 1.34-1.20 (m, 8), 0.869 (t, $J = 6\text{ Hz}$, 3

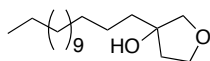
H). ^{13}C NMR (125 MHz, CDCl_3) δ 81.2, 78.9, 67.4, 39.8, 37.9, 31.7, 29.7, 24.6, 22.6, 14.0.



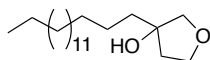
^1H NMR (500 MHz, CDCl_3) δ 4.01 (dd, $J = 8.5$ Hz, 16.5 Hz, 1 H), 3.87 (dd, $J = 9$ Hz, 16.5 Hz, 1 H), 3.68 (d, $J = 9.5$ Hz, 1 H), 3.54 (d, $J = 9.5$ Hz, 1 H), 1.90 (dd, $J = 6$ Hz, 8.5 Hz, 2 H), 1.63 (t, $J = 8.5$ Hz, 2 H), 1.33-1.13 (m, 16), 0.862 (t, $J = 6$ Hz, 3 H). ^{13}C NMR (125 MHz, CDCl_3) δ 81.2, 78.9, 67.4, 39.8, 37.9, 31.9, 30.1, 29.59, 29.57, 29.54, 29.3, 24.6, 22.7, 14.1.



^1H NMR (500 MHz, CDCl_3) δ 4.01 (dd, $J = 8.5$ Hz, 16.5 Hz, 1 H), 3.87 (dd, $J = 9$ Hz, 16.5 Hz, 1 H), 3.68 (d, $J = 9.5$ Hz, 1 H), 3.53 (d, $J = 9.5$ Hz, 1 H), 1.90 (dd, $J = 6$ Hz, 8.5 Hz, 2 H), 1.62 (t, $J = 8.5$ Hz, 2 H), 1.32-1.14 (m, 20), 0.861 (t, $J = 6$ Hz, 3 H). ^{13}C NMR (125 MHz, CDCl_3) δ 78.9, 67.5, 39.8, 37.9, 31.9, 30.1, 29.64, 29.58, 29.3, 24.6, 22.7, 14.1.



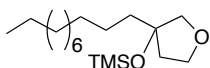
^1H NMR (500 MHz, CDCl_3) δ 4.00 (dd, $J = 8.5$ Hz, 16.5 Hz, 1 H), 3.87 (dd, $J = 9$ Hz, 16.5 Hz, 1 H), 3.68 (d, $J = 9.5$ Hz, 1 H), 3.53 (d, $J = 9.5$ Hz, 1 H), 1.90 (dd, $J = 6$ Hz, 8.5 Hz, 2 H), 1.62 (t, $J = 8.5$ Hz, 2 H), 1.34-1.18 (m, 24), 0.860 (t, $J = 7$ Hz, 3 H). ^{13}C NMR (125 MHz, CDCl_3) δ 81.2, 78.9, 67.4, 39.8, 37.9, 31.9, 30.1, 29.68, 29.67, 29.64, 29.57, 29.55, 29.3, 24.6, 22.7, 14.1.



^1H NMR (500 MHz, CDCl_3) δ 4.01 (dd, J = 8.5 Hz, 16.5 Hz, 1 H), 3.87 (dd, J = 9 Hz, 16.5 Hz, 1 H), 3.68 (d, J = 9.5 Hz, 1 H), 3.53 (d, J = 9.5 Hz, 1 H), 1.90 (dd, J = 6 Hz, 8.5 Hz, 2 H), 1.62 (t, J = 8.5 Hz, 2 H), 1.33-1.14 (m, 28), 0.860 (t, J = 7 Hz, 3 H). ^{13}C NMR (125 MHz, CDCl_3) δ 81.2, 78.9, 67.4, 39.8, 37.9, 31.9, 30.1, 29.68, 29.65, 29.57, 29.54, 29.3, 24.6, 22.7, 14.1.

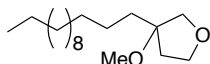
Protected Tetrahydrofuran Analogues

TMS-protected undecylhydroxytetrahydrofuran



Undecylhydroxytetrahydrofuran (1.0 equiv, 1.51 mmol, 365 mg) was dissolved in dried methylene chloride along with TMS chloride (1.1 equiv, 1.66 mmol, 0.21 mL) and imidazole (1.1 equiv, 1.66 mmol, 113 mg). The reaction was stirred at room temperature for 10 hours. The reaction mixture was diluted with diethyl ether and washed with brine (3 x 30 mL). The organic layer was dried over sodium sulfate and concentrated. The crude was purified using column chromatography (10% ethyl acetate in hexanes), yielding the clear product in 69%. ^1H NMR (500 MHz, CDCl_3) δ 3.94 (dd, J = 8.5 Hz, 16.5 Hz, 1 H), 3.84 (td, J = 4 Hz, 8.5 Hz, 1 H), 3.71 (d, J = 9 Hz, 1 H), 3.52 (d, J = 9 Hz, 1 H), 1.98-1.92 (m, 1 H), 1.86-1.78 (m, 1 H), 1.58 (t, J = 8.5 Hz, 2 H), 1.35-1.18 (m, 18), 0.862 (t, J = 7 Hz, 3 H), 0.109 (s, 9 H). ^{13}C NMR (125 MHz, CDCl_3) δ 83.9, 78.8, 67.8, 40.2, 39.6, 32.1, 30.3, 29.88, 29.87, 29.84, 29.6, 24.9, 22.9, 14.3, 2.29.

Methyl protected tridecylhydroxytetrahydrofuran



60% sodium hydride (1.5 equiv, 0.61 mmol, 24 mg) was added to a flame-dried flask with a stirbar. Dry THF was added to the flask before sealing and purging with nitrogen gas. 110 mg of tridecylhydroxytetrahydrofuran (1.0 equiv, 0.41 mmol) was added to the suspension and the solution was left stirring for 30 minutes. Finally, methyl iodide (1.5 equiv, 0.61 mmol, 0.04 mL) was added to the stirring solution and allowed to stir to completion observed via TLC. Water was added to the solution and it was left stirring for 8 hours. The solution was extracted with ethyl acetate. The organic layers were combined and dried over sodium sulfate. The organic solution was concentrated. The pure clear compound was isolated via column chromatography (20% ethyl acetate in hexanes) in 53% yield. ^1H NMR (500 MHz, CDCl_3) δ 4.00 (dd, $J = 7$ Hz, 14 Hz, 1 H), 3.87 (dd, $J = 9$ Hz, 16.5 Hz, 1 H), 3.89 (s, 3 H), 3.67 (d, $J = 9$ Hz, 1 H), 3.53 (d, $J = 9$ Hz, 1 H), 1.90 (dd, $J = 6$ Hz, 7.5 Hz, 2 H), 1.62 (t, $J = 8.5$ Hz, 2 H), 1.32-1.18 (m, 22), 0.860 (d, $J = 7$ Hz, 3 H). ^{13}C NMR (125 MHz, CDCl_3) δ 81.2, 78.9, 67.4, 60.4, 55.7, 39.8, 37.9, 31.9, 30.1, 29.7, 29.6, 29.5, 29.3, 24.6, 22.7, 21.0, 14.2, 14.1.

General Hemolysis Assay. A buffered solution of rabbit blood cells was diluted with an isotonic phosphate buffer solution (40 mL 0.066 M NaH_2PO_4 , 60 mL 0.0667 M Na_2HPO_4 , pH = 7.0, .46g/100mL NaCl) to 5×10^7 cells/mL. An eppendorf tube was filled with 400 μL of the cell solution and 20 μL of 10 $\mu\text{g/mL}$ of the analyzed compound or control. Triton X-100 served as the positive control. 20 μL of pure DMSO was used as a negative control along with a 400 μL sample of the

cell solution without any added compounds. The solutions were stirred via vortex and allowed to sit for 30 minutes. 100 μ L of the cell solution was added to a 96 well plate for microscopic evaluation. Microscopic photos were taken to keep record of the cell samples. The remaining portion of each cell solution was centrifuged at 11,000 rpm for 5 minutes. The supernatant was added to a 96 well plate to be analyzed by a Benchmark Biorad microplate reader at 550 nm.

REFERENCES

REFERENCES

1. Lesch, J. E. *The First Miracle Drugs : How the Sulfa Drugs Transformed Medicine*; Oxford University Press: Oxford, 2007.
2. Spellberg, B.; Guidos, R.; Gilbert, D.; Bradley, J.; Boucher, H. W.; Scheld, W. M.; Bartlett, J. G.; Edwards, J.; Archer, G. F.; Archer, G. F. "The Epidemic of Antibiotic-Resistant Infections: A Call to Action for the Medical Community from the Infectious Diseases Society of America" *Clinical Infectious Diseases* **2008**, *46*, 155.
3. Boucher, H. W.; Talbot, G. H.; Bradley, J. S.; Edwards, J. E.; Gilbert, D.; Rice, L. B.; Scheld, M.; Spellberg, B.; Bartlett, J. "Bad Bugs, No Drugs: No ESCAPE! An Update from the Infectious Diseases Society of America" *Clinical Infectious Diseases* **2009**, *48*, 1.
4. "The 10 × '20 Initiative: Pursuing a Global Commitment to Develop 10 New Antibacterial Drugs by 2020" *Clinical Infectious Diseases* **2010**, *50*, 1081.
5. Ling, L. L.; Schneider, T.; Peoples, A. J.; Spoering, A. L.; Engels, I.; Conlon, B. P.; Mueller, A.; Schabner, T. F.; Hughes, D. E.; Epstein, S.; Jones, M.; Lazarides, L.; Steadman, V. A.; Cohen, D. R.; Felix, C. R.; Fetterman, K. A.; Millett, W. P.; Nitti, A. G.; Zullo, A. M.; Chen, C.; Lewis, K. "A new antibiotic kills pathogens without detectable resistance" *Nature* **2015**, *517*, 455.
6. Gonzalez, R. J.; Tarloff, J. B. "Evaluation of hepatic subcellular fractions for Alamar blue and MTT reductase activity" *Toxicology in vitro : an international journal published in association with BIBRA* **2001**, *15*, 257.
7. Ahmed, S. A.; Gogal, R. M., Jr.; Walsh, J. E. "A new rapid and simple non-radioactive assay to monitor and determine the proliferation of lymphocytes: an alternative to [3H]thymidine incorporation assay" *Journal of immunological methods* **1994**, *170*, 211.
8. O'Brien, J.; Wilson, I.; Orton, T.; Pognan, F. "Investigation of the Alamar Blue (resazurin) fluorescent dye for the assessment of mammalian cell cytotoxicity" *European journal of biochemistry / FEBS* **2000**, *267*, 5421.
9. Moore, K. S.; Wehrli, S.; Roder, H.; Rogers, M.; Forrest, J. N., Jr.; McCrimmon, D.; Zasloff, M. "Squalamine: an aminosterol antibiotic from the shark" *Proceedings of the National Academy of Sciences of the United States of America* **1993**, *90*, 1354.

10. Hofmann, A. F.; Eckmann, L. "How bile acids confer gut mucosal protection against bacteria" *Proceedings of the National Academy of Sciences of the United States of America* **2006**, *103*, 4333.
11. Inagaki, T.; Moschetta, A.; Lee, Y.-K.; Peng, L.; Zhao, G.; Downes, M.; Yu, R. T.; Shelton, J. M.; Richardson, J. A.; Repa, J. J.; Mangelsdorf, D. J.; Kliewer, S. A. "Regulation of antibacterial defense in the small intestine by the nuclear bile acid receptor" *Proceedings of the National Academy of Sciences of the United States of America* **2006**, *103*, 3920.
12. Shai, Y. "Mechanism of the binding, insertion and destabilization of phospholipid bilayer membranes by alpha-helical antimicrobial and cell non-selective membrane-lytic peptides" *Biochimica et biophysica acta* **1999**, *1462*, 55.
13. Savage, P. B.; Li, C.; Taotafa, U.; Ding, B.; Guan, Q. "Antibacterial properties of cationic steroid antibiotics" *FEMS Microbiology Letters* **2002**, *217*, 1.
14. Savage, Paul B. "Design, Synthesis and Characterization of Cationic Peptide and Steroid Antibiotics" *European Journal of Organic Chemistry* **2002**, *2002*, 759.
15. Deng, G.; Dewa, T.; Regen, S. L. "A Synthetic Ionophore That Recognizes Negatively Charged Phospholipid Membranes" *Journal of the American Chemical Society* **1996**, *118*, 8975.
16. Kikuchi, K.; Bernard, E. M.; Sadownik, A.; Regen, S. L.; Armstrong, D. "Antimicrobial activities of squalamine mimics" *Antimicrobial agents and chemotherapy* **1997**, *41*, 1433.
17. Velkov, T.; Roberts, K. D.; Nation, R. L.; Thompson, P. E.; Li, J. "Pharmacology of polymyxins: new insights into an 'old' class of antibiotics" *Future microbiology* **2013**, *8*, 10.2217/fmb.13.39.
18. Ding, B.; Guan, Q.; Walsh, J. P.; Boswell, J. S.; Winter, T. W.; Winter, E. S.; Boyd, S. S.; Li, C.; Savage, P. B. "Correlation of the Antibacterial Activities of Cationic Peptide Antibiotics and Cationic Steroid Antibiotics" *Journal of Medicinal Chemistry* **2002**, *45*, 663.
19. Shamsuzzaman; Dar, A. M.; Khanam, H.; Gatoo, M. A. "Anticancer and antimicrobial evaluation of newly synthesized steroidal 5,6 fused benzothiazines" *Arabian Journal of Chemistry* **2014**, *7*, 461.
20. Coughlin, S. A.; Danz, D. W.; Robinson, R. G.; Klingbeil, K. M.; Wentland, M. P.; Corbett, T. H.; Waud, W. R.; Zwelling, L. A.; Altschuler, E.; Bales,

- E.; Rake, J. B. "Mechanism of action and antitumor activity of (S)-10-(2,6-dimethyl-4-pyridinyl)-9-fluoro-3-methyl-7-oxo-2,3-dihydro-7H-pyridol [1,2,3-de]-[1,4]benzothiazine-6-carboxylic acid (WIN 58161)" *Biochemical Pharmacology* **1995**, *50*, 111.
21. Wang, H.-j.; Gloer, K. B.; Gloer, J. B.; Scott, J. A.; Malloch, D. "Anserinones A and B: New Antifungal and Antibacterial Benzoquinones from the Coprophilous Fungus *Podospora anserina*" *Journal of Natural Products* **1997**, *60*, 629.
 22. Lana, E. J. L.; Carazza, F.; Takahashi, J. A. "Antibacterial Evaluation of 1,4-Benzoquinone Derivatives" *Journal of Agricultural and Food Chemistry* **2006**, *54*, 2053.
 23. COLWELL, C. A.; MCCALL, M. "STUDIES ON THE MECHANISM OF ANTIBACTERIAL ACTION OF 2-METHYL-1,4-NAPHTHOQUINONE" *Science* **1945**, *101*, 592.
 24. Johnson, J. H.; Meyers, E.; O'Sullivan, J.; Phillipson, D. W.; Robinson, G.; Trejo, W. H.; Wells, J. S. "Culpin, a novel hydroquinone antibiotic of fungal origin" *The Journal of antibiotics* **1989**, *42*, 1515.
 25. Cariello, L.; Zanetti, L.; Cuomo, V.; Vanzanella, F. "Antimicrobial activity of avarol, a sesquiterpenoid hydroquinone from the marine sponge, *dysidea avara*" *Comparative Biochemistry and Physiology Part B: Comparative Biochemistry* **1982**, *71*, 281.
 26. Ooi, N.; Chopra, I.; Eady, A.; Cove, J.; Bojar, R.; O'Neill, A. J. "Antibacterial activity and mode of action of tert-butylhydroquinone (TBHQ) and its oxidation product, tert-butylbenzoquinone (TBBQ)" *Journal of Antimicrobial Chemotherapy* **2013**, *68*, 1297.
 27. Zahler, R.; Jacobs, G. A.; Google Patents: 1989.
 28. Li, S.; Hao, L.; Bao, W.; Zhang, P.; Su, D.; Cheng, Y.; Nie, L.; Wang, G.; Hou, F.; Yang, Y. "A novel short anionic antibacterial peptide isolated from the skin of *Xenopus laevis* with broad antibacterial activity and inhibitory activity against breast cancer cell" *Archives of Microbiology* **2016**, *198*, 473.
 29. Cavallito, C. J.; Bailey, J. H. "Allicin, the Antibacterial Principle of *Allium sativum*. I. Isolation, Physical Properties and Antibacterial Action" *Journal of the American Chemical Society* **1944**, *66*, 1950.
 30. Ankri, S.; Mirelman, D. "Antimicrobial properties of allicin from garlic" *Microbes and Infection* **1999**, *1*, 125.

31. Hocquellet, A.; le Senechal, C.; Garbay, B. "Importance of the disulfide bridges in the antibacterial activity of human hepcidin" *Peptides* **2012**, *36*, 303.
32. Ganz, T. "Hepcidin, a key regulator of iron metabolism and mediator of anemia of inflammation" *Blood* **2003**, *102*, 783.
33. Keyes, R. F.; Carter, J. J.; Englund, E. E.; Daly, M. M.; Stone, G. G.; Nilius, A. M.; Ma, Z. "Synthesis and Antibacterial Activity of 6-O-Arylbutynyl Ketolides with Improved Activity against Some Key Erythromycin-Resistant Pathogens" *Journal of Medicinal Chemistry* **2003**, *46*, 1795.
34. Patel, S. K.; Tirkey, V.; Mishra, S.; Dash, H. R.; Das, S.; Shukla, M.; Saha, S.; Mobin, S. M.; Chatterjee, S. "Synthesis of mono- and bi-metallic dithiocarboxylate-alkyne complexes from sunlight driven insertion reaction and their antibacterial activity" *Journal of Organometallic Chemistry* **2014**, *749*, 75.
35. Schomaker, J. M.; Pulgam, V. R.; Borhan, B. "Synthesis of Diastereomerically and Enantiomerically Pure 2,3-Disubstituted Tetrahydrofurans Using a Sulfoxonium Ylide" *Journal of the American Chemical Society* **2004**, *126*, 13600.
36. Corey, E. J.; Venkateswarlu, A. "Protection of hydroxyl groups as tert-butyldimethylsilyl derivatives" *Journal of the American Chemical Society* **1972**, *94*, 6190.
37. Hamouda, T.; Myc, A.; Donovan, B.; Shih, A. Y.; Reuter, J. D.; Baker, J. R., Jr. "A novel surfactant nanoemulsion with a unique non-irritant topical antimicrobial activity against bacteria, enveloped viruses and fungi" *Microbiological research* **2001**, *156*, 1.
38. Kubo, I.; Muroi, H.; Kubo, A. "Antibacterial activity of long-chain alcohols against *Streptococcus mutans*" *Journal of Agricultural and Food Chemistry* **1993**, *41*, 2447.
39. Kubo, I.; Muroi, H.; Kubo, A. "Structural functions of antimicrobial long-chain alcohols and phenols" *Bioorganic & Medicinal Chemistry* **1995**, *3*, 873.
40. Norred, W. P.; Ansel, H. C.; Roth, I. L.; Peifer, J. J. "Mechanism of Dimethyl Sulfoxide-Induced Hemolysis" *Journal of Pharmaceutical Sciences* **1970**, *59*, 618.

41. Vollmer, W.; Höltje, J.-V. "The Architecture of the Murein (Peptidoglycan) in Gram-Negative Bacteria: Vertical Scaffold or Horizontal Layer(s)?" *Journal of bacteriology* **2004**, *186*, 5978.
42. Demchick, P.; Koch, A. L. "The permeability of the wall fabric of Escherichia coli and Bacillus subtilis" *Journal of bacteriology* **1996**, *178*, 768.
43. Malanovic, N.; Lohner, K. "Gram-positive bacterial cell envelopes: The impact on the activity of antimicrobial peptides" *Biochimica et Biophysica Acta (BBA) - Biomembranes* **2016**, *1858*, 936.
44. Martin, N. I.; Breukink, E. "The expanding role of lipid II as a target for lantibiotics" *Future Microbiology* **2007**, *2*, 513.
45. Marcos, J. F.; Gandía, M. "Antimicrobial peptides: to membranes and beyond" *Expert opinion on drug discovery* **2009**, *4*, 659.
46. Percy, M. G.; Gründling, A. "Lipoteichoic Acid Synthesis and Function in Gram-Positive Bacteria" *Annual Review of Microbiology* **2014**, *68*, 81.
47. Oku, Y.; Kurokawa, K.; Matsuo, M.; Yamada, S.; Lee, B.-L.; Sekimizu, K. "Pleiotropic Roles of Polyglycerolphosphate Synthase of Lipoteichoic Acid in Growth of Staphylococcus aureus Cells" *Journal of bacteriology* **2009**, *191*, 141.
48. Nikaido, H.; Nakae, T. In *Advances in Microbial Physiology*; Rose, A. H., Morris, J. G., Eds.; Academic Press: 1980; Vol. Volume 20, p 163.
49. Alakomi, H. L.; Skyttä, E.; Saarela, M.; Mattila-Sandholm, T.; Latva-Kala, K.; Helander, I. M. "Lactic Acid Permeabilizes Gram-Negative Bacteria by Disrupting the Outer Membrane" *Applied and environmental microbiology* **2000**, *66*, 2001.

Chapter II

Steps Towards the Total Synthesis of (+)-Alexine via One-Carbon Homologative Relay Ring Expansion

II.1. Introduction

II.1.1. Discovery of Alexine

Alexine (**II-1**) is a polyhydroxylated pyrrolizidine isolated from *Alexa leiopetala* in 1988 by Robert Nash and coworkers³. (1R, 2R, 3R, 7S, 8S)-3-hydroxymethyl-1, 2, 7-trihydroxypyrrolizidine, given the common name alexine, was the first example of a pyrrolizidine with a carbon substituent on C3. It was also found to closely resemble (2R, 5R)-dihydroxymethyl-(3R, 4R)-dihydroxypyrrolidine (DMDP) (**II-2**), a known glucosidase inhibitor found in *leguminosae derris* and *leguminosae lonchocarpus*.

II.1.2. Biological Activity of Alexine

Due to this resemblance to DMDP, alexine was tested for glucosidase inhibition. In initial screenings in 1988, alexine barely performed, inhibiting the hydrolysis of 6 mM *p*-nitrophenyl- α -D-glucopyranoside and 10 mM *p*-nitrophenyl- β -D-glucopyranoside by less than 50% at $>3.3 \times 10^{-4}$ M and 10 mM *p*-nitrophenyl- β -D-galactopyranoside by 50% at 1.5×10^{-4} M. While DMDP exhibited weak inhibition of α -D-glucopyranosidase, the inhibition of the β -anomer disaccharidase and the galactopyranosidase was much more effective (3.0×10^{-4}

M, 1.0×10^{-5} M, and 2.0×10^{-6} M, respectively). Additional biological testing by Nash in 1990 showed that alexines as a general class provided a weak activity, if any, with regard to mammalian glycosidases compared to castanosperamine (**II-7**).⁴

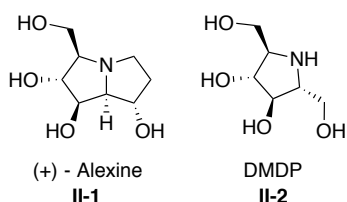


Figure II-1: Alexine structural comparison to DMDP.

In an overall sense, the evaluated alexines are not very effective against mammalian glucosidases. It is important to note, however, that there are varying activities that are solely dependent on the variation of particular stereocenters. When comparing alexine (**II-1**) and 3, 7a-diepialexine (**II-3**), the change in the two stereocenters decreases a moderate 50% inhibition (5.9×10^{-5} M for alexine) in trehalase to no observable inhibition at all ($>3.3 \times 10^{-4}$ M for 3, 7a-diepialexine). Interestingly, 1, 7a- and 7, 7a-diepialexines show an opposite effect when compared to alexine with regards to *p*-nitrophenyl- α -D-glucopyranoside (9.5×10^{-5} M, 1.5×10^{-5} M, and $>3.3 \times 10^{-4}$ M, respectively).

It is important to note that the alexines have exhibited a more significant inhibitory activity on fungal glucan1,4- α -glucosidase (amyloglucosidase). Alexine (**II-1**) has

also been found to effectively inhibit specific thioglucosidases. While castanospermine seems to have a promiscuous mode of action with regard to enzyme inhibition, the pyrrolizidines seem to be much more selective in their operation. It is, in this regard, apparent that though alexine seems to have inferior activity towards mammalian glycosides, the activities can potentially be manipulated by synthesizing alternative diastereomers and analogues.

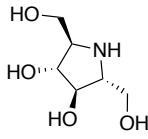
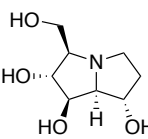
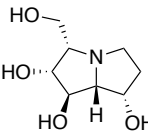
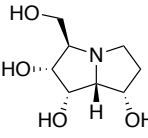
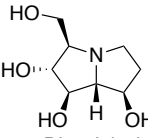
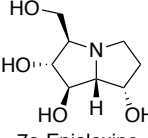
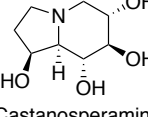
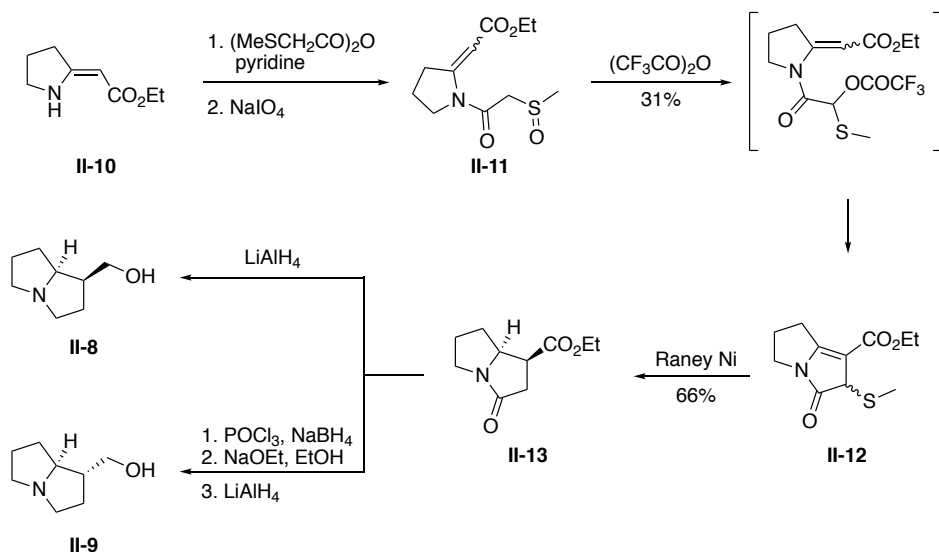
Entry	Inhibitor	p-Nitrophenyl- α -D-glucopyranosidase	p-Nitrophenyl- β -D-glucopyranosidase	p-Nitrophenyl- β -D-galactopyranosidase	Trehalase
1	 DMDP (II-2)	3.0×10^{-4}	1.0×10^{-5}	2.0×10^{-6}	--
2	 Alexine (II-1)	$>3.3 \times 10^{-4}$	$>3.3 \times 10^{-4}$	1.5×10^{-4}	5.9×10^{-5}
3	 3, 7a-Diepialexine (II-3)	$>3.3 \times 10^{-4}$	$>3.3 \times 10^{-4}$	--	$>3.3 \times 10^{-4}$
4	 1, 7a-Diepialexine (II-4)	9.5×10^{-5}	$>3.3 \times 10^{-4}$	--	$>3.3 \times 10^{-4}$
5	 7, 7a-Diepialexine (II-5)	1.6×10^{-5}	2.3×10^{-4}	--	1.0×10^{-4}
6	 7a-Epialexine (II-6)	$>3.3 \times 10^{-4}$	3.3×10^{-4}	--	$>3.3 \times 10^{-4}$
7	 Castanosperamine (II-7)	2.8×10^{-6}	1.7×10^{-5}	--	9.8×10^{-6}

Table II-1: Action of naturally occurring alexines on mouse gut digestive glucosidase activity compared with those of DMP and castanospermine. Concentration (M) of alkaloid giving 50% inhibition. $>3.3 \times 10^{-4}$ required for 50% inhibition.^{3 4}

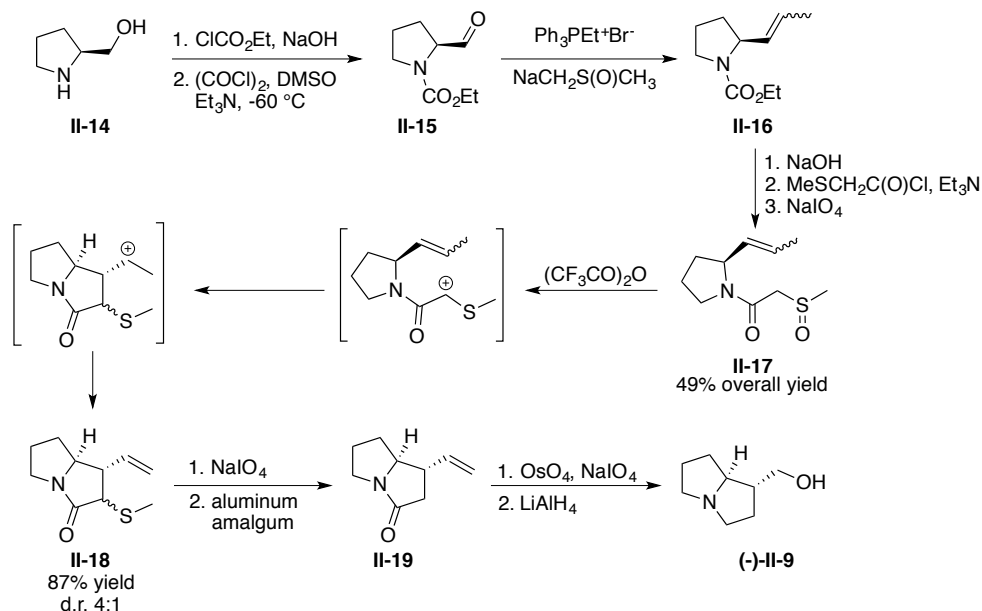
II.1.3. Previous Synthetic Approaches to Alexine and Other Members of the Family

Most approaches to pyrrolizidines involved naturally chiral compounds, specifically amino acids, sugars, and their derivatives. Earlier pyrrolizidine synthesis included the synthesis of necines and necic acids.⁵⁴ Synthesis of racemic isoretronecanol (**II-8**) and trachelanthamidine (**II-9**) utilized an unsaturated pyrrolidine ester (**II-10**) that, after amidation, oxidative esterification, and cyclization, afforded an unsaturated pyrrolizidine (**II-12**) in 66% yield. This compound produced **II-8** after a two-step reduction sequence. In order to form trachelanthamidine, the ester α -carbon of lactam **II-13** was flipped under basic conditions, producing the desired compound after the final hydride reduction.



Scheme II-1: Synthesis of pyrrolizidine natural products isoretronecanol (**II-8**) and trachelanthamidine (**II-9**).

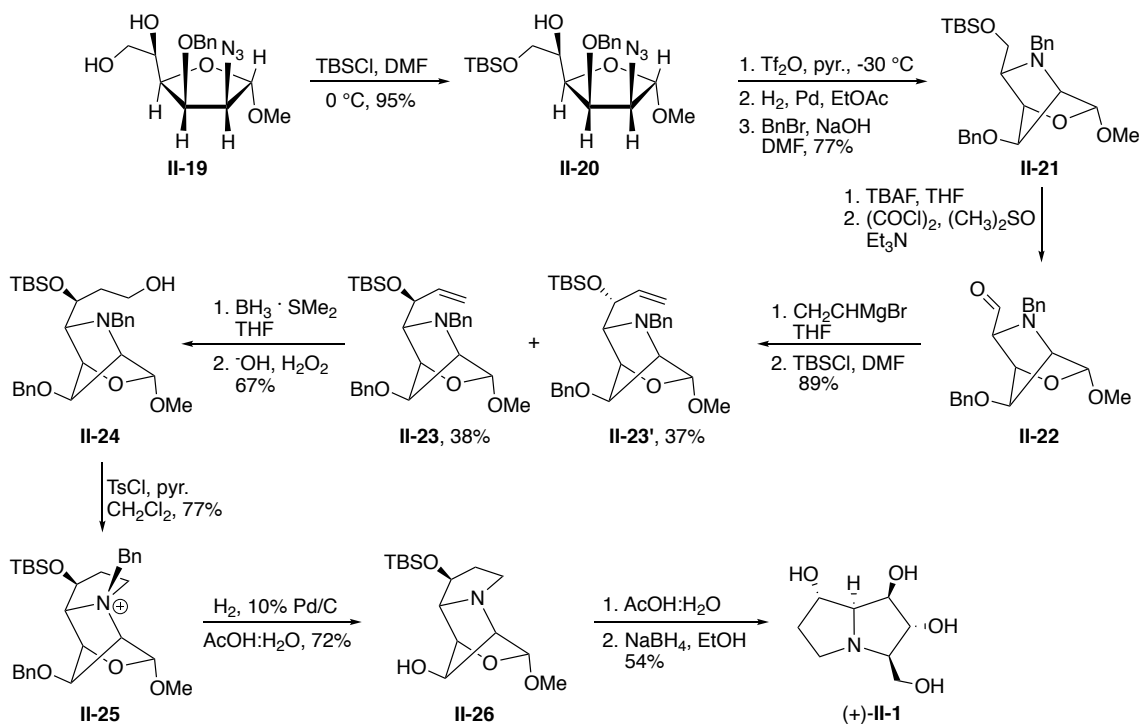
In order to synthesize trachelanthamidine chirally,⁵⁵ Ishibashi turned to L-prolinol (**II-14**) to provide the initial chirality on which the synthesis would depend (Scheme II-2). *N*-protection and Swern oxidation gave pyrrolidinal (**II-15**), followed by Wittig olefination to produce olefin (**II-16**) unselectively. After *N*-deprotection of (**II-16**), the pyrrolidine nitrogen was amidated using MeSCH₂C(O)Cl and triethylamine followed by oxidation to sulfoxide (**II-17**) with sodium periodate with an overall yield of 49% from L-prolinol. Trifluoroacetic anhydride was used to form pyrrolizidine **II-18** in 87% yield through a carbocation sequence similar to the mechanisms of the racemic synthesis that would form a terminal olefin handle for further functionalization. It is important to note that cyclization occurred stereospecifically and gave the desired stereochemistry of the pendant olefin. Formation of the olefin was regiospecific.



Scheme II-2: Synthesis of (-)-Trachelanthamidine (**II-9**).

^1H NMR showed the existence of two diastereomers in a ratio of 4:1. Sulfur was removed by oxidation to the sulfoxide and removal with aluminum amalgam to give compound (**II-19**). Oxidative cleavage of the olefin followed by global reduction produced (-)-trachelanthamidine (-)-**II-9**.

Similarly, many syntheses of pyrrolizidine natural products begin with simple chiral compounds, usually amino acids, sugars and their derivatives. For example, the first synthesis of (+)-alexine was accomplished using D-glucose as the template,⁵⁶ featured in Scheme II-3.



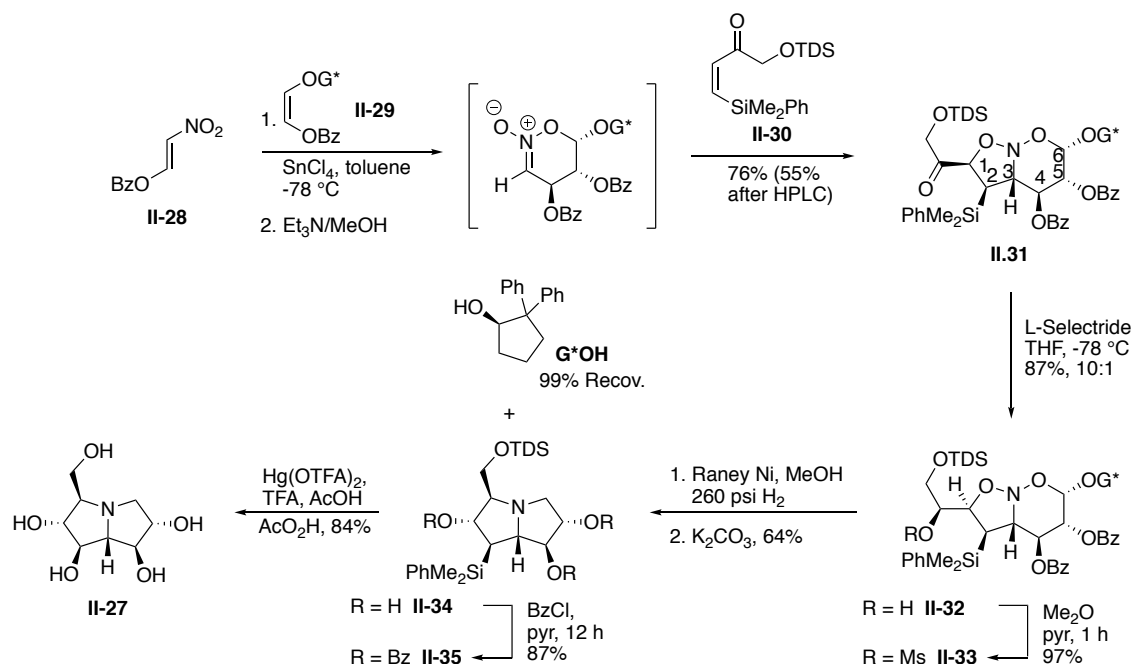
Scheme II-3: First synthesis of (+)-Alexine (**II-1**). This initial synthesis was based on the inherent chirality of D-glucose.

Methyl-2-azido-3-O-benzyl-2-deoxy- α -D-mannofuranoside (**II-19**), a compound synthesized from D-glucose by Fleet and coworkers,⁵⁷ was submitted to a selective silyl protection of the primary alcohol. Silyl ether **II-20** was triflated and the azide reduced, resulting in immediate cyclization to form bicyclic compound **II-21** after benzyl protection of the secondary amine.

Deprotection and Swern oxidation of **II-21** gave aldehyde **II-22**, which was submitted to nucleophilic addition of vinylmagnesium bromide. Epimeric alcohols **II-23** and **II-23'** were formed in almost equal amounts (38% and 37%) and subsequently, silyl protected with TBSCl. While compound **II-23'** was used to synthesize 7-epialexine, researchers continued with **II-23** to make (+)-alexine by hydroborating and oxidizing the terminal alkene to form primary alcohol **II-24** in 67% yield. Tosylation of the primary alcohol resulted in spontaneous cyclization to form ammonium **II-25**. Global benzyl deprotection followed by acid mediated silyl deprotection and hydrolysis of the furanoside provided **II-1** in 54% after sodium borohydride reduction of the lactol and ion exchange chromatographic purification.

Much of the synthesis of members of the alexine family, including every synthesis of (+)-alexine (**II-1**), was achieved by the same means as this initial synthesis of alexine and the pyrrolizidines before it.

The first achiral to chiral synthesis of a member of the alexine family, featured in Scheme II-4, was the Denmark synthesis of (+)-casuarine (**II-27**),⁵⁸ a pentahydroxypyrrolizidine effective in the inhibition of glucosidase I. Utilizing a tandem [4+2]/[3+2] bicyclization of nitroalkene (**II-28**), chiral auxillary-protected cis-vinyl ether (**II-29**), and dipolarophile (**II-30**), researchers were able to synthesize the key nitroso acetal intermediate that would provide **II-27** after reduction, oxidation of C-Si bond, and global deprotection.



Scheme II-4: Synthesis of (+)-Casuarine.

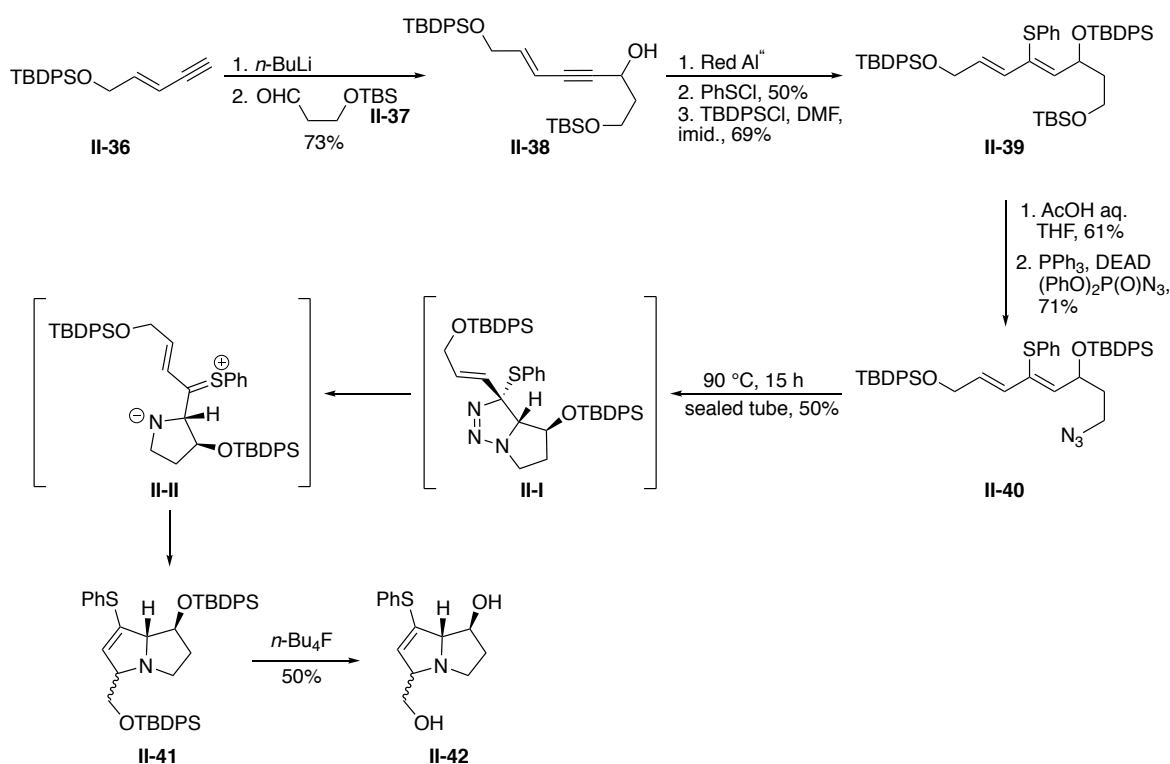
As mentioned previously, the chirality is induced using a chiral auxiliary during the [4+2] cyclization. This sets stereocenters at C4, C5, and C6, which in turn, along with the rigidity of the newly constructed 6-member heterocycle, establish the stereochemistry at carbons C1, C2, and C3 via the subsequent [3+2]

cyclization to form bicyclic ketone **II-31**. Denmark utilizes a similar method in the synthesis of (+)-1-epiaustraline,⁵⁹ incorporating tethered components for the [3+2] cyclization but inducing the intermolecular [4+2] cyclization prior.

Pearson and coworkers attempted a racemic synthesis utilizing the cyclization of an azodiene (**II-40**),⁶⁰ forming the desired pyrrolizidine with incorporation of the fully arranged and complete carbon skeleton. Though this synthesis is racemic, it is of note because of introduction of chirality to an achiral substrate followed by the incorporation of all other stereocenters in a process reliant on the originally introduced stereocenter. They propose the formation of triazoline (**II-I**), which undergoes fragmentation to zwitterion (**II-II**) and release of nitrogen gas to then recyclize via a slightly favored exo cyclization.

The synthesis began with the nucleophilic addition of enyne (**II-36**) to aldehyde (**II-37**). This synthesis had the potential to be an asymmetric synthesis of alexine or the C7 diastereomer of alexine with the formation of alcohol **II-38**. However, the use of a general and nonselective nucleophilic addition produced **II-38** a racemic mixture. Red Al alkyne reduction followed by a PhSCI quench resulted in vinyl thiol ether (**II-40**). Secondary alcohol protection followed by primary deprotection and Mitsunobu led to azide (**II-40**), the precursor to the key step of this synthesis. Cyclization produced lower yields (50%) and selectivities (70:30 diastereoselectivity) of pyrrolizidine **II-41** than would have been preferred. Global

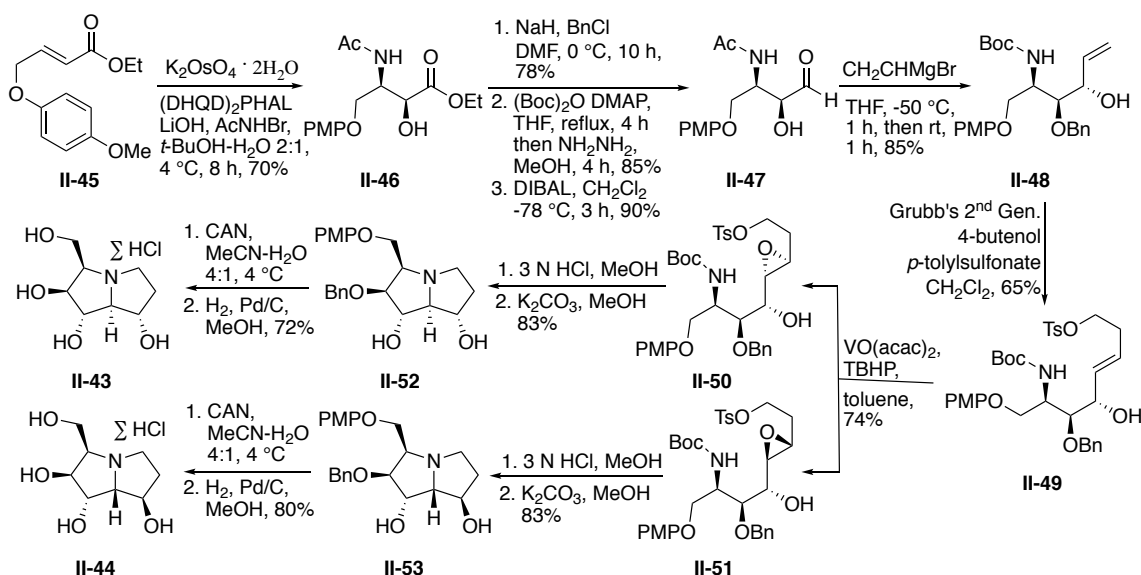
deprotection was also low yielding at 50%. All final attempts to use the vinyl sulfide to introduce the remaining hydroxyl groups failed leaving the synthesis incomplete and causing researchers to pursue other methods of synthesis.



Scheme II-5: Attempted synthesis of 3-epialexine analogues.

Han and coworkers⁶¹ chose a more fragmented synthesis utilizing Sharpless asymmetric aminohydroxylation to impose the chirality of the initial stereoisomers. In this case, the carbon skeleton is pieced together and the oxygens placed before culmination in a double cyclization of the amine to form the alexines of choice, 1,2-diepi-alexine (**II-43**) and 1,2,7-triepi-australine (**II-44**).

Aminohydroxylation of achiral ester (**II-45**) produced amino alcohol (**II-46**) in 70% yield and excellent regio- (>20:1) and enantioselectivity (>99% ee after recrystallization). After protection and reduction to form aldehyde (**II-47**), vinylmagnesium bromide was used to form alcohol (**II-48**) in a diastereomeric ratio of 4:1. Cross metathesis installs the remaining carbons with a primary



Scheme II-6: Asymmetric synthesis of 1,2-diepi-alexine and 1,2,7-triepi-australine via Sharpless aminohydroxylation.

tosylate leaving group. Vanadium-mediated epoxidation provided epoxides **II-50** and **II-51** as an inseparable mixture of diastereomers in a ratio of 2:3, respectively. Acidic deprotection followed by basification led to double cyclization producing pyrrolizidines **II-52** and **II-53** in 83% yield. Final deprotections removed the PMP and benzyl groups, giving 72% of diepi-alexine hydrochloric acid salt (**II-43**) and 80% of triepti-australine hydrochloric acid salt (**II-44**).

II.1.4. Retrosynthesis of Alexine

While all previous alexine syntheses and most general syntheses of polyhydroxylpyrrolidines were based on the chirality of an amino acid, a sugar, or a derivative of either, we devised a synthesis that would begin with an achiral starting material, with each additional step amenable for the synthesis of any diastereomer of alexine. In our synthesis of alexine, we desired the early incorporation of the necessary carbons with the later stage chiral addition of the hydroxyl groups. A working synthesis of this type would allow for synthesis of alexine analogues with little augmentation of the reaction sequence. We visualized the synthesis culminating in a chiral anti-dihydroxylation and benzyl deprotection to produce the final hydroxylated pyrrolizidine **II-1** (Figure II-2). Tosyl deprotection and palladium-mediated amino-cyclization of pyrrolidine (**II-55**) will form unsaturated pyrrolizidine (**II-54**). The construction of the pyrrolidine ring will be achieved via one carbon homologative relay ring expansion of

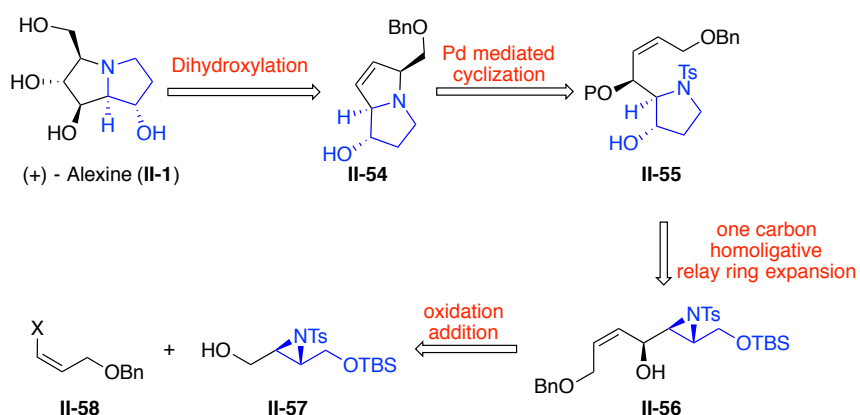


Figure II-2: Retrosynthetic analysis of (+)-Alexine (**II-1**) via one-carbon homologative relay ring expansion.

aziridine (**II-56**), a methodology developed by Borhan and coworkers (Figure (II-3)).⁶² This methodology relies on the basic and nucleophilic nature of a ylide created under basic conditions from sulfoxonium iodide (**II-61**) to react with an aziridinol (**II-59**) to form a 2,3-disubstituted pyrrolidine (**II-60**) with stereochemistry determined by the substitution of the aziridinol. Aziridinol deprotonation by the ylide causes formation of aza-Payne rearrangement product (**II-B**). Subsequent ylide attack creates dianion (**II-D**). 5-Exo-tet cyclization gives rise to the ring-expanded pyrrolidine (**II-E**). It should be noted that the aziridine submitted to this methodology in this synthesis is the most complex compound

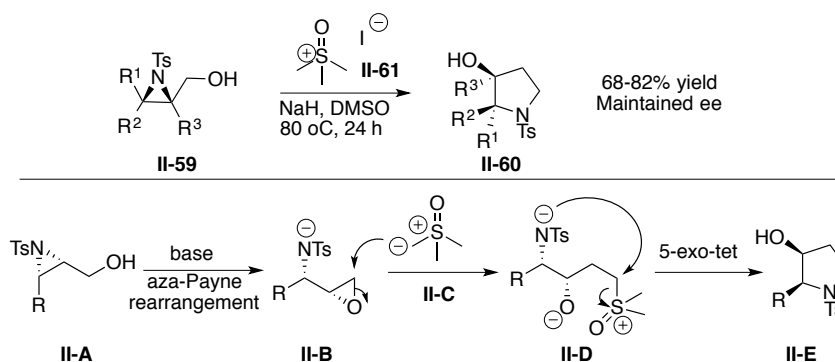


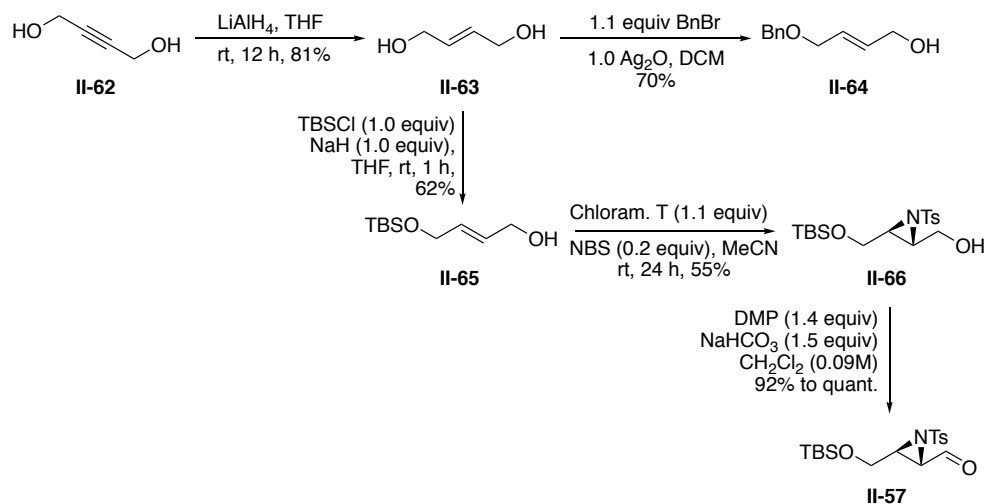
Figure II-3: One-carbon homoligative relay ring expansion of aziridinols.

submitted to this reaction, producing all of the required carbons for the alexine skeleton after cyclization. This aziridinol (**II-56**) can be synthesized using oxidation of a simpler disubstituted aziridinol followed by nucleophilic addition of protected allyl alcohol (**II-58**) to the aldehyde (**II-57**).

II.2. Results and Discussion

II.2.1. Synthesis of Alexine

Our synthesis of alexine began with the synthesis of the simple aziridinol **II-57** via the reduction of commercially available 2-butyne-1,4-diol with LiAlH_4 (Scheme II-7). This reaction produced trans-1,4-butanediol in 54% yield. Decreasing the equivalents of LAH from 2.0 equivalents to 1.2 equivalents and adding Celite® to the work up to prevent the coagulation of the aluminum gel and the sequestration of the diol produced gave the alkene diol **II-63** in 81% yield. Initial monoprotection of trans-alkenediol **II-63** with benzyl bromide proceeded in 70% of **II-64**. Though this procedure normally provides higher yields,⁶³ the reaction was not optimized. We decided it would be more feasible to use a less permanent protecting group and reserve the benzyl protection for a functionality that would endure to the end of the total synthesis, namely the allyl alcohol **II-69**. In searching for a new protecting group, initial attempts at mono protection using silyl chlorides and dehydropyran provided low yields, of which *tert*-butyldimethylsilyl chloride provided the highest at 34%. Later optimizations using sodium hydride brought the yield up to 62% approximately doubling the yield. Allyl alcohol **II-65** was submitted to a racemic aziridination using chloramine-T and *N*-bromosuccinimide to provide 55% of aziridinol **II-66**. Dess-Martin periodinane oxidation gave high yields of aziridinal **II-57** (92% to quantitative yield).

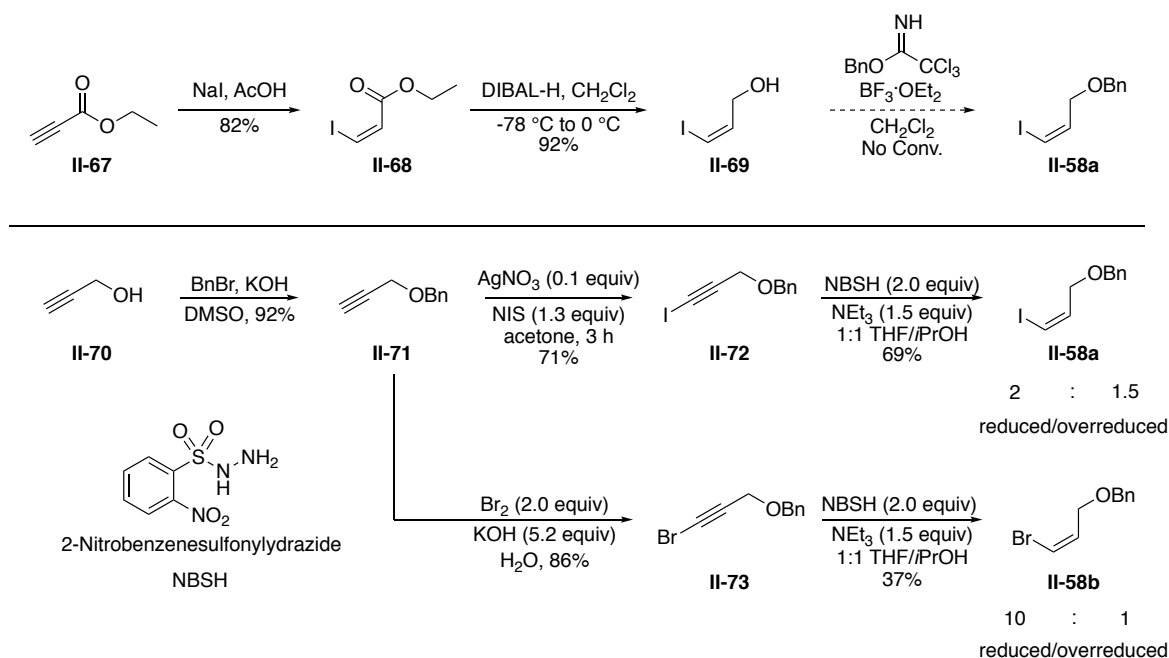


Scheme II-7: Synthesis of aziridinal fragment **II-57**.

As shown in Scheme II-8, synthesis of vinyl halide **II-58** began with a procedure done by Beruben et. al.⁶⁴ that incorporated the hydroiodination of commercially available ethyl propiolate **II-67** (82%) and subsequent DIBAL-H reduction of (Z)-b-iodo ethyl acrylate (**II-68**), giving cis-allyl alcohol **II-69** in 92% yield. In order to avoid elimination and formation of the protected propargyl alcohol, we attempted the acidic benzyl protection of **II-69**. All attempts at benzyl protection under acidic conditions failed, giving rise to a change in the method for the synthesis of ether **II-58**.

Commercially available propargyl alcohol (**II-70**) was benzyl protected under basic conditions giving benzyl propargyl ether (**II-71**). Alkyne iodination gave **II-72** in 71% yield. Utilizing NBSH reduction, **II-58a** was formed in a decent yield (69%) but produced a substantial amount of overreduced alkyl halide in

combination with the desired vinyl iodide (3:4, respectively). In a similar sequence, benzyl propargyl ether was brominated in aqueous potassium



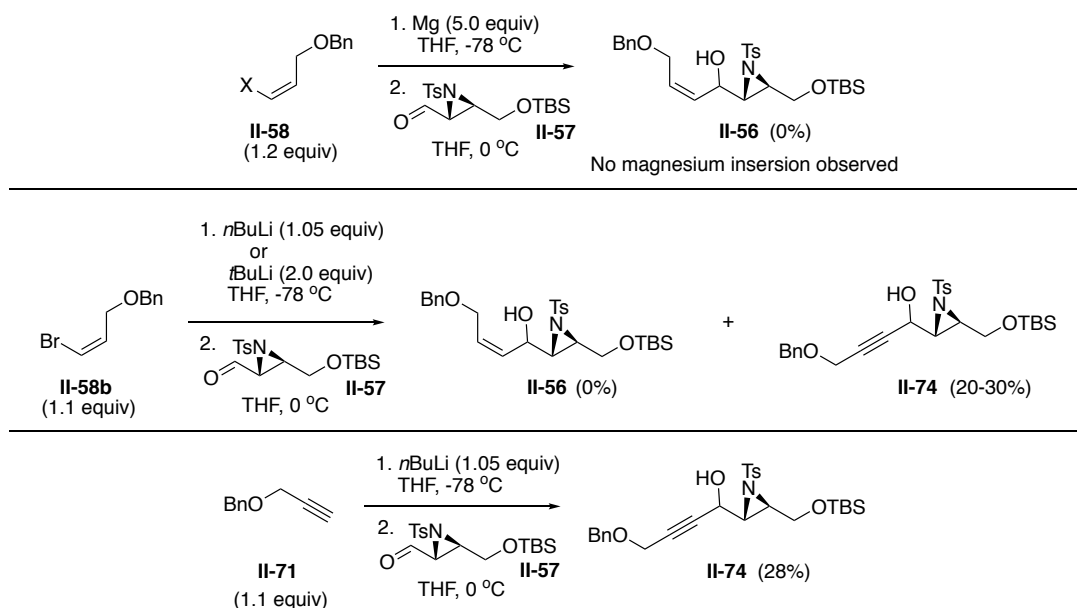
Scheme II-8: Synthesis of vinyl halide fragment **II-58**.

hydroxide. NBSH alkyne reduction to produce **II-58b** proceeded much less efficiently, giving 37% yield with a much lower instance of overreduction (10:1, alkene to alkane). It should also be noted that while iodination of the alkyne utilizes expensive reagents, bromination is significantly more economical and produces a greater overall selectivity in the end.

In an exploration of nucleophilic addition of organometallic reagents to aziridinals,

⁶⁵ Kulshrestha et. al. found that the aziridine substitution and the nitrogen protecting group affect the stereochemistry and selectivity of the resulting

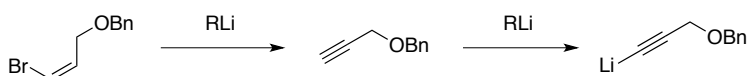
alcohol. While this study is thorough, addressing aliphatic, aromatic, and acetylenic organometallics, it does not extend to cis-vinyl organometallics. Therefore, the nucleophilic addition of **II-58** to aziridinal **II-57** featured in Scheme II-9 would expand on the previous study.



Scheme II-9: Initial nucleophilic combination of fragments.

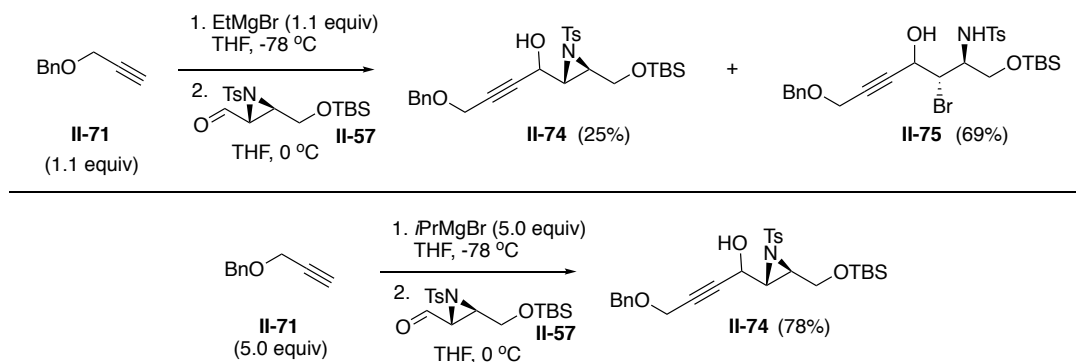
Initial attempts to nucleophilically introduce vinyl halide **II-58** to aziridinal **II-57** via Grignard addition failed using both the vinyl bromide **II-58b** and the vinyl iodide **II-58a**. Since the vinyl halide was not consumed, it appeared that the vinyl Grignard was not forming. Lithium-halogen exchange resulted in the complete consumption of the vinyl halide though the expected allyl aziridinol **II-56** was not observed. Instead, the propargyl aziridinol **II-74** formed in 20-30% yield. It appears that alkyl lithium was causing the dehydrohalogenation of the vinyl halide resulting in the formation of **II-71** in situ, followed by formation of the

alkynyl lithium nucleophile (Scheme II-10). This is a surprising outcome because Beruben and coworkers were able to form the cis-vinyl lithium adduct under similar conditions with the only difference being the substrate protecting group. In order to verify the synthesis of **II-74**, benzyl protected propargyl alcohol **II-71** was submitted directly to the nucleophilic addition to aziridinal **II-56**, producing **II-74** in 28% yield.



Scheme II-10: Dehydrohalogenation of cis-vinyl halide **II-58b** and lithiation of in situ formed alkyne.

Ethylmagnesium bromide as a base was much more reactive (Scheme II-11), giving **II-74** and bromoamine **II-75** in a ratio of 1:3 favoring the ring opened product. We theorize that the ethylmagnesium bromide disproportionated into diethyl magnesium and magnesium bromide via the Schlenck equilibrium, both a Lewis acid and a source of nucleophilic bromide. This has long been used as a



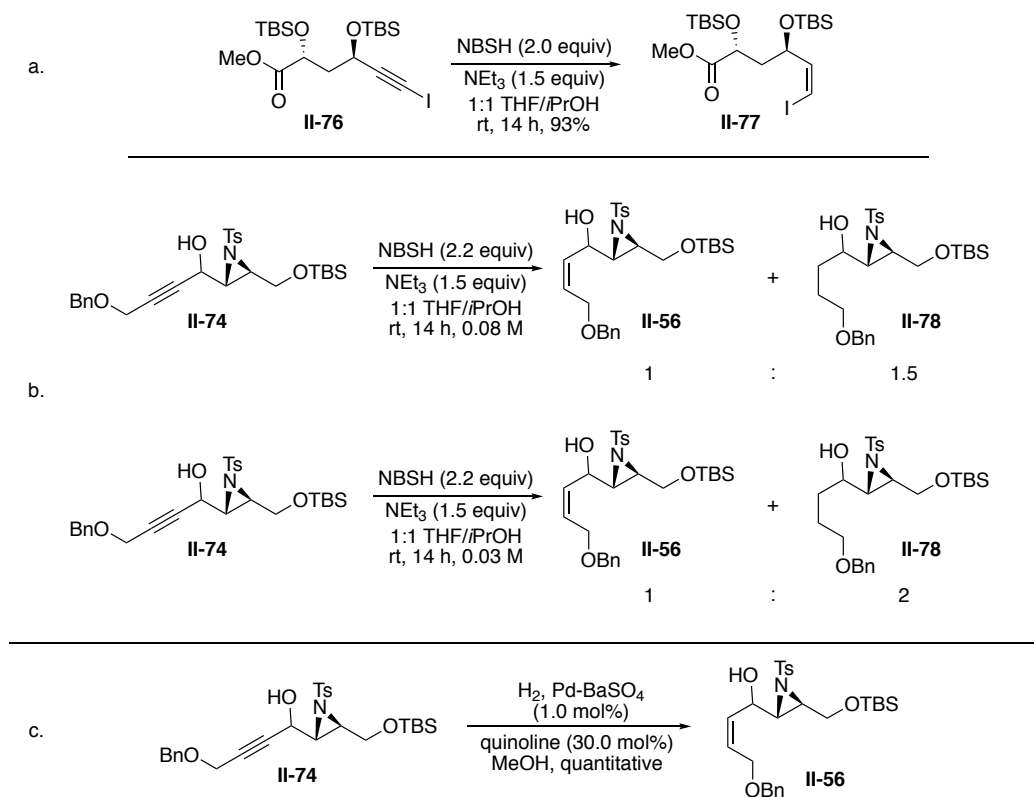
Scheme II-11: Nucleophilic addition using Grignard bases.

method for preparing dialkylmagnesium compounds.⁶⁶ In order to discourage the formation of the dialkylmagnesium, isopropylmagnesium bromide was submitted as a base. The modified reaction provided 78% of **II-74** with no formation of the ring-opened **II-75**.

It should be noted that only one diastereomeric product was produced by this addition. This is intriguing because Kulshrestha showed that trans substituted tosyl-protected aziridinals should produce a ratio of 70:30 of syn to anti when acetylene magnesium bromide is the nucleophile of choice. Due to the formation of this single diastereomer, we decided to postpone syn/anti assignment because the new stereocenter is and will be on a freely rotating portion of the synthetic intermediate until after the ring expansion.

Initial reduction of complex alkyne **II-74** featured in Scheme II-12 was attempted using NBSH reduction. Wulff and coworkers showed the utility of NBSH for the purposes of partial alkyne reduction in the synthesis of Fostriecin.⁶⁷ Attempting this partial reduction of **II-74** with NBSH was much less effective, providing mixtures of products at different reductive levels-from unreduced to completely saturated. Even after employing observed optimizations, overreduction was a major product. We found that palladium on barium sulfate provided a quantitative yield of **II-56**.

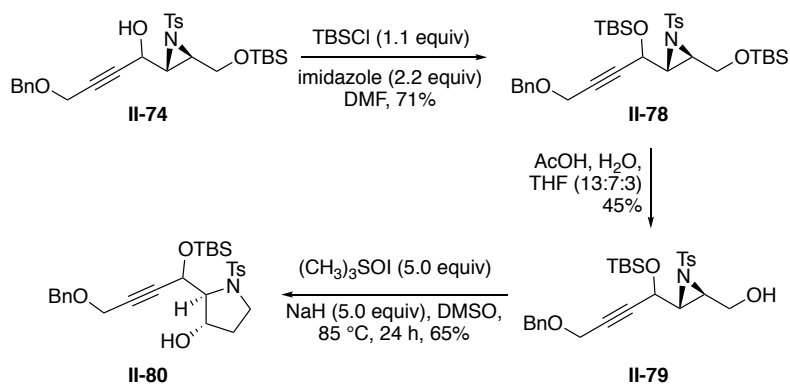
With aziridinol **II-56** in hand, it was important to protect the secondary alcohol and free the primary alcohol in order to prepare the compound for one-carbon homologative relay ring expansion. To this end and in attempts to protect and selectively free the primary alcohol, we initially attempted MOM protection with MOMCl in diisopropyl ethylamine only retrieving starting material. More reactive conditions, MOMCl with sodium iodide and diisopropyl ethylamine in dimethoxyethane (DME), led to small amounts of product and deterioration of the starting material. Even methyl etherification using dimethyl sulfate and TBAI



Scheme II-12: Alkyne reduction. a. The NBSH reduction performed by Phillips et al. provided 93% of desired product. b. NBSH reduction of propargyl aziridinol proved more reactive and difficult to partially reduce. c. Palladium on barium sulfate proved sufficient for a quantitative partial reduction to give the desired *cis*-alkene.

(0.5%) in a biphasic solution of 30% aqueous sodium hydroxide and light petroleum ether gave no noticeable yield of the desired product. Acidic PMB protections catalyzed by PPTS also showed no conversion. Silyl protection using TBDPSCI and TBSCl were also ineffective.

The difficulty in protecting allyl aziridinol **II-56** led us to consider protection of propargyl aziridinol **II-74** instead. Reactive MOMCl protection with sodium iodide also failed using this substrate. TBSCl provided the only successful protection of the secondary alcohol with 71% yield of diprotected aziridine **II-78** (Scheme II-13). An economic selective deprotection of the primary alcohol proceeded to give 45% yield of aziridinol **II-79** before the formation of significant amounts of doubly deprotected aziridinediol. As an analogue of **II-56**, **II-79** was submitted to the one-carbon homologative relay ring expansion and produced pyrrolidine **II-80** in 65% yield with what appeared to be two diastereomers (d.r. = 3.5:1). While this is on the lower side of the yields seen in Schomaker's chemistry, the result is



Scheme II-13: Silyl exchange and one-carbon homologative relay ring expansion.

reasonably good in lieu of the complexity of the substrate with no real optimization. Additionally, the diastereomeric ratio is interesting. It is known that the pyrrolidines formed using the one-carbon homologative relay ring expansion generally produce a single diastereomer with little change in the purity of enantiomerically enriched substrates. The fact that pyrrolidine II-80 was produced in two diastereomers suggests that a previous step in which diastereomers could be produced, namely, the nucleophilic addition of the metalloalkyne of propargyl ether II-71 to aziridinal II-57, did produce diastereomers but did not show obvious signs of the two molecules via general spectroscopic means. These ratios are comparable to those seen in tosyl-protected trans-aziridinals with ethynylmagnesium bromide (70:30, *syn* : *anti*).⁶⁵

In initial attempts to deprotect the secondary TBS group with tetrabutylammonium fluoride and to remove the tosyl group from the nitrogen with magnesium powder in methanol produced inconclusive results. Further advancements into the total synthesis of alexine (II-1) are still being investigated.

II.3. Conclusion

Pyrrolizidine syntheses have generally utilized small chiral compounds as initial building blocks in their synthesis and impose subsequent modifications on the original chiral center. More specifically, alexine has had very few syntheses that did not begin with a chiral building block of some sort. Our synthesis was

designed to impose the desired chirality upon an achiral substrate and cleverly and predictably add carbon skeleton and hydroxyl moieties that would, with little change to the total synthesis, be able to create new and different diastereomeric analogues of alexine. To this end and in attempts to explore cis-vinylmagnesium bromide addition to aziridinals, we attempted the nucleophilic addition of vinyl halide **II-58** to aziridinal **II-57**. Instead of the desired product, propargyl ether incorporation was the only product observed. Utilizing the lithium acetylenide provided the newly desired propargyl aziridinol in low yields. The desire to increase nucleophile reactivity and prevent Grignard disproportionation left us with isopropylmagnesium bromide as the ideal base to provide the necessary acetylene magnesium bromide in adequate yields. Due to the ineffectivity of the partially reduced **II-56**, alkyne **II-74** was submitted to a silyl exchange, protecting the new secondary alcohol and liberating the primary alcohol in preparation for the one-carbon homologative relay ring expansion. This reaction resulted in the complex disubstituted pyrrolidine in comparable yield to that of the more simple substrates initially tested in the development of this method. It should be noted that this is the most complex substrate submitted to this reaction.

In order to complete this synthesis, it will be necessary to remove the tosyl protecting group. While it is a necessary protecting group for the efficiency of the relay ring expansion, it is a somewhat temperamental process and must be tested

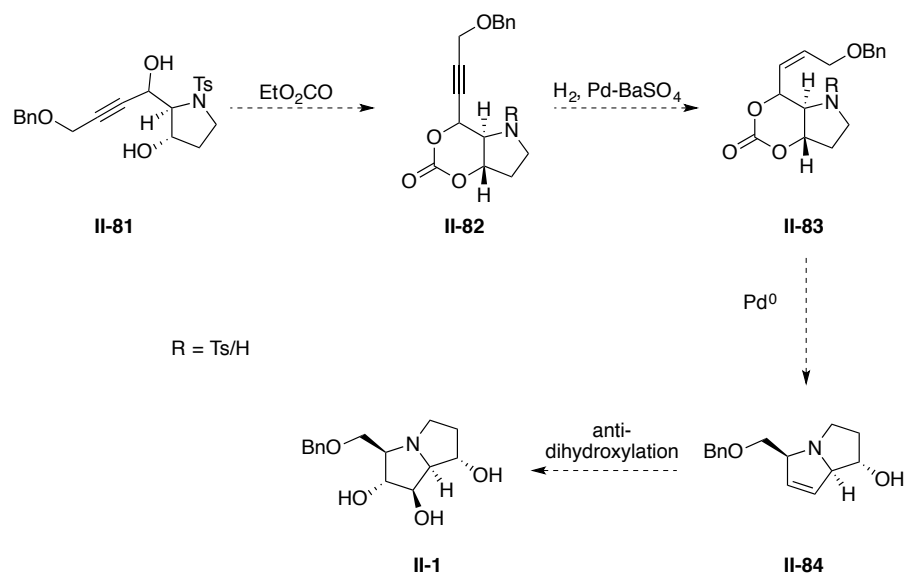
for the most optimal removal after every step beginning with the ring expansion itself.

While there are many ways to continue this synthesis, a protection of diol **II-81** as a carbonate provides many benefits: (1.) it enables us to find the relative stereochemistry of the unknown chiral center created by the nucleophilic addition by creating a rigidified ring system, (2.) it locks the alkyne in a position that would better educate us in the feasibility of tosyl removal at this stage, (3.) it provides the necessary handle for the palladium insertion for the upcoming aminocyclization, and (4.) it provides us with a predictive model of the aminocyclization based on the stereochemistry of the unknown center.

Reduction of the alkyne **II-82** to the cis-alkene **II-83** provides the ideally prepared substrate for a palladium-mediated aminocyclization. With a stereochemically salt-directed aminocyclization, **II-84** requires only an anti-dihydroxylation to give a benzyl-protected alkyne requiring only a mild deprotection of a primary alcohol.

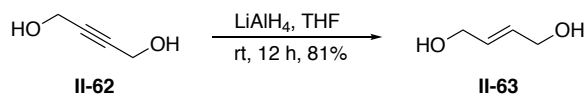
This racemic synthesis can be made asymmetric utilizing simple known methodology.⁶² Schomaker used Sharpless epoxidation, azide ring opening, and aziridine ring closing followed by tosyl protection to form the necessary chiral aziridinol. Córdova and coworkers⁶⁸ rely on the asymmetric aziridination of α,β -unsaturated aldehydes to give the necessary aziridinal.

In closing, while this synthesis is not complete, it provides a few colorful steps in the synthesis of alexine from completely achiral starting materials that is amenable to subtle changes to create other analogues. More studies will be undertaken to complete this and, ultimately, the asymmetric syntheses of alexine.

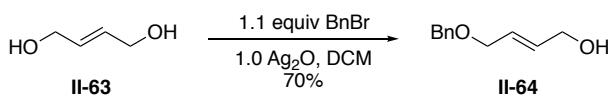


Scheme II-14: Remaining steps in the synthesis of alexine.

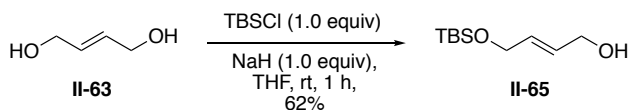
II.4. Experimental



Preparation of (*E*)-2-butene-1,4-diol. THF was cooled to 4 °C in a flame dried flask with a stir bar. Lithium aluminum hydride (1.2 equivalents, 139.39 mmol) was added slowly while monitoring changes in temperature and rate of bubbling. A dry THF solution of 2-butyne-1,4-diol (1.0 equivalent, 116.16 mmol) was added drop wise via cannula slowly while monitoring changes in temperature. The solution was allowed to slowly warm to room temperature and left for 14 hours. After verification of completion of the reaction via TLC in EtOAc (*R_f* = 0.3), the solution was cooled again to 4 °C. Celite (2.5g for every 10g of diol) was added to the stirring solution. Saturated ammonium sulfate solution was added slowly allowing for evolution of hydrogen gas and maintenance of cooled temperature. A saturated solution of sodium sulfate was slowly added followed by a 15% sodium hydroxide solution. The solution was filtered through a pad of Celite. The pad was washed several times with EtOAc. The solution was concentrated via reduced pressure giving a clear oil. The oil was distilled via kugelrohr (177 °C, 40 Torr) to give a more homogeneous clear oil. Alternately, the crude residue can be purified via flash column chromatography in ethyl acetate with yields of 81%. ¹H NMR (500 MHz, CDCl₃) δ 5.9 (dt, *J* = 1 Hz, 1.5 Hz, 2 H), 4.2 (s, 4 H), 1.6 (brs, 2 H); ¹³C NMR (62.8 MHz, CDCl₃) δ 130.5, 62.8.

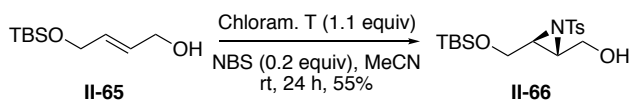


Preparation of (E)-4-(benzyloxy)but-2-en-1-ol. 2-butene-1,4-diol (1.0 equivalent, 124.7 mmol) was dissolved in methylene chloride along with silver oxide (1.0 equivalents, 124.7 mmol) and allowed to stir for minutes. Benzyl bromide (1.1 equivalents, 137.2 mmol) was added to the solution and allowed to stir for 24 hours. The reaction was monitored via TLC and upon completion, filtered through a silica gel plug. Concentration en vacuo was followed by additional filtration through another silica gel plug, yielding a clear oil. The crude was purified via column chromatography (30% EtOAc in hexanes) to give a clear oil in 70% yield. ^1H NMR (500 MHz, CDCl_3) δ 7.31 (m, 5 H), 5.91 (dt, $J = 16.0$ Hz, 5.5 Hz, 1.5 Hz, 1 H), 5.84 (dt, $J = 15.5$ Hz, 5.5 Hz, 1.5 Hz, 1 H), 4.51 (s, 2 H), 4.16 (tq, $J = 5.0$ Hz, 1.0 Hz, 2 H), 4.03 (dq, $J = 5.5$ Hz, 1.0 Hz, 2 H); ^{13}C NMR (62.8 MHz, CDCl_3) δ 132.37, 128.82, 128.64, 128.21, 127.99, 127.89, 72.59, 70.31, 63.32.



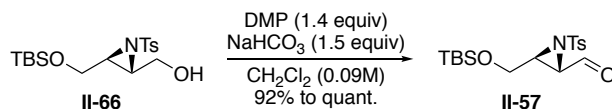
Preparation of (E)-4-((*tert*-butyldimethylsilyl)oxy)but-2-en-1-ol. Sodium hydride (1.0 equivalent, 93.8 mmol) was charged into a flame dried flask with a stir bar and 100 mL of dry tetrahydrofuran. After sealing, the container was purged with nitrogen gas. 2-butene-1,4-diol (1.0 equivalent, 93.8 mmol) was dissolved in 60mL of dry tetrahydrofuran and added dropwise to the suspension

and allowed to stir for 45 minutes. *Tert*-butyldimethylsilylchloride (1.0 equivalent, 93.8 mmol) dissolved in 15 mL of dry tetrahydrofuran was added to the solution in one portion, providing a milky white solution that was allowed to stir for another 45 minutes. After monitoring the consumption of the alcohol using TLC (20% EtOAc in hexanes), 450 mL of ether was added to the solution. 300 mL of 10% K₂CO₃ solution is used to wash the ether solution followed by 40 mL of a brine solution. The aqueous layers were washed with diethyl ether. Organic layers were combined, dried over sodium sulfate, filtered, and concentrated en vacuo. The crude residue was purified using column chromatography initially using 10% EtOAc in hexanes and after elution of excess TBS chloride, 20% EtOAc in hexanes was used to elute the desired product in 62% yield of a clear liquid. ¹H NMR (500 MHz, CDCl₃) δ 5.86 (dt, *J* = 5.5 Hz, 15.5 Hz, 2 H), 5.78 (dt, *J* = 3.5 Hz, 15.5 Hz, 2 H), 4.16 (dd, *J* = 1.5 Hz, 4.5 Hz, 2 H), 4.14 (d, *J* = 5.5 Hz, 2 H), 1.35 (brs, 1 H), 0.89 (s, 9 H), 0.05 (s, 6 H); ¹³C NMR (62.8 MHz, CDCl₃) δ 131.26, 129.15, 63.43, 63.33, 26.18, 18.65, -5.02.



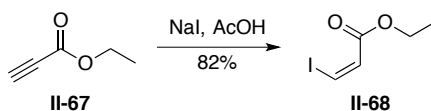
Preparation of (3-(((*tert*-butyldimethylsilyl)oxy)methyl)-1-tosylaziridin-2-yl)methanol. The mono-protected diol, (*E*)-4-((*tert*-butyldimethylsilyl)oxy)but-2-en-1-ol (1.0 equivalent, 1.96 mmol) was dissolved in dry acetonitrile along with a stir bar. Chloramine-T trihydrate (1.1 equivalents, 2.16 mmol) dried 60 °C under vacuum was added along with recrystallized NBS (0.2 equivalents, 0.39 mmol) were added to the solution and the flask was sealed. After purging with nitrogen gas, the solution was allowed to stir at room temperature for 19 hours. Upon

completion, an equal volume of water was added and the solution was extracted with ethyl acetate. The combined organics were dried over sodium sulfate and concentrated en vacuo. The viscous crude was purified via column chromatography (20% EtOAc in Hexanes) to give a slightly yellow viscous oil in 55% yield. ^1H NMR (500 MHz, CDCl_3) δ 7.83 (d, J = 8.0, 2 H), 7.29 (d, J = 8.5, 2 H), 4.13 (ddd, J = 13.0 Hz, 9.5 Hz, 3.0 Hz, 1 H), 3.96 (ddd, J = 13.0 Hz, 8.0 Hz, 4.5 Hz, 1 H), 3.76 (dd, J = 11.5 Hz, 4.0 Hz, 1 H), 3.58 (dd, J = 11.5 Hz, 6.0 Hz, 1 H), 3.15 (dd, J = 10.5 Hz, 4.5 Hz, 1 H), 3.03 (ddd, J = 8.0 Hz, 4.5 Hz, 3.0 Hz, 1 H), 2.86 (dd, J = 9.0 Hz, 4.5 Hz, 1 H), 2.41 (s, 3 H), 0.78 (s, 9 H), - 0.089 (s, 3 H), - 0.114 (s, 3 H).

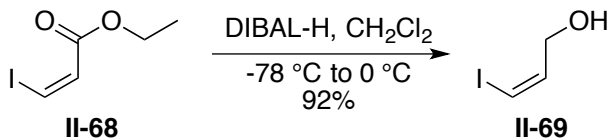


Preparation of (3-(((*tert*-butyldimethylsilyl)oxy)methyl)-1-tosylaziridine-2-carbaldehyde. DMP (1.4 equivalents, 0.377 mmol) and sodium bicarbonate (1.5 equivalents, 0.412 mmol) were charged into a flame dried flask with a stir bar. The flask was cooled in an acetone/dry ice bath and a prepared solution (0.09M) of aziridinol **II-66** (1.0 equivalents, 0.269 mmol) in dry methylene chloride was added. The flask was moved from a -78 °C bath to a 0 °C bath and allowed to stir without monitoring for 3 hours. After TLC verification of completion, a saturated aqueous solution of sodium thiosulfate was added to the solution. It caused a change in the color of the solution to white opaque and then clear. Saturated sodium bicarbonate solution was then added followed by water. The solution was extracted with methylene chloride and the organics were dried over sodium sulfate to be concentrated en vacuo giving a viscous yellow oil in quantitative

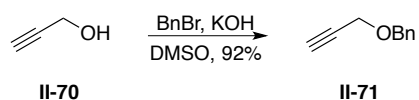
yield. ^1H NMR (500 MHz, CDCl_3) δ 9.54 (d, $J = 12.0$ Hz, 1 H), 7.83 (d, $J = 14.0$ Hz, 2 H), 7.32 (d, $J = 13.5$ Hz, 2 H), 3.83 (dd, $J = 19.0$ Hz, 6.0 Hz, 1 H), 3.70 (dd, $J = 19.0$ Hz, 8.0, 1 H), 3.60 (dt, $J = 8$ Hz, 6.5 Hz, 1 H), 3.18 (dd, $J = 11.0$ Hz, 6.5 Hz, 1 H), 2.43 (s, 3 H), 0.79 (s, 9 H), - 0.077 (s, 3 H), - 0..91 (s, 3 H).



Preparation of (Z)-ethyl 3-iodoacrylate. Sodium iodide (1.0 equivalent, 51 mmol) was dissolved in acetic acid in a flame-dried flask with a stir bar. The solution was purged with nitrogen gas and heated to 80 °C. Ethyl propionate (1.0 equivalent, 51 mmol) was added dropwise while noting the color change in the solution (slightly darker yellow). Water was added to the solution after cooling to room temperature. The solution was extracted with diethyl ether (3 x 50 ml). The organic phase was then washed with 4M potassium hydroxide until the aqueous layer had become neutral. The organic layer was dried over sodium sulfate and concentrated en vacuo. Purification has proven unnecessary since by NMR the compound appears pure. 82% yield. ^1H NMR (500 MHz, CDCl_3) δ 7.42 (d, $J = 9.0$ Hz, 1 H), 6.87 (d, $J = 9.0$ Hz, 1 H), 4.23 (q, $J = 7.0$ Hz, 2 H), 1.26 (t, $J = 7.0$ Hz, 3 H); ^{13}C NMR (62.8 MHz, CDCl_3) δ 164.8, 130.2, 94.8, 61.0, 14.4.

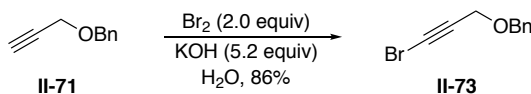


Preparation of (Z)-3-iodoprop-2-en-1-ol. (Z)-ethyl-3-iodoacrylate (1.0 equivalents, 4.4 mmol) was dissolved in dry methylene chloride in a flame-dried flask with a stir bar. The flask was sealed, purged with nitrogen gas, and cooled to -78 °C. Diisobutylaluminum hydride (2.2 equivalents, 9.8 mmol) was slowly added to the solution and after 10 minutes of stirring, it was warmed to 0 °C and left for 30 more minutes. After verification of completion using TLC (25% EtOAc in hexanes), a saturated solution of Rochelle's salt was added very slowly over an hour. After bubbling ceased, Glycerine was added and methylene chloride was used to dilute the solution. The solution was allowed to stir for 12 hours. The solution was filtered over Celite and washed with water and then with brine. The organic layer was dried over sodium sulfate and concentrated en vacuo. Reaction yielded 77% of mildly impure (peaks for toluene, the DIBAL-H solvent were apparent) light yellow oil. ¹H NMR (500 MHz, CDCl₃) δ 6.48 (dt, *J* = 8.0 Hz, 5.5 Hz, 1 H), 6.35 (dt, *J* = 8.0 Hz, 1.5 Hz, 1 H), 4.23 (t, *J* = 4.0 Hz, 2 H), 1.54 (s, 1 H); ¹³C NMR (62.8 MHz, CDCl₃) δ 140.2, 82.9, 66.0.

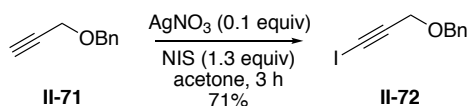


Preparation of ((prop-2-yn-1-yloxy)methyl)benzene. Potassium hydroxide (3.0 equivalents, 160.54 mmol) and DMSO were charged into a flask with a stir bar and cooled to 0 °C. Stirring had to be maintained during the process of cooling. Propargyl alcohol (1.0 equivalent, 53.51 mmol) was added at 0 °C and the solution was allowed to stir for 10 minutes, periodically warming to prevent total freezing of DMSO. Benzyl bromide (1.0 equivalent, 53.51 mmol) was also added at 0 °C and the solution was allowed to warm to room temperature. The reaction

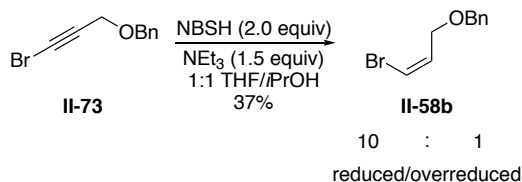
was allowed to stir for 15 hours. Upon completion of the reaction, water was added to the solution followed by diethyl ether. The aqueous layer was washed with diethyl ether (3 x 50 ml) and the organic layers were combined and dried over sodium sulfate. After concentration, the compound was proven to be quite pure. 92% yield. ^1H NMR (500 MHz, CDCl_3) δ 7.35 (m, 4 H), 7.29 (m, 1 H), 4.60 (s, 2 H), 4.16 (d, $J = 2.5$ Hz, 2 H), 2.45 (t, $J = 2.5$ Hz, 1 H).



Preparation of (((3-bromoprop-2-yn-1-yl)oxy)methyl)benzene. Potassium hydroxide pellets (5.2 equivalents, 7.11 mmol) were added to a round bottom flask with a stir bar and dissolved in water. The solution was then cooled to 0 °C and bromine liquid (0.75 equivalents, 1.03 mmol) was added in small portions. The solution was allowed to stir for 15 minutes. The alkyne (1.0 equivalents, 1.37 mmol) was then added drop wise before allowing to stir for 30 minutes at 0 °C. After cooling to room temperature, the aqueous solution was extracted with diethyl ether (3 x 10 ml). The combined organic phase was dried over magnesium sulfate and concentrated en vacuo. Purification was not required. 86% yield. ^1H NMR (500 MHz, CDCl_3) δ 7.32 (m, 5 H), 4.58 (s, 2 H), 4.18 (s, 2 H).

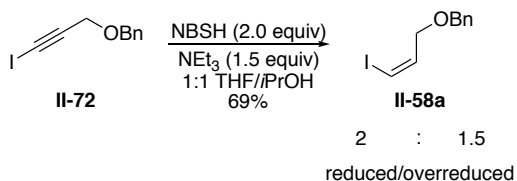


Preparation of (((3-iodoprop-2-yn-1-yl)oxy)methyl)benzene. Silver nitrate (0.1 equivalent, 0.14 mmol) and NIS (1.3 equivalents, 1.78 mmol) were added to a solution of the alkyne (1.0 equivalent, 1.37 mmol) in magnesium sulfate-dried acetone. The solution was allowed to stir for 3 hours. Hexanes were added to the solution and filtered over Celite. In the dark, water was added to the solution and the solution was extracted with hexanes. The organics were combined, dried over sodium sulfate, and concentrated en vacuo. Purification of this light yellow oil was not required. 71% yield. ^1H NMR (500 MHz, CDCl_3) δ 7.33 (m, 4 H), 7.29 (m, 1 H), 4.58 (s, 2 H), 4.30 (s, 2 H).



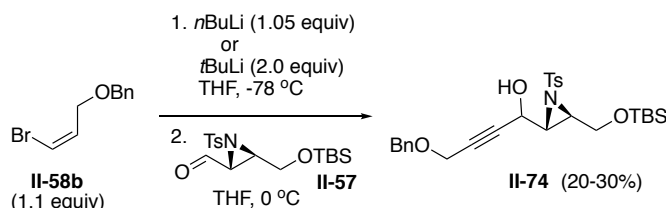
Preparation of (Z)-(((3-bromoallyl)oxy)methyl)benzene. The alkynyl bromide (1.0 equivalent, 0.755 mmol) was dissolved in a 1:1 mixture of tetrahydrofuran and isopropyl alcohol. Nitrobenzene sulfonic hydrazide (NBSH) (2.0 equivalents, 1.511 mmol) was added to the solution and the flask was sealed and purged with nitrogen gas. Triethylamine (1.5 equivalents, 1.133 mmol) was added to the solution and the flask was purged with nitrogen gas. The solution was allowed to stir for 14 hours. The reaction was quenched with saturated sodium bicarbonate and diluted with ethyl acetate. The aqueous layer was extracted with ethyl acetate (3 x 5 ml) and the organic layers were combined and dried over sodium

sulfate. The solution was concentrated en vacuo. The crude was purified via column chromatography to yield a slight yellow mixture of the alkene and its overreduced equivalent in a ratio of 10:1 in favor of the alkene with a total yield of 37%. Alkene: ^1H NMR (500 MHz, CDCl_3) d 7.31 (m, 5 H), 6.48 (dt, $J = 6.5$ Hz, 4.5 Hz, 1 H), 6.39 (dt, $J = 6.5$ Hz, 1.5, 1 H), 4.53 (s, 2 H), 4.12 (dd, $J = 4.5$ Hz, 1.5 Hz, 2 H). Overreduced: ^1H NMR (500 MHz, CDCl_3) d 7.31 (m, 5 H), 6.48 (dt, $J = 6.5$ Hz, 4.5 Hz, 1 H), 6.39 (dt, $J = 6.5$ Hz, 1.5, 1 H), 4.51 (s, 2 H), 3.53 (t, $J = 5.0$ Hz, 2 H), 3.29 (t, $J = 6.0$ Hz, 2 H), 2.08 (quint, $J = 5.0$ Hz, 2 H).



Preparation of (*Z*)-(((3-iodoallyl)oxy)methyl)benzene. The alkynyl iodide (1.0 equivalent, 0.967 mmol) was dissolved in a 1:1 mixture of tetrahydrofuran and isopropyl alcohol. Nitrobenzene sulfonic hydrazide (NBSH) (2.0 equivalents, 1.933 mmol) was added to the mixture and the flask was purged with nitrogen gas. Triethyl amine (1.5 equivalents, 1.450 mmol) was added and the solution was allowed to stir for 14 hours. The reaction was quenched with saturated sodium bicarbonate and diluted with ethyl acetate. The aqueous layer was extracted with ethyl acetate (3 x 5 ml). The organic layers were combined, dried over sodium sulfate, and concentrated en vacuo. The crude was purified via column chromatography to yield a light yellow mixture of the alkene and the overreduced equivalent in a ratio of 2:1.4 with a total yield of 69%. ^1H NMR (500 MHz, CDCl_3) d 7.34 (m, 4 H), 7.28 (m, 1 H), 6.48 (dt, $J = 6.5$ Hz, 4.5 Hz, 1 H),

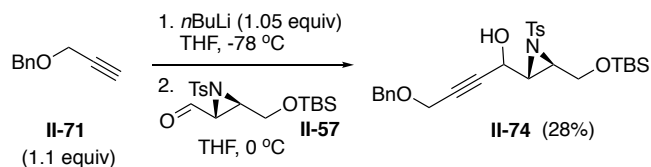
6.39 (dt, $J = 6.5$ Hz, 1.5 Hz, 1 H), 4.53 (s, 2 H), 4.12 (dd, $J = 4.5$ Hz, 1.5 Hz, 2 H); ^{13}C NMR (62.8 MHz, CDCl_3) δ 138.5, 138.0, 128.7, 128.1, 127.9, 83.4, 72.9, 69.8.



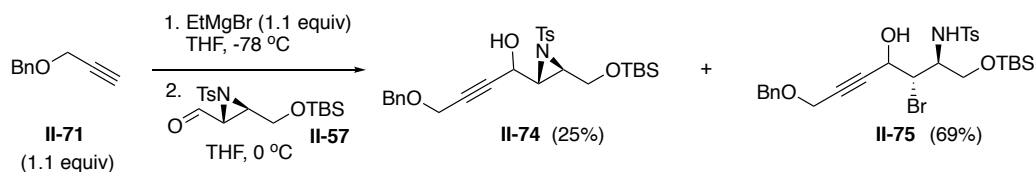
Preparation of 4-(benzyloxy)-1-(3-(((*tert*-butyldimethylsilyl)oxy)methyl)-1-tosylaziridin-2-yl)but-2-yn-1-ol. The (*Z*)-(((3-bromoallyl)oxy)methyl)benzene (1.0 equivalent, 0.434 mmol) was dissolved in dry tetrahydrofuran with a stir bar. After sealing, the flask was purged with nitrogen gas. After cooling to $-78\text{ }^\circ\text{C}$, *n*-butyllithium (1.3 equivalents, 0.564 mmol) was added to the solution and allowed to stir for 1 hour. A solution of the aziridinal (0.9 equivalents, 0.391 mmol) was added to the reaction and monitored via TLC (30% EtOAc in hexanes). Upon completion, 10 mL of ammonium chloride saturated solution was added dropwise to the solution and allowed to stir for 5 minutes. The solution was extracted with ethyl acetate, the organics were combined, washed with brine, and dried over sodium sulfate before concentrating en vacuo. The residue was purified using column chromatography (20% EtOAc in hexanes) to provide 20-30% of a light yellow liquid. ^1H NMR (500 MHz, CDCl_3) δ 7.83 (d, 8.5 Hz, 2 H), 7.31 (m, 7 H), 4.74 (dd, $J = 5.0$ Hz, 7.0 Hz, 1 H), 4.68 (s, 2 H), 4.56 (d, $J = 1.5$ Hz, 2 H), 4.17 (d, $J = 1.5$ Hz, 2 H), 3.85 (dd, 4.5 Hz, 11.5 Hz, 1 H), 3.73 (dd, 5.5 Hz, 11.0 Hz, 1 H), 3.14 (m, 2 H), 3.07 (d, 4.5 Hz, 1 H), 2.40 (s, 3H), 0.80 (s, 9 H), - 0.052 (s, 3 H), -

0.072 (s, 3 H); ^{13}C NMR (62.8 MHz, CDCl_3) d 129.8, 128.8, 128.7, 128.3, 128.2, 127.9, 127.8, 127.2, 72.0, 65.6, 61.5, 61.4, 57.5, 51.0, 47.2, 26.0, 21.8, 18.4.

The (*Z*)-(((3-bromoallyl)oxy)methyl)benzene (1.0 equivalent, 0.44 mmol) was dissolved in dry tetrahydrofuran with a stir bar. After sealing, the flask was purged with nitrogen gas. After cooling to $-78\text{ }^{\circ}\text{C}$, *tert*-butyllithium (2.0 equivalents, 0.88 mmol) was added to the solution and allowed to stir for 30 minutes. A solution of the aziridinal (1.0 equivalents, 0.44 mmol) was added to the reaction dropwise and monitored via TLC (30% EtOAc in hexanes). After stirring overnight (increasing to room temperature slowly), 4 mL of ammonium chloride saturated solution was added dropwise to the solution and allowed to stir for 10 minutes. The solution was extracted with ethyl acetate (4 x 4 mL), the organics were combined, and dried over sodium sulfate before concentrating *en vacuo*. The residue was purified using column chromatography (20% EtOAc in hexanes) to provide 20% of a light yellow liquid. . ^1H NMR (500 MHz, CDCl_3) d 7.83 (d, 8.5 Hz, 2 H), 7.31 (m, 7 H), 4.74 (dd, $J = 5.0\text{ Hz}$, 7.0 Hz , 1 H), 4.68 (s, 2 H), 4.56 (d, $J = 1.5\text{ Hz}$, 2 H), 4.17 (d, $J = 1.5\text{ Hz}$, 2 H), 3.85 (dd, 4.5 Hz, 11.5 Hz, 1 H), 3.73 (dd, 5.5 Hz, 11.0 Hz, 1 H), 3.14 (m, 2 H), 3.07 (d, 4.5 Hz, 1 H), 2.40 (s, 3H), 0.80 (s, 9 H), - 0.052 (s, 3 H), - 0.072 (s, 3 H); ^{13}C NMR (62.8 MHz, CDCl_3) d 129.8, 128.8, 128.7, 128.3, 128.2, 127.9, 127.8, 127.2, 72.0, 65.6, 61.5, 61.4, 57.5, 51.0, 47.2, 26.0, 21.8, 18.4.

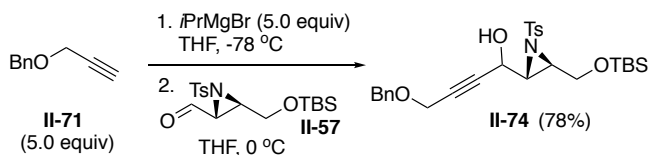


The ((prop-2-yn-1-yloxy)methyl)benzene (1.0 equivalent, 1.37 mmol) was charged into a flame dried flask with a stir bar. After sealing, the flask was purged with nitrogen gas and dry THF was added via syringe. The solution was cooled to -78°C and *n*-butyllithium (1.05 equivalents, 1.44 mmol) was added to the solution and allowed to stir for 30 minutes. A solution of the aziridinal (1.0 equivalents, 1.37 mmol) was added to the reaction dropwise and the color changed noted. After stirring overnight (increasing to room temperature slowly), 4 mL of ammonium chloride saturated solution was added dropwise to the solution and allowed to stir for 10 minutes. The solution was extracted with ethyl acetate (4 x 4 mL), the organics were combined, and dried over sodium sulfate before concentrating en vacuo. The residue was purified using column chromatography (20% EtOAc in hexanes) to provide 28% of a light yellow liquid. ^1H NMR (500 MHz, CDCl_3) δ 7.83 (d, 8.5 Hz, 2 H), 7.31 (m, 7 H), 4.74 (dd, J = 5.0 Hz, 7.0 Hz, 1 H), 4.68 (s, 2 H), 4.56 (d, J = 1.5 Hz, 2 H), 4.17 (d, J = 1.5 Hz, 2 H), 3.85 (dd, 4.5 Hz, 11.5 Hz, 1 H), 3.73 (dd, 5.5 Hz, 11.0 Hz, 1 H), 3.14 (m, 2 H), 3.07 (d, 4.5 Hz, 1 H), 2.40 (s, 3H), 0.80 (s, 9 H), - 0.052 (s, 3 H), - 0.072 (s, 3 H); ^{13}C NMR (62.8 MHz, CDCl_3) δ 129.8, 128.8, 128.7, 128.3, 128.2, 127.9, 127.8, 127.2, 72.0, 65.6, 61.5, 61.4, 57.5, 51.0, 47.2, 26.0, 21.8, 18.4.



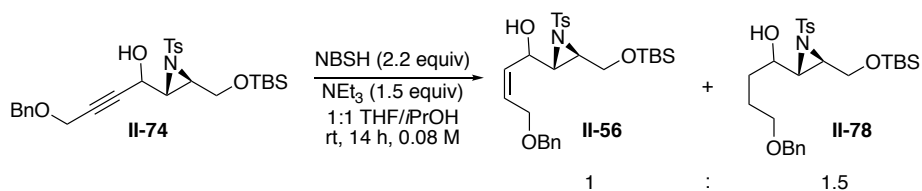
Preparation of 4-(benzyloxy)-1-(3-(((*tert*-butyldimethylsilyl)oxy)methyl)-1-tosylaziridin-2-yl)but-2-yn-1-ol. The ((prop-2-yn-1-yloxy)methyl)benzene (1.1 equivalent, 0.613 mmol) was charged into a flame dried flask with a stir bar. After sealing, the flask was purged with nitrogen gas and 15 mL dry THF was added via syringe. Ethylmagnesium bromide (1.1 equivalents, 0.613 mmol) was added to the solution at room temperature and allowed to stir for 1 hour before reducing the temperature to -78 °C. A 16 mL solution of aziridinal (1.0 equivalents, 0.557 mmol) was added to the reaction dropwise and the solution was allowed to stir at the lowered temperature for 10 minutes before raising the temperature to 0 °C. The reaction was left stirring for 2 hours before quenching with 4 mL of saturated ammonium chloride solution. The solution was extracted with ethyl acetate (3 x 10 mL). The organics were combined and washed with water and then with brine before drying over sodium sulfate and concentrating en vacuo. The residue was purified using column chromatography (20% EtOAc in hexanes) to provide 25% of the light yellow desired product. ¹H NMR (500 MHz, CDCl₃) δ 7.83 (d, 8.5 Hz, 2 H), 7.31 (m, 7 H), 4.74 (dd, *J* = 5.0 Hz, 7.0 Hz, 1 H), 4.68 (s, 2 H), 4.56 (d, *J* = 1.5 Hz, 2 H), 4.17 (d, *J* = 1.5 Hz, 2 H), 3.85 (dd, 4.5 Hz, 11.5 Hz, 1 H), 3.73 (dd, 5.5 Hz, 11.0 Hz, 1 H), 3.14 (m, 2 H), 3.07 (d, 4.5 Hz, 1 H), 2.40 (s, 3H), 0.80 (s, 9 H), - 0.052 (s, 3 H), - 0.072 (s, 3 H); ¹³C NMR (62.8 MHz, CDCl₃) δ 129.8, 128.8, 128.7, 128.3, 128.2, 127.9, 127.8, 127.2, 72.0, 65.6, 61.5, 61.4, 57.5, 51.0, 47.2, 26.0, 21.8, 18.4.

Preparation of *N*-(7-(benzyloxy)-3-bromo-1-((*tert*-butyldimethylsilyl)oxy)-4-hydroxyhept-5-yn-2-yl)-4-methylbenzenesulfonamide. *N*-((2*S*,3*S*)-7-(benzyloxy)-3-bromo-1-((*tert*-butyldimethylsilyl)oxy)-4-hydroxyhept-5-yn-2-yl)-4-methylbenzenesulfonamide was a large byproduct of the attempt to form 4-(benzyloxy)-1-((2*R*,3*R*)-3-(((*tert*-butyldimethylsilyl)oxy)methyl)-1-tosylaziridin-2-yl)but-2-yn-1-ol using ethylmagnesium bromide as the base and was isolated in 69% yield. ¹H NMR (500 MHz, CDCl₃) δ 7.75 (d, *J* = 8.5 Hz, 4 H), 7.36-7.25 (m, 7 H), 6.05 (d, *J* = 8.0 Hz, 1 H), 4.69 (d, *J* = 5.0 Hz, 1 H), 4.54 (s, 2 H), 4.30 (q, *J* = 4.0 Hz, 1 H), 4.09-4.02 (m, 3), 3.81 (dd, *J* = 5.0 Hz, 12 Hz, 2 H), 3.24 (br s, 1 H), 2.37 (s, 3 H), 0.905 (s, 9 H), 0.073 (s, 3 H), 0.062 (s, 3 H); ¹³C NMR (62.8 MHz, CDCl₃) δ 143.6, 137.2, 137.1, 129.5, 128.5, 128.1, 128.0, 127.6, 83.6, 83.4, 71.9, 65.1, 63.9, 62.0, 57.2, 51.5, 26.0, 25.7, 21.6, 18.2, -5.5, -5.6.



Preparation of 4-(benzyloxy)-1-(3-(((*tert*-butyldimethylsilyl)oxy)methyl)-1-tosylaziridin-2-yl)but-2-yn-1-ol. The ((prop-2-yn-1-yloxy)methyl)benzene (5.0

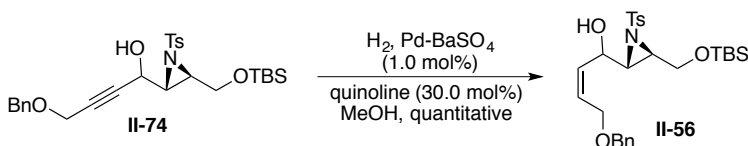
equivalent, 1.356 mmol) was charged into a flame dried flask with a stir bar. After sealing, the flask was purged with nitrogen gas and 2 mL dry methylene chloride was added via syringe. Isopropylmagnesium bromide (5.0 equivalents, 1.356 mmol) was added to the solution at room temperature and allowed to stir for 30 minutes before reducing the temperature to -78 °C. A solution of aziridinal (1.0 equivalents, 0.271 mmol) was added to the reaction dropwise and the solution was allowed to stir for 2 hours before TLC monitoring. Upon completion, 4 mL of saturated ammonium chloride solution was added and the solution was allowed to slowly return to room temperature. The solution was extracted with methylene chloride (3 x 40 mL) and washed with brine before combining the organic layers, drying over sodium sulfate, and concentrating en vacuo. The residue was purified using a short chromatographic column (5% EtOAc in hexanes to remove the excess propargyl ether before increasing to 20% EtOAc in hexanes) to provide 78% of the light yellow desired product. ¹H NMR (500 MHz, CDCl₃) δ 7.83 (d, 8.5 Hz, 2 H), 7.31 (m, 7 H), 4.74 (dd, *J* = 5.0 Hz, 7.0 Hz, 1 H), 4.68 (s, 2 H), 4.56 (d, *J* = 1.5 Hz, 2 H), 4.17 (d, *J* = 1.5 Hz, 2 H), 3.85 (dd, 4.5 Hz, 11.5 Hz, 1 H), 3.73 (dd, 5.5 Hz, 11.0 Hz, 1 H), 3.14 (m, 2 H), 3.07 (d, 4.5 Hz, 1 H), 2.40 (s, 3H), 0.80 (s, 9 H), - 0.052 (s, 3 H), - 0.072 (s, 3 H); ¹³C NMR (62.8 MHz, CDCl₃) δ 129.8, 128.8, 128.7, 128.3, 128.2, 127.9, 127.8, 127.2, 72.0, 65.6, 61.5, 61.4, 57.5, 51.0, 47.2, 26.0, 21.8, 18.4.



Preparation of (Z)-4-(benzyloxy)-1-(3-(((tert-butyl dimethylsilyl)oxy)methyl)-1-tosylaziridin-2-yl)but-2-en-1-ol.

A 1:1 solution of tetrahydrofuran and isopropyl alcohol (0.969 mL) was charged into a flask with a stir bar and 4-(benzyloxy)-1-((2*R*,3*R*)-3-(((tert-butyl dimethylsilyl)oxy)methyl)-1-tosylaziridin-2-yl)but-2-yn-1-ol (1.0 equivalents, 0.078 mmol). NBSH (2.2 equivalents, 0.171 mmol) was added to the solution and it was capped. Triethylamine (1.5 equivalents, 0.116 mmol) was added to the solution and it was allowed to stir for 14 hours. The reaction was quenched with 2 mL of saturated sodium bicarbonate solution and diluted with 4 mL of ethyl acetate. The aqueous portion was extracted with ethyl acetate (3 x 3 mL) before the combined organic layers were dried over sodium sulfate and concentrated en vacuo. The mixture of products (desired and overreduced, 1:1.5), though identifiable by NMR, were inseparable via chromatography. Dilution of this reaction to 2.65 mL decreased access to the cis alkene even further (1:2, desired to overreduced). **Alkene:** ^1H NMR (500 MHz, CDCl_3) δ 7.84 (d, J = 8.5 Hz, 2 H), 7.29 (m, 7 H), 5.79 (dt, J = 6.5 Hz, 6.0 Hz, 1 H), 5.59 (dd, J = 7.0 Hz, 9.5 Hz, 1 H), 4.75 (dd, J = 8.5 Hz, 8.5 Hz, 1 H), 4.51 (d, J = 5.5 Hz, 2 H), 4.17 (d, J = 6.0 Hz, 2 H), 3.69 (dd, J = 4.5 Hz, 11.5 Hz, 1 H), 3.58 (dd, J = 6.0 Hz, 11.5 Hz, 1 H), 3.06 (dt, J = 4.5 Hz, 6.0 Hz, 1 H), 2.88 (dd, J = 4.0 Hz, 8.0 Hz, 1 H), 2.42 (s, 3 H), 0.78 (s, 9 H), - 0.099 (s, 3H), - 0.121

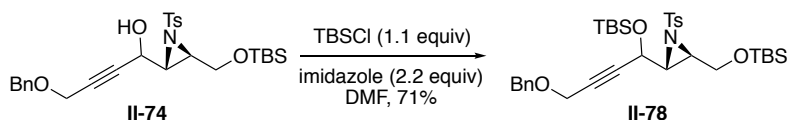
(s, 3 H); ^{13}C NMR (62.8 MHz, CDCl_3) δ 144.6, 130.7, 130.6, 129.8, 128.7, 128.2, 128.0, 127.8, 72.9, 67.1, 66.4, 61.7, 51.8, 47.5, 26.0, 21.9. **Overreduced:** ^1H NMR (300 MHz, CDCl_3) δ 7.84 (d, $J = 13.5$ Hz, 2 H), 7.29 (m, 7 H), 4.54 (dt, $J = 3.3$ Hz, 8.4 Hz, 1 H), 4.49 (s, 2 H), 4.15 (dt, $J = 1.8$ Hz, 6.0 Hz, 2 H), 3.66 (m, 1 H), 3.49 (m, 1 H), 3.16 (m, 1 H), 3.07 (m, 1 H), 2.41 (s, 3 H), 0.79 (s, 9 H), - 0.053 (s, 3H), - 0.75 (s, 3 H)



Preparation of (Z)-4-(benzyloxy)-1-(3-(((*tert*-butyldimethylsilyl)oxy)methyl)-1-tosylaziridin-2-yl)but-2-en-1-ol. 4-

(benzyloxy)-1-((2*R*,3*R*)-3-(((*tert*-butyldimethylsilyl)oxy)methyl)-1-tosylaziridin-2-yl)but-2-yn-1-ol (1.0 equivalents, 0.078 mmol) was charged into a flame-dried flask and dissolved in 10 mL of methanol. Distilled quinoline (30 mol%, 0.14 mmol) was added followed by Pd/BaSO₄ (1.0 mol%, 0.005 mmol). After purging with hydrogen gas, the solution was allowed to stir for approximately 19 hours to complete conversion. Filtration over Celite and concentration gave a clear residue. NMR showed quantitative conversion to the desired alkene. ^1H NMR (500 MHz, CDCl_3) δ 7.84 (d, $J = 8.5$ Hz, 2 H), 7.29 (m, 7 H), 5.79 (dt, $J = 6.5$ Hz, 6.0 Hz, 1 H), 5.59 (dd, $J = 7.0$ Hz, 9.5 Hz, 1 H), 4.75 (dd, $J = 8.5$ Hz, 8.5 Hz, 1 H), 4.51 (d, $J = 5.5$ Hz, 2 H), 4.17 (d, $J = 6.0$ Hz, 2 H), 3.69 (dd, $J = 4.5$ Hz, 11.5 Hz, 1 H), 3.58 (dd, $J = 6.0$ Hz, 11.5 Hz, 1 H), 3.06 (dt, $J = 4.5$ Hz, 6.0 Hz, 1 H), 2.88

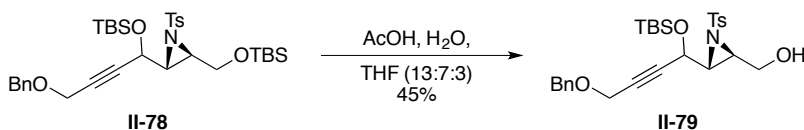
(dd, $J = 4.0$ Hz, 8.0 Hz, 1 H), 2.42 (s, 3 H), 0.78 (s, 9 H), -0.099 (s, 3 H), -0.121 (s, 3 H); ^{13}C NMR (62.8 MHz, CDCl_3) δ 144.6 , 130.7 , 130.6 , 129.8 , 128.7 , 128.2 , 128.0 , 127.8 , 72.9 , 67.1 , 66.4 , 61.7 , 51.8 , 47.5 , 26.0 , 21.9 .



Preparation of 2-(4-(benzyloxy)-1-(((*tert*-butyldimethylsilyl)oxy)but-2-yn-1-yl)-3-(((*tert*-butyldimethylsilyl)oxy)methyl)-1-tosylaziridine. 4-(benzyloxy)-1-

((*2R,3R*)-3-(((*tert*-butyldimethylsilyl)oxy)methyl)-1-tosylaziridin-2-yl)but-2-yn-1-ol (1.0 equivalent, 0.097 mmol), TBSCl (1.1 equivalent, 0.107 mmol), and imidazole (2.2 equivalents, 0.214 mmol) were charged into a flask and dissolved in DMF. The reaction was allowed to stir overnight before TLC verification of completion. Water was added at three times the volumetric amount of DMF and the solution was allowed to stir for 20 minutes. Extraction was done with diethyl ether (4×10 mL) before combining and drying the organic layers over sodium sulfate. The solution was concentrated under nitrogen gas. The residue was purified using column chromatography (3% EtOAc in hexanes) to yield 71% of the desired product. ^1H NMR (500 MHz, CDCl_3) δ 7.83 (d, $J = 8.5$ Hz, 2 H), 7.30 (m, 5 H), 7.24 (d, $J = 8.5$ Hz, 2 H), 4.51 (d, $J = 2.0$ Hz, 2 H), 4.35 (dt, $J = 1.5$ Hz, 6.5 Hz, 1 H), 4.18 (dd, $J = 5.0$ Hz, 11.5 Hz, 1 H), 4.09 (d, $J = 1.5$ Hz, 2 H), 3.97 (dd, $J = 7.0$ Hz, 11.5 Hz, 1 H), 3.15 (dd, $J = 4.5$ Hz, 6.5 Hz, 1 H), 2.94 (dt, $J = 4.5$ Hz, 7.0 Hz, 1 H), 2.38 (s, 3 H), 0.85 (s, 9 H), 0.80 (s, 9 H), 0.038 (s, 6 H), 0.017 (s, 3 H), -0.061 (s, 3 H); ^{13}C NMR (62.8 MHz, CDCl_3) δ 129.69 , 128.69 , 128.29 , 128.14 ,

128.09, 71.75, 63.16, 60.55, 57.43, 50.44, 47.25, 26.05, 25.93, 21.80, -4.52, -4.79.



Preparation of 3-(4-(benzyloxy)-1-((*tert*-butyldimethylsilyl)oxy)but-2-yn-1-yl)-1-tosylaziridin-2-yl)methanol.

2-(4-(benzyloxy)-1-((*tert*-butyldimethylsilyl)oxy)but-2-yn-1-yl)-3-(((*tert*-butyldimethylsilyl)oxy)methyl)-1-tosylaziridine (0.048 mmol) was charged into a flame-dried flask and dissolved in 1 mL of a 13:7:3 solution of acetic acid, water, and tetrahydrofuran, respectively. The reaction was allowed to stir at room temperature with continuous monitoring to prevent global deprotection using TLC (20% EtOAc in hexanes). After 13 hours, the reaction was quenched using saturated sodium bicarbonate solution. The solution was extracted with ethyl acetate (3 x 10 mL). The organic were combined and dried over sodium sulfate before concentration. The compound was purified via column chromatography (15% EtOAc in hexanes) yielding 45% of selectively silyl deprotected product. It should be noted that there was little diol found at this time and substantial reactant after quenching. ^1H NMR (500 MHz, CDCl_3) δ 7.84 (d, J = 8.5 Hz, 2 H), 7.29 (m, 7 H), 4.51 (d, J = 1.5 Hz, 2 H), 4.18 (m, 2 H), 4.10 (d, J = 2.0 Hz, 2 H), 4.05 (m, 1 H), 3.31 (dd, J = 4.5 Hz, 6.5 Hz, 1 H), 3.08 (ddd, J = 3.0 Hz, 4.5 Hz, 9.0 Hz, 1 H), 3.02 (dd, J = 4.0 Hz, 10.0 Hz, 1 H), 2.39 (s, 3 H), 0.76 (s, 9 H), -0.035 (s, 3 H), -0.13 (s, 3 H); ^{13}C NMR (62.8

4.93 (m, 1 H), 4.87 (m, 1 H), 4.51 (s, 2 H), 4.47 (m, 1 H), 4.11 (d, $J = 3.5$ Hz, 1H), 3.99 (d, $J = 2.0$ Hz, 2 H), 3.69 (dd, $J = 11.5$ Hz, 2.5 Hz, 1 H), 3.48 (dd, $J = 11.5$ Hz, 7.5 Hz, 1 H), 3.39 (d, $J = 2.0$ Hz, 1 H), 2.93 (s, 3 H), 0.88 (s, 9 H), 0.143 (s, 3 H), 0.113 (s, 3 H).

^1H NMR (500 MHz, CDCl_3) d 7.73 (d, $J = 8.5$ Hz, 2 H), 7.31 (m, 5 H), 7.21 (m, 2 H), 4.96 (m, 1 H), 4.89 (m, 1 H), 4.51 (s, 2 H), 4.47 (m, 1 H), 4.11 (d, $J = 3.5$ Hz, 1H), 3.99 (d, $J = 2.0$ Hz, 2 H), 3.69 (dd, $J = 11.5$ Hz, 2.5 Hz, 1 H), 3.48 (dd, $J = 11.5$ Hz, 7.5 Hz, 1 H), 3.39 (d, $J = 2.0$ Hz, 1 H), 2.94 (s, 3 H), 0.88 (s, 9 H), 0.132 (s, 3 H), 0.098 (s, 3 H).

REFERENCES

REFERENCES

1. Nash, R. J.; Fellows, L. E.; Dring, J. V.; Fleet, G. W. J.; Derome, A. E.; Hamor, T. A.; Scofield, A. M.; Watkin, D. J. "Isolation from *Alexa-Leiopetala* and X-Ray Crystal-Structure of Alexine, (1r,2r,3r,7s,8s)-3-Hydroxymethyl-1,2,7-Trihydroxypyrrolizidine [(2r,3r,4r,5s,6s)-2-Hydroxymethyl-1-Azabicyclo[3.3.0]Octan-3,4,6-Triol], a Unique Pyrrolizidine Alkaloid" *Tetrahedron Letters* **1988**, 29, 2487.
2. Nash, R. J.; Fellows, L. E.; Dring, J. V.; Fleet, G. W. J.; Girdhar, A.; Ramsden, N. G.; Peach, J. M.; Hegarty, M. P.; Scofield, A. M. "2 Alexines [3-Hydroxymethyl-1,2,7-Trihydroxypyrrolizidines] from *Castanospermum-Australe*" *Phytochemistry* **1990**, 29, 111.
3. Robins, D. J. "Pyrrolizidine alkaloids" *Natural Product Reports* **1995**, 12, 413.
4. Ishibashi, H.; Ozeki, H.; Ikeda, M. "Synthesis of optically active (-)-trachelanthamidine from L-prolinol" *Journal of the Chemical Society, Chemical Communications* **1986**, 654.
5. Fleet, G. W. J.; Haraldsson, M.; Nash, R. J.; Fellows, L. E. "Synthesis from D-glucose of alexine [(1R,2R,3R,7S,8S)-3-hydroxymethyl-1,2,7-trihydroxypyrrolizidine], 3-epialexine and 7-epialexine" *Tetrahedron Letters* **1988**, 29, 5441.
6. Fleet, G. W. J.; Smith, P. W. "Methyl 2-azido-3-O-benzyl-2-deoxy- α -D-mannofuranoside as a divergent intermediate for the synthesis of polyhydroxylated piperidines and pyrrolidines: synthesis of 2,5-dideoxy-2,5-imino-D-mannitol [2R,5R-dihydroxymethyl-3R,4R-dihydroxypyrrolidine]" *Tetrahedron* **1987**, 43, 971.
7. Denmark, S. E.; Hurd, A. R. "Synthesis of (+)-casuarine" *The Journal of organic chemistry* **2000**, 65, 2875.
8. Denmark, S. E.; Cottell, J. J. "Synthesis of (+)-1-epiaustraline" *The Journal of organic chemistry* **2001**, 66, 4276.
9. Pearson, W. H.; Hines, J. V. "Total syntheses of (+)-australine and (-)-7-epialexine" *The Journal of organic chemistry* **2000**, 65, 5785.
10. Chikkanna, D.; Singh, O. V.; Kong, S. B.; Han, H. "A general asymmetric route for the synthesis of the alexine and australine family of pyrrolizidine

- alkaloids. The first asymmetric synthesis of 1,2-diepi-alexine and 1,2,7-triepi-australine" *Tetrahedron Letters* **2005**, 46, 8865.
11. Schomaker, J. M.; Bhattacharjee, S.; Yan, J.; Borhan, B. "Diastereomerically and enantiomerically pure 2,3-disubstituted pyrrolidines from 2,3-aziridin-1-ols using a sulfoxonium ylide: A one-carbon homologative relay ring expansion" *Journal of the American Chemical Society* **2007**, 129, 1996.
 12. Dressel, M.; Restorp, P.; Somfai, P. "Total Synthesis of (+)-Alexine by Utilizing a Highly Stereoselective [3+2] Annulation Reaction of an N-Tosyl- α -Amino Aldehyde and a 1,3-Bis(silyl)propene" *Chemistry – A European Journal* **2008**, 14, 3072.
 13. Beruben, D.; Marek, I.; Normant, J. F.; Platzer, N. "Stereodefined Substituted Cyclopropyl Zinc Reagents from Gem-Bismetallics" *The Journal of organic chemistry* **1995**, 60, 2488.
 14. Kulshrestha, A.; Schomaker, J. M.; Holmes, D.; Staples, R. J.; Jackson, J. E.; Borhan, B. "Selectivity in the Addition Reactions of Organometallic Reagents to Aziridine-2-carboxaldehydes: The Effects of Protecting Groups and Substitution Patterns" *Chemistry – A European Journal* **2011**, 17, 12326.
 15. Cope, A. C. "The Preparation of Dialkylmagnesium Compounds from Grignard Reagents" *Journal of the American Chemical Society* **1935**, 57, 2238.
 16. Phillips, G. W.; University, M. S. *Synthetic Studies Toward the Total Synthesis of Fostriecin and Some Analogs*; Michigan State University, 2006.
 17. Deiana, L.; Dziedzic, P.; Zhao, G.-L.; Vesely, J.; Ibrahim, I.; Rios, R.; Sun, J.; Córdova, A. "Catalytic Asymmetric Aziridination of α,β -Unsaturated Aldehydes" *Chemistry – A European Journal* **2011**, 17, 7904.

Chapter III

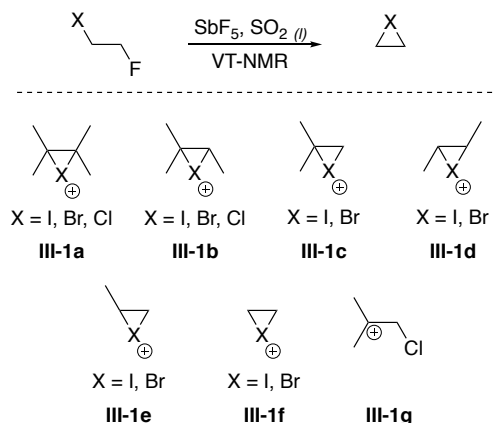
Mechanistic Investigation of (DHQD)₂PHAL Catalysis in Chlorination and Dihydroxylation Reactions Using a Naphthalene-Based Analogue

III.1. Introduction

III.1.1. Overview

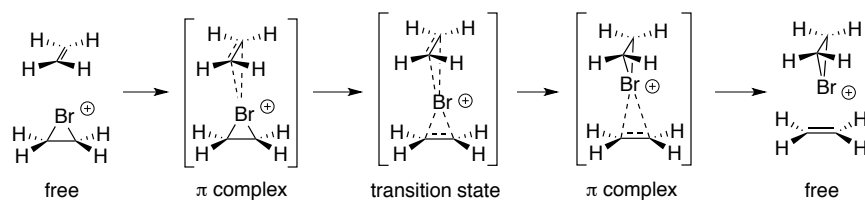
Halogenation is an old reaction first seen in textbooks as early as 1938.⁶⁹ Almost 30 years after,⁷⁰⁻⁷² Olah et. al. proved the existence of the haliranium ion, an intermediate proposed by Kimball and Roberts to explain the specific stereochemistry seen in bromination and chlorination of disubstituted olefins.⁷³ A haliranium ion can be described as a three membered ring containing a positively charged halogen. This haliranium intermediate (pictured in Scheme III-1) was observed via ¹H NMR by Olah et. al., who showed that all bromonium and iodonium and some chloronium exist as cyclized haliranium ions at -60 to -80 °C. Among the observable ions, the 2-chloro-tert-butyl carbocation **III-1g** stood out as a chloronium equivalent to haliraniums **III-1c**. It is here that we can initially see the implicit difference between the chloronium and that of the bromonium and iodonium ions. Interestingly, almost 30 years had passed before the publication of an asymmetric halofunctionalization was achieved. In order to illustrate some of the reasons that may have contributed to this, the major mechanistic challenges that befell the development of an asymmetric

halofunctionalization and the success that address these issues will be discussed.



Scheme III-1:
Spectroscopically observable
haliranium ions.

One of the main problems with achieving a selective halofunctionalization was brought to light by Brown and coworkers.^{74,75 76} It was observed that the sterically encumbered olefin adamantylidene adamantane participated in rapid olefin-to-olefin transfer with its isolable bromiranium and iodonium ions. In a general sense, a bromiranium (like the one featured in Scheme III-2) on a catalytic scale is surrounded by a high concentration of alkene that, upon attacking, will create the same product in a nonselective way. This implies that any face selective formation of bromiranium and iodonium that could lead to enantioenriched halofunctionalization would be compromised because of the racemization due to olefin-to-olefin transfer.



Scheme III-2: Mechanisms of olefin-to-olefin transfer of bromenium ions.

Denmark and coworkers were able to shed further light on the olefin-to-olefin transfer mechanism when they showed that they could form the bromiranium from the β -bromotosylate **III-2a** and capture it enantiospecifically (Table III-1).⁷⁷ However, in the presence of olefin **III-3**, they saw substantial erosion of enantiospecificity. The degree of erosion depends on the concentrations of the olefin and the nucleophile as well as the identity of the nucleophile counterion. A more loosely coordinated counter ion, like tetrabutylammonium, was found to provide for a greater retention of stereospecificity because of the increase in trapping rate. Interestingly, when a chlorine containing substrate **III-2b** was submitted to the same reaction with olefin **III-3**, they saw retention of enantioenrichment in the trapped product **III-4b**.

entry	Substrate	M	III-3 (equivalence)	es (%)
1	III-2a	Na	0.0	100
2	III-2a	Na	1.0	28
3	III-2a	<i>n</i> Bu ₄ N	1.0	81
4	III-2b	<i>n</i> Bu ₄ N	1.0	100

Table III-1: Erosion of enantiospecificity in acetolysis from olefin-to-olefin transfer. HFIP = hexafluoroisopropanol, Tf = trifluoromethanesulfonyl, Ts = 4-toluenesulfonyl.

It is important to point out a trend in these previously discussed works that would lend to a means by which the problems address can be overcome. From the work of Olah et. al. to Denmark's acetolysis, it becomes apparent that the halogen subjected to the halofunctionalization has a strong effect on the mechanism itself. While iodine and bromine, the larger and less electronegative halogens, tend to adopt a haliranium intermediate, the smaller and more electronegative halogens have a greater tendency to exist in open carbocation forms. This is especially visible when considering the case of fluorine in the cation synthesis reaction previously addressed (Scheme III-1). When a difluorinated substrate was submitted to antimony pentafluoride in liquid SO₂, NMR gave indications of a β-fluoro carbocation intermediate equilibrating between classical fluorinated ions at temperatures as low as -90 °C. Merritt similarly proposes the formation of fluorinated carbocation as the key

intermediate in the fluorination of propenyl benzene due to the stereo- and regioselectivity observed.⁷⁸ Interestingly, chlorine can exist as the chloriranium or “bridged chloronium” or the open carbocation depending on the substrate (Scheme III-1). This has the potential to introduce new mechanisms based on substrate tuning.

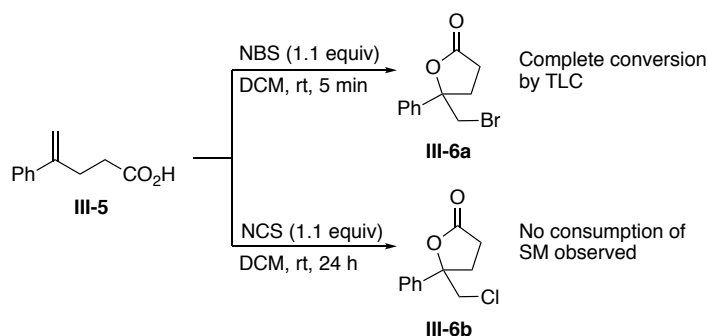
With this in mind, it is not difficult to resolve that limiting halofunctionalizations to chlorgenium sources could prevent the erosion of stereospecificity by eliminating olefin-to-olefin transfer.⁷⁹ Borhan and coworkers exemplified this in their seminal work on asymmetric chlorolactonization. Using (DHQD)₂PHAL as an organic catalyst in chloroform at room temperature, they showed that they could produce lactone **III-6a** in 35% enantimeric excess. Utilizing NCS in lieu of NBS dramatically increased the enantioselectivity to 65% *ee* (Table III-2, entry 3).

entry	X ⁺ source	solvent	temp (°C)	Prdt	% <i>ee</i>
1	NBS	CH ₂ Cl ₂	RT	III-6a	22
2	NBS	CHCl ₃	RT	III-6a	35
3	NCS	CHCl ₃	RT	III-6b	65
4	NCS	CHCl ₃	-40	III-6b	NR ^a
5	DCDMH	CHCl ₃	RT	III-6b	71
6	DCDMH	CHCl ₃	-40	III-6b	83

DCDMH
III-7

Table III-2: (DHQD)₂PHAL mediated halolactonization. ^a NR = no reaction after 3 h.

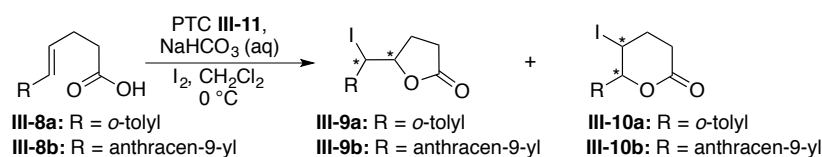
Interestingly, Borhan and coworkers were able to bring light to another problem with asymmetric halofunctionalization within the same context of the lactonization.⁸⁰ They were able to show that the reactivity of the halenium source is of significant importance. Highly reactive halenium reagents can cause an uncatalyzed background reaction in competition with the catalyzed reaction, eroding the stereoselectivity imbued by the catalyst. In Scheme III-3, alkene acid **III-5** was completely consumed in a bromolactonization with NBS that proceeded without catalyst to give lactone **III-6a** after only 5 minutes. However, chlorolactonization showed no conversion after 24 hours. In an ideal asymmetric catalysis, there is no background reaction to compete with the selective halofunctionalization. This would seem to suggest that simply switching to chlorenium sources in general would be a solution to both problems, but it is important to note that some chlorenium sources may not be reactive enough. When the Borhan lab attempted to lower the temperature of the selective NCS chlorolactonization in order to further bolster the enantioselectivity, there was no reaction after 3 hours (Table III-2, entry 4). Switching to 1,3-dichloro-5,5-dimethylhydantoin (DCDMH, **III-7**) at room temperature resulted in an increase in selectivity (71% *ee*) and lowering the temperature to -40 °C gave still higher enantioselectivities (83% *ee*).



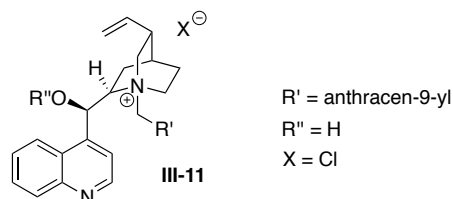
Scheme III-3: Comparison of halenium source reactivity exhibited through bromolactonization with NBS and chlorolactonization with NCS.

III.1.2. Phase-transfer Catalysis in Asymmetric Halofunctionalization

Phase-transfer catalysis has the potential to address these two issues with halofunctionalization in a different way. It can keep the halenium source and the olefin separate outside of the context of the catalyst, preventing competition from background reactions. Depending on the structure of the starting material relative to that of the product, it also has the potential to reduce the concentration of unreacted olefin in the presence of the haliranium intermediate, preventing olefin-to-olefin transfer. Gao and coworkers were the first to attempt halofunctionalization with phase-transfer catalysis.⁸¹ Under optimal conditions addressed in Scheme III-4, *trans*-4-pentenoic acid **III-8** was submitted to a biphasic mixture of aqueous sodium bicarbonate and methylene chloride with stoichiometric molecular iodine in the presence of 30 mol% of a cinchonidine derived ammonium salt **III-11**, producing *exo* cyclized iodolactone **III-9a** in 42% *ee* from **III-8a** and *endo* cyclized iodolactone **III-10b** in 31% *ee* from **III-8b**.



entry	S.M.	% yield (III-9+III-10)	III-9:III-10	% ee III-9	% ee III-10
1	III-8a	89	22:78	42.0	10.0
2	III-8b	38	0:100	--	31.0



Scheme III-4: Iodolactonization using phase-transfer catalysis.

This system effectively prevents background reaction by separating the olefin and the halonium source without the help of the phase-transfer catalyst (Figure III-1). However, it does not segregate the iodonium intermediate from the unreacted olefin. Therefore, the propensity for olefin-to-olefin transfer remains high, especially in the presence of the highly reactive iodonium ion. While this first attempt at asymmetric catalytic halofunctionalization produced only moderate yields, it serves as a platform to further investigate the use of phase-transfer systems to asymmetrically functionalize olefins with larger halogens.

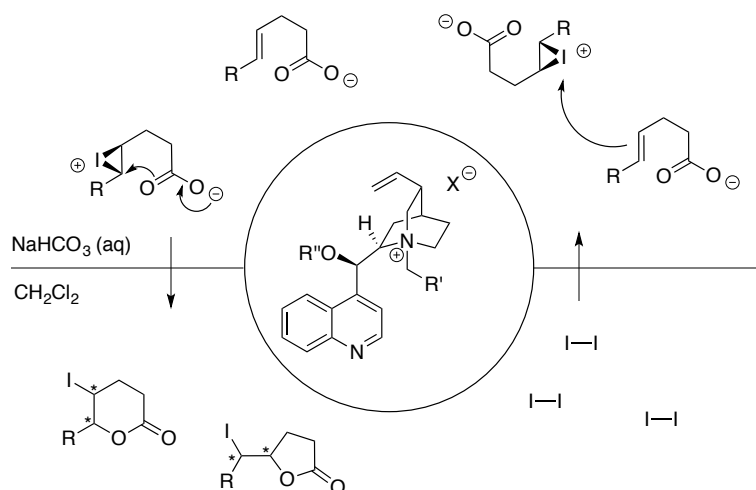
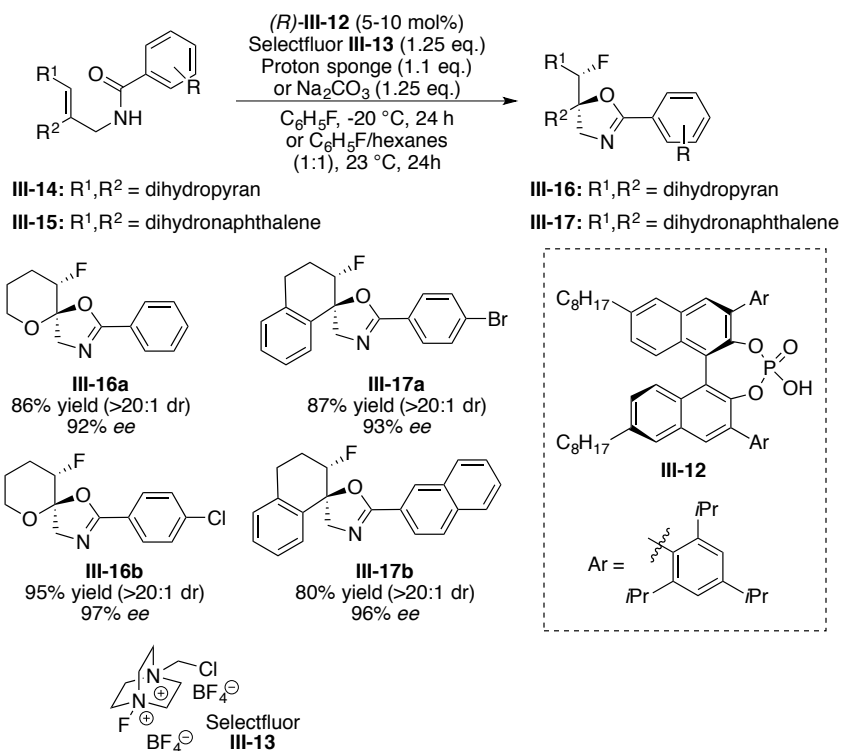


Figure III-1: Iodolactonization via phase-transfer catalysis.

Toste and coworkers were more successful in their phase-transfer catalysis (Scheme III-5).⁸² Toste utilized a chiral BINOL phosphoric acid derived anion **III-12** to transport Selectfluor (**III-13**), a dicationic fluorination reagent, into a nonpolar solvent to fluorocyclize allyl benzamides **III-14** and **III-15**. Dihydropyran substrates **III-14**, with products exemplified by **III-16a** and **III-16b**, proved to be highly enantio- and diastereoselective with enantioselectivities generally ranging from 87% to 97% *ee* and diastereoselectivities generally over 20 to 1. Electron deficient olefins **III-15** were similarly effective with enantioselectivities of 92% to 96% *ee* and diastereoselectivities as high as the previous substrates (>20:1).



Scheme III-5: Fluorocyclization of benzamides using an anionic phase-transfer catalyst.

This halofunctionalization incorporated the controlled separation of the olefin and the halonium source as seen prior with phase-transfer catalysis. However, in this case, Toste and coworkers were also able to prevent olefin-to-olefin transfer not by separating the cationic halogen intermediate from the unreacted olefin, but by utilizing a small halogen with decreased susceptibility to the olefin-to-olefin transfer mechanism.

III.1.3. Mechanistic Insights into Asymmetric Chlorocyclization

One of the advantages of the Borhan methodology is the ease with which it can be modified. Borhan and coworkers have not only used this as an opportunity to

broaden the chlorofunctionalization substrate scope, but also as an opportunity to increased understanding of chlorofunctionalization chemistry and mechanism.

In the previously addressed chlorolactonization methodology,⁷⁹ Borhan and coworkers have shown clear implications with regards to substrate scope. Electron rich aryl substituted 4-pentenoic acids **III-18b-c** (Table III-3) exhibited a loss in enantioselectivity, especially in the case of *p*-methoxy substituent. This can be attributed to the stabilization of the open carbocationic form. The effect is significantly milder in the case of *p*-methyl substituted acid **III-18b**. *Para*-halogenated aryl substituents slightly lowered yields (**III-19d** with 80%, **III-19e** with 81%), but showed no real effect on selectivity. The highly electron deficient trifluoromethyl substrate **III-19f** showed a significant drop in yield (61%) with little effect on enantioselectivity. Though no insight was given, it seems apparent that the electron-withdrawing propensity of the halogens is deactivating the olefin to some extent. Cyclohexyl substrate **III-19h** gave a moderate yield (55%) and compromised selectivity (43% *ee*). This substrate is the only one that saw a significant drop in both yield and enantioselectivity. Apparently, an aryl handle is necessary for the success of this reaction.

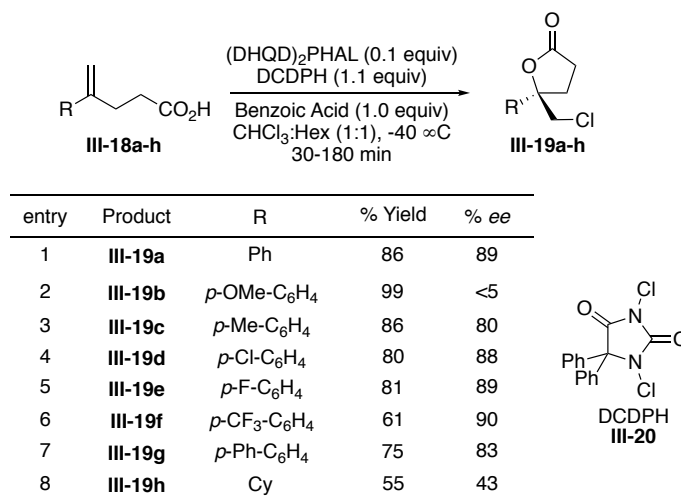


Table III-3: Selections from the chlorolactonization substrate scope.

Broadening the substrate scope to include unsaturated amides provided new handles for tuning along with new oxazolines and dihydrooxazines products. Utilizing DCDPH with 2 mol% of (DHQD)₂PHAL in trifluoroethanol (TFE) at -30 °C, Borhan and coworkers provided substituted oxazolines **III-22a-g** from 1,1-disubstituted allyl amides **III-21a-g**.⁸³ The pendant benzoyl moiety represented a new malleable group that could easily removed under acidic conditions. Changes made to this functionality, while able to directly affect the reaction progression and selectivity, would have little permanent effect on the product unless desired.

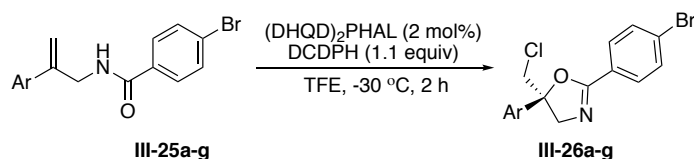
$(\text{DHQD})_2\text{PHAL}$ (2 mol%)
 DCDPH (1.1 equiv)
 TFE, $-30\text{ }^\circ\text{C}$, 2 h

III-23a-g **III-24a-g**

entry	Product	Ar	% Yield	% ee
1	III-24a	Ph	96	90
2	III-24b	<i>p</i> -NO ₂ -C ₆ H ₄	97	93
3	III-24c	<i>p</i> -OMe-C ₆ H ₄	90	93
4	III-24d	3,5(NO ₂) ₂ -C ₆ H ₃	83	86
5	III-24e	3,5(NO ₂) ₂ -4-MeC ₆ H ₂	95	98
6	III-24f	<i>p</i> -Br-C ₆ H ₄	98	98
7	III-24g	<i>p</i> - <i>t</i> Bu-C ₆ H ₄	93	88

Table III-4: Effect of benzoyl substitution on 1,1-disubstituted amide chlorocyclization.

When comparing these compounds, it is easy to see that there are both steric and electronic implications. The effectiveness of *para*-substitution is based a steric component. This becomes evident when comparing unsubstituted benzoyl **III-21a** with 4-nitro (**III-21b**) and 4-methoxybenzoyl (**III-21c**) substrates. The presence of a *para*-substituent increased the enantioselectivity irrespective of the electronic composition (90%, 93%, and 93%, respectively). This is further demonstrated in the comparison of **III-21d** and **III-21e**, differing only in the presence of a methyl substituent in the *para* position. The meta positioning of the nitro groups in the 3,5-dinitrobenzoyl group produced a notable decreased in selectivity (86%) but the presence of the methyl substituent in **III-21e** restored full activity, giving an enantioselectivity of 98% *ee*.



entry	Product	Ar	% Yield	% ee
1	III-26a	Ph	93	98
2	III-26b	3-NO ₂ -C ₆ H ₄	75	68
3	III-26c	3-OMe-C ₆ H ₄	72	93
4	III-26d	4-F-C ₆ H ₄	65	87
5	III-26e	4-Br-C ₆ H ₄	89	84
6	III-26f	4-Cl-C ₆ H ₄	94	87

Table III-5: Olefinic aryl effects on chlorocyclization of 1,1-disubstituted amides.

Changes in olefinic aromatic substituents appeared to produce interesting effects on yields and enantioselectivities (Table III-5). For example, the lowest selectivity seen in the tested compounds comes from the *meta*-nitrophenyl substrate (75% yield, 68% *ee*). Halogens, while tolerated, were also slightly deficient in enantioselectivity (**III-26d** at 87% *ee*, **III-26e** at 84% *ee*, and **III-26f** at 87% *ee*). *Meta*-methoxy substituted substrate **III-26c** gave moderate yields but high enantioselectivity. In this case, it is important to note that *meta* placement of the methoxy group prevents electron donation through resonance normally seen in *ortho* and *para* substituted systems. In this case, we rely only on the inductively withdrawing nature of the methoxy oxygen. There for it can be surmised that electron withdrawing substituents adversely affect the enantioselectivity. This trend seems to be exactly opposite to that of the chlorolactonization. Whether this trend speaks to the need for stabilization of the open β -chloro carbocation or the deactivation of the olefin has not been addressed.

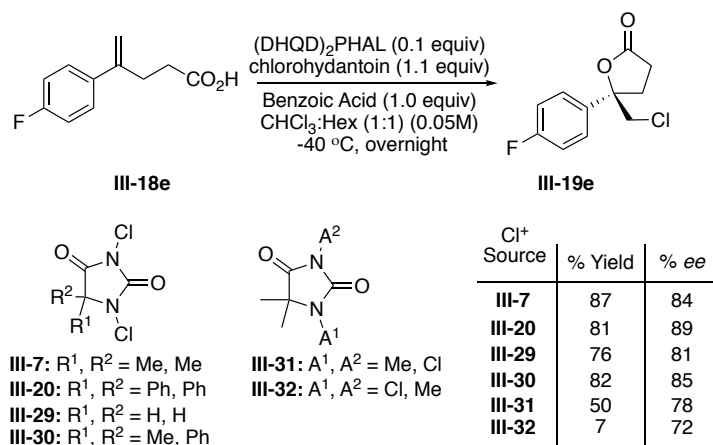
entry	R ¹	R ²	Ar	Prdt	Yield (%)	ee (%)
1	C ₆ H ₅	H	4-Br-C ₆ H ₄	III-28a	91	99
2	C ₆ H ₅	H	4-OMe-C ₆ H ₄	III-28b	93	>99
3	4-F-C ₆ H ₄	H	4-Br-C ₆ H ₄	III-28c	99	95
4	4-Br-C ₆ H ₄	H	4-Br-C ₆ H ₄	III-28d	85	93
5	4-CF ₃ -C ₆ H ₄	H	4-Br-C ₆ H ₄	III-28e	94	95
6	4-OMe-C ₆ H ₄	H	4-Br-C ₆ H ₄	III-28f	84	20
7	4-Me-C ₆ H ₄	H	4-Br-C ₆ H ₄	III-28g	93	60
8	2-Me-C ₆ H ₄	H	4-Br-C ₆ H ₄	III-28h	99	87
9	2-Me-C ₆ H ₄	H	4-OMe-C ₆ H ₄	III-28i	64	91
10	C ₆ H ₅	C ₆ H ₅	4-Br-C ₆ H ₄	III-28j	92	86
11	C ₆ H ₅	Me	4-Br-C ₆ H ₄	III-28k	52 ^a	91
12	Cy	H	4-Br-C ₆ H ₄	III-28l	77 ^a	>99
13	<i>n</i> -C ₅ H ₁₁	H	4-Br-C ₆ H ₄	III-28m	90 ^a	>99
14	CH ₂ Cy	H	4-Br-C ₆ H ₄	III-28n	80 ^a	88

Table III-6: Chlorocyclization of 1,2-disubstituted and trisubstituted allyl amides.

^aReaction was run in 1-nitropropane in the presence of 300 wt% molecular sieves (4Å).

Finally, Borhan and coworkers explored the potential of 1,2-disubstituted and trisubstituted allylic amides (Table III-6). These substrates were more robust, maintaining selectivity under a greater variety of changes. The optimal selectivity seen using the *p*-bromobenzoyl amide protecting group (91% yield, 99% *ee*) made it the ideal starting point for analysis of these new substrates. Electron deficient rings provided relatively high yields and enantioselectivities (Entries 3-5). However, electron rich aryl substitution on the olefin led to extensive erosion of enantioselectivities (**III-28f** at 20% *ee* and **III-28g** at 60%). *Ortho*-methyl substitution (**III-28h**) better maintained good enantioselectivities (87% *ee*) and gave an excellent yield (99%). Introduction of a comparable substrate with a *p*-methoxybenzoyl protection provided a slightly higher enantioselectivity (91% *ee*

of **III-28i**). Trisubstituted systems performed well with only slightly lower enantioselectivities (**III-28j** at 86% *ee* and **III-28k** at 91% *ee*). These are likely attributed to the marginal stabilization of the open carbocation intermediate.



Scheme III-6: Importance of hydantoin structure in chlorolactonization.

Interestingly, the compounds with aliphatic olefin substitutions (**III-28k-n**) did not perform well in TFE. However, 1-nitropropane in the presence of molecular sieves (4 Å) performed with comparably high enantioselectivities (**III-28k-n** at 88% to >99% *ee*) when compared to the best performing aryl compounds (for example, **III-28a** at 91% yield and 99% *ee*).

In order to fully gain an understanding of the chlorine source, Borhan and coworkers initially probed analogues of the 1,3-dichlorohydantoin that has proven so effective (Scheme III-6). Analysis of the methylated analogues (**III-31** and **III-32**) of the hydantoin chlorine source showed that with the transfer of the chlorine

from N-3 of **III-31** was much more facile (50% yield) than that of N-1 on analogue **III-32** (7% yield), insinuating that the chlorine on N-3 is exclusively delivered to the substrate. Moreover, the low yield observed in the case of **III-31** in comparison to that of **III-7** suggests that the chlorine on N-1 is instrumental in inductively activating the chlorine on N-3, preparing it for transfer. Additionally, a comparison of hydantoins **III-7** with **III-20**, **III-29**, and **III-30** exhibits a direct correlation between the steric load on C-5 and the enantioselectivity seen in chlorolactonization product. This suggests that the dichlorohydantoin is intimately involved in the enantioselective transfer of chlorine and not just a chlorgenium donor. This was confirmed through ^1H NMR analysis of C-5 protons when unsubstituted hydantoin **III-21** was incubated with $(\text{DHQD})_2\text{PHAL}$ and benzoic acid in CDCl_3 at $-40\text{ }^\circ\text{C}$. The singlet representing the C-5 hydrogens was split into a clear AB quartet that coalesced into a singlet as the temperature was warmed to room temperature, indicating the association of the hydantoin with the catalyst.

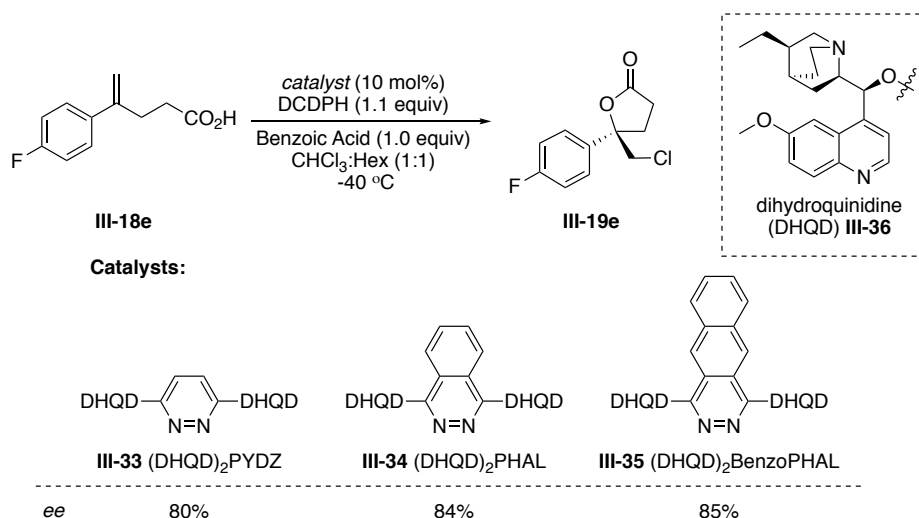
Recently, Borhan and coworkers were able to exclude hydantoins as the sole electrophilic chlorine reagent that could provide the high efficiency in the chlorocyclizations up to this point.⁸⁴ It was found that the use of Chloramine T-trihydrate in the presence of an HFIP additive at $24\text{ }^\circ\text{C}$ could provide comparable yields to the originally optimized hydantoin system (Table III-7). Conveniently, this reaction does not require the cryogenic temperatures required by the original process.

entry	R ¹	R ² , R ³	Ar	Prdt	yield/ ee (TsNNaCl)	yield/ ee (DCDPH)
1	C ₆ H ₅	H, H	C ₆ H ₅	III-24a	85%, 92% ee	96%, 90% ee
2	C ₆ H ₅	H, H	4-Br-C ₆ H ₄	III-26a	87%, 97% ee	93%, 98% ee
3	C ₆ H ₅	H, H	4-Me-C ₆ H ₄	III-28o	92%, 92% ee	90%, 83% ee
4	4-Br-C ₆ H ₄	H, H	4-Br-C ₆ H ₄	III-26e	87%, 90% ee	89%, 84% ee
5	4-OMe-C ₆ H ₄	H, H	4-Br-C ₆ H ₄	III-26c	86%, 92% ee	72%, 93% ee
6	H	C ₆ H ₅ , H	4-OMe-C ₆ H ₄	III-28b	93%, >99% ee	93%, >99% ee
7	H	4-CF ₃ -C ₆ H ₄ , H	4-Br-C ₆ H ₄	III-28e	90%, 97% ee	94%, 95% ee
8	H	2-Me-C ₆ H ₄	4-Br-C ₆ H ₄	III-28h	95%, 91% ee	99%, 87% ee
9	H	C ₆ H ₅ , C ₆ H ₅	4-Br-C ₆ H ₄	III-28j	84%, 92% ee	92%, 86% ee
10	H	C ₆ H ₅ , Me	4-Br-C ₆ H ₄	III-28k	64%, 92% ee	52%, 91% ee
11	H	4-Me-C ₆ H ₄ , H	4-Br-C ₆ H ₄	III-28g	86%, 40% ee	73%, 37% ee

Table III-7: Comparison of Chloramine-T·3H₂O/(DHQD)₂PHAL to DCDPH/(DHQD)₂PHAL in the cyclization of allyl amines.

In order to gain a deeper understanding of the dimeric (DHQD)₂PHAL the catalyst and its role in halofunctionalization, Marshall et al. performed structure enantioselectivity relationship (SER) studies of various chlorocyclization reactions, some of which were previously discussed.⁸⁵

Analogues of (DHQD)₂PHAL were synthesized and divided into 5 classifications: (1) the linker, (2) the sterics of the quinoline substituent, (3) the sterics of the quinuclidine substituents, (4) the quinuclidine nitrogens, and (5) the stereochemistry of the C-9 carbinol center.

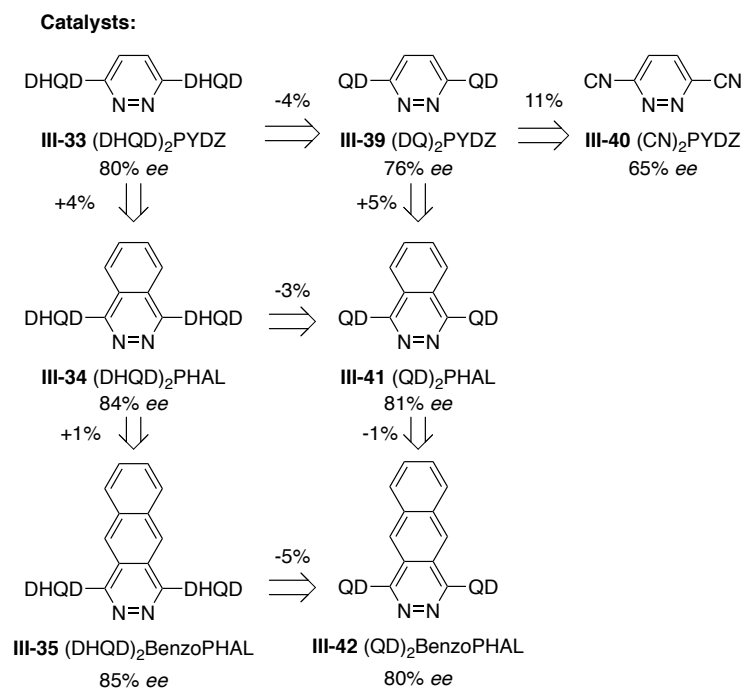
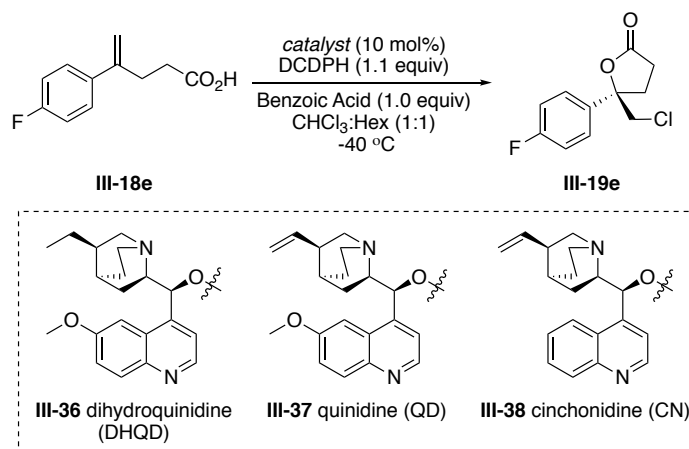


Scheme III-7: Evaluation of the importance of phthalazine linker in relation to enantioselectivity.

Initial studies addressed the necessary length of the linker using the chlorolactonization of 4-*p*-fluorophenyl-4-pentenoic acid **III-18e** as the model reaction (Scheme III-7). (DHQD)₂PHAL (**III-34**) gave 84%. Shortening the linker to 2,6-pyridazine (PYDZ) **III-33** gave a slightly less selective reaction (80% *ee*) while lengthening the linker to a 1,4-benzophthalazine (BenzoPHAL) **III-35** provided an even more slight (and possibly negligible) increase (85%). The change in enantioselectivity has been attributed to a computational study by Sharpless and coworkers addressing the preferred torsion angle about the C-O-C=N bonds. In the end, they conclude that introducing the larger aromatic linker rigidifies the optimal conformation, leading to stronger enantioinduction.

In order to probe the sterics of the quinoline substituents, researchers synthesized pyridazine dimers using other two other well-known commercially

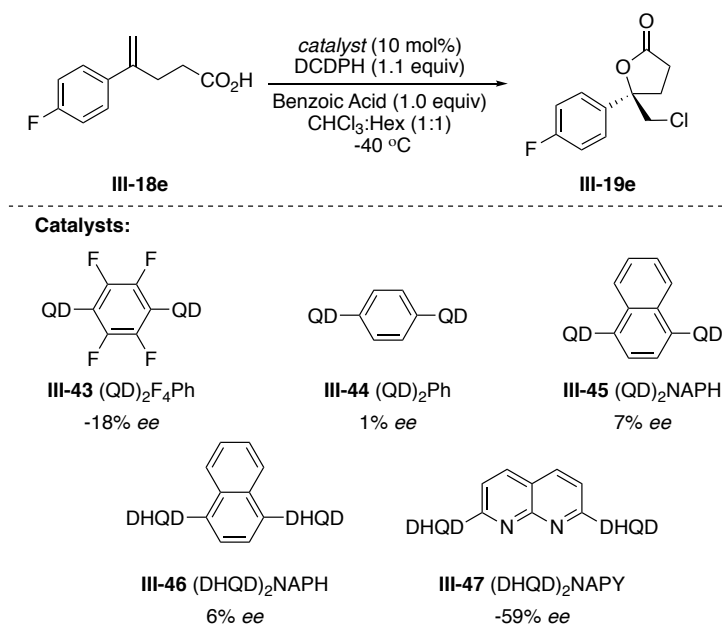
available cinchona alkaloids, namely quinidine (**III-37**) and cinchonidine (**III-38**). This evaluation featured in Scheme III-8 compared the approximate enantioselective “cost” of each modification of the monomeric units. When comparing (DHQD)₂PYDZ (**III-33**) to (QD)₂PYDZ (**III-39**), researchers found a drop of 5% *ee*, the “cost” of switching the saturated quinuclidine ethyl group for the vinyl moiety of the quinidine. A similar comparison of (QD)₂PYDZ (**III-39**) with (CN)₂PYDZ (**III-40**) was made, differing solely in the pendant methoxy group of the quinidine. The enantioselectivity fell 11%. In order to verify the additive effect the phthalazine and benzophthalazine compounds were also compared. (DHQD)₂benzoPHAL (**III-35**) provided a 5% higher enantiomeric access than did (QD)₂benzoPHAL (**III-42**). It should be noted that these values are close approximations. For example, while the cost of going from a saturated ethyl group to a vinyl group costs 5% *ee*, (DHQD)₂PHAL (**III-34**) to (DQ)₂PHAL (**III-41**) decreased the enantioselectivity by 3% *ee*.



Scheme III-8: Enantioselective cost evaluation of monomer modification in dimeric chlorolactonization catalysts. ^aThe enantioselectivities of lactone **III-19e** are documented below the structure of the catalyst used. ^bEach arrow indicates the enantioselective cost of a specified modification.

Borhan and coworkers then synthesized a number of catalyst analogues for the purposes of probing the importance of the phthalazine nitrogens (Scheme III-9). It

was observed that the fluorinated ether **III-43** led to a significant drop in enantioselectivity (-18% *ee*). Being aware of the fact that fluorine is capable of hydrogen bonding, Borhan and coworkers sought reassurance with Dissertation1,4-disubstitued benzene **III-44**. This use of this catalyst resulted in the complete erosion of the enantioselectivity. This observation showed that the nitrogens are important in conferring selectivity and not the added electronic alteration provided by the fluorine atoms. Dimer **III-44** gave 1% *ee*. In order to round out the series (QD)₂NAPH **III-45**, one of the most telling of the series, was examined. This catalyst produced near racemic product with 7% *ee*. While the quinidine (QD) monomer provides an effective catalyst when dimerized with phthalazine, it does not represent the catalyst with the most optimal activity. For this reason, (DHQD)₂NAPH (**III-46**) and (DHQD)₂NAPY (**III-47**) were also tested. The naphthyridine linker (NAPY), remarkably provided a moderate enantioselectivity of the opposite enantiomer (-59% *ee*). Researchers suggest that this 143% difference in enantioselectivity is most likely the result a very different conformation due to the wide separation of the alkaloids.



Scheme III-9: Probing the importance of the phthalazine nitrogens.

(DHQD)₂NAPH, the most similar analogue to (DHQD)₂PHAL in this sequence provided a 6% *ee*. The summation of these results affirms the importance of the phthalazine nitrogens as essential to the induction of stereoselectivity in (DHQD)₂PHAL.

In light of these findings, especially those seen in (DHQD)₂NAPH, Borhan and coworkers suggest two hypotheses:

1. The conformation of the naphthalene analogue of DHQD₂PHAL is not as rigid. This could be attributed to the absence of nitrogen lone pairs to repel the oxygen lone pairs, allowing for greater rotation about the C₉-O-C=C. Another suggested contributor is the decreased sp²-

character of the C₉ oxygen associated with the more electron rich naphthalene linker. This is a contrast to the donation of the oxygen into the electron deficient phthalazine linker, giving the oxygen with a greater sp²-character.

Calculations done by Sharpless and coworkers seem to support this hypothesis.⁸⁶ Using direct Hartree-Fock calculation ([6-31G*] basis set), they simulated the simultaneous turn of the methoxy units to the desired C-O-C=N torsion angle of 2,6-dimethoxypyridazine. The geometry was then optimized in C_s-symmetry at each point, fixing only the aforementioned torsion angle. The relative energies of the point MP2 (6-31G*) calculations were recorded. A comparison of the relative energies at 0° and 180° (an increase of approximately 52 kJ/mol) supports the suggestion that the oxygen lone pairs repel the nitrogen lone pairs at 180°. The initial increase of 15 kJ/mol seen when rotating from 0° to 30° underscores the broken conjugation of the oxygen lone pairs with the pyridazine ring.

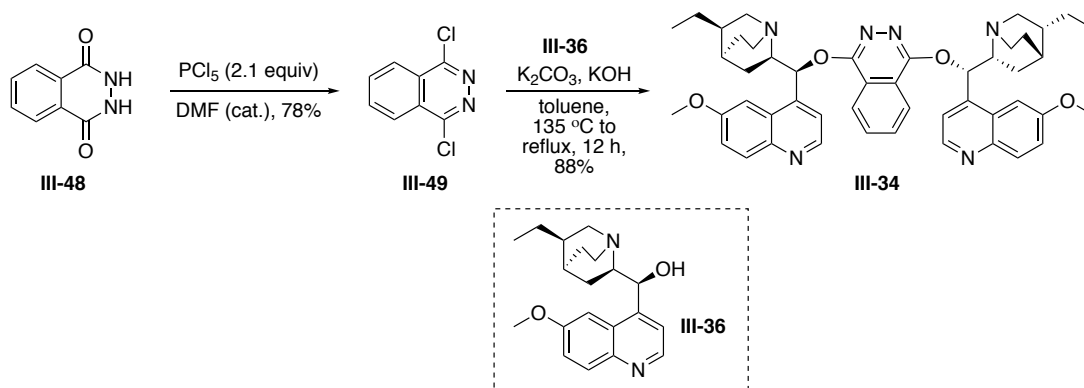
2. The phthalazine nitrogens may play a role in masking the carbocation generated by the chloronium addition step. Attack of the nucleophile displaces the nitrogen, producing the syn product, a process that could not be ruled out (though unlikely) by experiments done by Yousefi et al.

III.2. Results and Discussion

III.2.1. Synthesis of (DHQD)₂NAPH

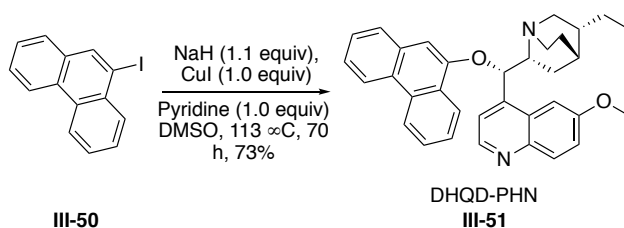
The idea that the phthalazine nitrogens play a key roll in the rigidity of the catalyst, and inadvertently the selectivity of the entire chlorofunctionalization methodology, is an intriguing prospect that we believed can and should be tested. To this end, we began with synthesizing the analogue that most closely represents the original structure of the optimal phthalazine dimer catalyst, (DHQD)₂PHAL **III-34**. This analogue, (DHQD)₂NAPH (**III-46**), because of the electronics of the naphthalene linker, can not be synthesized using the same methods used to synthesize the original catalyst.

Synthesis of (DHQD)₂PHAL by Sharpless and coworkers began with chlorination of phthalhydrazide **III-48** to form electron deficient phthalazine **III-49** in 78% yield. Basic coupling of dihydroquinidine **III-36** in toluene with azeotropic removal of water gave 88% of the desired (DHQD)₂PHAL dimer (Scheme III-10).²



Scheme III-10: Synthesis of (DHQD)₂PHAL.

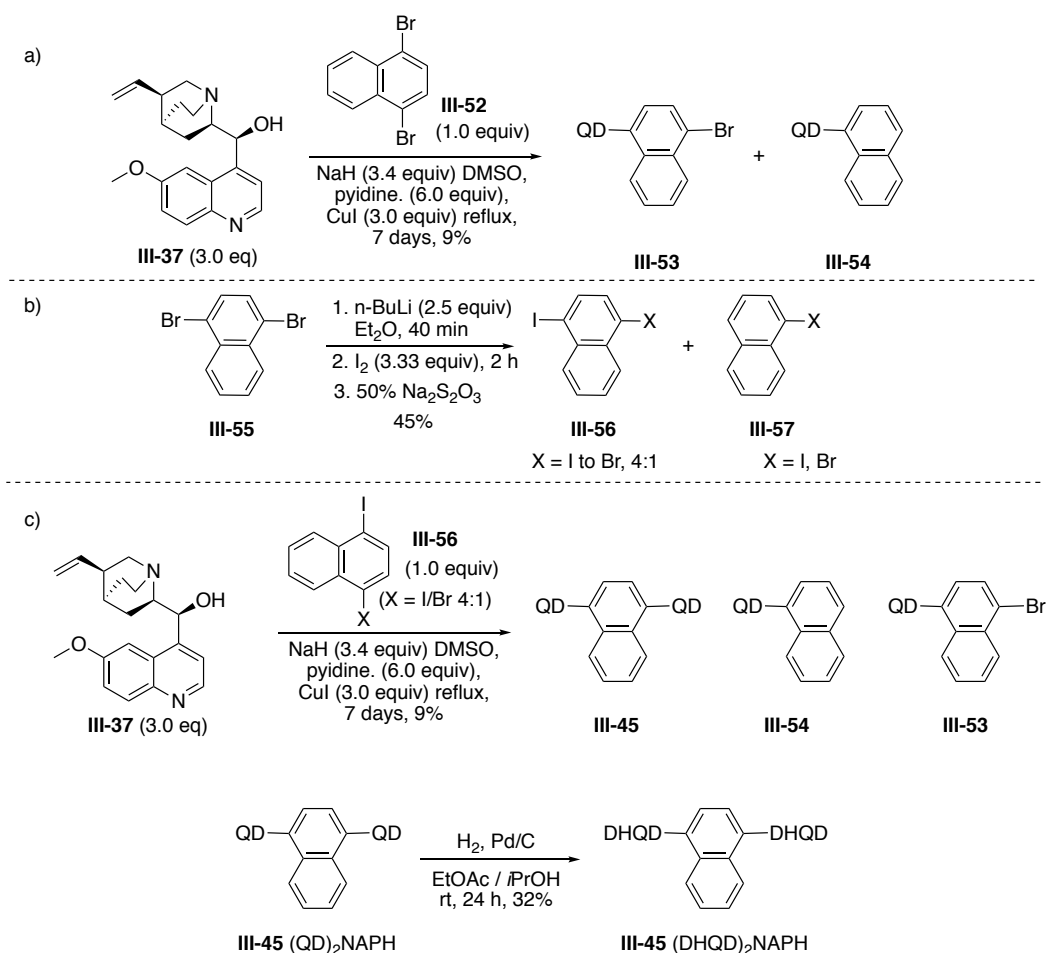
Synthesis of (DHQD)₂NAPH needed to follow a different method due to the electron rich nature of the naphthalene linker. To this end, we used the copper mediated Ullmann coupling, a method known to be effective in formation of biaryl systems from aryl halides⁸⁸ and the coupling of aryl halides with heteroatoms.^{89,90} Sharpless used this coupling to synthesize the phenanthryl ether catalysts featured in the catalyst screening of the asymmetric dihydroxylation (Scheme III-11).



Scheme III-11: Sharpless synthesis of dihydroquinidine 9-*O*-(9'-phenanthryl)ether (DHQD-PHN) using Ullmann coupling.²

Initial attempts to synthesize the (DHQD)₂NAPH dimer by Marshall et al. failed when the commercially available 1,4-dibromonaphthalene produced only the monoaddition products **III-53** and **III-54** (Scheme III-12a). It is known that aryl bromides require higher reaction temperatures, higher concentrations of substrates, and longer reaction times in order to undergo Ullmann coupling than their iodide counterparts.⁹¹

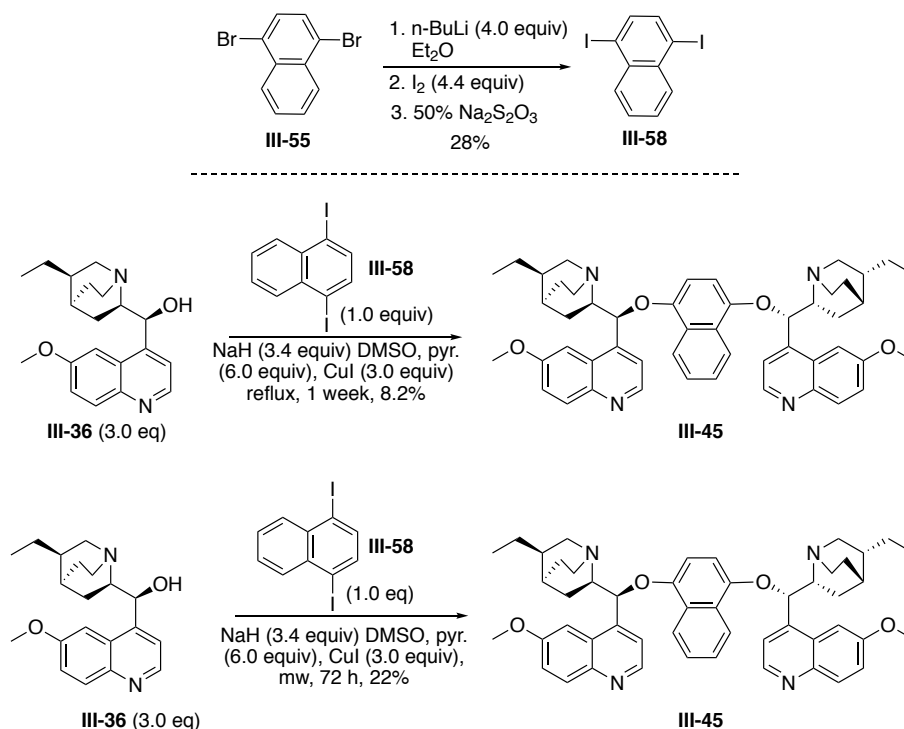
Consequently, they attempted the synthesis of 1,4-diiodonaphthalene using commercially available 1,4-dibromonaphthalene⁸⁵ via metal-halogen exchange, producing mixtures of the desired diiodonaphthalene and the single halogen exchange product 1-bromo-4-iodonaphthalene, along with monohalogenated naphthalenes **III-57**. After removing the monohalogenated naphthalene byproducts via column chromatography and crystallization of the remaining 1,4-disubstituted naphthalenes, researchers submitted a 4:1 mixture of dihalide **III-56** to the Ullmann reaction producing a mixture of products and isolating naphthalene dimer **III-45** in 9% yield (Scheme III-12c). Hydrogenation of the quinidine dimer provided dihydroquinidine dimer **III-45** in 32% yield.



Scheme III-12: Synthesis of naphthyl dimer (DHQD)₂NAPH. (a) Attempted Ullmann coupling with 1,4-dibromonaphthalene. (b) Synthesis of 1,4-diiodonaphthalene. (c) Ullmann coupling and reduction to form (DHQD)₂NAPH dimer.

In order to streamline this synthesis, we made a slight change to the halogen exchange submitting 1,4-dibromonaphthalene to increased equivalents of *n*-butyllithium and iodine (Scheme III-13). The isolated residue was submitted to a recrystallization, providing pure 1,4-diiodonaphthalene with no single halogen exchange product, though the yields were not as high (28%).⁹² We followed with Ullmann coupling of dihydroquinone **III-36** to remove the necessity for the low

yielding hydrogenation. The coupling, while possible, has proven difficult under the current conditions, giving yields of 8% pure product. We found that heating using microwaves for 72 hours provided almost three times the pure product (22%) than heating to 140 °C for 7 days. We also noticed this reaction gave a cleaner reaction, which provided us with a more efficient purification.

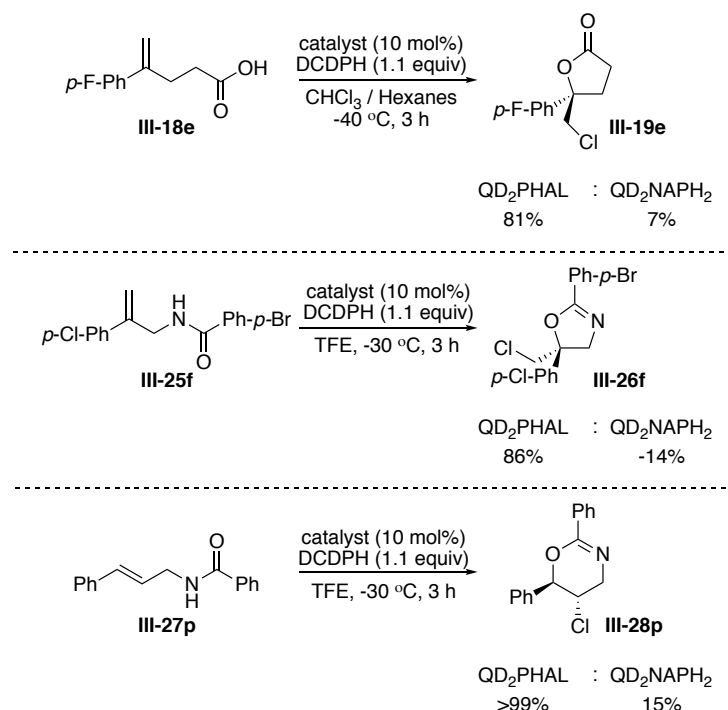


Scheme III-13: Synthesis of hydroquinidine-1,4-naphthalenediyl diether (DHQD)₂NAPH.

III.2.2. Intramolecular Chlorofunctionalization

Chlorofunctionalization using the Borhan lab methodologies has proven to be valuable with regard to their broad scope, high enantioselectivities and generalized procedure. Because of their success, they can serve as effective tools to probe the importance of the phthalazine nitrogens.

Initial SER studies performed by Marshall et al.⁸⁵ spanned approximately 25 catalysts and five reactions. For our purposes, we will look at 2 catalysts and 3 reactions. Unfortunately, due to the low yield of (DHQD)₂NAPH in the previously discussed synthesis (Scheme III-12c), there was not sufficient catalyst to test the 5 previously tested reactions, and therefore, not enough data to do a direct comparison of the optimal (DHQD)₂PHAL with its naphthalene analogue. However, the quinidine dimers were in sufficient supply to test against the desired reactions (Scheme III-14).

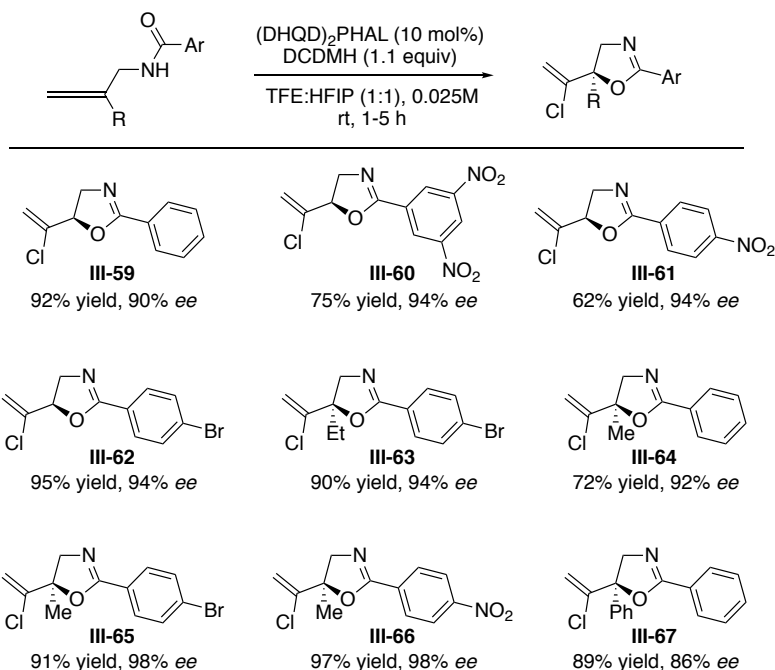


Scheme III-14: Comparison of (QD)₂PHAL and (QD)₂NAPH in chlorolactonization and allyl amide chlorocyclization.

The chlorolactonization of 4-(*para*-fluorophenyl)-4-pentenoic acid **III-18e** discussed earlier gave good enantioselectivities (81% *ee*) when (QD)₂PHAL was used as the catalyst. Switching to (QD)₂NAPH resulted in a significant drop in enantioselectivities (7% *ee*). Cyclization of 1,1-disubstituted allylic amide **III-25f** gave 86% *ee* in the presence of (QD)₂PHAL. The same cyclization oxazoline **III-26f** gave in 14% *ee* of the opposite enantiomer when catalyzed by (QD)₂NAPH. *Trans*-allyl amide **III-27p** cyclized with excellent enantioselectivity (>99% *ee*) when catalyzed by the phthalazine dimer (QD)₂PHAL. Again, the naphthalene analogue (QD)₂NAPH gave highly eroded stereoselectivities (15% *ee*). The SER studies done by Marshall et al. clearly show a consistent loss of enantioselectivity when using the naphthalene dimer analogue.

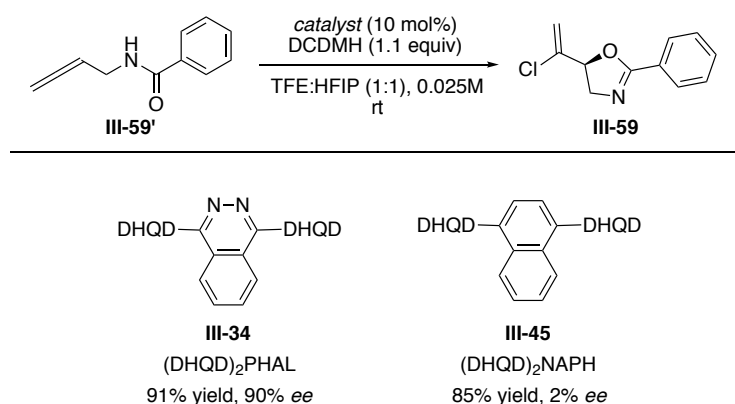
Allene halocyclization is a handy tool for the modification of organic molecules, providing a stereogenic center along with a vinyl halide with the potential to undertake cross-coupling reactions among other transformations. Ma and coworkers developed an iodoetherification and an iodolactonization that exhibited high region- and stereoselectivities without the use of a catalyst, instead relying on the intrinsic axial chirality of the allene.^{93 94} Hennecke and coworkers established an asymmetric bromolactonization of allenoic acids using (DHQD)₂PHAL as their catalyst but were met with low to moderate enantioselectivities (12-66% *ee*).

With this information in hand, we decided to continue our SER studies by addressing an allenyl chlorocyclization, a further advancement in the chlorocyclization reaction scope developed in the Borhan lab (Scheme III-15).⁹⁵ When investigating the substrate scope, compounds **III-60** and **III-61** showed lower enantioselectivities. This is due to the electron deficient nature of the amide benzoyl group. It is theorized that the nucleophilicity of the amide oxygen is reduced to the point of competition with intermolecular processes because of the electron withdrawing nature of the benzoyl ring. This was confirmed by the appearance of TFE-incorporated intermolecular byproduct. Conversely, 1,1-disubstitued allenes **III-63-66** performed very well with generally yields and enantioselectivities (90-97% yield, 92-98% *ee*). These compounds seemed to exhibit a greater eletrophilicity at the site of C-O bond formation. Unfortunately, this can lead to a greater background reaction as exhibited in the case of phenyl substituted **III-67** where enantioselectivities fell to 86%. The temperature was therefore lowered to regain selectivity.



Scheme III-15: Substrate scope for the intramolecular chlorocyclization of allene amides.

Under optimized conditions (Scheme III-16), (DHQD)₂PHAL-assisted allene amide **III-59'** was cyclized to form the corresponding vinyl chloride in 91% yield and 90% *ee*. Utilizing DHQD₂NAPH produced a yield of 85% but a low enantioselectivity of 2% *ee* remaining consistent with the previously seen deterioration of enantioselectivities due to the absence of the phthalazine nitrogens.

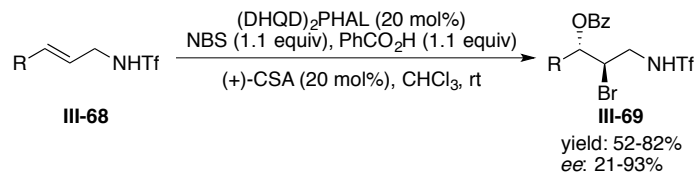


Scheme III-16: Allene chlorocyclization enantioselectivities.

III.2.3. Intermolecular Chlorofunctionalization

An overview of previous advancements in asymmetric halofunctionalization illustrates another method used to avoid the selectivity problems resulting from olefin-to-olefin transfer and β -halocarocation formation. The increased local concentration provided by tethered nucleophiles has been instrumental in the rate enhancement required for routinely higher enantioselectivities seen using a variety of halonium precursors and nucleophiles.

Intermolecular halofunctionalization opens up new direct routes for asymmetric aminohalogenation, haloesterification, dihalogenation, and halohydrin formation. Zhang et. al. exemplified this shift to intermolecular halofunctionalization in 2013 with the bromoesterification of allyl sulfonamides (Scheme III-17).⁹⁶ Using 20 mol% of (DHQD)₂PHAL in the presence of the same equivalence of camphorsulfonic acid (CSA), researchers were able to functionalize alkenes **III-68** providing benzoyl esters **III-69** in yields of 52-82% and *ee*'s of 21-93%.



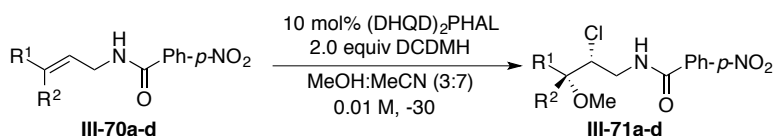
Scheme III-17: Bromoesterification of allyl sulfonamides using (DHQD)₂PHAL.

III.2.3.1. Chloroetherification

In a recent publication Borhan and coworkers,⁹⁷ the chlorination reaction profiles were increased to include intermolecular reactions, specifically chloroetherification (Table III-8). This system relies on a mixed solvent system (3:7, MeOH/MeCN) and a lowered temperature (-30 °C) to imbue upon intermolecular reactions a similar selectivity seen in intramolecular chlorination reactions using the same organic catalysts. Under the optimized conditions, allyl amides provided high enantioselectivities of halo-ethers, halo-esters, and halohydrins in both aryl and alkyl substrates. In the originally optimized chloroetherification reactions, it was found that a solution of DCDMH in the optimal methanol/acetonitrile solution with (DHQD)₂PHAL provided 56% yield and 84% *ee* of *anti*-2-chloro-3-methoxy amide **III-71a** from the *trans*-aryl alkene **III-70a** and 93% yield and 99% *ee* of the *syn* diastereomer (Table III-8, Entries 1 and 2). These compounds also exhibited high regioselectivity (both greater than 99:1) and seemed only to fall short in diastereoselectivity, showing ratios of 3.4:1

and 3.3:1, respectively. Both of these results can presumably be attributed to the carbocationic character of the benzylic carbon.

Aliphatic compounds **III-70c** and **III-70d** (Table III-8, entries 3 and 4) showed greater selectivity with both *trans* and *cis* propyl alkenes, giving high diastereo- (>99:1) and regioselectivities (>20:1). While the *trans* substrate provided adequate enantioselectivity (74%), the *cis* substrate was yet higher with *ee*'s of 99%. These regioselectivities are somewhat remarkable as there is not much distinguishing the difference between the two olefinic carbons.



Entry		Starting material		Product	Yield (%)	<i>d.r.</i>	<i>r.r.</i>	<i>e.r.</i>
		R ¹	R ²					
1	III-70a	Ph	H	anti	56	3.4:1	>99:1	92:8
2	III-70b	H	Ph	syn	93	3.3:1	>99:1	99.5:0.5
3	III-70c	C ₃ H ₇	H	anti	86	>99:1	>20:1	87:13
4	III-70d	H	C ₃ H ₇	syn	87	>99:1	>20:1	99.5:0.5

Table III-8: Limited substrate scope of intermolecular chloroetherification by Soltanzadeh, et al.

Due to the interesting and promising results seen with these substrates, these compounds were also used to explore the comparison of DHQD₂PHAL and DHQD₂NAPH as catalysts in intermolecular chloroetherification. The reactions

were compared at room temperature in order to eliminate possible inconsistency of varying low temperatures that may complicate the comparison of the two catalysts. We believed this would lead to a decrease in the enantioselectivities seen previously in DHQD₂PHAL. However, we believed the difference in enantioselectivity between the two catalysts would still be large enough to assess their effectiveness.

We had already reasoned that some of the selectivities seen in the literature would be lower because of the change in temperature. Therefore, the lower diastereoselectivities and enantioselectivities seen in the (DHQD)₂PHAL-catalyzed reactions were seen as consequences of the higher temperature. With this in mind, there were still stark differences in the effectiveness of the two catalysts. We were able to confirm the deterioration of the enantioselectivities and surprisingly regioselectivities with (DHQD)₂NAPH. For example, the *cis*-propyl allyl amide **III-70d** was converted to *syn*-β-chloromethoxy ether **III-71d** with little regioisomer (94:6) and 85% *ee* when mediated by (DHQD)₂PHAL. **III-70d** mediated by (DHQD)₂NAPH produced the desired methoxy ether **III-71d** with no selectivity (0% *ee*) along with higher quantities of the regioisomer **III-72d** and a substantial amount of the intramolecular oxazoline byproduct **III-74d** (regioselectivity was 49:12:39, respectively).

III-70 a-d

10 mol% *catalyst*
2.0 equiv DCDMH
MeOH:MeCN (3:7)
0.02 M, rt

III-71
Desired Product (CE)

III-72
Regioisomer (RI)

III-73
6-member ring
(6-memb)

III-74
5-member ring
(5-memb)

Entry	Substrate	DHQD ₂ PHAL				DHQD ₂ NAPH			
		84% Yield				100% Yield			
		C.E.	R.I.	6-memb	5-memb	C.E.	R.I.	6-memb	5-memb
1		94	0	6	0	78	0	22	0
	III-70a	<i>Syn</i> 36	<i>Anti</i> 58			<i>Syn</i> 30	<i>Anti</i> 48		
		86% ee	-32% ee			16% ee	-8% ee		
		73% Yield				23% Yield			
		C.E.	R.I.	6-memb	5-memb	C.E.	R.I.	6-memb	5-memb
2		100	0	0	0	100	0	0	0
	III-70b	<i>Syn</i> 62	<i>Anti</i> 38			<i>Syn</i> 59	<i>Anti</i> 41		
		94% ee	-90% ee			10% ee	-20% ee		
		75% Yield				85% Yield			
		C.E.	R.I.	6-memb	5-memb	C.E.	R.I.	6-memb	5-memb
3		87	7	2	3	50	11	30	9
	III-70c	60% ee				15% ee			
		80% Yield				98% Yield			
		C.E.	R.I.	6-memb	5-memb	C.E.	R.I.	6-memb	5-memb
4		94	6	0	0	49	12	0	39
	III-70d	85% ee				0% ee			

Table III-9: A comparison of intermolecular chloroetherification of aliphatic and aromatic allylic amides using (DHQD)₂PHAL and (DHQD)₂NAPH catalysts.

Similarly to the previously discussed literature findings, aliphatic substrates submitted to chloroetherification catalyzed by (DHQD)₂NAPH were found to have high diastereoselectivity. In each aliphatic compound, whether *cis* or *trans*, there was only one detectable diastereomer. Aromatic substrates, on the other hand,

were found to produce poor diastereoselectivities of approximately 2:1. These results can be explained in one of two ways: (1) Classical halogenation mechanisms suggest that the formation of a chloriranium intermediate that, in aliphatic, systems should not differentiate between the two carbon sites as a point of nucleophilic attack unless the nitrogen inductively reduces the electrophilicity of the closer carbon. This explains the 5-*exo-trig* oxazoline byproducts seen in the cyclization of aliphatic systems. This could also explain erosion in regioselectivity seen in the use of (DHQD)₂NAPH. Aromatic systems produce β-chlorocarocations that erode the diastereoselectivity whilst enhancing regioselectivity. (2) These results are also supported by Ashtekar's nucleophile assisted alkene activation theory,⁹⁸ a concept that contradicts the driving force for the formation of bridged halonium species often represented in Organic Chemistry textbooks. This paper suggests that reactivity of an unactivated alkene comes from the polarizing of the pi bond through the close proximity of the nucleophile. While this paper addresses appended nucleophiles to establish this point, it is not difficult to justify the use of this theory in explaining the diastereoselectivities seen in these intermolecular reactions. The product **III-71** is dependent on the approach of an external nucleophile to polarize the olefinic carbon distal to the nitrogen. Unactivated aliphatic olefins (represented by propyl allyl amines **III-70c** and **III-70d**) produce a small amount of regioisomer **III-72c** and **III-72d**, likely due to the closeness in electrophilicity of the olefinic carbons. The increase in regioisomer seen in the case of (DHQD)₂NAPH

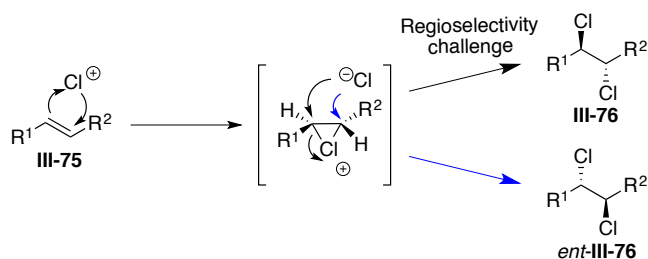
suggests a change in conformation that allows the external nucleophile an easier approach of the olefinic carbon proximal to the nitrogen. Interestingly, in the case of *cis* versus *trans* aliphatic systems, cyclized byproducts ratios vary substantially. *Trans*-**III-70c** provides 30% of 6-membered cyclized byproduct **III-73c** while *cis*-**III-70d** yielded 39% of 5-membered cyclized byproduct **III-74d**. This suggests that the nucleophilic amide nears the olefin at different positions depending on the alkene isomer.

In the case of mildly activated alkenes, namely aryl alkenes, there was a breakdown in diastereoselectivity that could justifiably be attributed to one of two scenarios: (1) the formation of a benzylic carbocation allowing the formation of significant amounts of both diastereomers with any selectivity mitigated by the catalyst or (2) the temporary formation of a six membered ring through cyclization of the pendant amide nucleophile later reopened by an external nucleophile. The first condition is much more easily justified than the second due to the formation of the six-membered oxazoline in the *trans*-aryl alkene and lack thereof in the *cis*-aryl alkene. On the other hand, these compounds were highly regioselective, yielding no recognizable regioisomer. This also points to the formation of a benzylic carbocation and no chance of any opposing polarization of the pi bond by a nucleophile.

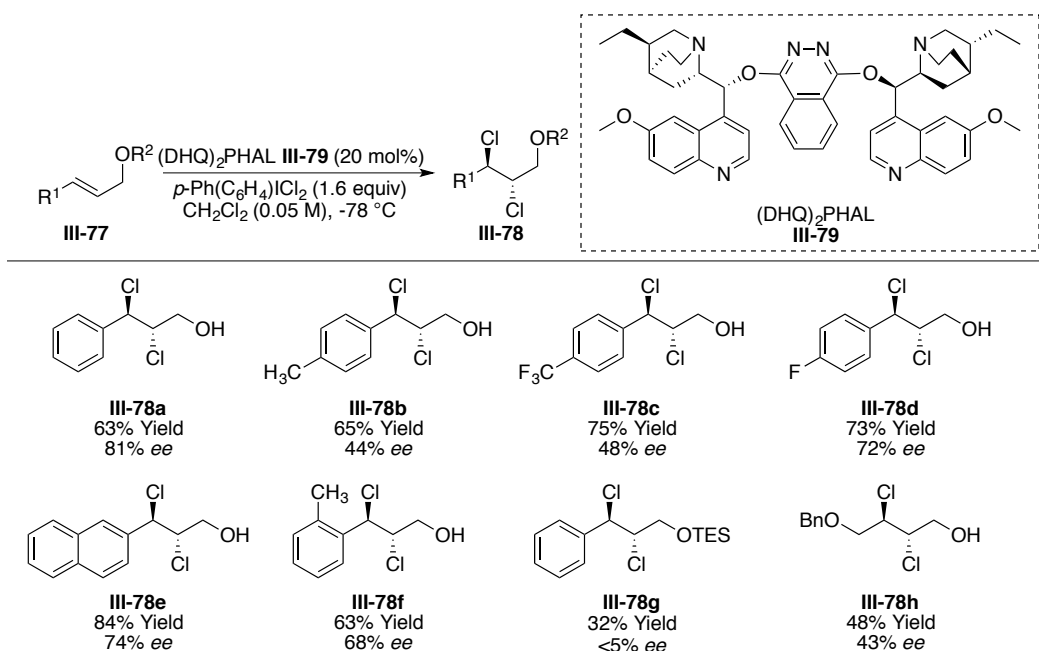
When evaluating the enantioselectivities in the comparison of (DHQD)₂PHAL and (DHQD)₂NAPH, the results seem comparable to those in the intramolecular cases. There is a drastic loss in selectivity in every instance with the use of the naphthyl catalyst. This is exemplified best with the *cis*-aryl and aliphatic substrates.

III.2.3.2. Dichlorination

In order to further explore the difference between the two catalysts, we began to evaluate the dichlorination of the previously tested substrates. Dihalogenation provides a new challenge not previously seen with other forms of halofunctionalization (Scheme III-18). The formation of the chloriranium ion, whether in a facially selective manner or not, is undermined by the low regioselectivity of unactivated alkenes. In order to address this issue, Nicolaou and coworkers relied in major part on a substrate scope limitation of cinnamyl alcohols illustrated in Scheme III-19.⁹⁹ The increased electrophilicity of the phenyl-adjacent olefinic carbon provides an electron deficient trap for the nucleophilic chloride.



Scheme III-18: Regioselectivity challenge associated with asymmetric dichlorination of unactivated olefins.



Scheme III-19: Nicolaou asymmetric dichlorination of allyl alcohols.

The procedure used was developed by Borhan, and coworkers,¹⁰⁰ using dichlorodimethylhydantoin, (DHQD)₂PHAL catalyst, and one hundred equivalents of lithium chloride to decrease byproduct formation in trifluoroethanol at cold temperatures (Table III-10). Soltanzadeh et. al. has been able to transform allyl amides **III-70a-d** into chiral dihalides **III-80a-d** with moderate to high

enantioselectivities (84:16 to 99.5:0.5). As seen in the chloroetherification, the tested aryl alkenes give moderate to high enantioselectivities (84:16 for *trans* and 97:3 for *cis*) with a similar drop in diastereoselectivities, the greater of which was seen in *cis*-aryl substrates at 15.6:1. Alkyl substrates showed impressively high enantio- and diastereoselectivities with ratios of 90.5:9.5 and 98.2 for *trans* and *cis*, respectively, with regard to enantiomer selectivity and greater than 99:1 with regard to both diastereomers.

Entry	Starting material		Yield (%)	d.r.	e.r.	
	R ¹	R ²				
1	III-70a	Ph	H	63	53:1	84:16
2	III-70b	H	Ph	62	15.6:1	97:3
3	III-70c	C ₃ H ₇	H	76	>99:1	90.5:9.5
4	III-70d	H	C ₃ H ₇	91	>99:1	98:2

Table III-10: Limited substrate scope of intermolecular dichlorination by Soltanzadeh, et al.

When this reaction was explored with both catalysts at room temperature (Table III-11), the greatest selectivities were seen with (DHQD)₂PHAL, as expected. With regard to the *cis*- and *trans*-aliphatic compounds, the major product was the desired dichlorination product **III-80c-d** with small amounts of trifluoroethanol (TFE) incorporation (1% and 8% for *trans* and *cis*, respectively) and no apparent

formation of the 5-membered ring **III-74**. The enantioselectivity was moderate in the *trans* aliphatic compound (64% *ee*) and good in the *cis* at 86% *ee*.

The *trans* aliphatic allyl amide **III-70c** in the case of (DHQD)₂NAPH was less chemoselective, providing 14% TFE incorporation. The *cis* aliphatic amide provided much still less chemoselectivity, with greater amounts of TFE incorporation (30%) and, additionally, cyclization to form the 5-membered oxazoline ring (12%).

With regards to the enantioselectivity, the expected erosion was observed with (DHQD)₂NAPH as the catalyst. The aliphatic amide yielded 12% *ee* and 16% *ee* with regards to *trans* and *cis* compounds, respectively.

With little data available on the torsional strain of 1,4-dialkoxy naphthalene and phthalazine systems, we sought out their single ring analogues (*p*-dimethoxybenzene and 1,4-dimethoxypyridazine) to shed light on their torsional energies. Kollman and Houk,¹⁰¹ in an exploration of the nonplanarity of *o*-dimethoxybenzenes, showed using STO-3G calculations that the relative energy difference between a *p*-substituted benzene wherein both methoxy groups are planar (0° and 0°) and one wherein a single methoxy group is orthogonal (0° and 90°) is near zero ($E_{\text{rel}} = 0.16$ kcal/mol)(Figure III-2). It should be noted that this value is lower than the energy of a 90° rotation of anisole (0.94kcal/mol). This low relative energy allows the free and easy rotation of the methoxy group.

III-82		III-83			III-84			III-85		
deg	E_{rel}	deg ₁	deg ₂	E_{rel}	deg ₁	deg ₂	E_{rel}	deg ₁	deg ₂	E_{rel}
0°	0	0°	0°	0	0°	0°	0	0°	0°	0
45°	1.05	90°	0°	2.25	90°	0°	0.16	30°	0°	1.90
90°	0.94							60°	0°	0.98
								90°	0°	0.34
								180°	0°	10.14

Figure III-2: Relative energy of rotation of anisole and dimethoxybenzenes. ^a Relative energy (E_{rel}) is in kcal/mol.

Sharpless and coworkers, in a discussion of two models for asymmetric induction in osmium-catalyzed dihydroxylation, presented the relative torsion angle energies of 1,4-dimethoxypyridazine.⁸⁶ Both methoxy units were synchronously rotated along the C_{Ar}-O in the N=C-O-CH₃ sequence to the desired torsion angle. Using Hartree-Fock calculations (6-31G* basis set) to calculate the relative

energies at each optimized point, Sharpless was able to show that the relative energy required to rotate a methoxy group a mere 30° would be approximately 15 kJ/mol (3.6 kcal/mol) (Figure III-3). At 90°, the energies reached as high as 60 kJ/mol (14 kcal/mol). It should be noted that this system is unlike the singular bond rotations addressed Kollman and Houk and should not be directly compared. The synchronous movement of both methoxy groups may have additional destabilizing effects not addressed herein. However, both studies shed light on the possible mechanistic underpinnings that govern the observed catalyst functionality.

Pople and coworkers explored the torsional barriers of *p*-substituted phenols using an STO-3G basis set.¹⁰² Understanding that phenols have increased double bond character in their C-O bonds, they sought to highlight the effects specific substituents in the *para* position would have on the π -donating ability of the attached oxygen. They were able to show that electron-donating moieties, such as another hydroxyl group, decreased the π donation from the phenol oxygen and consequently, decreasing the double bond character and the barrier to rotation.

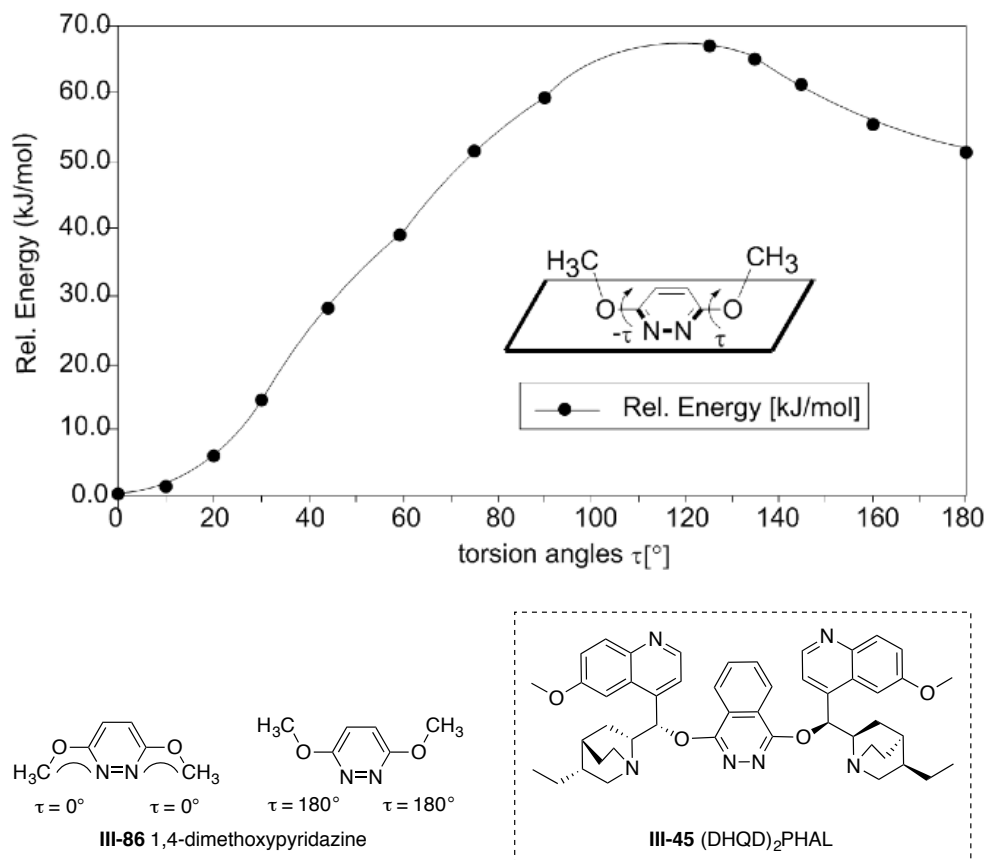


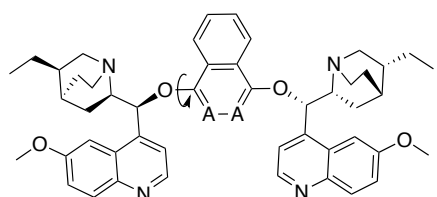
Figure III-3: Relative rotational energy of 1,4-dimethoxypyridazine, a simple model system for (DHQD)₂PHAL bond rotation.

In our attempts to clarify the role of the phthalazine nitrogens, we calculated the relative energies of the rotomers of (DHQD)₂PHAL and (DHQD)₂NAPH using density functional theory (DFT) B3LYP 6-31G* in vacuum with post solvent = trichloromethane. After initial geometry optimization, all bonds of the molecule were locked save the dihedral angle of N=C-O-C₉ in the case of phthalazine and C=C-O-C₉ in the case of naphthalene. This bond was rotated by 36° intervals for 360° and the relative energies recorded at each interval.

Initial observation of the optimized catalysts revealed that the optimal dihedral angle was not 0° as some may expect, but 13.03° (Figure III-4). With an approximately 109° between the C_9 -O bond and the oxygen lone pair, the lone pair becomes orthogonal to the plane of the aromatic linker (96° from line of lone pair orbital to the linker C=C or C=N bond). This appears to be the optimal angle by which donation into the ring can occur. Comparison of the two catalysts at this optimal dihedral angle showed that $(DHQD)_2PHAL$ was the most stable (-2.65 kcals). $(DHQD)_2NAPH$ was more than two times less stable in the initial conformation than its phthalazine counterpart (-1.23 kcals). This is reasonable when considering Pople's phenol study. The electron deficient phthalazine ring is further stabilized by the lone pair donation of the pendant oxygen atoms. On the other hand, naphthalene is more electron rich and will not be equally stabilized by the π -donation of their analogous counterparts.

Though we analyzed the full 360° rotation of the catalysts, we were only interested in the initial rotational conformations, noting that other factors, such as sterics could play a more significant role in the observed energies of conformers of greater than 60° (Table III-12). We found that $(DHQD)_2PHAL$ requires 1.4 kcals more energy (13.03° at -2.64 kcal to 49.03° at 0 kcal) to rotate 36° than the more electron rich $(DHQD)_2NAPH$ catalyst (13.03° at -1.23 kcal to 49.03° at 0 kcal). While the difference becomes even more drastic when considering the rotation from 13.03° to 85.03° (72° bond rotation requires 6.65 kcals of energy in

(DHQD)₂PHAL and 4.87 kcal in (DHQD)₂NAPH), we believed that the larger differences were due to the addition of alternate destabilizing effects, such as sterics.



A = N, **III-34** (DHQD)₂PHAL
A = CH, **III-46** (DHQD)₂NAPH

	A=C-O-C dihedral angle [°]	<i>E</i> _{res} ^a
(DHQD) ₂ PHAL	13.03	-2.64
	49.03	0
	85.03	4.01
(DHQD) ₂ NAPH	13.03	-1.23
	49.03	0
	85.03	3.64

Table III-12: DFT B3LYP 6-31G* energies (kcal) of single (DHQD)₂Ar bond rotation.

These results confirm that the phthalazine nitrogens provide an electron deficient environment that causes greater π -donation from the pendant ether oxygen lone pairs. This, in turn, rigidifies the catalyst giving the high enantioselectivities exhibited in the chlorofunctionalization reactions.

We have not yet addressed the possible lone pair repulsion also suggested in the hypothesis.

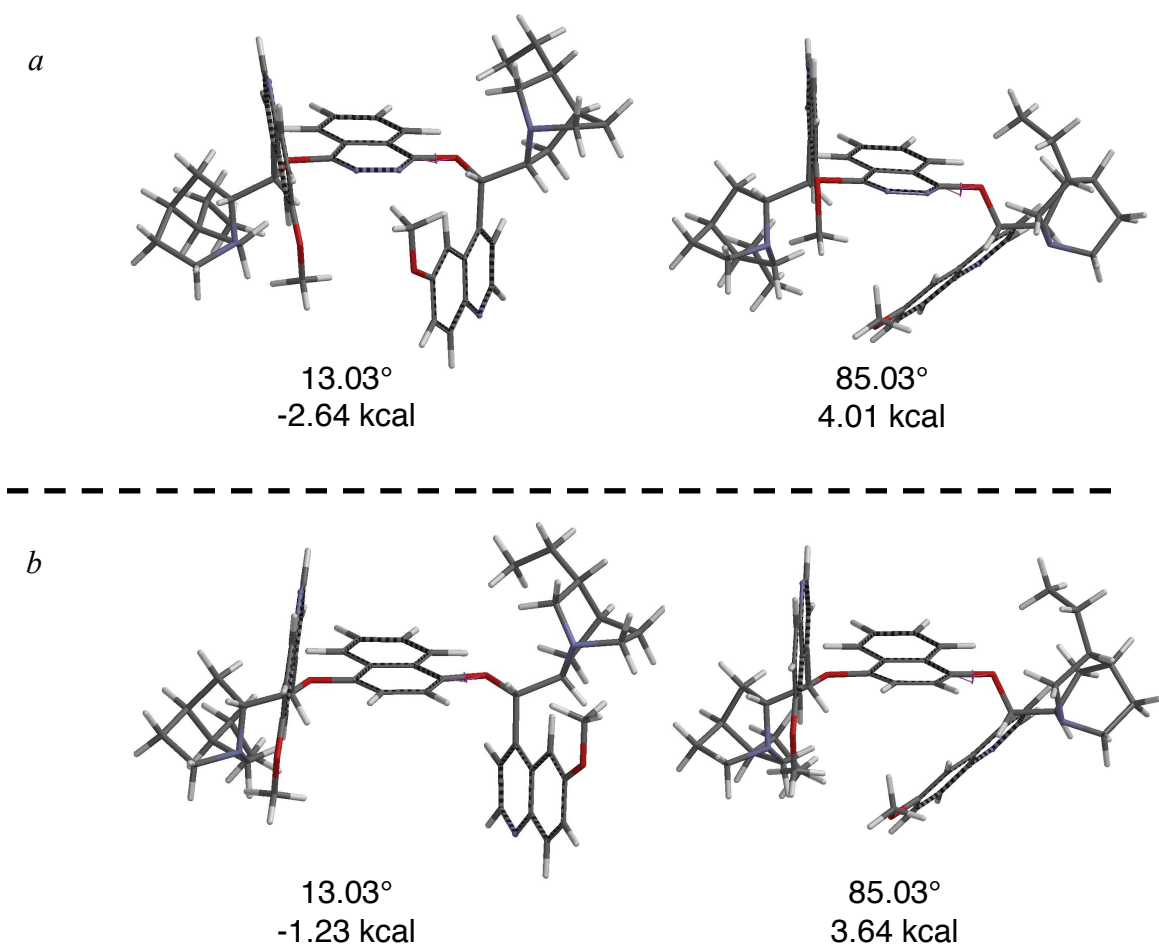
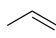
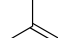
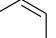
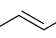
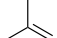
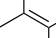


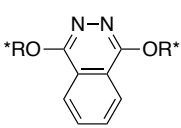
Figure III-4: DFT calculation (B3LYP 6-31G*) of relative energy of (DHQD)₂PHAL (*a*) and (DHQD)₂NAPH (*b*). =C-O-C dihedral angle and relative energy for each structure is written below.

III.2.5. Sharpless Dihydroxylation

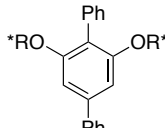
Asymmetric dihydroxylation is a well studied reaction¹ developed and expounded upon by Sharpless and many others. This reaction uses (DHQD)₂PHAL and (DHQ)₂PHAL ligands, among other ligands with pendant cinchona alkaloids, with

catalytic potassium osmate to form a chiral vicinal diol. In evaluating a multitude of alkenes, studies showed that, with the exception of *cis*-disubstituted olefins, cinchona alkaloid dimerized phthalazines were the preferred ligand linker among the tested systems with *trans*-disubstituted and trisubstituted alkenes providing the best range of enantioselectivity (90-99.8% *ee*, pictured in Scheme III-20). Testing of *trans*-disubstituted substrate scope revealed that *trans*-5-decene and *trans*-stilbene showed high selectivity using both phthalazine ligands (93-97% and >99.5% *ee*, respectively).¹

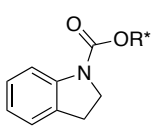
Olefin class						
Preferred ligand	PYR PHAL	PHAL	IND	PHAL	PHAL	PYR PHAL
<i>ee</i> range	30-97%	70-97%	20-80%	90-99.8%	90-99%	20-97%



PHAL-class



PYR-class



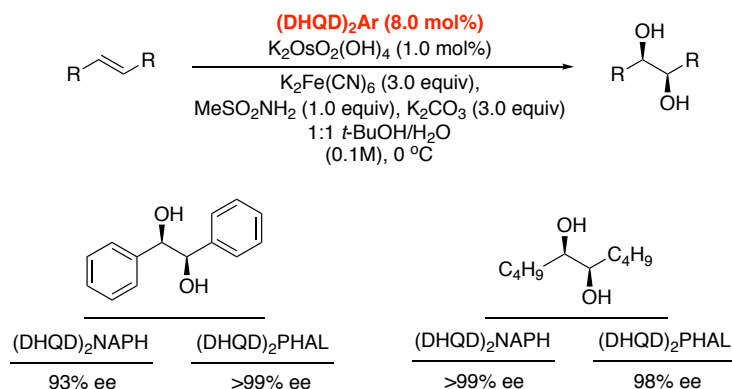
IND-class

R* = DHQD
or DHQ

Scheme III-20: Recommended ligand for each olefin class and their enantioselectivity range.¹

Since these compounds are easily accessible, they were used to probe the viability of (DHQD)₂NAPH in comparison to the phthalazine catalyst. It would be reasonable to believe that, similarly to the halogenation reactions, (DHQD)₂NAPH would produce selectivity much lower than that of (DHQD)₂PHAL.

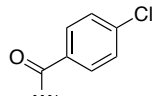
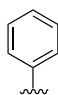
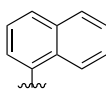
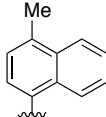
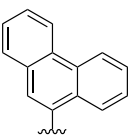
It was found, however, that the naphthalene linker changed the enantioselectivity of the dihydroxylation very little (Scheme III-21). Using Chiral HPLC, hydrobenzoin produced using (DHQD)₂NAPH was highly enantioselective at 93% *ee*. (DHQD)₂PHAL provided still higher selectivity at greater than 99% *ee*. Even more interestingly, (DHQD)₂NAPH produced a slightly more selective diol in the case of *trans*-5-decene (>99% *ee*) than (DHQD)₂PHAL (98% *ee*).



Scheme III-21: Dihydroxylation of *trans*-stilbene and *trans*-5-decene with (DHQD)₂NAPH and (DHQD)₂PHAL.

While dimeric dihydroquinidine naphthyl ether has not been published, these results are somewhat consistent with those seen in the structure-enantioselectivity studies done by the Sharpless group in 1991.¹⁰³ The *p*-chlorobenzoyl ester, the phenyl ether, the (1'-naphthyl) ether, (1'-(4-methylnaphthyl)), and (9'-phenanthryl) ether, among with quite a few others, were probed using stilbene and *trans*-5-decene to represent aromatic and aliphatic substrates in the evaluation of catalyst effectiveness with regards to

enantioselectivity (Table III-13). Seemingly, all four catalysts showed an excellent enantioselectivity with stilbene with a slight drop when using the phenyl ether. More interestingly, 9-O-(1'-naphthyl), 9-O-(1'-(4-methylnaphthyl), and 9-O-(9'-phenanthryl) ethers (Table III-13, entries 3,4, and 5) compared favorably against the phenyl ether and *p*-chlorobenzoyl ester (entries 1 and 2) in the oxidation of *trans*-decene. The phenyl ether selectivity was significantly lower at 88% *ee* than that of the naphthyl (94%), 4-methylnaphthyl (95%) and phenanthryl (95%) catalysts, with the *p*-chlorobenzoyl still lower (79% *ee*).

entry			decene (% ee)	stilbene (% ee)
1		III-87	79	99
2		III-88	88	94
3		III-89	94	99
4		III-90	95	98
5		III-91	95	99

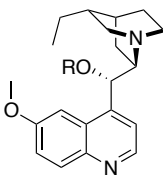

 (DHQD)

Table III-13: Dihydroxylation of *trans*-5-decene and *trans*-stilbene using a variety of 9-O-aromatic DHQD catalysts.

It was reasoned, based on x-ray crystallographic data, that when directly overlapped, the catalysts showed the greatest steric difference in the upper left

quadrant (Figure III-5). The steric filling of this quadrant appeared to increase enantioselectivities in the case the aliphatic olefin. In accordance with this observation, the *p*-chlorobenzoyl catalyst showed much lower selectivity when compared to the naphthyl and phenanthryl catalysts. The phenyl catalyst also showed lower enantioselectivities though not as low as those of the benzoyl catalyst. This point is further illustrated by the slight difference in the enantioselectivity imposed by the less sterically bulky (1'-naphthyl) ether when compared to the (1'-(4-methylnaphthyl)) and phenanthryl catalysts, the latter of which show a slight increase in selectivity. This suggests that filling right quadrants is also important though the absence of sterics there is not as detrimental to enantioselectivity.

When this logic is applied to the dihydroxylation of olefins using (DHQD)₂NAPH in place of (DHQD)₂PHAL, it suggests that they should impose similar enantioselectivities on both aromatic and aliphatic olefins since they have similar groups in the most significant quadrants.

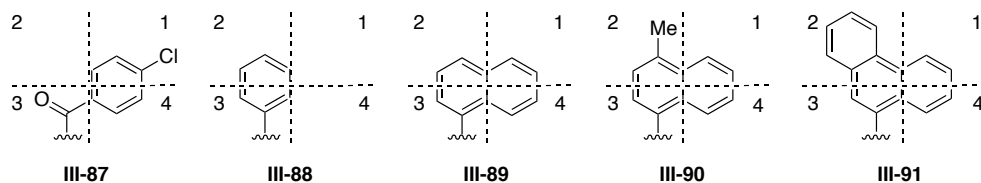


Figure III-5: A comparison of DHQD ether catalysts divided into quadrants.

III.3. Conclusion

In the asymmetric halogenation of alkenes, the specific composition, the difference between phthalazine and naphthalene, is important. There is a marked difference in the enantioselectivity of both intra- and intermolecular halogenation. This difference is directly attributable to the electron deficient nature of the phthalazine ring, leading to an increase in the sp^2 character of the ether oxygen and restricting the rotation around the O-C_{Ar} bond. This creates high concentrations of the rigid catalyst conformation responsible for producing the high enantioselectivities. When the phthalazine nitrogens are removed, the electron withdrawing nature of the ring is replaced by the electron donating nature of the naphthalene, dispelling the oxygen sp^2 character seen previously and lowering the conformational energy. The result is a much less rigid catalyst and greatly diminished *ee*'s.

In the asymmetric dihydroxylation of olefins, the composition, as it corresponds to the electronics of the linker, appears not to be as important as the general structure of the catalyst. This has been shown in singly and doubly substituted linkers that are both electron deficient and electron rich. This is likely due to the fact that the cinchonidine-based catalysts are operating as ligands.

While it was never assumed that the mechanisms for asymmetric halogenation and dihydroxylation were the same, the research shows that the mechanisms

differ even in the importance of basic configuration of (DHQD)₂PHAL. It is important to note that (DHQD)₂PHAL plays the role of a catalyst in halogenation but the role of a ligand in dihydroxylation. Further study is necessary to explore the importance of rigidity in a catalyst as opposed to a ligand in the case of (DHQD)₂PHAL and hopefully in a more generally applicable sense. To this end, (QD)₂NAPH can be synthesized to provide another handle for the manipulation of catalyst orientation.

In order to further prove the claims that the electron deficiency of the aryl linker lends itself to a more rigid system and higher enantioselectivities, it seems logical to synthesize electron deficient naphthalene catalysts. Catalysts like **III-92**, **III-93** and **III-94** featured in Figure III-6 should regain rigidity and with it, the high selectivities seen in chlorofunctionalization reactions performed in our lab using (DHQD)₂PHAL catalysts.

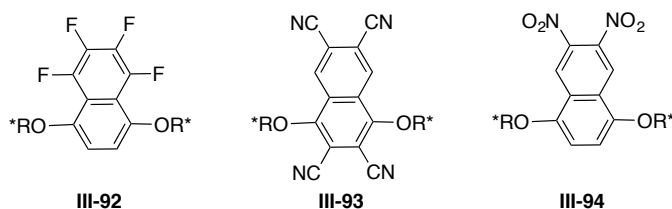
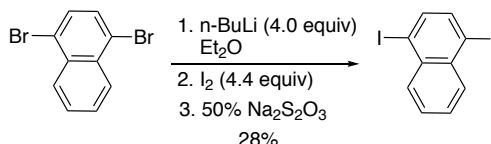


Figure III-6: Possible electron deficient naphthyl linkers to test for the recovery of selectivity in chlorofunctionalization.

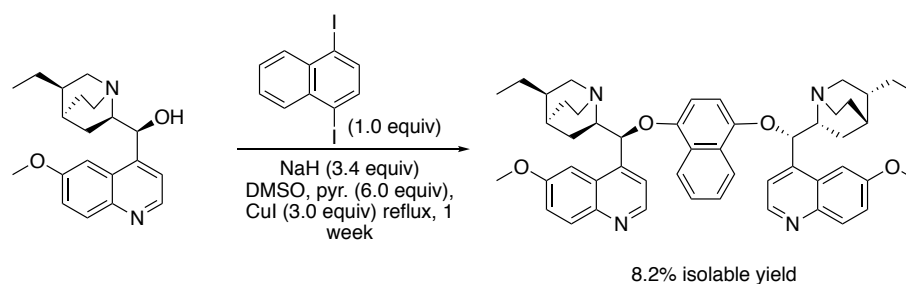
III.4. Experimental

III.4.1. Synthesis



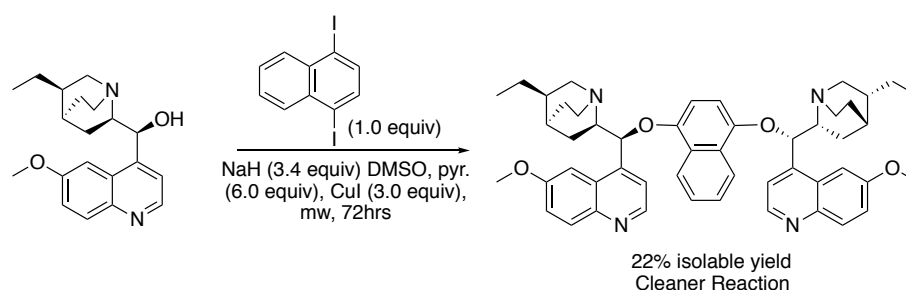
Preparation of 1,4-diiodonaphthalene. 1,4-dibromonaphthalene (1.0 equivalents, 6.99 mmol) was charged into a flame dried flask with a stir bar, sealed and purged with nitrogen gas. *n*-Butyllithium (4.0 equivalents, 27.98 mmol) was added slowly to the stirring solution. A yellow precipitate began to form. The suspension was allowed to stir for 10 minutes before the addition of iodine (4.4 equivalents, 30.77 mmol). The solution bubbled and then turned a dark brown. The solution was left to stir overnight in darkness. More diethyl ether was added to the solution and it was transferred to a separatory funnel and washed with 25% w/w aqueous sodium thiosulfate (3 x 20 mL). This was followed by washing with 50 mL of water. The organic phase was dried over sodium sulfate, filtered and concentrated en vacuo. The yellow residue was dissolved in methylene chloride and run through a plug of silica gel. The solvent was completely removed and the residue redissolved in ethanol while warming. The solution was refrigerated overnight. The yellow needle crystals were filtered through filter paper and the solid (28% yield) was transferred to a vial. ¹H NMR (500 MHz, CDCl₃) δ 8.06 (dd, *J* = 6.4, 3.2 Hz, 1H), 7.79 (s, 1H), 7.62 (dd, *J* = 6.4,

3.3 Hz, 1H); ^{13}C NMR (126 MHz, CDCl_3) δ 138.16, 134.75, 133.05, 128.66, 100.75.



Preparation of Hydroquinidine 1,4-naphthalenediyl diether. A stir bar was charged into a flask of dried hydroquinidine. The flask was purged with argon for 30 minutes. Dry DMSO (8.2 mL) was added to the flask and left stirring until the solid was completely dissolved. Sodium hydride was added in one portion. The solution changed from a light brown to an orange hue. The reaction was allowed to stir for 30 minutes. Dry pyridine and copper (I) iodide were both added, changing the solution color to a dark brown, and the solution was stirred for another 45 minutes. Finally, 1,4-diiodonaphthalene was added and the reaction was heated to 120 °C and allowed to stir for 7 days. After cooling to room temperature, 30% ammonium hydroxide was carefully added and the reaction was left stirring for 10 minutes before addition 50 mL of ethyl acetate. The organic layer was washed with 30% ammonium hydroxide until the blue color had dissipated in the aqueous layer. The organic layer was dried over

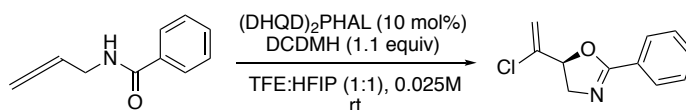
sodium sulfate and concentrated. Two columns, the first with 5% methanol in chloroform and the second in 10% methanol in ethyl acetate to 40% methanol in ethyl acetate, were necessary to purify the compound, a tan solid in 8.2% yield. ^1H NMR (500 MHz, CDCl_3) δ 8.58 (d, J = 4.6 Hz, 2H), 8.59 – 8.49 (m, 2H), 8.02 (d, J = 9.1 Hz, 2H), 7.65 (dt, J = 6.4, 3.6 Hz, 2H), 7.47 – 7.34 (m, 6H), 6.08 (s, 2H), 6.03 (s, 1H), 5.30 (s, 0H), 4.01 – 3.93 (m, 1H), 3.93 (s, 5H), 3.25 (td, J = 9.2, 3.9 Hz, 2H), 3.07 (t, J = 10.9 Hz, 2H), 2.96 (d, J = 13.4 Hz, 1H), 2.90 (dt, J = 18.2, 7.2 Hz, 3H), 2.74 (dt, J = 13.2, 8.9 Hz, 2H), 2.30 (t, J = 11.4 Hz, 2H), 1.59 (dtd, J = 35.8, 16.2, 15.0, 7.9 Hz, 7H), 1.44 (td, J = 14.2, 13.3, 7.6 Hz, 1H), 1.27 (p, J = 5.1, 4.3 Hz, 1H), 0.93 (t, J = 7.3 Hz, 6H); ^{13}C NMR (126 MHz, CDCl_3) δ 157.95, 147.59, 146.41, 144.55, 144.11, 131.97, 126.70, 126.50, 126.03, 121.93, 121.87, 118.27, 105.60, 100.78, 60.53, 55.71, 51.10, 50.19, 37.46, 29.71, 27.19, 26.67, 25.28, 22.04, 11.93.



Preparation of Hydroquinidine 1,4-naphthalenediyl diether. A microwave vial for 2 to 5 mL of solution was flamed dried with a stir bar. Upon addition of the hydroquinidine, the vial was closed with a rubber septum, purged with argon gas, and 2 mL of dry DMSO was added. Sodium hydride was added

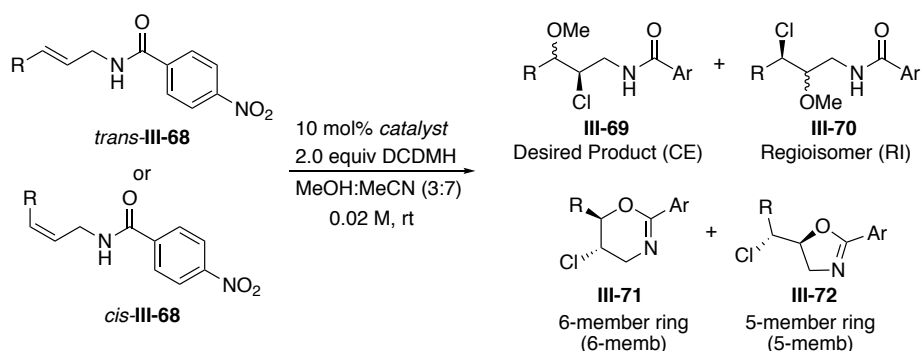
in one portion and the solution was allowed to stir for 30 minutes. Dry pyridine and copper (I) iodide were added to the stirring solution. The solution stirred for 45 minutes before addition of diiodonaphthalene solution (3 mL DMSO). Argon was bubbled into the solution. The reaction was sealed with the vial cover and put into the microwave. The reaction was set to microwave for a combination of 38 hours at 120 °C. After cooling to room temperature, 4 mL of 30% ammonium hydroxide was carefully added and the reaction was left stirring for 10 minutes before transfer to a separatory funnel and addition 10 mL of ethyl acetate. The organic layer was washed with 30% ammonium hydroxide (10 mL increments) until the blue color had dissipated in the aqueous layer. The organic layer was dried over sodium sulfate and concentrated. Two columns, the first with 5% methanol in chloroform and the second in 10% methanol in ethyl acetate to 40% methanol in ethyl acetate, were necessary to purify the compound, a tan solid in 22% yield. It should be noted that the reaction was cleaner and more easily separable. ¹H NMR (500 MHz, CDCl₃) δ 8.58 (d, *J* = 4.6 Hz, 2H), 8.59 – 8.49 (m, 2H), 8.02 (d, *J* = 9.1 Hz, 2H), 7.65 (dt, *J* = 6.4, 3.6 Hz, 2H), 7.47 – 7.34 (m, 6H), 6.08 (s, 2H), 6.03 (s, 1H), 5.30 (s, 0H), 4.01 – 3.93 (m, 1H), 3.93 (s, 5H), 3.25 (td, *J* = 9.2, 3.9 Hz, 2H), 3.07 (t, *J* = 10.9 Hz, 2H), 2.96 (d, *J* = 13.4 Hz, 1H), 2.90 (dt, *J* = 18.2, 7.2 Hz, 3H), 2.74 (dt, *J* = 13.2, 8.9 Hz, 2H), 2.30 (t, *J* = 11.4 Hz, 2H), 1.59 (dtd, *J* = 35.8, 16.2, 15.0, 7.9 Hz, 7H), 1.44 (td, *J* = 14.2, 13.3, 7.6 Hz, 1H), 1.27 (p, *J* = 5.1, 4.3 Hz, 1H), 0.93 (t, *J* = 7.3 Hz, 6H); ¹³C NMR (126 MHz, CDCl₃) δ 157.95, 147.59, 146.41, 144.55, 144.11, 131.97, 126.70, 126.50, 126.03,

121.93, 121.87, 118.27, 105.60, 100.78, 60.53, 55.71, 51.10, 50.19, 37.46, 29.71, 27.19, 26.67, 25.28, 22.04, 11.93.



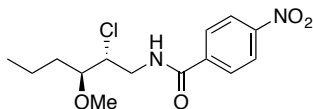
Preparation of (S)-5-(1-chlorovinyl)-2-phenyl-4,5-dihydrooxazole. A small stir bar was charged into a small test tube followed by *N*-(buta-2,3-dien-1-yl)benzamide (1.0 equivalent, 0.06 mmol), the desired catalyst (10 mol %, 0.1 equivalents, 0.006 mmol), and 0.18 mL of the solvent (trifluoroethanol/hexafluoroisopropanol, 1:1). Finally DCDMH was added and the reactions were allowed to stir until completion, with TLC monitoring occurring every 10 minutes. After completion, 2 mL of saturated sodium thiosulfate were added to the reactions. The reactions were allowed to stir for 2 minutes before addition of methylene chloride. The aqueous layer was extracted with portions of methylene chloride (2 mL x 3). The organics were combined, dried over sodium sulfate, and concentrated en vacuo. The crude compounds were purified using column chromatography (10% EtOAc in hexanes to 20% EtOAc in hexanes). The yields were generated via NMR using MTBE. The enantioselectivity was evaluated using chiral HPLC. Yield for DHQD₂PHAL catalyst: 91%. Yield for DHQD₂PHAL catalyst: 85%. ¹H NMR (500 MHz, CDCl₃) δ 7.95 (d, *J* = 7.0 Hz, 2 H), 7.48 (dd, *J* = 7.0 Hz, 7.5 Hz, 1 H), 1.6 (t, *J* = 7.5 Hz, 2 H), 5.55 (s, 1 H), 5.37

(s, 1 H), 5.19 (dd, J = 6.5 Hz, 9.0 Hz, 1 H), 4.24 (dd, 10.5 Hz, 15.0 Hz), 4.05 (dd, 7.5 Hz, 15.0 Hz, 1 H).



General procedure for catalytic asymmetric chloroetherification of unsaturated amides. Small stir bars were added to medium test tubes. The allylic amide was added with the tested catalysts (DHQD₂PHAL and DHQD₂NAPH) into the tubes along with 2 mL of a 7 : 3 mixture of acetonitrile and methanol. Finally, DCDMH was added and the solution was allowed to stir for 3 hours. The reaction was quenched with saturated sodium thiosulfate solution (2 mL). Water (2 mL) and methylene chloride (2 mL) were added. The organic were combined and dried over sodium sulfate before concentrating en vacuo. The crude material was purified using column chromatography (10% EtOAc in hexanes) after documenting crude MTBE-based NMR yields.

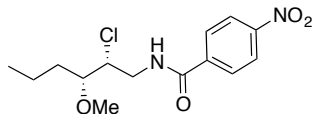
a-2c-OMe-NO₂: **N-((2*R*,3*S*)-2-chloro-3-methoxyhexyl)-4-nitrobenzamide**



R_f : 0.38 (30% EtOAc in hexanes, UV)

¹H NMR (500 MHz, CDCl₃) δ 8.29 (d, *J* = 9.0 Hz, 2H), 7.93 (d, *J* = 9.0 Hz, 2H), 7.24 (br s, 1H), 4.16-4.10 (m, 2H), 3.60-3.56 (m, 1H), 3.49-3.47 (m, 4H), 1.68-1.62 (m, 2H), 1.54-1.35 (m, 2H), 0.95 (m, 3H); ¹³C NMR (125 MHz, CDCl₃) δ 165.40, 149.70, 139.86, 128.14, 123.90, 83.90, 61.78, 59.37, 42.92, 33.69, 18.46, 14.09. HRMS analysis (ESI): Calculated for [M-H]⁻: C₁₄H₁₈ClN₂O₄: 313.0955; Found: 313.0953; Resolution of enantiomers: DAICEL Chiralcel[®] AD-H column, 7% IPA-Hexanes, 0.5 mL/min, 254 nm, RT1 (major) = 32.6 min, RT2 (major) = 34.7 min. α_D²⁰ = -30 (c 0.25, CHCl₃, *er* = 87:13)

s-2c-OMe-NO₂: **N-((2*R*,3*R*)-2-chloro-3-methoxyhexyl)-4-nitrobenzamide**

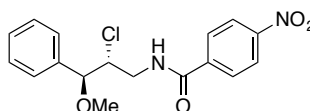


R_f : 0.25 (30% EtOAc in hexanes, UV)

¹H NMR (500 MHz, CDCl₃) δ 8.29 (d, *J* = 9.0 Hz, 2H), 7.93 (d, *J* = 9.0 Hz, 2H), 6.79 (br s, 1H), 4.25-4.23 (m, 1H), 4.13-4.08 (m, 1H), 3.61-3.55 (m, 1H), 3.45 - 3.41 (m, 4H), 1.68-1.62 (m, 2H), 1.54-1.35 (m, 2H), 0.95 (t, *J* = 7.5 Hz, 3H); ¹³C

NMR (125 MHz, CDCl₃) δ 165.44, 149.74, 139.73, 128.14, 123.90, 82.70, 61.04, 58.27, 43.78, 32.08, 18.90, 14.04. HRMS analysis (ESI): Calculated for [M+H]⁺: C₁₄H₂₀ClN₂O₄: 315.1112; Found: 315.1116; Resolution of enantiomers: DAICEL Chiralcel[®] AD-H column, 10% IPA-Hexanes, 1.0 mL/min, 254 nm, RT1 (major) = 12.1 min, RT2 (minor) = 14.0 min. α_D^{20} = +19.0 (c 0.1, CHCl₃, *er* = 99.5:0.5)

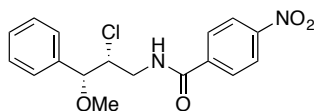
a-2b-OMe-NO₂: *N*-((2*R*,3*S*)-2-chloro-3-methoxy-3-phenylpropyl)-4-nitrobenzamide



R_f : 0.20 (30%EtOAc in hexanes, UV)

¹H NMR (500 MHz, CDCl₃) δ 8.29 (d, *J* = 9.0 Hz, 2H), 7.88 (d, *J* = 9.0 Hz, 2H), 7.40-7.33 (m, 5H), 6.82 (br s, 1H), 4.45 (d, *J* = 4.5 Hz, 1H), 4.25-4.22 (m, 1H), 4.11-4.06 (m, 1H), 3.66-3.61 (m, 1H), 3.34 (s, 3H); ¹³C NMR (125 MHz, CDCl₃) δ 165.26, 149.64, 139.66, 136.87, 137.22, 128.76, 128.12, 127.18, 123.87, 86.33, 62.60, 57.98, 42.54. HRMS analysis (ESI): Calculated for [M+H]⁺: C₁₇H₁₈ClN₂O₄: 349.0955; Found: 349.0950; Resolution of enantiomers: DAICEL Chiralcel[®] OJ-H column, 20% IPA-Hexanes, 1.0 mL/min, 265 nm, RT1 (minor) = 27.0 min, RT2 (major) = 30.1 min. α_D^{20} = +46.7 (c 0.5, CHCl₃, *er* = 92:8)

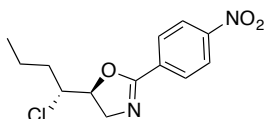
s-2b-OMe-NO₂: N-((2*R*,3*R*)-2-chloro-3-methoxy-3-phenylpropyl)-4-nitrobenzamide



R_f : 0.22 (30% EtOAc in hexanes, UV)

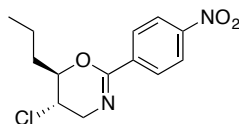
¹H NMR (500 MHz, CDCl₃) δ 8.27 (d, *J* = 9.0 Hz, 2H), 7.86 (d, *J* = 9.0 Hz, 2H), 7.41-7.24 (m, 5H), 6.57 (br s, 1H), 4.41 (d, *J* = 4.5 Hz, 1H), 4.29-4.28 (m, 1H), 4.00-3.95 (m, 1H), 3.56-3.52 (m, 2H), 3.27(s, 3H); ¹³C NMR (125 MHz, CDCl₃) δ 165.32, 149.75, 139.66, 136.83, 123.84, 128.68, 128.13, 127.49, 123.87, 85.03, 63.63, 57.44, 43.80. HRMS analysis (ESI): Calculated for [M+H]⁺: C₁₇H₁₈ClN₂O₄: 349.0955; Found: 349.0955; Resolution of enantiomers: DAICEL Chiralcel[®] AD-H column, 10% IPA-Hexanes, 1.0 mL/min, 254 nm, RT1 (major) = 22.8 min, RT2 (minor) = 29.9 min. α_D²⁰ = -8.0 (c 0.1, CHCl₃, *er* = 99.5:0.5)

a-4c-NO₂: chlorobutyl-2-(4-nitrophenyl)-4,5-dihydrooxazole

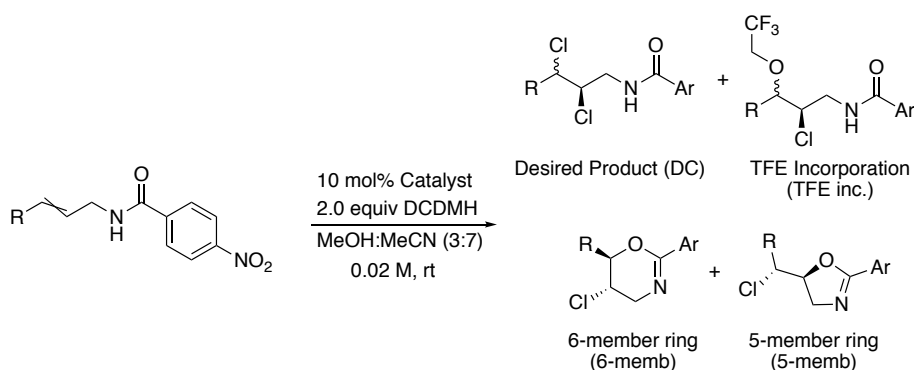


¹H NMR (500 MHz, CDCl₃) δ 8.26 (d, *J* = 8.5 Hz, 2H), 8.10 (d, *J* = 8.5 Hz, 2H), 4.82-4.77 (m, 1H), 4.21 (dd, *J* = 16.0, 10.0 Hz, 1H), 4.09-4.03 (m, 2H), 1.85-1.83 (m, 1H), 1.69-1.66 (m, 2H), 1.47-1.43 (m, 1H), 0.98 (t, *J* = 7.5 Hz, 3H); ¹³C NMR (125 MHz, CDCl₃) δ 161.86, 149.54, 133.11, 129.19, 123.59, 82.03, 63.02, 57.96, 35.85, 19.28, 13.49.

***t*-3c-NO₂: 5-chloro-2- (4-nitrophenyl)-6-propyl-5,6-dihydro-4*H*-1,3-oxazine**



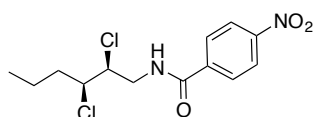
¹H NMR (500 MHz, CDCl₃) δ 8.21 (d, *J* = 8.5 Hz, 2H), 8.06 (d, *J* = 8.5 Hz, 2H), 4.26 (dt, *J* = 8.5, 3.0 Hz, 1H), 3.02-3.94 (m, 2H), 3.70 (dd, *J* = 16.5, 7.0 Hz, 1H), 1.99-1.94 (m, 1H), 1.71-1.64 (m, 2H), 1.55-1.51 (m, 1H), 1.03 (t, *J* = 7.5 Hz, 3H);
¹³C NMR (125 MHz, CDCl₃) δ 153.32, 149.22, 138.64, 128.19, 123.30, 78.85, 52.44, 50.48, 34.48, 18.02, 13.84. HRMS analysis (ESI): Calculated for [M+H]⁺: C₁₃H₁₆N₂O₃Cl: 283.0849; Found: 283.0863.



General procedure for catalytic asymmetric dichlorination of unsaturated amides. The substrate (0.04 mmol, 1.0 equiv) and LiCl (4 mmol, 100 equiv) were suspended in trifluoroethanol (TFE, 1.0 mL) in a small septum-covered test tube equipped with a stir bar. (DHQD)₂PHAL (3 mg, 10 mol%) was then introduced. After stirring for 2 min DCDMH (16 mg, 0.08 mmol, 2.0 equiv) was added. The

stirring was continued at -30 °C till the reaction was complete (TLC). The reaction was quenched by the addition of saturated aq. Na₂SO₃ (1 mL) and diluted with DCM (3 mL). The organics were separated and the aqueous layer was extracted with DCM (3 × 3 mL). The organics were combined and dried over sodium sulfate before concentrating en vacuo. The crude material was purified using column chromatography (10% EtOAc in hexanes) after documenting crude MTBE-based NMR yields.

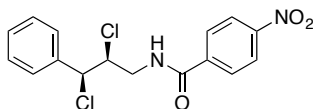
5a: *N*-((2*S*,3*S*)-2,3-dichlorohexyl)-4-nitrobenzamide



R_f : 0.60 (30% EtOAc in hexanes, UV)

¹H NMR (500 MHz, CDCl₃) δ 8.30 (d, *J* = 8.5 Hz, 2H), 7.94 (d, *J* = 8.5 Hz, 2H), 6.52 (br s, 1H), 4.41-4.38 (ddd, *J* = 9.5, 4.5, 2.5 Hz, 1H), 4.18-4.15 (ddd, *J* = 9.0, 4.5, 2.0 Hz, 1H), 4.13-4.07 (ddd, *J* = 14.0, 7.5, 4.5 Hz, 1H), 3.66-3.61 (ddd, *J* = 13.5, 8.5, 5.0 Hz, 1H), 1.93-1.80 (m, 2H), 1.62-1.54 (m, 1H), 1.46-1.38 (m, 1H), 0.96 (t, *J* = 7.0 Hz, 3H); ¹³C NMR (125 MHz, CDCl₃) δ 165.77, 149.81, 139.27, 128.22, 123.96, 63.49, 62.76, 44.92, 37.45, 19.67, 13.40. HRMS analysis (ESI): Calculated for [M+H]⁺: C₁₃H₁₇Cl₂N₂O₃: 319.0616; Found: 319.0609; Resolution of enantiomers: DAICEL Chiralcel[®] AD-H column, 15% IPA-Hexanes, 1.0 mL/min, 254 nm, RT1 (major) = 8.3 min, RT2 (minor) = 10.8 min. α_D²⁰ = +47.1 (c 0.65, CHCl₃, *er* = >99:1)

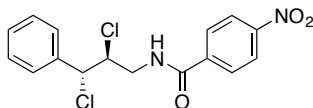
5h: *N*-((2*S*,3*S*)-2,3-dichloro-3-phenylpropyl)-4-nitrobenzamide



R_f : 0.50 (30% EtOAc in hexanes, UV)

¹H NMR (500 MHz, CDCl₃) δ 8.29 (d, *J* = 9.0 Hz, 2H), 7.88 (d, *J* = 9.0 Hz, 2H), 7.47-7.35 (m, 5H), 6.50 (br s, 1H), 5.18 (d, *J* = 5.0 Hz, 1H), 4.59-4.55 (m, 1H), 4.14-4.01 (ddd, *J* = 14.0, 7.5, 4.0 Hz, 1H), 3.52-3.46 (ddd, *J* = 14.0, 8.5, 4.5 Hz, 1H); ¹³C NMR (125 MHz, CDCl₃) δ 165.53, 149.81, 139.21, 136.71, 129.23, 128.71, 128.17, 127.80, 123.94, 64.97, 64.25, 44.38. HRMS analysis (ESI): Calculated for [M+H]⁺: C₁₆H₁₅Cl₂N₂O₃: 353.0460; Found: 353.0452; Resolution of enantiomers: DAICEL Chiralcel[®] AD-H column, 15% IPA-Hexanes, 1.0 mL/min, 254 nm, RT1 (major) = 13.5 min, RT2 (minor) = 27.6 min. α_D²⁰ = -11.3 (c 0.6, CHCl₃, *er* = >99:1)

5m: *N*-((2*S*,3*R*)-2,3-dichloro-3-phenylpropyl)-4-nitrobenzamide

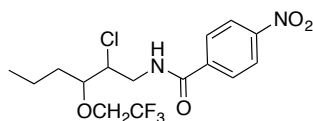


R_f : 0.44 (30% EtOAc in hexanes, UV)

¹H NMR (500 MHz, CDCl₃) δ 8.29 (d, *J* = 8.5 Hz, 2H), 7.91 (d, *J* = 8.5 Hz, 2H), 7.43-7.35 (m, 5H), 6.56 (br s, 1H), 5.02 (d, *J* = 8 Hz, 1H), 4.59-4.55 (dt, *J* = 11, 3.5 Hz, 1H), 4.49-4.44 (ddd, *J* = 14.5, 7.0, 3.5 Hz, 1H), 3.67-3.62 (ddd, *J* = 13.5, 8.5, 5.0 Hz, 1H); ¹³C NMR (125 MHz, CDCl₃) δ 165.47, 149.77, 139.36, 137.47,

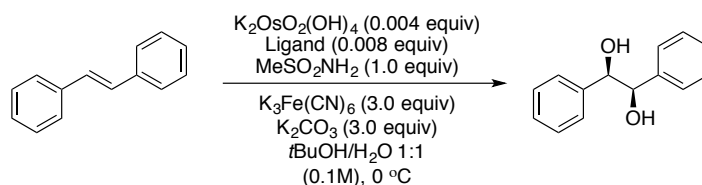
129.22, 128.79, 128.21, 127.75, 123.91, 63.98, 63.55, 43.89. HRMS analysis (ESI): Calculated for $[M+H]^+$: $C_{16}H_{15}Cl_2N_2O_3$: 353.0460; Found: 353.0462; Resolution of enantiomers: DAICEL Chiralcel[®] AD-H column, 20% IPA-Hexanes, 1.0 mL/min, 254 nm, RT1 (minor) = 10.5 min, RT2 (major) = 11.6 min. $\alpha_D^{20} = +5.6$ (c 1.0, $CHCl_3$, $er = 90:10$)

6a: *N*-(2-chloro-3-(2,2,2-trifluoroethoxy)hexyl)-4-nitrobenzamide



R_f : 0.60 (30% EtOAc in hexanes, UV)

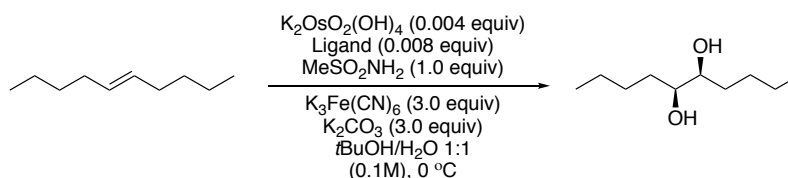
1H NMR (500 MHz, $CDCl_3$) δ 8.30 (d, $J = 8.5$ Hz, 2H), 7.93 (d, $J = 8.5$ Hz, 2H), 6.68 (br s, 1H), 4.28-4.25 (m, 1H), 4.15-4.10 (ddd, $J = 14.5, 7.0, 4.5$ Hz, 1H), 3.99-3.91 (m, 2H), 3.73-3.70 (dt, $J = 10.5, 3.5$ Hz, 1H), 3.59-3.54 (ddd, $J = 13.5, 9.0, 5.0$ Hz, 1H), 1.78-1.73 (m, 1H), 1.67-1.60 (m, 1H), 1.45-1.35 (m, 2H), 0.96 (t, $J = 7.5$ Hz, 3H); ^{13}C NMR (125 MHz, $CDCl_3$) δ 165.63, 149.76, 139.46, 128.16, 127.03 (q, $J_{CF} = 277.8$ Hz), 123.93, 82.57, 67.33 (q, $J_{CF} = 34.1$ Hz), 60.76, 43.44, 32.18, 18.53, 13.96. HRMS analysis (ESI): Calculated for $[M+H]^+$: $C_{15}H_{19}ClN_2O_4F_3$: 383.0985; Found: 383.0970



Preparation of (*R,R*)-Hydrobenzoin. The required catalysts [(DHQD)₂PHAL and (DHQD)₂NAPH] (0.008 equiv, 1.1×10^{-2} mmol, 8.5 mg), potassium osmate (0.004 equiv, 5.0×10^{-3} mmol, 2 mg), potassium ferrocyanate (3.0 equiv, 4.07 mmol, 1.340 g), potassium carbonate (3.0 equiv, 4.07 mmol, 563 mg), methanesulfonamide (1.0 equiv, 1.36 mmol), and 13.6 mL of a 1:1 solution of tert-butyl alcohol and distilled water (0.1 M) were combined in a flask with small stir bar and left to stir for 20 minutes. The solution was cooled to 0 °C before addition of stilbene (1.0 equiv, 1.36 mmol, 245 mg). Similar reaction conditions were repeated using AD-mix β (1.4g/mmol, 1.904g). In order to quench the reaction, a saturated sodium thiosulfate solution was added to the solution. Water was added to the stirring solution, followed by methylene chloride. The organic layers were combined and dried over anhydrous sodium sulfate. The opaque residue was purified using column chromatography (20% EtOAc/Hexanes). ¹H NMR (500 MHz, CDCl₃) δ 7.11-7.22 (m, 10H), 4.68 (s, 2H), 3.05 (br s, 2H); ¹³C NMR (125 MHz, CDCl₃) δ 139.8, 128.1, 127.9, 126.9, 79.1. Enantiomeric excess was determined by HPLC: HP Series 1100, Chiralcel OJ-H Column (hexane/2-propanol = 90:10, flow rate 1 ml/min, RT1 (minor) = 15.25 min, RT2 (major) = 17.55 min), $\alpha_D^{28} = +93^\circ$ (lit.), c = 2.5 in EtOH.

Catalytic System	Product Yield	α_D^{28}	HPLC
AD-mix β	113 mg	+69	99% <i>ee</i>
(DHQD) ₂ PHAL	43 mg	+73.2	65-98% <i>ee</i>
(DHQD) ₂ NAPH	50 mg	+79.2	77-99% <i>ee</i>

Table III-14: Oxidation of *trans*-stilbene via Sharpless Dihydroxylation with (DHQD)₂PHAL and (DHQD)₂NAPH ligands.



Preparation of (5*R*,6*R*)-5,6-decanediol. The required catalysts [(DHQD)₂PHAL and (DHQD)₂NAPH] (0.008 equiv, 1.1×10^{-2} mmol, 8.5 mg), potassium osmate (0.004 equiv, 5.0×10^{-3} mmol, 2 mg), potassium ferrocyanate (3.0 equiv, 4.07 mmol, 1.340 g), potassium carbonate (3.0 equiv, 4.07 mmol, 563 mg), methanesulfonamide (1.0 equiv, 1.36 mmol), and 13.6 mL of a 1:1 solution of tert-butyl alcohol and distilled water (0.1 M) were combined in a flask with small stir bar and left to stir for 20 minutes. The solution was cooled to 0 °C before addition of stilbene (1.0 equiv, 1.36 mmol, 245 mg). Similar reaction conditions were repeated using DABCO as a catalyst (0.008 equiv, 1.1×10^{-3} mmol, 100 μL of a 1.23mg/mL solution, 0.123 mg). In order to quench the reaction, a saturated sodium thiosulfate solution was added to the solution. Water was added to the stirring solution, followed by methylene chloride. The organic layers were combined and dried over anhydrous sodium sulfate. The opaque

residue was purified using column chromatography (20% EtOAc/Hexanes). ^1H NMR (500 MHz, CDCl_3) δ 3.41 (2H, s), 2.03–1.98 (2H, br), 1.47–1.33 (12H, m), 0.94–0.90 (6H, t, $J = 6.8$ Hz). Enantiomeric resolution was determined via Chiral GC: HP 6890 Series GC System, GAMA DEX 225 Column 30M x 0.25, 0.25 film, Column # 19951-01B (90 °C to 250 °C, 3 °C/min, holding for 60 min, RT1 (minor) = 22.48 min, RT2 (major) = 22.77 min).

Catalyst	Enantioselectivities (% ee)
DABCO	6%
(DHQD) ₂ PHAL	99%
(DHQD) ₂ NAPH	99%

Table III-15: Oxidation of *trans*-decene via Sharpless Dihydroxylation with (DHQD)₂PHAL and (DHQD)₂NAPH ligands.

III.4.2. Quantum Mechanics Modeling Experiments

Full optimization of the all conformations of DHQD₂PHAL and DHQD₂NAPH truncated structures, including their rotamers locked at 30° increments about the C-O-C=C bond, was performed using density functional calculations at the B3LYP/6-31G*/SM8(CHCl_3) level in the Spartan-10 software running on Macintosh and Linux platforms.

1,4-Dimethoxynaphthalene

Standard Nuclear Orientation (Angstroms)

I	Atom	X	Y	Z
1	H	1.222840	-2.786393	-0.000075
2	C	0.710165	-1.831628	-0.000066
3	C	1.413306	-0.648901	-0.000044
4	C	-1.413304	-0.648902	-0.000029
5	C	0.714167	0.603283	-0.000019
6	C	-0.710161	-1.831629	-0.000055
7	C	-0.714167	0.603282	-0.000013
8	C	1.401507	1.843292	-0.000005
9	H	-1.222838	-2.786393	-0.000054
10	H	-2.485556	1.835200	0.000003
11	C	0.706132	3.033812	0.000018
12	H	2.485555	1.835202	-0.000014
13	H	1.246611	3.976742	0.000028
14	C	-0.706136	3.033810	0.000021
15	H	-1.246615	3.976741	0.000034
16	C	-1.401508	1.843290	0.000004
17	O	2.778645	-0.549607	-0.000043
18	C	3.533071	-1.746856	0.000152
19	H	3.330804	-2.351748	0.894780
20	H	4.581709	-1.442867	0.000083

21	H	3.330786	-2.352062	-0.894260
22	O	-2.778643	-0.549610	-0.000025
23	C	-3.533076	-1.746856	0.000077
24	H	-3.330768	-2.352007	-0.894367
25	H	-4.581712	-1.442862	0.000005
26	H	-3.330828	-2.351806	0.894671

Nuclear Repulsion Energy = 852.4788794914 hartrees

There are 50 alpha and 50 beta electrons.

Incremental DFT

Cycle	Energy	DIIS Error
1	-618.1244544228	5.28×10^{-2}
2	-614.7728026387	4.79×10^{-3}
3	-614.7800062000	4.84×10^{-3}
4	-614.9323128850	8.27×10^{-4}
5	-614.9366783091	3.41×10^{-5}
6	-614.9365856275	1.16×10^{-4}
7	-614.9366783091	3.41×10^{-5}
8	-614.9366860498	5.03×10^{-6}
9	-614.9366860710	2.01×10^{-6}
10	-614.9366861992	2.80×10^{-7}

11	-614.9366862824	2.61×10^{-7}
12	-614.9366863036	4.17×10^{-8}

Ground-State Mulliken Net Atomic Charges

	Atom	Charge (a.u.)
1	H	0.128044
2	C	-0.217919
3	C	0.329123
4	C	0.329123
5	C	0.058723
6	C	-0.217919
7	C	0.058723
8	C	-0.179911
9	H	0.128044
10	H	0.146630
11	C	-0.132817
12	H	0.146630
13	H	0.126009
14	C	-0.132816
15	H	0.126009
16	C	-0.179911
17	O	-0.513688

18	C	-0.211011
19	H	0.149834
20	H	0.167151
21	H	0.149832
22	O	-0.513689
23	C	-0.211011
24	H	0.149832
25	H	0.167151
26	H	0.149833
Sum of Atomic Charges		0.000000

Cartesian Multipole Moments

Charge (ESU x10¹⁰)

0.0000

Dipole Moment (Debye)

X	0.0000	Y	-2.2642	Z	0.0003
---	--------	---	---------	---	--------

Tot 2.2642

Quadrupole Moments (Debye-Ang)

XX	-68.5954	XY	0.0000	YY	-69.6703
----	----------	----	--------	----	----------

XZ	0.0003	YZ	-0.0003	ZZ	-85.0054
----	--------	----	---------	----	----------

Traceless Quadrupole Moments (Debye-Ang)

QXX	17.4849	QYY	14.2603	QZZ	-31.7452
-----	---------	-----	---------	-----	----------

QXY	0.0000	QXZ	0.0010	QYZ	-0.0009
Octapole Moments (Debye-Ang ²)					
XXX	-0.0004	XXY	-33.0225	XYY	0.0000
YYY	-5.0212	XXZ	0.0031	XYZ	-0.0005
YYZ	-0.0001	XZZ	0.0014	YZZ	-6.8222
ZZZ	-0.0005				
Traceless Octapole Moments (Debye-Ang ²)					
XXX	-0.0024	YYY	328.4750	ZZZ	-0.0303
XXY	-360.7399	XXZ	0.0392	XYY	0.0010
XYZ	-0.0072	XZZ	0.0014	YYZ	-0.0089
YZZ	32.2650				
Hexadecapole Moments (Debye-Ang ³)					
XXXX	-1840.1259	XXXY	0.0002	XXYY	-535.9420
XYYY	0.0000	YYYY	-1523.2672	XXXZ	-0.0001
XXYZ	-0.0040	XYYZ	-0.0013	YYYZ	0.0050
XXZZ	-374.2399	XYZZ	0.0000	YYZZ	-312.1990
XZZZ	-0.0043	YZZZ	0.0001	ZZZZ	-98.2987
Traceless Hexadecapole Moments (Debye-Ang ³)					
XXXX	1156.3993	XXXY	0.0166	XXXZ	0.2449
XXYY	2832.4692	XXYZ	-0.4328	XXZZ	-3988.8685
XYYY	-0.0111	XYYZ	-0.0506	XYZZ	-0.0055
XZZZ	-0.1943	YYYY	325.6009	YYYZ	0.4800

YYZZ	-3158.0701	YZZZ	-0.0472	ZZZZ	7146.9386
------	------------	------	---------	------	-----------

Gradient of SCF Energy

	1	2	3	4	5	6
1	-0.0000263	0.0000954	0.0000398	-0.0000391	-0.0001235	-0.0000945
2	0.0000001	0.0001118	-0.0000627	-0.0000616	-0.0000056	0.0001117
3	-0.0000002	-0.0000018	-0.0000004	0.0000003	0.0000009	-0.0000011
	7	8	9	10	11	12
1	0.0001231	-0.0000025	0.0000259	0.0000070	0.0000253	-0.0000068
2	-0.0000060	0.0000321	-0.0000000	-0.0000048	-0.0000404	-0.0000050
3	0.0000010	-0.0000003	0.0000002	-0.0000001	0.0000005	-0.0000002
	13	14	15	16	17	18
1	-0.0000060	-0.0000259	0.0000061	0.0000029	-0.0000526	-0.0000469
2	-0.0000022	-0.0000408	-0.0000022	0.0000323	-0.0001662	0.0001179
3	-0.0000001	0.0000001	-0.0000001	-0.0000004	0.0000001	0.0000009
	19	20	21	22	23	24
1	0.0000005	0.0000033	-0.0000007	0.0000530	0.0000474	0.0000009
2	0.0000173	-0.0000136	0.0000164	-0.0001669	0.0001183	0.0000163
3	-0.0000091	-0.0000003	0.0000096	0.0000000	0.0000002	0.0000097
	25	26				
1	-0.0000032	0.0000001	Max Gradient Component = 1.669×10^{-4}			
2	-0.0000136	0.0000173	RMS Gradient = 4.912×10^{-5}			

3 -0.0000002 -0.0000093 Gradient Time: CPU 3.72 s Wall 3.75 s

Geometry Optimization Parameters

NAtoms	NIC	NZ	NCons	NDum	NFix	NCnnct	MaxDiss
26	177	0	1	0	0	0	0

Optimization Cycle: 1

Coordinates (Angstroms)

	Atom	X	Y	Z
1	H	1.222840	-2.786393	-0.000075
2	C	0.710165	1.831628	-0.000066
3	C	1.413306	-0.648901	-0.000044
4	C	-1.413304	-0.648902	-0.000029
5	C	0.714167	0.603283	-0.000019
6	C	-0.710161	-1.831629	-0.000055
7	C	-0.714167	0.603282	-0.000013
8	C	1.401507	1.843292	-0.000005
9	H	-1.222838	-2.786393	-0.000054
10	H	-2.485556	1.835200	0.0000003
11	C	0.706132	3.033812	0.000018
12	H	2.485555	1.835202	-0.000014

13	H	1.246611	3.976742	0.000028
14	C	-0.706136	3.033810	0.000021
15	H	-1.246615	3.976741	0.000034
16	C	-1.401508	1.843290	0.000004
17	O	2.778645	-0.549607	-0.000043
18	C	3.533071	-1.746856	0.000152
19	H	3.330804	-2.3517480	0.894780
20	H	4.581709	-1.442867	0.000083
21	H	3.330786	-2.352062	-0.894260
22	O	-2.778643	-1.746856	-0.000025
23	C	-3.533076	-1.746856	0.000077
24	H	-3.330768	-2.352007	-0.894367
25	H	-4.581712	-1.442862	0.000005
26	H	-3.330828	-2.351806	0.894671

Point Group: c1

Number of degrees of freedom: 72

Energy is -614.936686304

Constraints and their Current Values

					Value	Constraint
Dihedral:	18	17	3	2	-0.010	-0.010

71 Hessian modes were used to form the next step

Hessian Eigenvalues					
0.002295	0.012401	0.019388	0.020757	0.021276	0.021450
0.023501	0.024386	0.025490	0.025971	0.026944	0.027795
0.028825	0.031015	0.033569	0.034389	0.035798	0.038869
0.078054	0.078079	0.078374	0.078564	0.126446	0.126616
0.129744	0.131989	0.134426	0.136072	0.142111	0.142840
0.150755	0.153538	0.160419	0.175073	0.175490	0.176540
0.184067	0.184165	0.188097	0.202916	0.212829	0.255909
0.273854	0.282001	0.294424	0.296822	0.297032	0.298030
0.298164	0.305604	0.308969	0.309720	0.310320	0.314779
0.316166	0.337017	0.339062	0.343240	0.344142	0.345008
0.347270	0.359256	0.361514	0.375724	0.384340	0.385366
0.387219	0.432373	0.458402	0.764108	0.771759	

1,4-Dimethoxyphthalazine

Standard Nuclear Orientation (Angstroms)				
I	Atom	X	Y	Z
1	H	1.241895	-4.016389	-0.000010
2	C	0.705224	-3.071643	-0.000006

3	H	2.493205	-1.868488	-0.000031
4	C	1.409006	-1.880755	-0.000017
5	C	-1.409006	-1.880755	0.000017
6	C	0.706365	-0.658348	-0.000012
7	C	-0.705223	-3.071643	0.000012
8	C	-0.706365	-0.658348	0.000004
9	C	1.333532	0.638688	-0.000019
10	H	-1.241895	-4.016389	0.000022
11	H	-2.493205	-1.868489	0.000031
12	N	0.685858	1.770827	-0.000018
13	N	-0.685858	1.770826	0.000001
14	C	-1.333532	0.638688	0.000009
15	O	2.685182	0.639628	-0.000016
16	O	-2.685182	0.639628	0.000017
17	C	3.328246	1.918992	-0.000012
18	H	3.051510	2.494401	-0.888269
19	H	4.397684	1.701547	0.000156
20	H	3.051238	2.494520	0.888081
21	C	-3.328247	1.918991	-0.000015
22	H	-3.051455	2.494446	0.888195
23	H	-4.397684	1.701547	-0.000109
24	H	-3.051293	2.494474	-0.888155

Nuclear Repulsion Energy = 864.6502624925 hartrees

There are 50 alpha and 50 beta electrons.

Incremental DFT

Cycle	Energy	DIIS Error
1	-650.2216189062	5.36×10^{-2}
2	-614.7728026387	4.78×10^{-3}
3	-614.7800062000	5.86×10^{-3}
4	-614.9323128850	1.51×10^{-3}
5	-614.9366783091	6.14×10^{-4}
6	-614.9365856275	1.90×10^{-4}
7	-614.9366783091	6.61×10^{-5}
8	-614.9366860498	2.26×10^{-5}
9	-614.9366860710	4.24×10^{-6}
10	-614.9366861992	1.30×10^{-6}
11	-614.9366862824	3.42×10^{-7}
12	-614.9366863036	1.25×10^{-7}
13	-647.0053338358	2.65×10^{-8}

Ground-State Mulliken Net Atomic Charges

Atom	Charge (a.u.)
------	---------------

1	H	0.140986
2	C	-0.127603
3	H	0.160903
4	C	-0.180929
5	C	-0.180929
6	C	0.083466
7	C	-0.127603
8	C	0.083466
9	C	0.522553
10	H	0.140986
11	H	0.160903
12	N	-0.390236
13	N	-0.390236
14	C	0.522553
15	O	-0.501180
16	O	-0.501180
17	C	-0.204327
18	H	0.169435
19	H	0.157485
20	H	0.169447
21	C	-0.204326
22	H	0.169438

23	H	0.157485
24	H	0.169444
Sum of Atomic Charges		0.000000

Cartesian Multipole Moments

Charge (ESU x10¹⁰)

0.0000

Dipole Moment (Debye)

X	0.0000	Y	-2.0292	Z	0.0000
---	--------	---	---------	---	--------

Tot 2.0292

Quadrupole Moments (Debye-Ang)

XX	-67.4048	XY	0.0000	YY	-74.5258
----	----------	----	--------	----	----------

XZ	0.0001	YZ	0.0000	ZZ	-81.3629
----	--------	----	--------	----	----------

Traceless Quadrupole Moments (Debye-Ang)

QXX	21.0792	QYY	-0.2840	QZZ	-20.7952
-----	---------	-----	---------	-----	----------

QXY	0.0000	QXZ	0.0003	QYZ	0.0000
-----	--------	-----	--------	-----	--------

Octapole Moments (Debye-Ang²)

XXX	0.0000	XXY	30.1599	XYY	0.0000
-----	--------	-----	---------	-----	--------

YYY	-27.3481	XXZ	0.0001	XYZ	0.0003
-----	----------	-----	--------	-----	--------

YYZ	0.0006	XZZ	0.0000	YZZ	11.6279
-----	--------	-----	--------	-----	---------

ZZZ	0.0009
-----	--------

Traceless Octapole Moments (Debye-Ang²)

XXX	-0.0001	YYY	-540.1790	ZZZ	-0.0007
XXY	409.0800	XXZ	-0.0028	XYY	0.0001
XYZ	0.0041	XZZ	0.0000	YYZ	0.0035
YZZ	131.0990				

Hexadecapole Moments (Debye-Ang³)

XXXX	-1695.5001	XXXY	0.0000	XXYY	-493.1787
XYYY	0.0000	YYYY	-1563.8100	XXXZ	0.0077
XXYZ	0.0000	XYYZ	0.0004	YYYZ	0.0022
XXZZ	-336.9152	XYZZ	0.0000	YYZZ	-305.2716
XZZZ	0.0023	YZZZ	0.0018	ZZZZ	-90.5634

Traceless Hexadecapole Moments (Debye-Ang³)

XXXX	-1309.4874	XXXY	-0.0006	XXXZ	0.3386
XXYY	4672.2351	XXYZ	-0.0313	XXZZ	-3362.7476
XYYY	0.0005	XYYZ	-0.1125	XYZZ	0.0000
XZZZ	-0.2261	YYYY	-2182.0575	YYYZ	0.1331
YYZZ	-2490.1776	YZZZ	-0.1018	ZZZZ	5852.9252

Gradient of SCF Energy

	1	2	3	4	5	6
1	0.0000055	-0.0000148	0.0000119	0.0000043	-0.0000043	0.0000043
2	-0.0000108	-0.0000136	0.0000017	0.0000171	0.0000171	0.0000049
3	0.0000000	-0.0000000	-0.0000000	0.0000001	0.0000000	-0.0000002

	7	8	9	10	11	12
1	0.0000148	-0.0000043	-0.0000652	-0.0000055	-0.0000119	0.0000739
2	-0.0000136	0.0000049	0.0000589	-0.0000108	0.0000017	-0.0000538
3	-0.0000000	-0.0000001	-0.0000003	0.0000000	0.0000000	0.0000001
	13	14	15	16	17	18
1	-0.0000739	0.0000652	0.0000276	-0.0000276	-0.0000055	-0.0000018
2	-0.0000538	0.0000589	-0.0000158	-0.0000158	-0.0000062	0.0000100
3	0.0000003	0.0000001	0.0000007	-0.0000001	-0.0000007	-0.0000105
	19	20	21	22	23	24
1	0.0000115	-0.0000036	0.0000055	0.0000022	-0.0000115	0.0000032
2	-0.0000018	0.0000094	-0.0000062	0.0000099	-0.0000018	0.0000095
3	-0.0000001	0.0000104	-0.0000000	0.0000106	0.0000001	-0.0000103

Max Gradient Component = 7.386×10^{-5}

RMS Gradient = 2.283×10^{-5}

Gradient Time: CPU 4.46 s Wall 5.23 s

Geometry Optimization Parameters

NAtoms	NIC	NZ	NCons	NDum	NFix	NCnnct	MaxDiss
24	160	0	1	0	0	0	0

Optimization Cycle: 1

Coordinates (Angstroms)

	Atom	X	Y	Z
1	H	1.222840	-2.786393	-0.000075
2	C	0.710165	1.831628	-0.000066
3	H	1.413306	-0.648901	-0.000044
4	C	-1.413304	-0.648902	-0.000029
5	C	0.714167	0.603283	-0.000019
6	C	-0.710161	-1.831629	-0.000055
7	C	-0.714167	0.603282	-0.000013
8	C	1.401507	1.843292	-0.000005
9	C	-1.222838	-2.786393	-0.000054
10	H	-2.485556	1.835200	0.0000003
11	H	0.706132	3.033812	0.000018
12	N	2.485555	1.835202	-0.000014
13	N	1.246611	3.976742	0.000028
14	C	-0.706136	3.033810	0.000021
15	O	-1.246615	3.976741	0.000034
16	O	-1.401508	1.843290	0.000004
17	C	2.778645	-0.549607	-0.000043
18	H	3.533071	-1.746856	0.000152
19	H	3.330804	-2.3517480	0.894780

20	H	4.581709	-1.442867	0.000083
21	C	3.330786	-2.352062	-0.894260
22	H	-2.778643	-1.746856	-0.000025
23	H	-3.533076	-1.746856	0.000077
24	H	-3.330768	-2.352007	-0.894367

Point Group: c1

Number of degrees of freedom: 66

Energy is -647.005333836

Constraints and their Current Values

					Value	Constraint
Dihedral:	12	9	15	17	0.000	0.000

62 Hessian modes were used to form the next step

Hessian Eigenvalues

0.001482	0.004489	0.008163	0.012866	0.021094	0.022009
0.022240	0.023652	0.025401	0.026202	0.026946	0.028666
0.030892	0.033135	0.034870	0.037114	0.075065	0.075244
0.076513	0.121466	0.121596	0.128577	0.130773	0.131641
0.132546	0.145799	0.151822	0.171100	0.177462	0.180070
0.181996	0.183760	0.191787	0.199235	0.236772	0.248401

0.280880	0.297922	0.305558	0.305853	0.305882	0.306755
0.310155	0.310519	0.314849	0.318101	0.320539	0.321098
0.336418	0.337515	0.338116	0.342488	0.346454	0.351732
0.374638	0.380298	0.428032	0.439884	0.450207	0.458218
0.604588	0.615563				

REFERENCES

REFERENCES

1. Kolb, H. C.; VanNieuwenhze, M. S.; Sharpless, K. B. "Catalytic Asymmetric Dihydroxylation" *Chemical reviews* **1994**, *94*, 2483.
2. Amberg, W.; Bennani, Y. L.; Chadha, R. K.; Crispino, G. A.; Davis, W. D.; Hartung, J.; Jeong, K. S.; Ogino, Y.; Shibata, T.; Sharpless, K. B. "Syntheses and crystal structures of the cinchona alkaloid derivatives used as ligands in the osmium-catalyzed asymmetric dihydroxylation of olefins" *The Journal of organic chemistry* **1993**, *58*, 844.
3. Nash, R. J.; Fellows, L. E.; Dring, J. V.; Fleet, G. W. J.; Derome, A. E.; Hamor, T. A.; Scofield, A. M.; Watkin, D. J. "Isolation from *Alexa-Leiopetala* and X-Ray Crystal-Structure of Alexine, (1r,2r,3r,7s,8s)-3-Hydroxymethyl-1,2,7-Trihydroxypyrrolizidine [(2r,3r,4r,5s,6s)-2-Hydroxymethyl-1-Azabicyclo[3.3.0]Octan-3,4,6-Triol], a Unique Pyrrolizidine Alkaloid" *Tetrahedron Letters* **1988**, *29*, 2487.
4. Nash, R. J.; Fellows, L. E.; Dring, J. V.; Fleet, G. W. J.; Girdhar, A.; Ramsden, N. G.; Peach, J. M.; Hegarty, M. P.; Scofield, A. M. "2 Alexines [3-Hydroxymethyl-1,2,7-Trihydroxypyrrolizidines] from *Castanospermum-Australe*" *Phytochemistry* **1990**, *29*, 111.
5. Lesch, J. E. *The First Miracle Drugs : How the Sulfa Drugs Transformed Medicine*; Oxford University Press: Oxford, 2007.
6. Spellberg, B.; Guidos, R.; Gilbert, D.; Bradley, J.; Boucher, H. W.; Scheld, W. M.; Bartlett, J. G.; Edwards, J.; Archer, G. F.; Archer, G. F. "The Epidemic of Antibiotic-Resistant Infections: A Call to Action for the Medical Community from the Infectious Diseases Society of America" *Clinical Infectious Diseases* **2008**, *46*, 155.
7. Boucher, H. W.; Talbot, G. H.; Bradley, J. S.; Edwards, J. E.; Gilbert, D.; Rice, L. B.; Scheld, M.; Spellberg, B.; Bartlett, J. "Bad Bugs, No Drugs: No ESCAPE! An Update from the Infectious Diseases Society of America" *Clinical Infectious Diseases* **2009**, *48*, 1.

8. "The 10 × '20 Initiative: Pursuing a Global Commitment to Develop 10 New Antibacterial Drugs by 2020" *Clinical Infectious Diseases* **2010**, 50, 1081.
9. Ling, L. L.; Schneider, T.; Peoples, A. J.; Spoering, A. L.; Engels, I.; Conlon, B. P.; Mueller, A.; Schaberle, T. F.; Hughes, D. E.; Epstein, S.; Jones, M.; Lazarides, L.; Steadman, V. A.; Cohen, D. R.; Felix, C. R.; Fetterman, K. A.; Millett, W. P.; Nitti, A. G.; Zullo, A. M.; Chen, C.; Lewis, K. "A new antibiotic kills pathogens without detectable resistance" *Nature* **2015**, 517, 455.
10. Gonzalez, R. J.; Tarloff, J. B. "Evaluation of hepatic subcellular fractions for Alamar blue and MTT reductase activity" *Toxicology in vitro : an international journal published in association with BIBRA* **2001**, 15, 257.
11. Ahmed, S. A.; Gogal, R. M., Jr.; Walsh, J. E. "A new rapid and simple non-radioactive assay to monitor and determine the proliferation of lymphocytes: an alternative to [3H]thymidine incorporation assay" *Journal of immunological methods* **1994**, 170, 211.
12. O'Brien, J.; Wilson, I.; Orton, T.; Pognan, F. "Investigation of the Alamar Blue (resazurin) fluorescent dye for the assessment of mammalian cell cytotoxicity" *European journal of biochemistry / FEBS* **2000**, 267, 5421.
13. Moore, K. S.; Wehrli, S.; Roder, H.; Rogers, M.; Forrest, J. N., Jr.; McCrimmon, D.; Zasloff, M. "Squalamine: an aminosterol antibiotic from the shark" *Proceedings of the National Academy of Sciences of the United States of America* **1993**, 90, 1354.
14. Hofmann, A. F.; Eckmann, L. "How bile acids confer gut mucosal protection against bacteria" *Proceedings of the National Academy of Sciences of the United States of America* **2006**, 103, 4333.
15. Inagaki, T.; Moschetta, A.; Lee, Y.-K.; Peng, L.; Zhao, G.; Downes, M.; Yu, R. T.; Shelton, J. M.; Richardson, J. A.; Repa, J. J.; Mangelsdorf, D. J.; Kliewer, S. A. "Regulation of antibacterial defense in the small intestine by the nuclear bile acid receptor" *Proceedings of the National Academy of Sciences of the United States of America* **2006**, 103, 3920.

16. Shai, Y. "Mechanism of the binding, insertion and destabilization of phospholipid bilayer membranes by alpha-helical antimicrobial and cell non-selective membrane-lytic peptides" *Biochimica et biophysica acta* **1999**, 1462, 55.
17. Savage, P. B.; Li, C.; Taotafa, U.; Ding, B.; Guan, Q. "Antibacterial properties of cationic steroid antibiotics" *FEMS Microbiology Letters* **2002**, 217, 1.
18. Savage, Paul B. "Design, Synthesis and Characterization of Cationic Peptide and Steroid Antibiotics" *European Journal of Organic Chemistry* **2002**, 2002, 759.
19. Deng, G.; Dewa, T.; Regen, S. L. "A Synthetic Ionophore That Recognizes Negatively Charged Phospholipid Membranes" *Journal of the American Chemical Society* **1996**, 118, 8975.
20. Kikuchi, K.; Bernard, E. M.; Sadownik, A.; Regen, S. L.; Armstrong, D. "Antimicrobial activities of squalamine mimics" *Antimicrobial agents and chemotherapy* **1997**, 41, 1433.
21. Velkov, T.; Roberts, K. D.; Nation, R. L.; Thompson, P. E.; Li, J. "Pharmacology of polymyxins: new insights into an 'old' class of antibiotics" *Future microbiology* **2013**, 8, 10.2217/fmb.13.39.
22. Ding, B.; Guan, Q.; Walsh, J. P.; Boswell, J. S.; Winter, T. W.; Winter, E. S.; Boyd, S. S.; Li, C.; Savage, P. B. "Correlation of the Antibacterial Activities of Cationic Peptide Antibiotics and Cationic Steroid Antibiotics" *Journal of Medicinal Chemistry* **2002**, 45, 663.
23. Shamsuzzaman; Dar, A. M.; Khanam, H.; Gatoo, M. A. "Anticancer and antimicrobial evaluation of newly synthesized steroidal 5,6 fused benzothiazines" *Arabian Journal of Chemistry* **2014**, 7, 461.
24. Coughlin, S. A.; Danz, D. W.; Robinson, R. G.; Klingbeil, K. M.; Wentland, M. P.; Corbett, T. H.; Waud, W. R.; Zwelling, L. A.; Altschuler, E.; Bales, E.; Rake, J. B. "Mechanism of action and antitumor activity of (S)-10-(2,6-dimethyl-4-pyridinyl)-9-fluoro-3-methyl-7-oxo-2,3-dihydro-7H-pyridol [1,2,3-

- de]-[1,4]benzothiazine-6-carboxylic acid (WIN 58161)" *Biochemical Pharmacology* **1995**, *50*, 111.
25. Wang, H.-j.; Gloer, K. B.; Gloer, J. B.; Scott, J. A.; Malloch, D. "Anserinones A and B: New Antifungal and Antibacterial Benzoquinones from the Coprophilous Fungus *Podospora anserina*" *Journal of Natural Products* **1997**, *60*, 629.
 26. Lana, E. J. L.; Carazza, F.; Takahashi, J. A. "Antibacterial Evaluation of 1,4-Benzoquinone Derivatives" *Journal of Agricultural and Food Chemistry* **2006**, *54*, 2053.
 27. COLWELL, C. A.; MCCALL, M. "STUDIES ON THE MECHANISM OF ANTIBACTERIAL ACTION OF 2-METHYL-1,4-NAPHTHOQUINONE" *Science* **1945**, *101*, 592.
 28. Johnson, J. H.; Meyers, E.; O'Sullivan, J.; Phillipson, D. W.; Robinson, G.; Trejo, W. H.; Wells, J. S. "Culpin, a novel hydroquinone antibiotic of fungal origin" *The Journal of antibiotics* **1989**, *42*, 1515.
 29. Cariello, L.; Zanetti, L.; Cuomo, V.; Vanzanella, F. "Antimicrobial activity of avarol, a sesquiterpenoid hydroquinone from the marine sponge, *dysidea avara*" *Comparative Biochemistry and Physiology Part B: Comparative Biochemistry* **1982**, *71*, 281.
 30. Ooi, N.; Chopra, I.; Eady, A.; Cove, J.; Bojar, R.; O'Neill, A. J. "Antibacterial activity and mode of action of tert-butylhydroquinone (TBHQ) and its oxidation product, tert-butylbenzoquinone (TBBQ)" *Journal of Antimicrobial Chemotherapy* **2013**, *68*, 1297.
 31. Zahler, R.; Jacobs, G. A.; Google Patents: 1989.
 32. Li, S.; Hao, L.; Bao, W.; Zhang, P.; Su, D.; Cheng, Y.; Nie, L.; Wang, G.; Hou, F.; Yang, Y. "A novel short anionic antibacterial peptide isolated from the skin of *Xenopus laevis* with broad antibacterial activity and inhibitory activity against breast cancer cell" *Archives of Microbiology* **2016**, *198*, 473.

33. Cavallito, C. J.; Bailey, J. H. "Allicin, the Antibacterial Principle of *Allium sativum*. I. Isolation, Physical Properties and Antibacterial Action" *Journal of the American Chemical Society* **1944**, *66*, 1950.
34. Ankri, S.; Mirelman, D. "Antimicrobial properties of allicin from garlic" *Microbes and Infection* **1999**, *1*, 125.
35. Hocquellet, A.; le Senechal, C.; Garbay, B. "Importance of the disulfide bridges in the antibacterial activity of human hepcidin" *Peptides* **2012**, *36*, 303.
36. Ganz, T. "Hepcidin, a key regulator of iron metabolism and mediator of anemia of inflammation" *Blood* **2003**, *102*, 783.
37. Keyes, R. F.; Carter, J. J.; Englund, E. E.; Daly, M. M.; Stone, G. G.; Nilius, A. M.; Ma, Z. "Synthesis and Antibacterial Activity of 6-O-Arylbutynyl Ketolides with Improved Activity against Some Key Erythromycin-Resistant Pathogens" *Journal of Medicinal Chemistry* **2003**, *46*, 1795.
38. Patel, S. K.; Tirkey, V.; Mishra, S.; Dash, H. R.; Das, S.; Shukla, M.; Saha, S.; Mobin, S. M.; Chatterjee, S. "Synthesis of mono- and bi-metallic dithiocarboxylate-alkyne complexes from sunlight driven insertion reaction and their antibacterial activity" *Journal of Organometallic Chemistry* **2014**, *749*, 75.
39. Schomaker, J. M.; Pulgam, V. R.; Borhan, B. "Synthesis of Diastereomerically and Enantiomerically Pure 2,3-Disubstituted Tetrahydrofurans Using a Sulfoxonium Ylide" *Journal of the American Chemical Society* **2004**, *126*, 13600.
40. Corey, E. J.; Venkateswarlu, A. "Protection of hydroxyl groups as tert-butyldimethylsilyl derivatives" *Journal of the American Chemical Society* **1972**, *94*, 6190.
41. Hamouda, T.; Myc, A.; Donovan, B.; Shih, A. Y.; Reuter, J. D.; Baker, J. R., Jr. "A novel surfactant nanoemulsion with a unique non-irritant topical antimicrobial activity against bacteria, enveloped viruses and fungi" *Microbiological research* **2001**, *156*, 1.

42. Kubo, I.; Muroi, H.; Kubo, A. "Antibacterial activity of long-chain alcohols against *Streptococcus mutans*" *Journal of Agricultural and Food Chemistry* **1993**, *41*, 2447.
43. Kubo, I.; Muroi, H.; Kubo, A. "Structural functions of antimicrobial long-chain alcohols and phenols" *Bioorganic & Medicinal Chemistry* **1995**, *3*, 873.
44. Norred, W. P.; Ansel, H. C.; Roth, I. L.; Peifer, J. J. "Mechanism of Dimethyl Sulfoxide-Induced Hemolysis" *Journal of Pharmaceutical Sciences* **1970**, *59*, 618.
45. Vollmer, W.; Höltje, J.-V. "The Architecture of the Murein (Peptidoglycan) in Gram-Negative Bacteria: Vertical Scaffold or Horizontal Layer(s)?" *Journal of bacteriology* **2004**, *186*, 5978.
46. Demchick, P.; Koch, A. L. "The permeability of the wall fabric of *Escherichia coli* and *Bacillus subtilis*" *Journal of bacteriology* **1996**, *178*, 768.
47. Malanovic, N.; Lohner, K. "Gram-positive bacterial cell envelopes: The impact on the activity of antimicrobial peptides" *Biochimica et Biophysica Acta (BBA) - Biomembranes* **2016**, *1858*, 936.
48. Martin, N. I.; Breukink, E. "The expanding role of lipid II as a target for lantibiotics" *Future Microbiology* **2007**, *2*, 513.
49. Marcos, J. F.; Gandía, M. "Antimicrobial peptides: to membranes and beyond" *Expert opinion on drug discovery* **2009**, *4*, 659.
50. Percy, M. G.; Gründling, A. "Lipoteichoic Acid Synthesis and Function in Gram-Positive Bacteria" *Annual Review of Microbiology* **2014**, *68*, 81.
51. Oku, Y.; Kurokawa, K.; Matsuo, M.; Yamada, S.; Lee, B.-L.; Sekimizu, K. "Pleiotropic Roles of Polyglycerolphosphate Synthase of Lipoteichoic Acid in Growth of *Staphylococcus aureus* Cells" *Journal of bacteriology* **2009**, *191*, 141.

52. Nikaido, H.; Nakae, T. In *Advances in Microbial Physiology*; Rose, A. H., Morris, J. G., Eds.; Academic Press: 1980; Vol. Volume 20, p 163.
53. Alakomi, H. L.; Skyttä, E.; Saarela, M.; Mattila-Sandholm, T.; Latva-Kala, K.; Helander, I. M. "Lactic Acid Permeabilizes Gram-Negative Bacteria by Disrupting the Outer Membrane" *Applied and environmental microbiology* **2000**, *66*, 2001.
54. Robins, D. J. "Pyrrolizidine alkaloids" *Natural Product Reports* **1995**, *12*, 413.
55. Ishibashi, H.; Ozeki, H.; Ikeda, M. "Synthesis of optically active (-)-trachelanthamidine from L-prolinol" *Journal of the Chemical Society, Chemical Communications* **1986**, 654.
56. Fleet, G. W. J.; Haraldsson, M.; Nash, R. J.; Fellows, L. E. "Synthesis from D-glucose of alexine [(1R,2R,3R,7S,8S)-3-hydroxymethyl-1,2,7-trihydroxypyrrolizidine], 3-epialexine and 7-epialexine" *Tetrahedron Letters* **1988**, *29*, 5441.
57. Fleet, G. W. J.; Smith, P. W. "Methyl 2-azido-3-O-benzyl-2-deoxy- α -D-mannofuranoside as a divergent intermediate for the synthesis of polyhydroxylated piperidines and pyrrolidines: synthesis of 2,5-dideoxy-2,5-imino-D-mannitol [2R,5R-dihydroxymethyl-3R,4R-dihydroxypyrrolidine]" *Tetrahedron* **1987**, *43*, 971.
58. Denmark, S. E.; Hurd, A. R. "Synthesis of (+)-casuarine" *The Journal of organic chemistry* **2000**, *65*, 2875.
59. Denmark, S. E.; Cottell, J. J. "Synthesis of (+)-1-epiaustraline" *The Journal of organic chemistry* **2001**, *66*, 4276.
60. Pearson, W. H.; Hines, J. V. "Total syntheses of (+)-australine and (-)-7-epialexine" *The Journal of organic chemistry* **2000**, *65*, 5785.
61. Chikkanna, D.; Singh, O. V.; Kong, S. B.; Han, H. "A general asymmetric route for the synthesis of the alexine and australine family of pyrrolizidine

- alkaloids. The first asymmetric synthesis of 1,2-diepi-alexine and 1,2,7-triepi-australine" *Tetrahedron Letters* **2005**, 46, 8865.
62. Schomaker, J. M.; Bhattacharjee, S.; Yan, J.; Borhan, B. "Diastereomerically and enantiomerically pure 2,3-disubstituted pyrrolidines from 2,3-aziridin-1-ols using a sulfoxonium ylide: A one-carbon homologative relay ring expansion" *Journal of the American Chemical Society* **2007**, 129, 1996.
 63. Dressel, M.; Restorp, P.; Somfai, P. "Total Synthesis of (+)-Alexine by Utilizing a Highly Stereoselective [3+2] Annulation Reaction of an N-Tosyl- α -Amino Aldehyde and a 1,3-Bis(silyl)propene" *Chemistry – A European Journal* **2008**, 14, 3072.
 64. Beruben, D.; Marek, I.; Normant, J. F.; Platzer, N. "Stereodefined Substituted Cyclopropyl Zinc Reagents from Gem-Bismetallics" *The Journal of organic chemistry* **1995**, 60, 2488.
 65. Kulshrestha, A.; Schomaker, J. M.; Holmes, D.; Staples, R. J.; Jackson, J. E.; Borhan, B. "Selectivity in the Addition Reactions of Organometallic Reagents to Aziridine-2-carboxaldehydes: The Effects of Protecting Groups and Substitution Patterns" *Chemistry – A European Journal* **2011**, 17, 12326.
 66. Cope, A. C. "The Preparation of Dialkylmagnesium Compounds from Grignard Reagents" *Journal of the American Chemical Society* **1935**, 57, 2238.
 67. Phillips, G. W.; University, M. S. *Synthetic Studies Toward the Total Synthesis of Fostriecin and Some Analogs*; Michigan State University, 2006.
 68. Deiana, L.; Dziedzic, P.; Zhao, G.-L.; Vesely, J.; Ibrahim, I.; Rios, R.; Sun, J.; Córdova, A. "Catalytic Asymmetric Aziridination of α,β -Unsaturated Aldehydes" *Chemistry – A European Journal* **2011**, 17, 7904.
 69. Gilman, H. *Organic chemistry: an advanced treatise*; J. Wiley & sons, inc: New York;London; U6 - ctx_ver=Z39.88-2004&ctx_enc=info%3Aofi%2Fenc%3AUTF-

8&rft_id=info%3Asid%2Fsummon.serialssolutions.com&rft_val_fmt=info%3Aofi%2Ffmt%3Akev%3Amtx%3Abook&rft.genre=book&rft.title=Organic+chemistry&rft.au=Gilman%2C+Henry&rft.au=Allen%2C+C.+F.+H&rft.date=1938-01-01&rft.pub=J.+Wiley+%26+sons%2C+inc&rft.externalDBID=I17&rft.externalDocID=b16114632¶mdict=en-US U7 - Book, 1938; Vol. 1.

70. Olah, G. A.; Bollinger, J. M. "Stable carbonium ions. XLVIII. Halonium ion formation via neighboring halogen participation. Tetramethylethylene halonium ions" *Journal of the American Chemical Society* **1967**, *89*, 4744.
71. Olah, G. A.; Bollinger, J. M. "stable carbonium ions. Ivii catalysts with olefins.ang. .ang" *Journal of the American Chemical Society* **1968**, *90*, 947.
72. Olah, G. A.; Bollinger, J. M.; Brinich, J. "Stable carbonium ions. LXII. Halonium ion formation via neighboring halogen participation: ethylenehalonium, propylenehalonium, and 1,2-dimethylethylenehalonium ions" *Journal of the American Chemical Society* **1968**, *90*, 2587.
73. Roberts, I.; Kimball, G. E. "The Halogenation of Ethylenes" *Journal of the American Chemical Society* **1937**, *59*, 947.
74. Brown, R. S. "Investigation of the Early Steps in Electrophilic Bromination through the Study of the Reaction with Sterically Encumbered Olefins" *Accounts of Chemical Research* **1997**, *30*, 131.
75. Brown, R. S.; Nagorski, R. W.; Bennet, A. J.; McClung, R. E. D.; Aarts, G. H. M.; Klobukowski, M.; McDonald, R.; Santarsiero, B. D. "Stable Bromonium and Iodonium Ions of the Hindered Olefins Adamantylideneadamantane and Bicyclo[3.3.1]nonylidenebicyclo[3.3.1]nonane. X-Ray Structure, Transfer of Positive Halogens to Acceptor Olefins, and ab Initio Studies" *Journal of the American Chemical Society* **1994**, *116*, 2448.
76. Neverov, A. A.; Brown, R. S. "Br⁺ and I⁺ Transfer from the Halonium Ions of Adamantylideneadamantane to Acceptor Olefins. Halocyclization of 1, ω -Alkenols and Alkenoic Acids Proceeds via Reversibly Formed Intermediates" *The Journal of organic chemistry* **1996**, *61*, 962.

77. Denmark, S. E.; Burk, M. T.; Hoover, A. J. "On the Absolute Configurational Stability of Bromonium and Chloronium Ions" *Journal of the American Chemical Society* **2010**, *132*, 1232.
78. Merritt, R. F. "The Polar Fluorination of Propenylbenzene" *Journal of the American Chemical Society* **1967**, *89*, 609.
79. Whitehead, D. C.; Yousefi, R.; Jaganathan, A.; Borhan, B. "An Organocatalytic Asymmetric Chlorolactonization" *Journal of the American Chemical Society* **2010**, *132*, 3298.
80. Whitehead, D. C. Ph.D., Michigan State University, 2009.
81. Wang, M.; Gao, L. X.; Mai, W. P.; Xia, A. X.; Wang, F.; Zhang, S. B. "Enantioselective Iodolactonization Catalyzed by Chiral Quaternary Ammonium Salts Derived from Cinchonidine" *The Journal of organic chemistry* **2004**, *69*, 2874.
82. Rauniyar, V.; Lackner, A. D.; Hamilton, G. L.; Toste, F. D. "Asymmetric Electrophilic Fluorination Using an Anionic Chiral Phase-Transfer Catalyst" *Science* **2011**, *334*, 1681.
83. Jaganathan, A.; Garzan, A.; Whitehead, D. C.; Staples, R. J.; Borhan, B. "A catalytic asymmetric chlorocyclization of unsaturated amides" *Angewandte Chemie* **2011**, *50*, 2593.
84. Jaganathan, A.; Borhan, B. "Chlorosulfonamide salts are superior electrophilic chlorine precursors for the organocatalytic asymmetric chlorocyclization of unsaturated amides" *Organic letters* **2014**, *16*, 3616.
85. Marshall, S. E., Michigan State University, 2013.
86. Becker, H.; Tong Ho, P.; Kolb, H. C.; Loren, S.; Norrby, P.-O.; Sharpless, K. B. "Comparing two models for the selectivity in the asymmetric dihydroxylation reaction (AD)" *Tetrahedron Letters* **1994**, *35*, 7315.
87. Yousefi, R.; Ashtekar, K. D.; Whitehead, D. C.; Jackson, J. E.; Borhan, B. "Dissecting the Stereocontrol Elements of a Catalytic Asymmetric

Chlorolactonization: Syn Addition Obviates Bridging Chloronium" *Journal of the American Chemical Society* **2013**, *135*, 14524.

88. Broady, S. D.; Golden, M. D.; Leonard, J.; Muir, J. C.; Maudet, M. "Asymmetric synthesis of (S)-(-)-N-acetylcolchinol via Ullmann biaryl coupling" *Tetrahedron Letters* **2007**, *48*, 4627.
89. Ma, D.; Cai, Q.; Zhang, H. "Mild method for Ullmann coupling reaction of amines and aryl halides" *Organic letters* **2003**, *5*, 2453.
90. Wolter, M.; Nordmann, G.; Job, G. E.; Buchwald, S. L. "Copper-Catalyzed Coupling of Aryl Iodides with Aliphatic Alcohols" *Organic letters* **2002**, *4*, 973.
91. Hassan, J.; Sévignon, M.; Gozzi, C.; Schulz, E.; Lemaire, M. "Aryl–Aryl Bond Formation One Century after the Discovery of the Ullmann Reaction" *Chemical reviews* **2002**, *102*, 1359.
92. Kajanus, J.; van Berlekom, S. B.; Albisson, B.; Martensson, J. "Synthesis of Bis(phenylethynyl)arylene-Linked Diporphyrins Designed for Studies of Intramolecular Energy Transfer" *Synthesis* **1999**, 1155.
93. Lü, B.; Jiang, X.; Fu, C.; Ma, S. "Highly Regio- and Stereoselective Cyclic Iodoetherification of 4,5-Alkadienols. An Efficient Preparation of 2-(1'(Z)-Iodoalkenyl)tetrahydrofurans" *The Journal of organic chemistry* **2009**, *74*, 438.
94. Zhang, X.; Fu, C.; Yu, Y.; Ma, S. "Stereoselective iodolactonization of 4-allenoic acids with efficient chirality transfer: development of a new electrophilic iodination reagent" *Chemistry* **2012**, *18*, 13501.
95. Salehi Marzijarani, N. Ph.D., Michigan State University, 2016.
96. Zhang, W.; Liu, N.; Schienebeck, C. M.; Zhou, X.; Izhar, I. I.; Guzei, I. A.; Tang, W. "Enantioselective intermolecular bromoesterification of allylic sulfonamides" *Chemical Science* **2013**, *4*, 2652.

97. Soltanzadeh, B.; Jaganathan, A.; Staples, R. J.; Borhan, B. "Highly Stereoselective Intermolecular Haloetherification and Haloesterification of Allyl Amides" *Angewandte Chemie* **2015**, *54*, 9517.
98. Ashtekar, K. D.; Vetticatt, M.; Yousefi, R.; Jackson, J. E.; Borhan, B. "Nucleophile Assisted Alkene Activation: Olefins Alone are Often Incompetent" *Journal of the American Chemical Society* **2016**.
99. Nicolaou, K. C.; Simmons, N. L.; Ying, Y.; Heretsch, P. M.; Chen, J. S. "Enantioselective Dichlorination of Allylic Alcohols" *Journal of the American Chemical Society* **2011**, *133*, 8134.
100. Soltanzadeh, B.; Jaganathan, A.; Yi, Y.; Yi, H.; Staples, R. J.; Borhan, B. "Highly Regio- and Enantioselective Vicinal Dihalogenation of Allyl Amides" *Journal of the American Chemical Society* **2017**, *139*, 2132.
101. Anderson, G. M.; Kollman, P. A.; Domelsmith, L. N.; Houk, K. N. "Methoxy group nonplanarity in o-dimethoxybenzenes. Simple predictive models for conformations and rotational barriers in alkoxyaromatics" *Journal of the American Chemical Society* **1979**, *101*, 2344.
102. Radom, L.; Hehre, W. J.; Pople, J. A.; Carlson, G. L.; Fateley, W. G. "Torsional barriers in para-substituted phenols from ab initio molecular orbital theory and far infrared spectroscopy" *Journal of the Chemical Society, Chemical Communications* **1972**, 308.
103. Ogino, Y.; Chen, H.; Manoury, E.; Shibata, T.; Beller, M.; Lubben, D.; Sharpless, K. B. "A Ligand Structure-Enantioselectivity Relationship for the Osmium-Catalyzed Asymmetric Dihydroxylation of Olefins" *Tetrahedron Letters* **1991**, *32*, 5761.